

**Tracing metals: An archaeo-metallurgical
investigation of metal working remains and
artefacts from Thaba Nkulu in the Waterberg,
South Africa**

Volume I



Name: Michael Lewis Naylor

Student Number: 318828

Division: Archaeology

School: Geography, Archaeology and Environmental Studies

Faculty: Faculty of Science

Supervisor: Dr M.H. Schoeman

Co-Supervisor: Prof L.A. Cornish

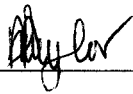
A dissertation submitted to the School of Geography, Archaeology and
Environmental Studies, Faculty of Science University of the Witwatersrand,

In fulfilment of the requirements for the degree of
Master of Science.

Johannesburg 2015

DECLARATION

I declare that this dissertation is my own unaided work. It has been submitted in partial fulfilment of the requirements of the Degree of Master of Science in Archaeology in the University of the Witwatersrand, Johannesburg. It has not been submitted before for any degree or examination in any other University.



(Signature of candidate)

13 day of October 20 15 in Johannesburg

ABSTRACT

Excavations conducted at Thaba Nkulu, an Early Farming Community homestead with associated metal working debris, led to the recovery of iron slag, tuyères, furnace lining, iron ore, copper artefacts and iron artefacts. Using the material recovered, this dissertation identified chemical signatures for metal artefacts and metal smelting and smithing associated material. This was achieved through the use of a combination of X-ray fluorescence spectrometry (XRF) and Scanning Electron Microscopy coupled with Energy-Dispersive X-Ray Spectroscopy (SEM-EDX). The artefacts recovered were analysed, and 3 sets of possible chemical signatures were recorded.

In addition, the excavations and material culture (both metal and non-metal) were used to grapple with the spatial configuration of Thaba Nkulu. This includes the position of metal working relative to the homestead.

ACKNOWLEDGEMENTS

First and foremost I would like to thank my friends and family, without whom, this dissertation would not have come to fruition. You all encouraged me, aided me and supported me throughout the course of this project, and for that I am truly grateful.

I especially thank my father, Stephen Leslie Naylor. Thank you for your support and aid, whether it was excavating, sorting through lab notes, aiding with words and editing, putting up with me and my randomness, and encouraging me to always carry on. Even though you may think you were of little help, you have aided me more than you will ever know.

Secondly, I would like to thank my supervisors Dr Alex Schoeman and Prof. Lesley Cornish.

To Dr Schoeman: Thank you for being my supervisor and guiding me along the course of archaeology. No matter what issues I had, you were there to aid and support me. Thank you for assisting with permit applications, acquisition of literature, knowledge and guidance.

To Prof. Lesley Cornish: Thank you for your help with the metallurgy, literature, proof reading, editing and in general aiding me in understanding the complexities of metallurgy. Without your knowledge and guidance this project's aims would still be in their infancy.

Finally, I would like to thank the two main financial and logistical contributors to this project:

The National Research Fund (NRF), freestanding bursary.

The owner and managers of Thaba Nkulu game farm.

The financial assistance of the National Research Foundation (N R F) towards this research is hereby acknowledged. Opinions expressed and conclusions arrived at, are those of the author and are not necessarily to be attributed to the N R F.

Finally, a big thank you to Mrs Ina Maria Lerchbaumer, the owner of Thaba Nkulu, as well as Mr Henry Hayward, the Farm Manager. Thank you both for granting me permission to work on your property and for taking care of me and those who excavated with me.

CONTENTS

	PAGE
DECLARATION	i
ABSTRACT	ii
ACKNOWLEDGEMENTS	iii
CONTENTS	v
LIST OF FIGURES	xvi
LIST OF TABLES	xxii
CHAPTER 1: INTRODUCTION	1
1.1: Research aims	2
1.2: Thaba Nkulu	3
1.3: Organisation of the dissertation	5
CHAPTER 2: BACKGROUND	6
Introduction:	6
2.1: Archaeology of the Waterberg	6
2.1.1: Introduction	6
2.1.2: Hunter-gatherers of the Waterberg	6
2.1.3: Farming communities of the Waterberg	10
2.2: Smelting vs. Smithing sites	16
2.2.1: Introduction	16
2.2.2: Smelting and smithing	17
2.2.3: Archaeo-metallurgy in the spatial belief debate	22
2.3: Archaeo-metallurgy: Various metals and their trace elements	24
2.3.1: History of archaeo-metallurgical research in the Waterberg	24
2.3.2: Various archaeo-metallurgy instruments, uses and discoveries	24
2.3.3: Early theories on sourcing artefacts	26

Conclusions:	28
CHAPTER 3: ARCHAEOLOGY METHODOLOGY	30
Introduction:	30
3.1: The excavations	30
3.1.1: The Area	30
3.1.2: Permit Application	31
3.1.3: Mapping	31
3.1.4: Excavations and test pits	32
3.1.5: Problems found on site	34
3.1.6: Excavation details	34
3.1.6.1: 2328 CA1 (1)	34
3.1.6.2: 2328 CA1 (2)	35
3.1.6.3: 2328 CA1 (3)	35
3.1.6.4: 2328 CA1 (4)	36
3.1.6.5: 2328 CA1 (10)	36
3.2: Storage and management of artefacts	36
3.2.1: Main artefacts	36
3.2.2: Secondary artefacts	37
Conclusions:	38
CHAPTER 4: ARCHAEOLOGY RESULTS	39
Introduction:	39
4.1: Site Results	39
4.1.1: The site of 2328 CA1	39
4.1.2: 2328 CA1 Shovel Test Pits	42
4.1.3: Excavation 2328 CA1 (1)	46
4.1.4: Excavation 2328 CA1 (1) stratigraphy	48
4.1.4.1: XIX/N	48
4.1.4.1.1: XIX/N/S	48

4.1.4.1.2: XIX/N/AD.....	49
4.1.4.1.3: XIX/N/2A.....	49
4.1.4.1.4: XIX/N/2B.....	49
4.1.4.2: XX/O.....	52
4.1.4.2.1: XX/O/S.....	52
4.1.4.2.2: XX/O/AD.....	52
4.1.4.2.3: XX/O/1B.....	52
4.1.4.2.4: XX/O/2A.....	53
4.1.4.2.5: XX/O/2B.....	53
4.1.4.3: XX/M.....	56
4.1.4.3.1: XX/M/S.....	56
4.1.4.3.2: XX/M/1A.....	56
4.1.4.3.3: XX/M/1B.....	56
4.1.4.3.4: XX/M/2A RB.....	56
4.1.4.3.5: XX/M/2B RG.....	57
4.1.4.3.6: XX/M/3A RG.....	57
4.1.4.3.7: XX/M/3B RG + XX/M/3B B (Hard).....	57
4.1.4.3.8: XX/M/4A Tuyère layer (grey).....	58
4.1.4.3.9: XX/M/4B Tuyère layer (grey).....	58
4.1.4.3.10: XX/M/5A (grey- tuyère pipes).....	58
4.1.4.3.11: XX/M/5B B + XX/M/5B BH.....	58
4.1.4.3.12: XX/M/6A.....	59
4.1.5: Excavation 2328 CA1 (2).....	62
4.1.6: Excavation 2328 CA1 (2) stratigraphy.....	64
4.1.6.1: XIII/E.....	64
4.1.6.1.1: XIII/E/S.....	64
4.1.6.1.2: XIII/E/1A.....	64
4.1.6.1.3: XIII/E/1B.....	64
4.1.6.1.4: XIII/E/2A.....	64
4.1.6.1.5: XIII/E/2B.....	65
4.1.6.1.6: XIII/E/3A.....	65
4.1.6.2: XIII/F.....	66
4.1.6.2.1: XIII/F/S.....	66
4.1.6.2.2: XIII/F/1A.....	66
4.1.6.3.2: XIII/F/1B.....	67
4.1.6.3.4: XIII/F/2A.....	67

4.1.6.3.5: XIII/F/2B.....	67
4.1.6.3.6: XIII/F/3A.....	68
4.1.6.3.7: XIII/F/3B.....	68
4.1.6.3.8: XIII/F/4A mixed.....	68
4.1.6.3.9: XIII/F/GA 4B	69
4.1.6.3.10: XIII/F/GA 5A.....	69
4.1.6.3.11: XIII/F/GA 5B	69
4.1.6.3.12: XIII/F/GA 6A.....	69
4.1.6.3.13: XIII/F/GA 6B	70
4.1.6.4: XIV/F.....	73
4.1.6.4.1: XIV/F/S.....	73
4.1.6.4.12: XIV/F/1A	73
4.1.6.4.3: XIV/F/1B.....	73
4.1.7: Excavation 2328 CA1 (10).....	73
4.1.8: Excavation 2328 CA1 (10) stratigraphy	75
4.1.8.1: Road Test X/I.....	75
4.1.8.1.1: Road Test X/I/S.....	75
4.1.8.1.2: Road Test X/I/1A	75
4.1.8.1.3: Road Test X/I 1B.....	75
4.1.8.2: VIII/G	76
4.1.8.2.1: VIII/G/S.....	76
4.1.8.2.2: VIII/G/1A + 1B	76
4.1.8.2.3: VIII/G/2A.....	77
4.1.8.3: IX/G	77
4.1.8.3.1: IX/G/S	77
4.1.8.3.2: IX/G/1A.....	77
4.1.8.3.3: IX/G/1B.....	77
4.1.8.3.4: IX/G/2A.....	77
4.1.8.3.5: IX/G/2B.....	78
4.1.8.3.6: IX/G/3A+ 3B.....	78
4.1.9: Excavations 2328 CA1 (3) and 2328 CA1 (4)	79
4.1.9.1: 2328 CA 1 (3) X/A	80
4.1.9.1.1: X/A/S.....	80
4.1.9.1.2: X/A/1A-2A.....	80
4.1.9.1.3: X/A/2B	81

4.1.9.1.4: X/A/3A	81
4.1.9.1.5: X/A/3B	81
4.1.9.1.6: X/A/4A	81
4.1.9.1.7: X/A/4B	82
4.1.9.1.8: X/A/5A	82
4.1.9.1.9: X/A/5B	82
4.1.9.2: 2328 CA 1 (4)	85
4.1.9.2.1: XX/J/S	85
4.1.9.2.2: XX/J/1A + 1B	85
4.1.9.2.3: XX/J/2A	85
4.1.9.2.4: XX/J/2B	85
4.1.9.2.5: XX/J/3A	86
4.1.9.2.6: XX/J/3B	86
4.1.9.2.7: XX/J/4A	86
4.1.10: 2328 CA1 Road surface Collection	88
4.2: Artefacts recovered	90
4.2.1: Artefacts recovered from each excavation	90
4.2.1.1: Artefacts recovered from Test pits and shovel test pits	90
4.2.1.2: Artefacts recovered from 2328 CA1 (1)	90
4.2.1.3: Artefacts recovered from 2328 CA1 (2)	91
4.2.1.4: Artefacts recovered from 2328 CA1 (10)	91
4.2.1.5: Artefacts recovered from 2328 CA1 (3) and 2328 CA1 (4)	92
4.2.1.6: Artefacts recovered from the Road surface collection	92
4.2.2: Metal artefacts, slag and tuyère	93
4.2.2.1: Metal artefacts	93
4.2.2.2: Slag	96
4.2.2.3: Tuyère	96
4.2.3: Ceramic fragments	99
4.2.4: Charcoal	106
4.2.5: Other material culture	107
4.2.5.1: Baked sand	107
4.2.5.2: Faunal remains	107
4.2.5.3: Beads	107

4.2.5.4: Orange compact soil/daga.....	107
4.2.6: Dating.....	108
4.2.6.1: Radiocarbon dating.....	108
Conclusion:.....	108
CHAPTER 5: EXCAVATIONS AND ARTEFACTS	
DISCUSSION	109
Introduction:	109
5.1: Excavations, meanings and interpretations.	109
5.1.1: Introduction:	109
5.1.2: 2328 CA1 (2) and 2328 CA1 (10) road pits, an indicator of the homestead	109
5.1.3: The occupation layer	112
5.1.4: The site overall.....	113
5.1.5: Excavation 2328 CA1 (1), the slag and tuyère dump.....	115
5.2: Main artefacts recovered interpretations.....	118
5.2.1: Introduction:	118
5.2.2: Metallic smelting and smithing materials.....	118
5.2.2.1: Slag	118
5.2.2.3: Copper artefacts	121
5.2.3.1: Tuyère.....	121
5.2.3.2: Ore	121
CHAPTER 6: LABORATORY METHODOLOGY.....	123
6.1: Analysis of samples.....	123
6.1.1: XRF Analysis.....	123
6.1.1.1: XRF preparation	124
6.1.1.2: XRF testing.....	125
6.1.2: Scanning Electron Microscope Analysis.....	126
6.1.2.1: SEM preparation.....	127
6.1.2.2: Etching.....	128

6.1.2.3: Optical microscopy	129
6.1.2.4: SEM analyses.....	129
6.1.3: Conversion of results	130
CHAPTER 7: XRF AND SEM RESULTS	131
7.1: XRF findings	131
7.1.1: Introduction	131
7.1.2: Slag.....	132
7.1.3: Tuyère fragments.....	152
7.1.4: Ore	156
7.1.5: Iron artefacts.....	161
7.1.6: Copper artefacts	165
7.2: Metallography.....	169
7.2.1: Copper artefacts	169
7.2.2: Iron artefacts.....	172
7.3: SEM-EDX findings.....	176
7.3.1: SEM-EDX slag.....	176
7.3.2: SEM-EDX tuyère and ore.....	180
7.3.3: SEM-EDX iron artefacts.....	182
7.3.4: SEM-EDX copper artefacts	184
7.4: Overall SEM-EDX analysis	186
Conclusions:	187
CHAPTER 8: CHEMICAL SIGNATURE DISCUSSION.....	188
Introduction:	188
8.1: Artefacts chemical signatures.....	188
8.1.1: Metallic smelting and smithing material	188
8.1.1.1: Slag chemical composition and signature.....	188
8.1.1.2: Iron artefacts chemical composition and signature.....	191
8.1.1.3: Copper artefact chemical composition and signature	193

8.1.2: Non-metallic smelting and smithing material	195
8.1.2.1: Tuyère	195
8.1.2.2: Ore	196
8.1.3: Thaba Nkulu’s chemical signatures	197
8.1.3.1: Ratio analysis	199
8.1.3.2: Comparison analysis	205
CHAPTER 9: CONCLUSIONS	214
Introduction:	214
9.1: Excavation outcomes	214
9.2: Thaba Nkulu’s chemical signature	215
9.3: Future research options	218
9.3.1: Future site options	218
9.3.2: Future analysis options	218
REFERENCES:	221
APPENDIX A: ARTEFACTS RECOVERED FROM SITE 2328	
CA1	237
A10.1: 2328 CA1 (1)	237
A10.2: 2328 CA1 (2)	243
A10.3: 2328 CA1 (3)	250
A10.4: 2328 CA1 (4)	252
A10.5: 2328 CA1 (10)	254
A10.6: 2328 CA1 Test Pits	258
A10.7: 2328 CA1 Road Collection	260
APPENDIX B: XRF RESULTS AND TABLES	264
B11.1: 2328 CA1 (1)	265
B11.2: 2328 CA1 (2)	285
B11.3: 2328 CA1 (3)	302

B11.4: 2328 CA1 (4)	306
B11.5: 2328 CA1 (10)	310
B11.6: 2328 CA1 Road Collection	320
B11.7: 2328 CA1 Test Pits	329
B11.8: 2328 CA1 Artefacts	332
APPENDIX C: XRF CONVERTED RESULTS	335
C12.1: XRF slag normalised oxides	335
C12.2: XRF tuyère normalised oxides	354
C12.3: XRF ore normalised oxides	357
C12.4: XRF iron artefacts normalised oxides	361
C12.5: XRF copper artefacts normalised oxides	364
APPENDIX D: SIGMA ZEISS SEM RESULTS	367
D13.1.1: 2328 CA1 (1) XIX/N/AD 1	367
D13.1.2: 2328 CA1 (1) XIX/N/AD 2	368
D13.1.3: 2328 CA1 (1) XIX/N/AD 3	369
D13.2.1: 2328 CA1 (1) XIX/N/2B 1	370
D13.2.2: 2328 CA1 (1) XIX/N/2B 2	371
D13.2.3: 2328 CA1 (1) XIX/N/2B 3	372
D13.3.1: 2328 CA1 (1) XX/M/2A RB 1	373
D13.3.2: 2328 CA1 (1) XX/M/2A RB 2	374
D13.3.3: 2328 CA1 (1) XX/M/2A RB 3	375
D13.4.1: 2328 CA1 (1) XX/M/1B 1	377
D13.4.2: 2328 CA1 (1) XX/M/1B 2	378
D13.4.3: 2328 CA1 (1) XX/M/1B 3	379
D13.5.1: 2328 CA1 (1) XX/O/AD	380
D13.5.2: 2328 CA1 (1) XX/O/AD (2)	381

D13.5.3: 2328 CA1 (1) XX/O/AD (3)	382
D13.6.1: 2328 CA1 (1) XX/O/2B 1	384
D13.6.2: 2328 CA1 (1) XX/O/2B 2	385
D13.7.1: 2328 CA1 (2) XIII/F/S thin wire earring 1	386
D13.7.2: 2328 CA1 (2) XIII/F/S thin wire earring 2	387
D13.8.1: 2328 CA1 (3) X/A/3A thick copper wire 1	389
D13.8.2: 2328 CA1 (3) X/A/3A thick copper wire 2	390
D13.9.1: 2328 CA1 (10) Road Test X/I/S 1	391
D13.9.2: 2328 CA1 (10) Road Test X/I/S 2	392
D13.10.1: 2328 CA1 Road collection 8 Slag 1	394
D13.10.2: 2328 CA1 Road collection 8 Slag 2	395
D13.11.1: 2328 CA1 Road collection 16 Ore	396
D13.12.1: 2328 CA1 57 Copper Earring 1	397
D13.12.2: 2328 CA1 57 Copper Earring 2	398
D13.12.3: 2328 CA1 57 Copper Earring 3	399
D13.12.4: 2328 CA1 57 Copper Earring 4	400
D13.13.1: 2328 CA1 Arrowhead 1	402
D13.13.2: 2328 CA1 Arrowhead 2	403
D13.13.3: 2328 CA1 Arrowhead 3	404
D13.13.4: 2328 CA1 Arrowhead 4	405
D13.13.5: 2328 CA1 Arrowhead 5	406
D13.14.1: 2328 CA1 Spear base 1	407
D13.14.2: 2328 CA1 Spear base 2	408
D13.14.3: 2328 CA1 Spear base 3	409
D13.14.4: 2328 CA1 Spear base 4	410
D13.15.1: 2328 CA1 Tang 1	411

D13.15.2: 2328 CA1 Tang 2	412
D13.15.3: 2328 CA1 Tang 3	413
D13.15.4: 2328 CA1 Tang 4	414
APPENDIX E: EDAX SEM RESULTS	416
E14.1: 2328 CA1 (3) X/A/5B tuyère	416
E14.2: 2328 CA1 (4) XX/J/3A slag	418
E14.3: 2328 CA1 (4) XX/J/3B tuyère	420
E14.4: 2328 CA1 (10) VIII/G/S Ore	422
E14.5: 2328 CA1 (10) IX/G/1B slag	424

LIST OF FIGURES

	PAGE
Figure 1.1: Map of the Waterberg region, showing various known sites and Thaba Nkulu (scale bar indicates 200m).....	4
Figure 2.1: Map indicating known Stone Age and Farming Community sites near Thaba Nkulu. Adapted from Van der Ryst (1998: iv) to include Thaba Nkulu.....	8
Figure 2.2: smelting slag from Miller & Killick (2004: 25).....	12
Figure 2.3: Low shaft furnace from Chirikure <i>et al.</i> (2014: 297).....	13
Figure 2.4: Tuyère pipes in a partially excavated furnace from Whitelaw (1991: 31).....	13
Figure 3.1: Excavation distribution on site 2328 CA1, including 2010 rescue excavation.....	31
Figure 4.1: Locations of excavations on site 2328CA1, including the 2010 rescue excavations.....	40
Figure 4.2: The 2328 CA1 site, with relevant archaeological information.....	41
Figure 4.3: Test pits and shovel test pit locations.....	43
Figure 4.4: Grid test pit 50cm x 50cm x ~40cm.....	44
Figure 4.5: Shovel test pit, dug to a depth of ~40cm.....	44
Figure 4.6: Shovel test pit with ceramic fragment.....	45
Figure 4.7: Ceramic with Diamant decoration, found in shovel test pit hole.....	45
Figure 4.8: Tuyère submersed in slag on surface of 2328 CA1 (1).....	46
Figure 4.9: 2328 CA1 (1) excavation.....	47
Figure 4.10: Excavation 2328 CA1 (1) location, with zoomed in grid layout.....	48
Figure 4.11: 2328 CA1 (1) XIX/N North facing wall stratigraphy.....	50
Figure 4.12: 2328 CA1 (1) XIX/N, base layer (with tree and animal hole).....	50
Figure 4.13: 2328 CA1 (1) XIX/N West facing wall stratigraphy.....	51
Figure 4.14: 2328 CA1 (1) XIX/N South facing wall stratigraphy, with layer indicators.....	51
Figure 4.15: 2328 CA1 (1) XX/O North facing wall stratigraphy.....	53
Figure 4.16: 2328 CA1 (1) XX/O East facing wall stratigraphy, with layer indicators.....	54

Figure 4.17: 2328 CA1 (1) XX/O Plan view.....	55
Figure 4.18: 2328 CA1 (1) XX/O at 25cm depth.....	55
Figure 4.19: 2328 CA1 (1) XX/M first slag and tuyère layer (3A RG), with root disturbance in top right corner.....	59
Figure 4.20: 2328 CA1 (1) XX/M Plan view.....	60
Figure 4.21: 2328 CA1 (1) XX/M final layer, showing the rock, slag walls and the final layer of excavation.....	60
Figure 4.22: 2328 CA1 (1) XX/M East facing wall stratigraphy, with layer indicators.....	61
Figure 4.23: 2328 CA1 (1) XX/M North facing wall stratigraphy.....	61
Figure 4.24: Excavation 2328 CA1 (2), with zoomed in grid layout.....	63
Figure 4.25: 2328 CA1 (2) XIII/E, final layer.....	66
Figure 4.26: 2328 CA1 (2) XIII/F/4A red soil mix with grey soil patch (bottom right (south-west corner)).....	70
Figure 4.27: 2328 CA1 (2) XIII/F Plan View.....	71
Figure 4.28: 2328 CA1 (2) XIII/F North facing wall stratigraphy, with layer indicators.....	71
Figure 4.29: 2328 CA1 (2) XIII/F South facing wall stratigraphy.....	72
Figure 4.30: 2328 CA1 (2) XIII/F/GA 5A final layer, showing pit base.....	72
Figure 4.31: Excavation 2328 CA1 (10), with enlarged in grid layout.....	74
Figure 4.32: Road Test X/I, bone on surface.....	76
Figure 4.33: 2328 CA1 (10) Plan view, with square IX/G to the left and square VIII/G to the right.....	78
Figure 4.34: Photo of excavation 2328 CA1 (10), at termination.....	79
Figure 4.35: Excavation 2328 CA1 (3) and 2328 CA1 (4).....	80
Figure 4.36: 2328 CA1 (3) X/A North facing wall stratigraphy, with layer indicators.....	83
Figure 4.37: 2328 CA1 (3) X/A South facing wall stratigraphy.....	83
Figure 4.38: 2328 CA1 (3) with test pit 3 in top left corner.....	84
Figure 4.39: 2328 CA1 (3) Plan view.....	84
Figure 4.40: 2328 CA1 (4) XX/J North facing wall stratigraphy, with layer indicators.....	87

Figure 4.41: 2328 CA1 (4) XX/J.....	87
Figure 4.42: 2328 CA1 (4) Plan View.....	88
Figure 4.43: Road surface collection distribution.....	88
Figure 4.44: AC 13, showing ceramics found on road surface.....	89
Figure 4.45: Iron arrowhead.....	94
Figure 4.46: Iron spear base.....	94
Figure 4.47 Iron tang.....	94
Figure 4.48: Copper thin wire earring.....	95
Figure 4.49: Thick copper wire.....	95
Figure 4.50: Copper earring (2328 CA1 57).....	95
Figure 4.51: Small tuyère (viewed across the width/diameter) from excavation 2328 CA1 (1).....	97
Figure 4.52: Small tuyère (viewed along the length) from excavation 2328 CA1 (1).....	97
Figure 4.53: Large tuyère (viewed across the width/diameter) from excavation 2328 CA1 (10).....	98
Figure 4.54: Large tuyère (viewed along the length) from excavation 2328 CA1 (10).....	98
Figure 4.55: 2328 CA1 (3) X/A/3B ceramic with incision decoration.....	100
Figure 4.56: 2328 CA1 Road collection 4 ceramic with herring bone impressed decoration, burnishing on a raised surface.....	100
Figure 4.57: 2328 CA1 (2) XIII/E/2B raised bump with impressed decoration...	101
Figure 4.58: 2328 CA1 (3) X/A/5A body section, with diagonal and horizontal incision lines.....	101
Figure 4.59: 2328 CA1 (4) XX/J/3A punctates below rim.....	102
Figure 4.60: 2328 CA1 (3) X/A/3B herringbone incision with incision running diagonally down the body, with a slight incision line.....	102
Figure 4.61: Wash down from 2328 CA1 (10) IX/G/S herringbone incisions....	103
Figure 4.62: 2328 CA1 (4) XX/J/4A two pieces of ceramic, with multiple horizontal incision, with apparent V separation design between.....	103
Figure 4.63: 2328 CA1 Road collection 3, comb stamping with diagonal and horizontal incisions.....	104

Figure 4.64: 2328 CA1 Road collection 18 multiple bands of comb stamping, separated by incisions.....	104
Figure 4.65: 2328 CA1 Test Pit 2 cross hatched decoration.....	105
Figure 4.66: 2328 CA1 (4) XX/J/3A multiple incisions varying in width, with some containing separate diagonal slashes.....	105
Figure 4.67: 2328 CA1 (4) XX/J/2B multiple lines of diagonal incisions, separated with horizontal incisions.....	106
Figure 5.1: Possible area zones, indicating homestead area relative to smelting site.....	114
Figure 5.2: Smelting slag, recovered from excavation 2328 CA1 (2).....	119
Figure 5.3: Flow slag, recovered from 2328 CA1 (1).....	120
Figure 5.4: Iron ore from Thaba Nkulu.....	122
Figure 7.1: Thaba Nkulu slag XRF low percentage element proportions (each colour represents one slag sample).....	150
Figure 7.2: Thaba Nkulu slag XRF higher percentage element proportions (each colour represents one slag sample).....	151
Figure 7.3: Thaba Nkulu tuyère XRF low percentage element proportions (colours represent individual samples).....	154
Figure 7.4: Thaba Nkulu tuyère XRF higher percentage element proportions (colours represent individual samples).....	155
Figure 7.5: Thaba Nkulu ore XRF low percentage element proportions (colours represent individual samples).....	159
Figure 7.6: Thaba Nkulu ore XRF higher percentage element proportions (colours represent individual samples).....	160
Figure 7.7: Thaba Nkulu iron artefacts XRF low percentage element proportions (colours represent individual samples).....	163
Figure 7.8: Thaba Nkulu iron artefacts XRF higher percentage element proportions (colours represent individual samples).....	164
Figure 7.9: Thaba Nkulu copper artefacts XRF low percentage element proportions. The blue column represents 2328 CA1 57.....	167
Figure 7.10: Thaba Nkulu copper artefacts XRF higher percentage element proportions. The blue column represents 2328 CA1 57.....	168

Figure 7.11: Optical micrograph of 2328 CA1 (3) X/A/3A copper artefact after sectioning and etching showing: grains (of different shades) with annealing twins (parallel sides (arrow 1)) and stringers of inclusions (grey (arrow 2)). Bar (bottom left) represents 50 microns.....	169
Figure 7.12: Optical micrograph at lower magnification micrograph of 2328 CA1 (2) XIII/F/S a thin copper earring after etching showing: grains with annealing twins (parallel sides) and aligned stringers of inclusions (grey). Bar represents 50 microns.....	170
Figure 7.13: Optical micrograph at intermediate magnification of 2328 CA1 (2) XIII/F/S, a thin copper earring after etching, showing: mainly equiaxed grains with annealing twins (parallel sides) and aligned stringers of inclusions (grey). Bar represents 50 microns.....	171
Figure 7.14: Optical micrograph at higher magnification of 2328 CA1 (2) XIII/F/S, a thin copper earring after etching, showing: mainly equiaxed grains with annealing twins (parallel sides) and aligned stringers of inclusions (grey). Bar represents 50 microns.....	171
Figure 7.15: Low magnification of 2328 CA1 iron arrow head, showing: ferrite grains (light), pearlite (darker) and sulphide stringers (very dark), and high proportion of oxides in the bottom right hand corner, grey. Red bar represents 50 microns.....	172
Figure 7.16: High magnification of 2328 CA1 iron arrow head microstructure, showing ferrite grains (light), pearlite (darker) and sulphide stringers (grey). Red bar represents 50 microns.....	173
Figure 7.17: Optical micrograph of 2328 CA1 iron spear head, showing mainly equiaxed ferrite grains (lighter) and irregular graphite (very dark). Bar represents 50 microns.....	174
Figure 7.18: Optical micrograph of 2328 CA1 iron spear head, showing ferrite grains (light) with graphite (dark).....	174
Figure 7.19: 2328 CA1 iron tang showing ferrite grains, needle like structure (arrow) and carbides, red bar equals 50 microns.....	175
Figure 7.20: 2328 CA1 iron tang, showing ferrite grains and carbides, red bar represents 50 microns.....	176

Figure 7.21: Slag 2328 CA1 (10) Road Test X/I/S SEM-BSE of a section through a slag fragment, showing a round hole with iron lining at the left hand side (dark), iron-aluminium silicate dendrites (light), iron-aluminium silicate needles (medium).....	178
Figure 8.1: Recalculated compositions of slag, plotted using FeO-SiO ₂ -Al ₂ O ₃ (Redrawn from Miller <i>et al.</i> 1995: Fig. 4).....	190
Figure 8.2: Iron artefacts plotted on the composition triangle for FeO-SiO ₂ -Al ₂ O ₃	193
Figure 8.3: Thaba Nkulu MgO (wt%) to CaO (wt%).....	201
Figure 8.4: Blakelock <i>et al.</i> (2009: 1750) MgO (wt%) to CaO (wt%).....	201
Figure 8.5: Thaba Nkulu MgO (wt%) to K ₂ O (wt%).....	202
Figure 8.6: Blakelock <i>et al.</i> (2009: 1750) MgO (wt%) to K ₂ O (wt%).....	202
Figure 8.7: Thaba Nkulu Al ₂ O ₃ (wt%) to SiO ₂ (wt%).....	203
Figure 8.8: Blakelock <i>et al.</i> (2009: 1750) Al ₂ O ₃ (wt%) to SiO ₂ (wt%).....	203
Figure 8.9: Various sites' slag, XRF analyses low proportion percentages (from Miller & Killick 2004) compared with Thaba Nkulu slag.....	209
Figure 8.10: Various sites' slag, XRF analyses higher proportion percentages (from Miller & Killick 2004) compared with Thaba Nkulu slag.....	210
Figure 8.11: Various sites slag, SEM-EDS analyses low proportion percentages (from Miller & Killick 2004) compared with Thaba Nkulu slag.....	211
Figure 8.12: Various sites slag, SEM-EDS analyses higher proportion percentages (from Miller & Killick 2004) compared with Thaba Nkulu slag.....	212

LIST OF TABLES

	PAGE
Table 2.1: Ten categories for metallurgical waste Miller and Killick (2004: 25-26).....	22
Table 4.1: Test pits and Spade test pit artefact summary.....	90
Table 4.2: Number of artefacts (slag and tuyère) and material culture (ceramics) recovered from each excavated square in excavation.....	90
Table 4.3: 2328 CA1 (2) Artefact breakdown.....	91
Table 4.4 2328 CA1 (10) artefact break down.....	92
Table 4.5: 2328 CA1 (3) and 2328 CA1 (4) artefact breakdown.....	92
Table 4.6: Road surface collection artefact breakdown.....	93
Table 4.7: Charcoal weights.....	106
Table 7.1: XRF slag results, low proportion percentages in wt%.....	134
Table 7.2: XRF slag results, higher proportion percentages in wt%.....	142
Table 7.3: XRF tuyère results, low proportion percentages in wt%.....	153
Table 7.4: XRF tuyère results, higher proportion percentages in wt%.....	153
Table 7.5: XRF ore results, low proportion percentages in wt%.....	157
Table 7.6: XRF ore results, high proportion percentages in wt%.....	158
Table 7.7: XRF iron artefacts results, low proportion percentages in wt%.....	162
Table 7.8: XRF iron artefacts results, higher proportion percentages in wt%....	162
Table 7.9: XRF copper artefacts results, low proportion percentages in wt%...	166
Table 7.10: XRF copper artefacts results, higher proportion percentages in wt%.....	166
Table 7.11: SEM-EDX slag results in wt%.....	179
Table 7.12: SEM-EDX tuyère and ore results in wt%.....	181
Table 7.13: SEM-EDX iron artefacts results in wt%.....	183
Table 7.14: SEM-EDX copper artefacts results in wt%.....	185
Table 8.1: Averages and standard deviations of slag samples.....	189
Table 8.2: Averages and standard deviations of slag and iron artefact samples.....	192
Table 8.3: Averages and standard deviations between tuyère and slag samples.....	196

Table 8.4: Averages and standard deviations between ore and
slag samples.....197

CHAPTER 1: INTRODUCTION

The study of archaeo-metallurgy traditionally focused on the identification of slag types, metal production, furnace designs and much more (e.g. Friede & Steel 1976; Miller & van der Merwe 1994a; Miller & Whitelaw 1994; Greenfield et al. 1997; Miller 2002; Miller & Killick 2004). A recent shift in focus, however, has led archaeo-metallurgy to concentrate on two main subjects: the sourcing of artefacts (e.g. Blakelock et al. 2009), and the identification of slag types (e.g. Miller & Killick 2004). These two shifts were, in part, the result of numerous debates concerning the Early Farming Community (EFC) period (pre – 1000 AD), and thus interpretations of events (cf. Maggs & Michael 1976; Maggs 1980a, 1980b, 1980c, 1993; Huffman 1982, 1990a, 1990b, 2000; Hall, S. 1981, 1985; Hall, M. 1984; Miller & Whitelaw 1994; Miller et al. 1995; Hall & Smith 2000; Miller 2002; Greenfield & Miller 2004; Miller & Killick 2004; Koursaris et al. 2007; Lyaya 2011).

Subsequent to the source linkage of tin leralé to Rooiberg (cf. Killick 1991; Grant 1994, 1999; Chirikure *et al.* 2010), archaeologists started to source other metallic alloys, such as those with iron (cf. Buchwald & Wivel 1998; Coustures *et al.* 2003; Blakelock *et al.* 2009). Unlike tin, however, iron is more common and can be produced over most of South Africa, and with this, a debate over sourcing iron artefacts began. As there is not yet a standard method for chemical signature analysis on artefacts, multiple experiments have been conducted (e.g. Buchwald & Wivel 1998; Coustures *et al.* 2003; Blakelock *et al.* 2009).

The most common techniques used for identifying chemical compositions, which are needed to identify a chemical signature, are X-ray Fluorescence Spectrometry (XRF) and Scanning Electron Microscopy coupled with Energy-Dispersive X-Ray Spectroscopy (SEM-EDX). In the past, however, this equipment was not easily available, or affordable. Today, these instruments have become more available, and with the ever-expanding development of instruments, it is possible to detect almost any element present in a sample. This made these two instruments ideal for achieving the aims of this project.

The second focus on slag identification came about due to a debate between Thomas Huffman (1980b, 1993) and Tim Maggs (1980a, 1992; 1994) which centred on the location of smelting areas in relation to the position of EFC settlements. This debate has led to research into slag type identification (cf. Miller & Killick 2004), settlement design identification (cf. Maggs 1973; Miller & Whitelaw 1994; Greenfield *et al.* 1997; Greenfield & Miller 2004), and metal production (Friede & Steel 1976; Miller & van der Merwe 1994a; Miller 2002), all of which would allow archaeologists to distinguish between smelting and smithing sites.

1.1: Research aims

This dissertation had two aims. The first was to identify a chemical signature for the metals and metal smelting, as well as smithing associated material culture found on site 2328 CA1 (Thaba Nkulu). Through the identification of a chemical signature, all metal artefacts and their associated production material culture could possibly be traced back to Thaba Nkulu. This data could aid in the identification of trade networks, and aid in understanding the complexity of metal production on EFC sites. This task, however, has had many challenges. The first setback was that, due to the fact that this field of study is relatively new, there is no standard for the identifying of chemical signatures in archaeology. The second problem faced was that all methods currently used are either being debated or the results have been incompatible (cf. Buchwald & Wivel 1998; Coustures *et al.* 2003; Blakelock *et al.* 2009).

The second aim of this dissertation was to engage in one of the most prominent debates on EFC metal production. This debate focuses on the spatial belief said to be implemented on EFC sites, in which smelting was viewed as a ritual and the symbolism behind it meant that smelting could not be performed within the homestead area. It has been suggested by Thomas Huffman (1980b, 1993) that smelting was performed away from the homestead in seclusion, whereas Tim Maggs (1980a, 1992; 1994) argued that this is not always the case. Through excavations performed on Thaba Nkulu and the analyses of materials and artefacts recovered, this dissertation engaged in this debate from Thaba Nkulu's perspective.

1.2: Thaba Nkulu

Thaba Nkulu is located in the northern Waterberg District Municipality of the Limpopo Province, South Africa (Figure 1.1). The Waterberg area contains dolomite hills in the north, which contain banded ironstone and ferruginous chert and is known as the Transvaal System, while a peculiar type of haematite found amongst overlapping layers of haematite and red dolomite can be found in the south (Bandama 2013: 56). This made the Waterberg region a source for metallic ores. This research follows on from a 2010 rescue excavation conducted at the site by Dr Alex Schoeman and Prof. Lyn Wadley. The purpose of their excavation was to remove ceramic pots exposed during the making of a dirt road on the property, as such little is known about the site. The excavation, however, yielded a metal artefact, as well as metal smelting and smithing associated material culture, which indicated possible EFC and LFC association to the area. This material and the possible EFC affiliation of the site and good state of preservation suggested that the research potential of the site was high.

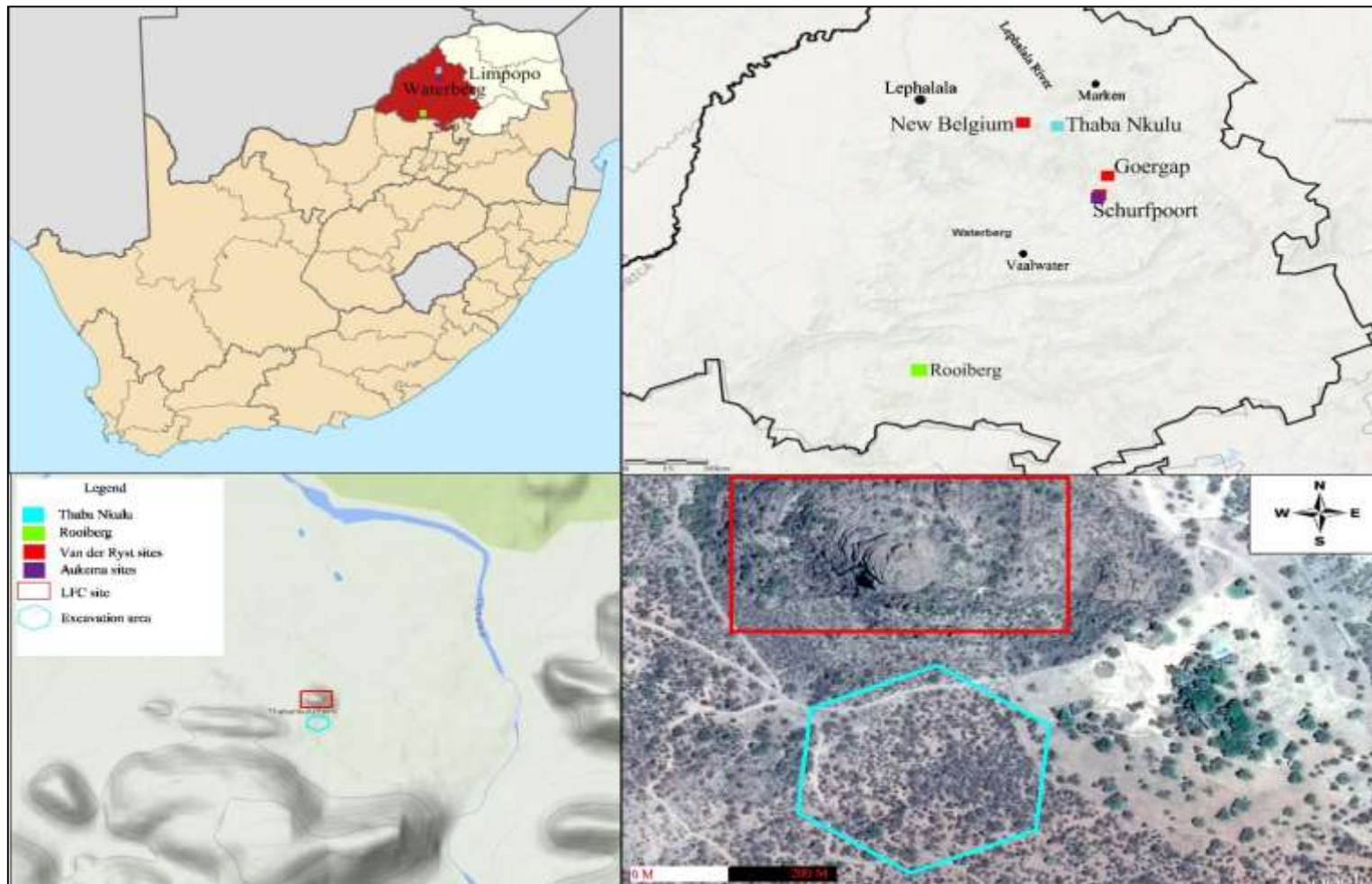


Figure 1.1: Map of the Waterberg region, showing various known sites and Thaba Nkulu (scale bar indicates 200m).

1.3: Organisation of the dissertation

This dissertation consists of archaeology (excavations and general artefacts) and metallurgy. Due to this, the chapters are split to reflect the different sections.

Following Chapter 1, the dissertation is organised as follows: Chapter 2 explores background information regarding the area where Thaba Nkulu is located. Next, the chapter deals with the history of archaeo-metallurgical research, with regard to both the spatial configuration debate and the history of chemical signature analysis.

Chapter 3 discusses the process and techniques used to excavate Thaba Nkulu, followed by the techniques and methods for storing and curating the artefacts recovered.

Chapter 4 presents the excavation results, as well as, artefact results.

Following this, Chapter 5 discusses the data and patterns in the data, relating to Thaba Nkulu, while locating these in the broader context.

Chapter 6 then proceeds to discuss the techniques and methods used to analyse the material recovered from the site, while focusing on the instruments used to record the chemical compositions of all artefacts subjected to chemical analyses.

Following this, Chapter 7 reveals the outcomes of the chemical composition analyses.

Chapter 8 deals with the discussion of the chemical composition results, and presents plausible chemical signatures for Thaba Nkulu's metal and metal smelting and smithing associated material culture.

The final chapter, Chapter 9, reflects on the outcomes of the project, and makes recommendations for future work.

CHAPTER 2: BACKGROUND

Introduction:

The first section of this chapter explores the history of the Waterberg region and surroundings, through focusing on known occupations, dates and material culture.

The second section discusses information pertaining to the EFC period, focusing in particular on metal production. It highlights the main points of the debate concerning the spatial configuration of smelting site location, relative to homesteads.

The final section discusses the archaeo-metallurgy, and the use of chemical signature and trace element analysis within the field of archaeology. This section overviews past usage of trace element analysis in archaeology, possible predictions, complications and techniques of this process.

2.1: Archaeology of the Waterberg

2.1.1: Introduction

Metal-based products have been produced in southern Africa since the first millennia AD (Miller 2002). This technology was introduced into the Waterberg region of South Africa by farming communities during the last two thousand years. The archaeology of the Waterberg area, however, extends deeper than the last two millennia AD (Van der Ryst 2007), and incorporates the Stone Age, Iron Age (Farming Communities) (Aukema 1989; Huffman 1990a; Van der Ryst 1998, 2007), and Historical Periods (Koursaris *et al.* 2007). Through exploring the different groups which occupied the area and the interactions and changes which occurred, one can examine how the social landscape of the Waterberg changed.

2.1.2: Hunter-gatherers of the Waterberg

The introduction of metal artefacts to the Waterberg region and the site of Thaba Nkulu specifically, must be understood in the context of interactions between the groups

which occupied the area. These encounters allowed for the development of a regional economy and changes within Farming Community settlements.

The Waterberg District Municipality was originally home to small groups of hunter-gatherers during the Later Stone Age (LSA). Evidence for their occupation is commonly found in rock shelters, rather than in open areas, due to the mobile settlement patterns of hunter-gatherers. Some rock shelters were often used by hunter-gatherer groups, and became imbued with ritual significance (Aukema 1989; Van der Ryst 1998, 2007).

The nearest known LSA sites to Thaba Nkulu hill are located on the farm New Belgium 608 LR, which forms part of the Thaba Nkulu reserve. New Belgium is located a few kilometres away from Thaba Nkulu (Figure 2.1). This site formed part of Van der Ryst's (1998) excavations along the Lephalala River on the Waterberg Plateau. Other sites were Schurfpoort and Goergap. These sites contained LSA artefacts, as well as material culture such as ceramics, which are traditionally associated with farming communities. Van der Ryst (1998, 2007) associated ceramics with farming communities, and suggested that they were either being brought in through trade or resulted from post hunter-gatherer occupations.

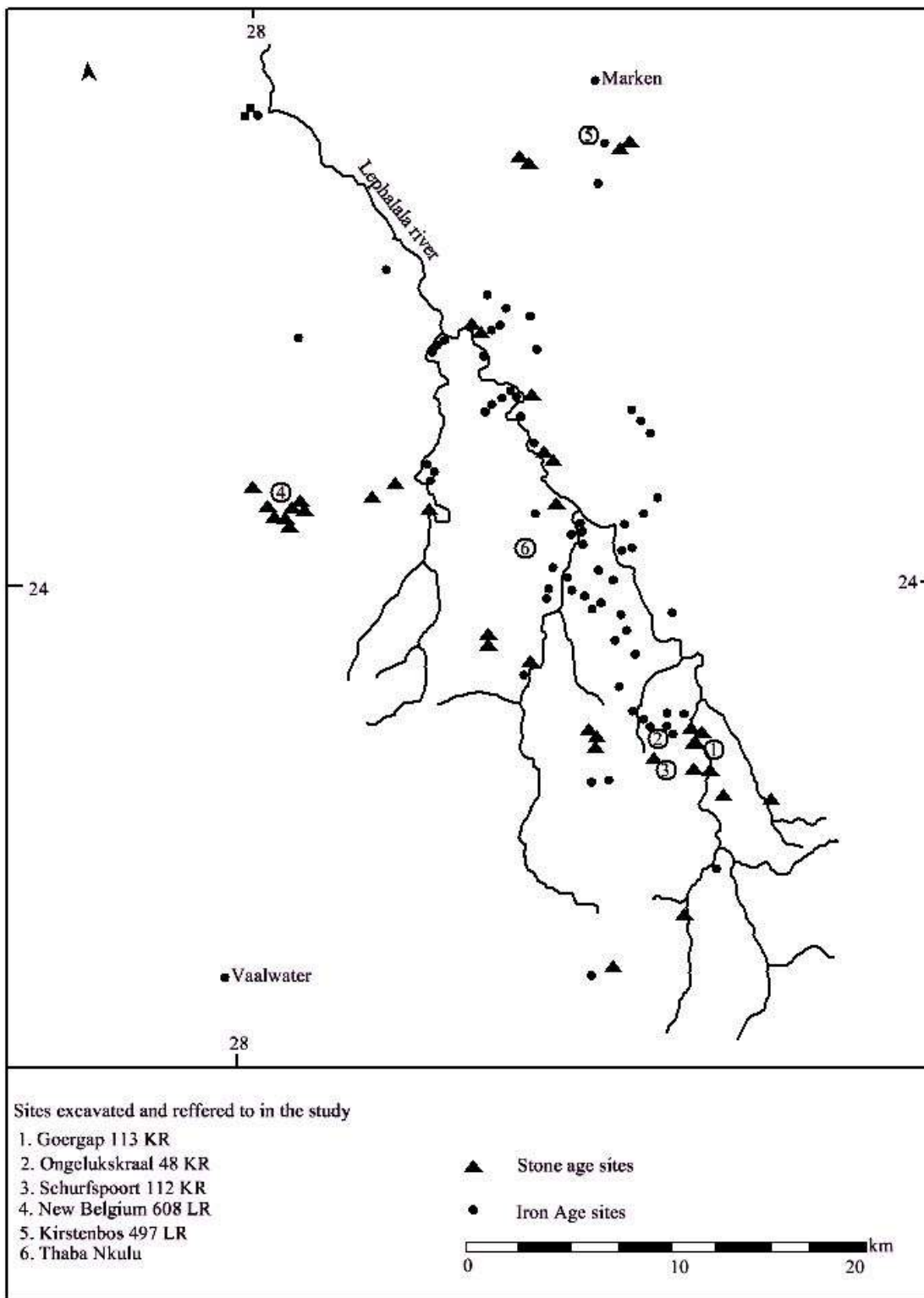


Figure 2.1: Map indicating known Stone Age and Farming Community sites near Thaba Nkulu. Adapted from Van der Ryst (1998: iv) to include Thaba Nkulu.

As New Belgium represents the nearest site to Thaba Nkulu, it can be used to construct an occupation sequence for the area. This sequence is particularly useful in a region where very little research has been conducted on open air farming community settlements. The excavations revealed not only Middle Stone Age (MSA) and LSA material, but also material culture such as pottery and glass beads. These are generally associated with farming communities. Unfortunately, due to contamination from past excavations in the lower level areas, the dates for early farming community occupations at New Belgium are problematic, levels 1 and 2 of 8, were dated (Van der Ryst 1998: 25-26). The dates obtained from level 2 were calibrated to 1663 AD, and 1532 AD for level 1.

Similar to New Belgium, Schurfpoot rock shelter (located within 20km south-east of Thaba Nkulu) revealed MSA and LSA material culture. Undecorated pots were found during the excavation, but no farming community associated material culture (Van der Ryst 1998: 26-27). Another shelter on the farm, however, studied by Aukema (1989) revealed farming community material culture. The LSA dates at Schurfpoot were around 1213 AD and 1291 AD.

Archaeologists developed two hypotheses to explain the presence of farming community artefacts in rock shelters. The first stated that rock shelters were used by farming communities as shelters during times of unrest. The second hypothesis suggested that the farmer artefacts were acquired by hunter-gatherers through trade (Aukema 1989:70). Jan Aukema (1989), however, found that there are additional explanations for the use of rock shelters. His research showed that rock shelters with little or no occupational debris were used by farmers for rain-making rituals, where evidence such as “clay pots, potsherds, grindstones, and in a number of shelters whole clay pots, buried up to their rims” (Aukema 1989: 70) were found. Rain-making rituals, however, were not only performed by farming communities, but by hunter-gatherers as well (Van der Ryst 1998:7).

Irrespective of the nature of the relationship, it is clear that hunter-gatherer and EFC groups interacted by the first millennium AD (Van der Ryst 1998; Hall & Smith 2000). With the continued development and expansion of farming communities, changes eventually occurred. During the period from AD 900 to AD 1270, the rise of hierarchical power and political structures caused new problems for hunter-gatherer societies (Hall & Smith 2000:30). By this time, most hunter-gatherer groups had entered into partnerships or other agreements within the farming communities who were occupying the same space (Van Doornum 2005). Eventually, these relationships changed, and the hunter-gatherer societies were forced to adapt and integrate into farming societies, or relocate. It was this displacement and forced change that created the initial destruction and removal of hunter-gatherer societies from the Waterberg region, and elsewhere within Southern Africa. Van der Ryst (1998) suggested that around the 14th Century AD, the disappearance of an independent hunter-gatherer identity in the region began. Hall and Smith (2000) equated the disappearance of hunter-gatherers in the Soutpansberg region to their integration into the farming communities. Historical records, however, suggest that there were still people of mixed Forager and Sotho descent groups living in the area as late as the 19th Century AD (Hall & Smith 2000: 44; Bradfield *et al.* 2009).

The changes are also spatially diverse, Van der Ryst's (1998, 2007) research shows that interactions between hunter-gatherers and EFCs began during the first millennium AD, and that population and land use expansion increased in the second millennium AD. The eastern side of the Waterberg, for example, was used by hunter-gatherers during the first millennium AD (Van der Ryst 1998). Only in the second millennium did hunter-gatherers and farming communities begin to intensively use the North Western part of the Waterberg (Van der Ryst 1998:17).

2.1.3: Farming communities of the Waterberg

Very little is known regarding EFCs in and around the Waterberg region, as only a handful of researchers have focused on the EFC period in and around the region (e.g.

Hall 1981; Hanisch 1981; Aukema 1989; Huffman 1990a; Boeyens & Küsel 1992; Miller *et al.* 1995; Van der Ryst 1998, 2007). Later Farming Community (LFC) archaeology in the Waterberg region has been researched more intensively, due to the identification of tin production and the rise of hierarchical societies in the north of the Limpopo Province (Friede & Steel 1976; Hall 1981; Killick 1991; Grant 1994, 1999; Miller & Hall 2008; Chirikure *et al.* 2010).

In general EFC sites were mainly located in river valleys (Maggs 1980a, 1980b; Greenfield & Miller 2004), unlike LFC settlements, which were built from stone and found on hills. This means that EFC sites are less visible. The possible forms of evidence are either the support structure holes or the remains of daga floors (Maggs 1980a: 133). The second form of possible evidence is the presence of artefacts, such as ceramics or beads.

Ceramics are the most common artefacts found on farming community sites (Sadr & Sampson 2006). It is also these ceramics which can help to distinguish between the different groups in an area (Calabrese 2005), through analysing decorative style, which can also provide information pertaining to occupation periods (e.g. Maggs 1980a; Huffman 1982; Hall 1984). These artefacts, however, were often traded and can also be present on LSA sites in areas where there are no EFC occupations (Boeyens & Küsel 1992; Van der Ryst 1998, 2006; Bandama 2013).

The presence of metal smelting and smithing informed the creation of the term “Iron Age”, and gives the identifying factor for the separation between hunter-gatherers and the EFC. The use of metallic-based artefacts, however, is not solely associated with EFC groups. For example, iron arrowheads have been used by hunter-gatherer groups in other areas (Wiesner 1983: 260). The use of iron arrowheads by hunter-gatherers during the EFC period, however, has not been confirmed. In general metal-based artefacts and their use have been mainly attributed to farming communities.

Where present, the smelting or smithing waste remains such as slag (molten silicates consisting of reduced iron, ore and other silica's (Figure 2.2) (Bandama *et al.* 2013), burnt clay, furnaces (Figure 2.3)/furnace lining and tuyère pipes (clay pipes used to funnel air into a furnace (Figure 2.4), are generally accepted as a by-product of farming communities (Maggs and Michael 1976; Maggs 1980a; Miller & Whitelaw 1994; Miller *et al.* 1995; Miller 2002; Miller & Killick 2004; Koursaris *et al.* 2007). As metal artefacts were produced by both EFC and LFC peoples, the mere existence of metal artefacts cannot identify the time period or associated people EFC or LFC, as multi-phase occupation can occur on farming community sites (Aukema 1989; Huffman 1990a). Through direct dating or the use of ceramic evidence, linked with a relative dating, metal associated material can be linked to either EFC or LFCs.



Figure 2.2: smelting slag from Miller & Killick (2004: 25).



Figure 2.3: Low shaft furnace from Chirikure *et al.* (2014: 297).



Figure 2.4: Tuyère pipes in a partially excavated furnace from Whitelaw (1991: 31).

Van der Ryst (1998) recovered Eiland ceramics. She stated “the earliest dates for hunter-gatherer LSA occupation of the Waterberg correspond with the Eiland phase of the early Iron Age” (Van der Ryst 1998:11). Jan Aukema’s (1988) preliminary unpublished report on the Waterberg Plateau, attributed the Eiland settlement phase to being the first EFC occupation in the region. In 1989, however, Jan Aukema amended this, stating that Eiland formed the third occupation phase (Aukema 1989), as earlier dates for occupation were found at the site of Diamant, which is located in the western part of the Waterberg District Municipality. When exactly farmers originally entered the Waterberg is still unknown. Earlier ceramic phases such as Happy Rest have been recorded in the Waterberg area (Van der Ryst 2007) and have been dated to roughly around 400 AD (Prinsloo 1974).

One of the earliest known dates for an EFC occupation in South Africa comes from the east of the Waterberg, in the Soutpansberg region of the Vhembe District of the Limpopo Province. This EFC site was dated to around AD 330 ± 45 (Pta 1168) and it is on this site that the ceramic style Happy Rest was first identified (Prinsloo 1974). In the western Waterberg area, EFC sites were discovered along the Motlhabatsi River (most probably derived from *motlhaba* = sand and *metsi* = water) and is the original (and current) Tswana name of the river, which was corrupted by early Europeans to the Matlabas River). These sites were first recorded by Aukema in 1989. The earliest site, Diamant, was dated to around AD 570 ± 50 (Prinsloo 1974) and around AD 600 (Hanisch 1981). The Diamant site had a second component dating to around AD 700 ± 45 and AD 710 ± 50 (Hall 1985). As these sites are situated to the east and west of Thaba Nkulu, it would be a reasonable assumption that the dates of initial occupation for the Thaba Nkulu area would fall within the first millennium AD.

Further north, near the Limpopo River, settlement structures containing Eiland ceramics were discovered and dated to around AD 990 ± 50 (Huffman 1990a: 117). Aukema (1989) suggested that the people living at Eiland settlements were probably the first EFC group to enter the northern Waterberg area. The shift to the northern areas

was been attributed to human factors. With early EFC cattle causing overgrazing and thus shrub development, the river valley areas, once tsetse fly free, now became infested. This in turn, forced the EFC groups to migrate further north to avoid endemic areas (Huffman 1990a: 117). The Eiland sites were amongst some of the last EFC settlements in the region (Boeyens & Küsel 1992).

Phase 2 settlements are marked by the arrival of LFCs and associated stone-walled sites, found on mountain tops. There are two groups of stone-walled settlements which appear in the Waterberg. The first contained undecorated ceramics and are associated with Northern Ndebele speakers, and date to around AD 1550 ± 70 and AD 1700 ± 50 (Boeyens and Küsel 1992; Huffman 1990a).

The second group arrived shortly after, and had a slightly different layout system from the Ndebele. In the Ndebele settlement structure, huts were placed at the back of the residential areas. Huffman (1990a:117) suggested that the "...undecorated pottery, hut type and back location indicates that these people were probably Nguni speakers". The second settlement structures' huts were placed in the middle of the settlement and are associated with Sotho-Tswana speakers (Huffman 1990a). Not only do these sites contain hut settlement patterns similar to Sotho-Tswana speakers, but they also have ceramics associated with them. The ceramic style is known as Moloko.

The earliest Moloko site, Icon, dating to the early 14th century is located in the nearby northern part of the Limpopo Province (Moore 1981). Moloko ceramics developed into a range of ceramics styles associated with Sotho-Tswana speakers. One of the first Moloko sites discovered in the Matlabas River area, Leamington 1, was dated to AD 1650 ± 40 (Huffman 1990a). As the dates begin after the arrival of the Nguni speakers, Boeyens and Küsel (1992) see this as the third occupation phase.

The Ndebele and the Sotho-Tswana both continued to occupy the Waterberg area until the historic period. Initially, it was thought that the Ndebele were living in the

Waterberg to control the tin trade between Rooiberg and Zimbabwe. Their settlements, however, also post-date the tin mining (Huffman 1990a:117-118). With the two groups occupying the same area, this could also have been the reason for the defensive formation (hilltop building) of Sotho-Tswana settlements to protect themselves against their Ndebele neighbours (Huffman 1990a: 118). The settlement of groups in the area was then further complicated during the 19th Century, as the *difaqane* forced large numbers of people to seek shelter in mountains (Huffman 1990a). After this, with the arrival of the colonialists, the Waterberg saw the decline of farming community traditions and practices, especially with regards to metal production (Koursaris *et al.* 2007).

2.2: Smelting vs. Smithing sites

2.2.1: Introduction

EFC metal smelting and working has been of great interest to archaeologists (e.g. Evers 1975; Avery & Schmidt 1979; Maggs 1980a, 1992; Huffman 1990b; Miller & Whitelaw 1994; Miller 2002, 2010; Miller & Killick 2004). Numerous research studies have attempted to understand the intricate workings of this period, both in terms of lifestyle and modes of production (e.g. Sandelowsky 1974; Evers 1975; Avery & Schmidt 1979; Friede 1979; Maggs 1980a, 1992; Mason 1982; Huffman 1990b; Miller & Whitelaw 1994; Miller 2002, 2010; Chirikure 2007; Miller & Hall 2008; Blakelock *et al.* 2009). One debate, however, has remained unresolved, and it pertains to the spatial relationship between EFC residential sites and smelting locations.

Before the debate argument can be discussed, it is imperative that the different terms used for metal working practices be explained. This is due to multiple terms being used to describe metal working/production, smelting, and smithing/forging, as well as, that these terms will be used consistently throughout this dissertation. The term metal working and/or metal production refer to the entire processes of creating metal products (Miller & Hall 2008; Bandama 2013). In some instances, however, the term “working

or iron-working” (e.g. Goucher 1981: 185-186; Whitelaw 1991: 37) is associated to the forging or smithing part of metal production.

The term smelting is used to describe the process of separating metals and non-metals from ore. During smelting, a bloom is created and it is on this bloom that metal smithing is performed. The terms metal forging and smithing refer to the post smelting production phase of metal working. In this phase, the bloom retrieved from the furnace is worked into a desired shape, or further refined to create a higher grade of metallic alloy, or in some instances repair a past creation (Delegorgue 1990; Maggs 1992).

2.2.2: Smelting and smithing

The spatial metal production debate centres on whether smelting was performed within the settlement area, as described by Maggs (1980a, 1992), or away from it in seclusion (due to ritual beliefs), as described by Huffman (1990b). The placement of a smelting area was further explored by other archaeologists (e.g. Miller & Whitelaw 1994; Miller 2002; Coustures *et al.* 2003; Greenfield & Miller 2004; Chirikure 2007; Lyaya 2011). The debate concerning spatial configuration plays an important role in understanding not only the metal smelting and working industry in the EFC, but also the complexities of belief and settlement organization. It is accepted that smithing was performed within the settlement, as it does not involve rituals which needed to be done in seclusion (Huffman 1990b).

One of the main reasons for the continuation of the debate is due to the lack of evidence for placement. Most of the evidence has either been destroyed (Miller 2002: 1100) or contextually, not all material for placement is available (cf. Miller & Whitelaw 1994 for lack of furnace argument; Miller & Killick 2004 context to link slag and material to smelting or smithing). A number of techniques have been developed to address this and other research questions (e.g. Coustures *et al.* 2003; Miller & Killick 2004; Blakelock *et al.* 2009; Chirikure *et al.* 2010). Due to this, archaeologists have tried to distinguish the difference between smelting and smithing sites. Smelting and smithing

sites have distinct differences in material, from furnaces to slags; each is an indicator of what was performed at the site (Miller 2010).

Some EFC sites such as Magogo, Mamba, Wosi, Ndongondwane, and even KwaGandaganda, have been interpreted as being EFC sites where smelting took place within the settlement area (Greenfield & Miller 2004). All of these sites, except for Ndongondwane however, have multi-period occupation or multiple occupations during a single period, and were interpreted as being contemporary, which may not have been the case (Greenfield & Miller 2004:1529-1530). At KwaGandaganda, it was argued that smelting had occurred in the settlement area as smelting slag evidence was present. Due to the lack of a furnace, the slag evidence can only support smelting nearby and not directly identify the smelting area, and as such, where smelting took place is still questioned (Miller & Whitelaw 1994: 82). As stated earlier, EFC homes were made from materials which were easily destroyed or were bio-degradable, and so might have perished, while new settlements were placed over older sites. In the case of Ndongondwane, however, evidence directly linked a furnace to the settlement area. In Ndongondwane, it was confirmed that smelting took place within the settlement due to the identification of slag and a furnace (Maggs 1984; Loubser 1993; Greenfield & Miller 2004: 1529).

The main debate over smelting and smithing, in archaeological terms, centres on spatial interpretations. Maggs (1980a, 1992) suggested that EFC smelting and smithing took place within or near the residential areas, whereas Huffman (1990b:7) stated that due to cultural beliefs, smelting was performed in seclusion away from the residential area. Maggs's argument is based on EFC data, and he argues that there is a possibility that EFCs' beliefs differed from those of the LFC. He (Maggs 1992) suggested that there is a definite shift in ritual behaviour and, that most LFC smelting sites were placed in secluded areas away from settlements.

Huffman's model of metal work is based on his understanding of "Bantu" ritual beliefs. Huffman (1990b) stated that smelting was associated with procreation, and as such, had to be performed in seclusion. Such beliefs have been recorded amongst Tswana speakers. Anderson (2009: 223) for example, suggested that the smelting areas were kept separate, and that smelting was done in seclusion, because they believed that smelting is "heat", and that heat is the source of all problems such as drought, illness, mishaps and death. He, however, noted that ethnography relating to Tswana iron production is scarce, and that his interpretation was drawn from ethnography of other areas, or other cultural domains not linked to metal working.

There is also a third approach which complicates the debate. In some cases, evidence has shown a combination of both debates (cf. Hall *et al.* 2006; Chirikure 2007). One such site is Marothodi in the Pilanesberg (an LFC site) which dates to the 19th century. Within the settlement area, iron smelting took place, although in order to follow the ritualistic belief, the smelting areas were walled, creating a sense of seclusion from the main settlement area (Hall *et al.* 2006: 29). A further example would be when the production of metal artefacts goes beyond the needs of a settlement. In the case of the LFC site Njanja, in Zimbabwe, women and children were required to participate in metal production, despite the belief system (Chirikure 2007: 81).

Smelting sites by definition are characterised by their function, which is the breaking down of ore in a furnace to produce metal which can subsequently be turned into artefacts. Smelting sites often contain large amounts of ash, slag and tuyère fragments, which were disposed of during or after the smelting process (Shinnie 1985; Miller 2002). In some cases, ore is stored in the vicinity of smelting sites, after having been collected from local deposits (Shinnie 1985). Although smelting can be performed in various ways, each smelt is different, as different metal elements melt into liquid at different temperatures (e.g. the melting point of pure iron is 1540°C) (Avery & Schmidt 1979). Research has shown that smelters were able to create iron blooms, using solid state reduction process at various temperatures, ranging from 1200°C to 1400°C and

maintain these temperatures during the smelting process (Friede 1979: 376; Miller *et al.* 1995:41), unlike European blast furnaces, which melted the ore and created what is known as cast/pig iron (Pleiner 2000; Pryce & Natapintu 2009: 251). Not only do the smelting temperatures vary, but the range of furnace types differs as well (Miller 2002).

Friede (1979:372, 375) states that in southern Africa, there were only two, or possibly three, furnace types. The first is the beehive or oval-shaped furnace (known as a low shaft furnace (Figure 2.3). This furnace is commonly found in Zimbabwe. The second type would be the *Venda furnace*, found mainly in the northern parts of South Africa (“eastern and north-eastern Transvaal”). The possible third furnace type is the *Melville Koppies* type furnace. Only one example of this type of furnace is known, making the third type the least used in South Africa. Newer studies, however, show that there was a fourth furnace type used in southern Africa, this type was the bowl type furnace and is found in both the Waterberg and KwaZulu-Natal (Maggs 1982; Crew 2001: 101; Bandama *et al.* 2013: 263; Chirikure & Bandama 2014: 299). This type is generally associated to belonging to Nguni speakers, and has been speculated to have been probably introduced to the Waterberg region, by Nguni-speaking people, however, there is too little research relating to the connection of furnace types to groups (Bandama *et al.* 2013: 248). The one thing all these furnaces have in common is that they are “all low-shaft furnaces, being bellows-blown and non-slag tapping” furnaces (Friede 1979: 372). Maggs (1992: 66) suggested that smelting sites can be identified by “large blocks of fired clay from the walls of furnaces, often showing vitrification on the inner surface, large quantities of slag including some of fist size or larger as well as iron ore”.

Along with the furnaces, there were tools such as ceramic pots or crucibles which were used to melt metal in, and ceramic shards which were used to remove excess waste from moulds or slag (Miller 2010). Unlike ceramic pots or crucibles, the ceramic shards can be used on both smelting and smithing sites.

Another type of ceramic artefact, commonly found on sites, is tuyère fragments. These fragments are found on both smelting and smithing sites, although more on smelting sites, as the tuyère pipes tended to break often. This is due to the tuyères being made from baked clay, which was not resilient to thermal shock, or in some cases, the clay contained trapped air which caused them to shatter. With the large temperature changes occurring in and around the furnace during smelting, the tuyères tended to shatter/break (Friede 1979: 376; Childs 2000:212)

Metal smithing sites may contain furnaces, which differ in use, such as to re-melt or heat up metal products. The main identifier of smithing sites are moulds, which are used to pour non-ferrous metals (e.g. tin, copper, bronze) into a mould to create a desired shape, although this casting technology only developed during the second millennium AD (Miller 2010: 45). Another indicator would be smithing tools such as anvils and hammers/hammer stones (Goucher 1981; Chirikure 2007), which are used in shaping moulded and re-heated metals to further desired shapes. Greenfield and Miller (2004) stated that metal forging sites are situated "close to hut floors in the middle of a settlement". A lot less slag is produced during metal smithing than during smelting (Maggs 1992). It, however, is difficult to directly link slag to the settlement areas, as multi-phase occupation often occur on sites, and new settlements can be placed on old furnaces or slag dumps (Greenfield & Miller 2004).

Miller and Killick (2004) created ten possible categories for metallurgical waste, and possible identifiers which belong to smelting, smithing or both. Table 2.1 summarises these ten categories.

Table 2.1: Ten categories for metallurgical waste Miller and Killick (2004: 25-26).

Type of metallurgical waste	Description of material	At Ndongondwane, cases of magnetism	Smelting or smithing association
Raw ore	Prepared ore in blocky pieces a few centimetres square	Ore was a mixture of magnetite and haematite, and was magnetic	None
Partially reduced ore	Partially reduced, slag-coated blocks	Strongly magnetic	Smelting
Smelting slag	Large chunks of only slightly vesicular slag		Smelting
Forge bases	Round oval buns of slag, palm-sized, and plano-convex in sections, with undulating upper surfaces showing fluid structures, and rough lower surfaces with impressions of numerous small charcoal fragments	Variably magnetic	Smithing
Tabular slag	Thin slag sheets, often with undulating upper surfaces and sandy bases	Tend to be less magnetic	Smithing
Frothy glassy slag	No identifiers, although tend to cluster around smithing forges	Non-magnetic	Smithing
Tuyère	Ceramics, sometimes with slag fused tips		Both, except if fused with slag, then smelting
Furnace lining	Overfired, bloated ceramic fragments with a slag coating		Smelting
Indeterminate slag	All slag, which could not be assigned with confidence to any of the above classes		
Iron bloom	Slag coated lumps of raw iron metal		

2.2.3: Archaeo-metallurgy in the spatial belief debate

Archaeo-metallurgy has contributed to the debate over spatial beliefs in farming community smithing and smelting practices, by seeking to use the products in determining their origin area in the production line (e.g. proving slag belongs to either a smelting area or a smithing area). This process, however, is difficult as the chemical composition of slag is fairly homogenous, and thus trace element analysis cannot distinguish these differences (Miller *et al.* 1995; Coustures *et al.* 2003: 600; Miller &

Killick 2004; Blakelock *et al.* 2009: 1752). The slags' physical appearances, however, can be inhomogeneous, and as such, can be distinguished from each other.

With regard to slags, archaeo-metallurgical research has aided in the possible identification of the differences between smelting and smithing slag (e.g. Miller & Whitelaw 1994). Some smelting slags contain partially reduced ore, which can be identified visibly with the naked eye (Greenfield & Miller 2004). These are associated with the smelting process, as smithing does not require further ore to be added. Conversely, smithing slag is identified through either being a *glassy slag* or *tabular slag*. These, however, are based on physical appearance, and in most cases this is not easily done due to some slags being able to form from both smelting and smithing.

As the *glassy slag* process can occur in both smelting and smithing, it is the non-magnetic *glassy slag* which is associated to smithing (Miller & Killick 2004; Greenfield & Miller 2004). *Tabular slag* is identified by its thin slag sheets or plate-like slag fragments, often with undulating upper surfaces, sandy bases and is often only slightly magnetic (Miller & Killick 2004: 26; Greenfield & Miller 2004: 1517). Further research in this field has shown that sometimes smithing can produce slag which is indistinguishable from smelting slag (Miller & Killick 2004). In situations such as these, trace element analysis is able to identify elements found within samples and give definitive evidence in support of this argument. By understanding the compositions of slag, one can determine whether it was smelting or smithing slag, based on what it contains and under what circumstances these occur (e.g. high melting temperature). Overall, one cannot simply assume or state where a piece of slag originated by sight alone; context and metallurgical studies are needed to affirmatively place slag into a smelting or smithing category (cf. Miller & Killick 2004).

2.3: Archaeo-metallurgy: Various metals and their trace elements

2.3.1: History of archaeo-metallurgical research in the Waterberg

A substantial amount of archaeo-metallurgical research in the Waterberg has focused on tin mining and production during the last millennium. Sotho-Tswana speakers produced and controlled the tin mining, smelting and production of artefacts during the sixteenth century (Hall 1981, 1985). This industry was centred on Rooiberg, located in the south western part of the Waterberg District Municipality (Friede & Steel 1976; Killick 1991; Grant 1994, 1999; Miller & Hall 2008; Chirikure *et al.* 2010). Rooiberg is located roughly 170-180 km from Thaba Nkulu.

The importance of the Rooiberg tin site stems from it being the only currently known archaeological tin source mined in pre-colonial South Africa (Hall 1981; Miller & Hall 2008). Studies, however, have shifted focus from the sourcing of tin, to expanding knowledge about production processes. These studies focused on the tin mining, smelting and smithing operations, and explaining settlement beliefs, culture, traditions, practices and settlement sequence were secondary (e.g. Miller & Hall 2008).

2.3.2: Various archaeo-metallurgy instruments, uses and discoveries

Tin is not the only important metal produced during the last two thousand years. Metallurgy has shown that multiple metallic ores have been mined and different metallic alloys have been worked since the first millennium AD (e.g. Stuiver & van der Merwe 1968; Mason 1974; Sandelowsky 1974; Friede 1979; Whitelaw 1991; Miller & van der Merwe 1994a). These include iron, copper, and bronze (rarely) (Grant 1994; Miller & Hall 2008), which were made into a variety of artefacts such as axes, bangles, beads, hoes, knives and spears (Krige 1936; Maggs 1991, 1992; Miller & Whitelaw 1994).

The use of metallurgy in archaeology is important, as this field of research allows not only for the recognition of groups through furnace identification (Robinson 1961; Friede & Steel 1985); but also facilitates the understanding of skill requirements in

metal production (Sandelowsky 1974). Through the use of element analysis, archaeologists can see the complexities required to alter mineral ore into a metallic alloy (Grant 1999). For example, by adding copper to tin, bronze is created (Grant 1999). Other areas of expertise are the addition of various metals to create a shorter slag time for metals with lower melting points, such as adding iron oxide to tin. These processes demonstrate skill and knowledge, as the over-addition of iron would create a substance known as hardhead (Grant 1994).

The process of identifying composition needs microscopy and an analytical technique. In most cases, the use of microscopy enables the identification of structures beyond the naked eye's capabilities. This research is called metallography, and is often complemented by element analysis (e.g. Miller 2002; Coustures *et al.* 2003; Miller & Killick 2004; Hall *et al.* 2006; Blakelock *et al.* 2009; Chirikure *et al.* 2010). One of the most commonly used instruments in modern microscopy is a scanning electron microscope (SEM) (Miller & Killick 2004; Koursaris *et al.* 2007; Blakelock *et al.* 2009). Coupled with *Energy-Dispersive X-Ray Spectroscopy* (EDX), this allows archaeologists to determine the elements which comprise their samples (Miller & Hall 2008). Another technique would be the use of X-Ray Fluorescence Spectrometry (XRF), which has proven successful in numerous studies (cf. Killick 1991; Grant 1994, 1999; Miller & Killick 2004; Chirikure *et al.* 2010). In some cases, multiple methods are used in order to identify trace elements on different substances/artefacts or similar substances/artefacts (Miller *et al.* 1995). As the Waterberg region contains multiple metallic elements: iron, copper, tin (Koursaris *et al.* 2007), and platinum (Environmental Management Framework for the Waterberg District 2010), researchers may need to use different equipment within the field of archaeo-metallurgy to record the elemental composition of artefacts.

Archaeologists can perform a variety of trace element analyses, in order to assess accurately the chemical signature of artefacts (Chirikure *et al.* 2010). For example, tin artefacts contain trace amounts of iron or copper, and in some cases, both elements

(Killick 1991; Grant 1999). The ratios vary between regions, allowing archaeologists to trace artefacts to their region of production (Buchwald & Wivel 1998; Coustures *et al.* 2003; Pollard *et al.* 2006: 5; Blakelock *et al.* 2009). The techniques and materials used in the smelting process create products that are unique to the smelters and/or location (Koursaris *et al.* 2007: 25), and the artefacts can be used to trace where the ore in the artefact or the artefact itself originates (Buchwald & Wivel 1998; Coustures *et al.* 2003; Blakelock *et al.* 2009).

Trace element research is not limited to identifying artefacts or metals. It has been used to explore ore quality, mining, smelting, final production and trade of metal based artefacts (cf. Killick 1991; Grant 1994, 1999; Chirikure *et al.* 2010). Due to the properties of metal-based artefacts, their chemical signature relates to their ore form, before it was smelted and made into an artefact (Killick 1991; Grigorova *et al.* 1998; Grant 1999).

2.3.3: Early theories on sourcing artefacts

Tracing the final product of the metal working process back to the sources has been the subject of numerous debates. On the one side, some archaeologists argue that the original chemical composition of ore is transferred to the slag during the smelting process (Buchwald & Wivel 1998; Crew 2000; Coustures *et al.* 2003). Elements that are preferentially concentrated in the liquid phase during melting and crystallization are termed incompatible, and are highly charged and are large-ion lithophile elements for iron (e.g. Rb, Sr, Ba, Zr and Th). Elements that are preferentially retained in residual solids (e.g. the bloom) during melting and extracted in the crystallizing solids, during fractional crystallization, are termed compatible (e.g. Cr, V, Mn and Ni). During the process of reduction and partial melting, the highly incompatible trace elements in slag will preserve the same ratios as in the initial ore samples (Coustures *et al.* 2003: 601-602). This allows the chemical signature to be traced from the slag to the ore and *vice versa*.

The assumption is that “for all the incompatible trace element pairs (e.g. Ba-Sr, Rb-Cs, Hf-Zr, Th-Zr, Th-Hf, Nb-Ta and La-Ce)” (Coustures *et al.* 2003), their ratios should remain the same throughout the smelting process, as their “ions have the same number of electrons and an equivalent ionic radius” (Coustures *et al.* 2003: 602). So when the ore and slag ratios are compared, their numbers should be linear on a correlation coefficient graph. During their analyses, Coustures *et al.* (2003: 608) noted that all the slags removed during the different parts of the smelting process maintained the chemical signature of the ore. Crew (2000) states that ore accounts for between 77.5% and 100% of the chemical signature of the slag. There will be some additives to the slag’s composition from ash or clay, although this is marginal (Coustures *et al.* 2003: 610).

With the possibility of being able to trace slag to ore, one further step would allow for the tracing of the complete production line. Final artefacts created from the bloom (post smelting) would have been hammered into a desired shape. During this process, slag left behind on the bloom would be incorporated into the artefact. These small amounts of slag are called slag inclusions (Coustures *et al.* 2003). By identifying the chemical composition of the overall artefact and focusing on these slag inclusions, the chemical composition of the slag should still remain, thus allowing a trace to be performed (Coustures *et al.* 2003; Blakelock *et al.* 2009).

Some archaeologists, such as Blakelock *et al.* (2009) and Miller and Killick (2004), have suggested an alternative view to tracing ore. They state that the different techniques, flux, controls, and temperature used within smelting can alter a chemical signature, make the composition untraceable if researchers’ do not have access to the full range of production material. Blakelock *et al.* (2009: 1745) admit that some of the impurities from the ore transmit to the slag during the smelting process. They go on to say, however, that changes do occur during smelting and post smelting, and these differences in the chemical compositions are caused by humans and not natural inclusions into the chemical composition of the final product (Blakelock *et al.* 2009:

1745). Furthermore, they state that studies which only focus on generic geological ores have not focused on comparing slags with the slag inclusions. All attempts to do this, however, are based on assumption and speculation (Blakelock *et al.* 2009: 1746).

Consequently, Blakelock *et al.* (2009) performed a controlled smelting experiment, from which possible links to provenancing artefacts, based on slag and slag inclusions, can be made. Using known substances (ore, charcoal and flux) and controlled techniques (fixed temperatures), three smelts were performed. From these, the respective changes in the materials' chemical compositions were recorded, between each stage in the production phases. Due to the knowledge of the smelt, influences and changes in the chemical makeup (ratios) could be recorded. Upon completion of the smelt, all materials involved were analysed for the non-reduced compounds found in slag inclusions. These were then compared in terms of four sets of ratios: MgO : CaO, MgO : K₂O, Al₂O₃ : SiO₂ and SiO₂ : MnO. When the results of all types of slag were compared on scatter plots, their type was identified through this ratio system. Originally the Al₂O₃ : SiO₂ was used to distinguish artefact and slag groups, although it was noted in this study that the comparison could lead to artefacts matching to slag from different sites. As such, Blakelock *et al.* (2009: 1756) argued that the MgO : K₂O and SiO₂ : MnO ratios should be used instead, as they show consistency between smelting slags and the slag inclusions.

Conclusions:

To date, most research in the Waterberg has focused on the LSA (cf. Boeyens & Küsel 1992; Van der Ryst 1998, 2007) and LFC occupations, as well as associated tin working sites. What little is known of the initial occupation and the EFC period is the result of Jan Aukema's (1989) research. Other archaeologists such as T. Huffman (1990a), J.C.A. Boeyens and M.M. Küsel (1992) have used Aukema's research to further understand the EFC sequence.

Through the use of archaeo-metallurgy, archaeologists have begun to explore new possibilities in understanding the complexities on EFC and LFC sites. Using these examples and methods, this dissertation aims to identify chemical signatures for the metal artefacts, and metal associated material culture recovered from Thaba Nkulu. The next chapter will deal with the techniques and methods used in this project to discover, identify, and present all the information and research needed to achieve the aims of this dissertation.

CHAPTER 3: ARCHAEOLOGY METHODOLOGY

Introduction:

This chapter is divided into two sections. Section one is the excavation section. It describes the techniques used to map the site, identify archaeological material culture, excavate, and store material relevant to this project. The second section deals with the laboratory work and describes how the material recovered was processed and analysed.

3.1: The excavations

3.1.1: The Area

The main objectives of the field work were, where possible, to determine the extent of the homestead, to identify possible smelting and/or smithing areas and their spatial position in the homestead. In order to understand the possible extent of the site, the 2010 rescue excavation location was used as a starting point (see Chapter 2 for details). From this earlier excavation, a foot survey of the surrounding area was performed, and an assessment of what was discovered was used to determine a starting point for the excavations. The sand over-burden and vegetation coverage hindered the visibility of obvious signs of occupation. As a result, and given the time constraints, a total of six areas were tested through excavations, and in some cases, test pits (Figure 3.1 for 2010 site location).

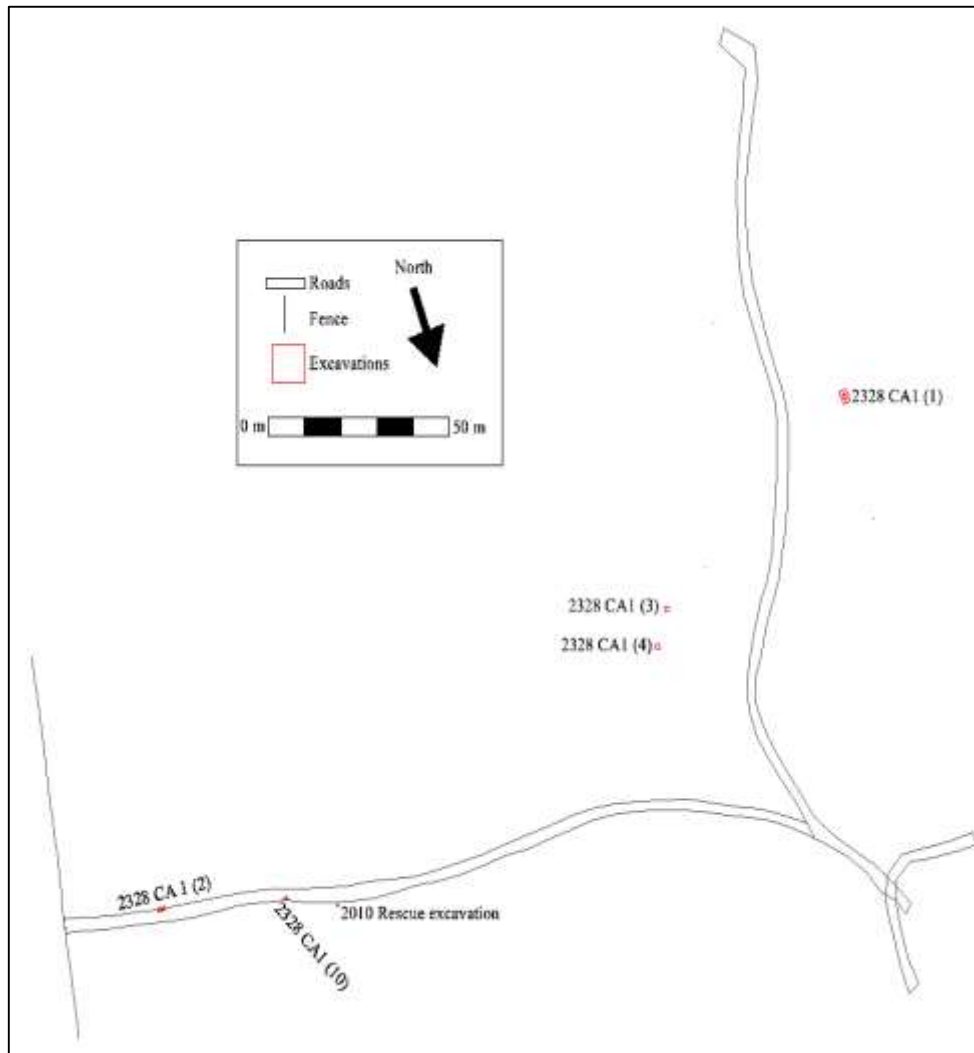


Figure 3.1: Excavation distribution on site 2328 CA1, including 2010 rescue excavation

3.1.2: Permit Application

The site was excavated under permit no. 189, issued by the South African Heritage and Resources Agency (SAHRA).

3.1.3: Mapping

Mapping aids in understanding the special relationships between various features on the site (David 2006). A hand held global positioning system (GPS) was used to map

Thaba Nkulu, during the initial foot survey. EFC artefacts such as ceramics, metal and metal associated material were recorded. Subsequently the site was mapped in detail with a Trimble Differential GPS R6 system (DGPS). Features, finds and excavations were plotted with the DGPS. A DGPS allowed for smaller margins of error than a GPS (Walter & Schultz 2013).

Due to the environment and season (late summer in February), physical field visibility was reduced. The tree cover at 2328 CA1 also formed an obstruction, which meant the manoeuvring of the DGPS device was limited and the accuracy would be slightly reduced.

The two forms of spatial data were later combined. This aided in the decisions of where to excavate, as well as where to dig test pits for possible homestead associated finds.

3.1.4: Excavations and test pits

A standard approach was followed for all excavations. When a possible excavation area had been identified, the area was cleared of vegetation by hand, using small tools such as secateurs (Edgeworth 2013). So as to not cause a major negative environmental impact on the site itself, only intended excavation areas were cleared. The clearing consisted of the removal of small grass and shrubs. Trees and larger vegetation were left untouched, except where small branches immediately affected the area.

Once an area was cleared, a grid was set up. Grid placement followed the methodology of Sir Mortimer Wheeler (1954). The grids were set up, varying in size, but always accounting for the size being equal to or less, than the site expected to be dug (cf. Higginbotham 1985). Once a potential area was discovered, and the grid's size determined, a north-south baseline was set up. Grids were labelled using Roman numerals (on the east to west lines) and alphabetical letters (along the north to south lines).

Excavations were then dug in 5cm spits, using trowels, and where necessary, geological pickaxes. The use of geological pickaxes was limited, in order to prevent destruction of artefacts. The 5cm spits were chosen for excavating (Balme & Paterson 2006:104). With the exception of excavations 2328 CA1 (3), 2328 CA1 (4) and 2328 CA1 (10), all other excavations followed 5 cm spits throughout. Excavations 2328 CA1 (3) and 2328 CA1 (4), started with 10cm spits, however, returned to 5cm spits after ~20-25cm following stratigraphic layers, whereas 2328 CA1 (10) was dug stratigraphically. All material recovered was sorted in sorting trays, and then stored. Excavations terminated at about ~50cm.

Test pits were used to explore potential excavation areas, or areas with the possible presence of material culture/cultural horizons. Test pits were either dug using a grid space, or using a spade. In the case of a grid test pit, a 50cm x 50cm grid was placed on sites that appeared to contain material culture, such as near the 2010 rescue excavation site. The spade test pits were dug to around 30-40cm in depth. These were dug to identify the extent of the site. When artefacts were discovered, they were mapped as test pits with artefacts, whereas the rest were marked as test pits. Material obtained from these pits was sieved and sorted.

Where possible, charcoal (dating samples) was collected *in situ* (cf. Holdaway 2006).

A sieve was used to separate material culture from the soil removed during excavation (cf. Huckleberry 2006). This project used a steel mosquito 1mm x 1mm grid. The grid size allowed for the retrieval of all farming community material culture, especially beads and seeds. All material culture would be collected in the sieve, which was then sorted on sorting trays.

Artefacts were placed into paper or plastic bags (depending on the artefact), which were labelled with the site name, the date when the soil was removed, grid and row letter, and finally the spit layer names. This ensured correct storage and allowed for accurate

recollection and management of the material recovered, as well as keeping them safe from degradation, breakage, and mixing with other deposits or stratigraphic layer artefacts (cf. O'Conner & Barrett 2006:274).

3.1.5: Problems found on site

All excavations faced shifting top sand. Since the site was occupied, large amounts of sand accumulated on the valley surface. In some areas, the sand was as deep as 20-40cm, and the implications of which could be the mixing of artefacts between stratified layers and the possible misinterpretation of artefact periods and ages (cf. Stockton 1973 regarding *in situ* artefact displacement). Where loose sand was discovered, possible artefact displacement was taken into account. It should be noted, however, that the sand on this site appeared to be sterile.

3.1.6: Excavation details

As this section describes the methods used to excavate each site, the details of excavation and stratigraphy are discussed in their respective chapters.

3.1.6.1: 2328 CA1 (1)

Excavation 2328 CA1 (1) consisted of a compressed slag + tuyère pit. It was discovered in an area where animal burrowing had brought material culture to the surface. Vegetation covered the area. Once the area was cleared, a 2m x 3m grid comprising 1m x 1m squares was set up.

The area was excavated in a checkerboard pattern. XIX/N and XX/O were chosen as the starting points for the excavation, followed later by XX/M. It was noted that the excavation was on a slope with the XIX row being the highest point. In order to dig in 5cm spits, datum points were created on the north-facing line of the squares.

3.1.6.2: 2328 CA1 (2)

A grey patch of soil marked the second excavation area. The grey patch suggested the presence of ash or dung, and could assist in the understanding of the site layout.

The sandy surface was uneven and not much vegetation was present. A 2m x 2m grid comprising 1m x 1m squares was placed over the area. The north–south line was labelled alphabetically from E and the east–west squares were identified by Roman numerals starting with XIII. The holes dug were XIII/E, XIII/F and XIV/F. Grids XIII/E and XIV/F, however, were discontinued as the grey soil became concentrated in grid XIII/F.

As the site was on an incline, the highest point of the excavation - the most westerly row - was chosen as the base line.

3.1.6.3: 2328 CA1 (3)

During the field survey, a large patch/area of grass, unlike most of the savannah grass type seen in the area. This new grass type was localized amongst the shrubveld, east of excavation 2328 CA1 (1). The area contained a substantial amount of ceramic sherds, which had been brought to the surface by animal burrowing. With the hopes that the grass might be linked to a possible cattle kraal as seen by Denbow (1979) and Jorge *et al.* (2008), two test pits were excavated in this area: Test pit 4 near a large baobab tree and Test pit 5 just east of the animal hole. The test pits were excavated in a 50cm x 50cm grid, and 10cm spits. At a depth of approximately 30cm, an occupation layer was uncovered.

Consequently, additional 1m x 1m squares were opened. One was directly next to the test pit 4 2328 CA1 (3), and one was next to test pit 5 2328 CA1 (4). Excavation 2328 CA1 (3) was given a label of X/A, while excavation 2328 CA1 (4) was labelled as XX/J.

3.1.6.4: 2328 CA1 (4)

This excavation was located approximately 5m north of excavation 2328 CA 1 (3). It was hoped that the residential material extended to the area. The excavation square was a 1m x 1m grid, and was placed next to Test pit 5. The square was excavated to ~45cm.

3.1.6.5: 2328 CA1 (10)

2328 CA1 (10) was an excavation consisting of three individual 50cm x 50cm grids. The first grid was labelled as X/I and was excavated due to the possible recovery of human remains, as it was near the location of the pot burial (cf. Boeyens *et al.* 2009, regarding burial pots) recovered by Schoeman and Wadley in 2010. It was a shallow excavation of approximately 10cm, although once it was discovered that the bones were of an animal origin, excavation stopped. The second grid was placed north of the X/I excavation and was excavated to retrieve a ≤ 20 cm long tuyère which was protruding from the surface. An additional 50cm x 50cm grid was placed, due to the discovery of a pit. The two grids were labelled VIII/G and IX/G respectively.

Once all excavations were complete, all the trenches and test pits were backfilled.

3.2: Storage and management of artefacts

3.2.1: Main artefacts

The artefacts collected were sorted into primary artefacts and secondary artefacts. The primary artefacts were materials directly associated with this research, whereas the secondary artefacts were those collected during the excavation that did not directly relate to the current research. The primary artefacts collected consisted of slag, tuyère, ore, metal-based artefacts, ceramics and charcoal. The methods used to store and record these artefacts were all similar.

The first components of the material culture were the slag, tuyère fragments and ore. All the slag and tuyère pieces were counted and placed into separate bags. The slag

was weighed. The total number of slag fragments and weight of the slag was recorded. For the recording of ore, just the presence of ore was noted.

All the ceramics were dipped in water and the outside surface of the ceramics were scrubbed with a tooth brush. This ensured that decoration was visible. Sherds had a white line painted on the inside, with a white alkaline paint, and on this paint the excavation, grid and layer where the sherd was retrieved was written. The ceramics were then classified, focussing on where on the pot they came from, rim, neck/shoulder or body. Once they were sorted by position, they were checked for thickness; any ceramic with a thickness of over 10mm was considered thick, while less was considered thin (cf. Sadr & Sampson 2006). Along with the thickness, any decoration was noted, and distinctive decoration would aid in the identification. If the decoration was identified, its style was recorded, which would aid in context and relative dating of the ceramic (cf. Huffman 2007 for ceramic styles relating to the Farming Community period). Once each ceramic sherd was recorded, the ceramics were placed in plastic bags and separated by category (e.g. decoration, sherd type (rim, neck), thin or thick).

Lastly, charcoal was examined. Dating charcoal recovered during excavation was removed *in situ* with tweezers to prevent contamination. Once it was removed, it was placed into tin foil and then placed into small plastic containers. Charcoal that was selected to be dated was stored in a plastic zip-lock bag and placed in a plastic container, with the relevant identification labels inside and outside the container. Charcoal found in the excavation bags during the sorting of slag, tuyère, ore and ceramics was discarded.

3.2.2: Secondary artefacts

The secondary artefacts consisted of bone, stone, seeds, beads, orange-coloured rock/daga and baked sand. The bulk of these were recorded as being present and separated into individual plastic zip-lock bags. Faunal remains were placed into paper bags to prevent moisture build up. All other material culture items were individually

placed into bags and recorded. Stones and baked sand, however, were bagged together. All artefacts were then placed back into their original excavation site bags, and were stored in cardboard boxes at the University of the Witwatersrand in the Archaeology Department.

Conclusions:

All the methods used in the field enabled the discovery of artefacts, and through a set of standardised techniques, artefacts were recovered, analysed and stored. The results obtained through these methods are discussed in the next chapter.

CHAPTER 4: ARCHAEOLOGY RESULTS

Introduction:

Using the techniques described in Chapter 3, this project explored the spatial configuration of metal working in relation to residential space at Thaba Nkulu. In this chapter, the results of the field and laboratory research are presented. It then reports on the discoveries made on the site, focussing on the five excavation areas which were identified through the techniques and methods discussed in the previous chapter. Following this, it reports on recovered material culture.

4.1: Site Results

4.1.1: The site of 2328 CA1

The surface of Thaba Nkulu (2328 CA1) (Figure 4.1) was littered with archaeological artefacts and material culture (Figure 4.2). The eastern section of the road surface (left middle section of Figure 4.2) contained the majority of artefacts, ranging from ceramics to slag. Figure 4.2 shows concentrations of ceramic sherds and slag, by representing both those found in clusters and those in wash lines. The majority of ceramic sherds were found in the road, where sherds were eroding out of pits. Slag was recorded where found in a cluster, or as individual pieces being larger than 5cm.

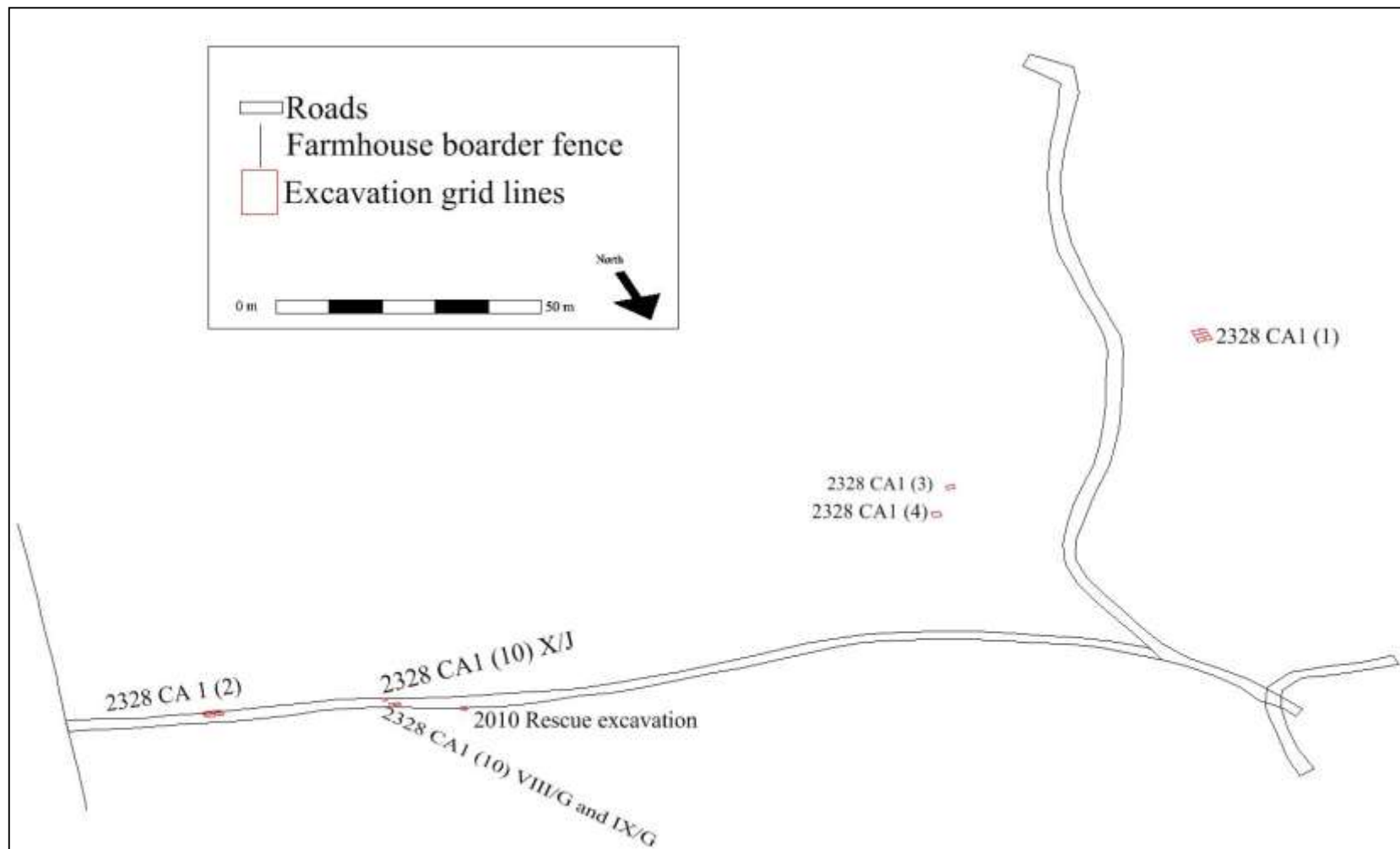


Figure 4.1: Locations of excavations on site 2328CA1, including the 2010 rescue excavations.

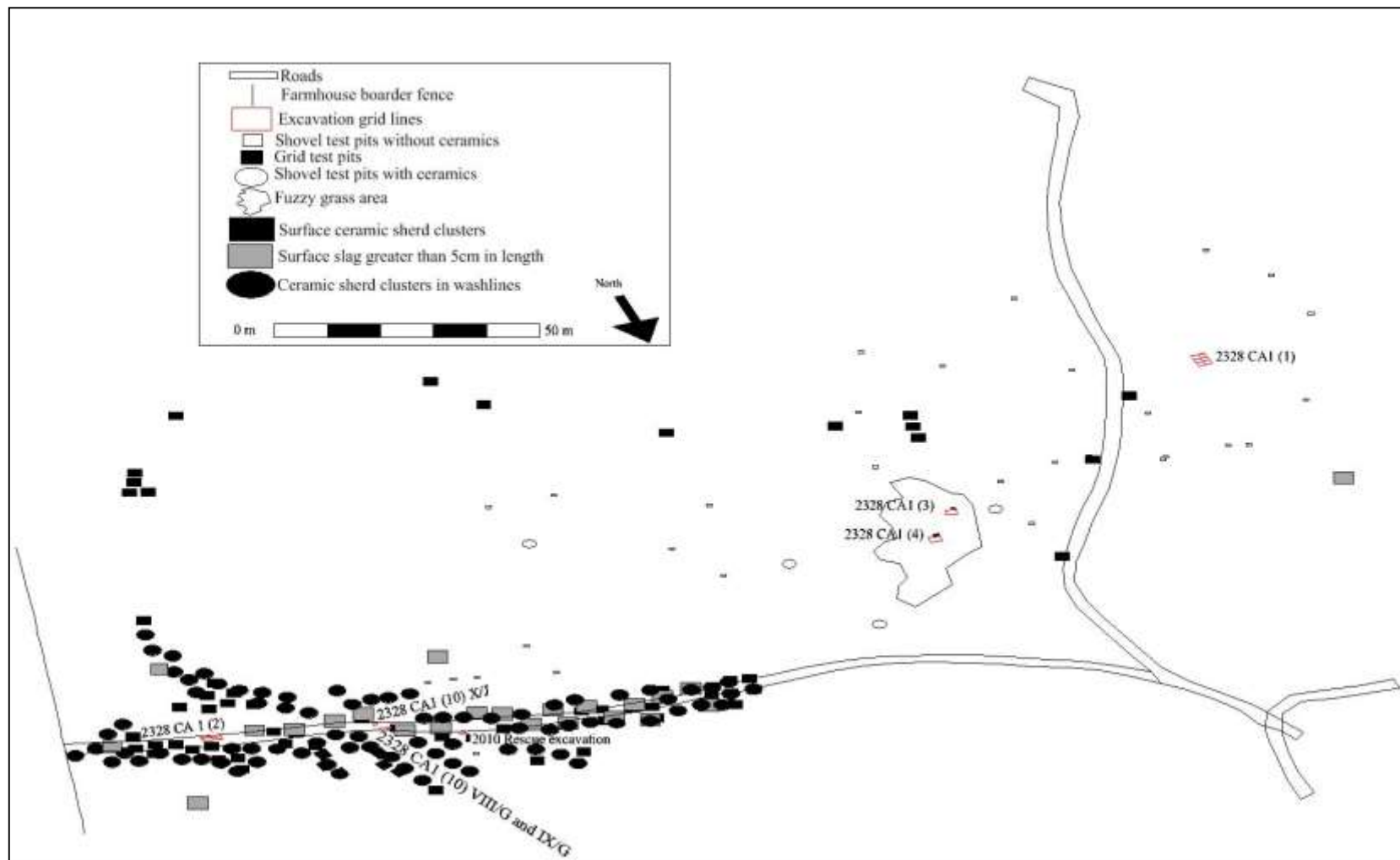


Figure 4.2: The 2328 CA1 site, with relevant archaeological information.

4.1.2: 2328 CA1 Shovel Test Pits

Shovel test pits were used to try and establish the extent of the site (Figure 4.3). Through both excavation and spade test pits, holes were dug near excavation sites, as well as in the open areas. Figure 4.4 shows the grid test pit excavation style. In addition to the grid style pits, 40 spade test pits (free dig) were dug. Figure 4.5 displays the free dig distribution.

All pits were checked for artefacts, and where present, the pit was marked, and mapped (Figure 4.3). Figures 4.6 and 4.7 show an EFC (Diamant style) ceramic found in one of the shovel test pits.

The stratigraphy in the tests pits was largely uniform, with 30cm to 40cm sterile sand (without artefacts) overlaying the cultural layers. When ceramics were discovered in the spade test pits, the hole was marked, in order to see the extent of the possible occupation area.

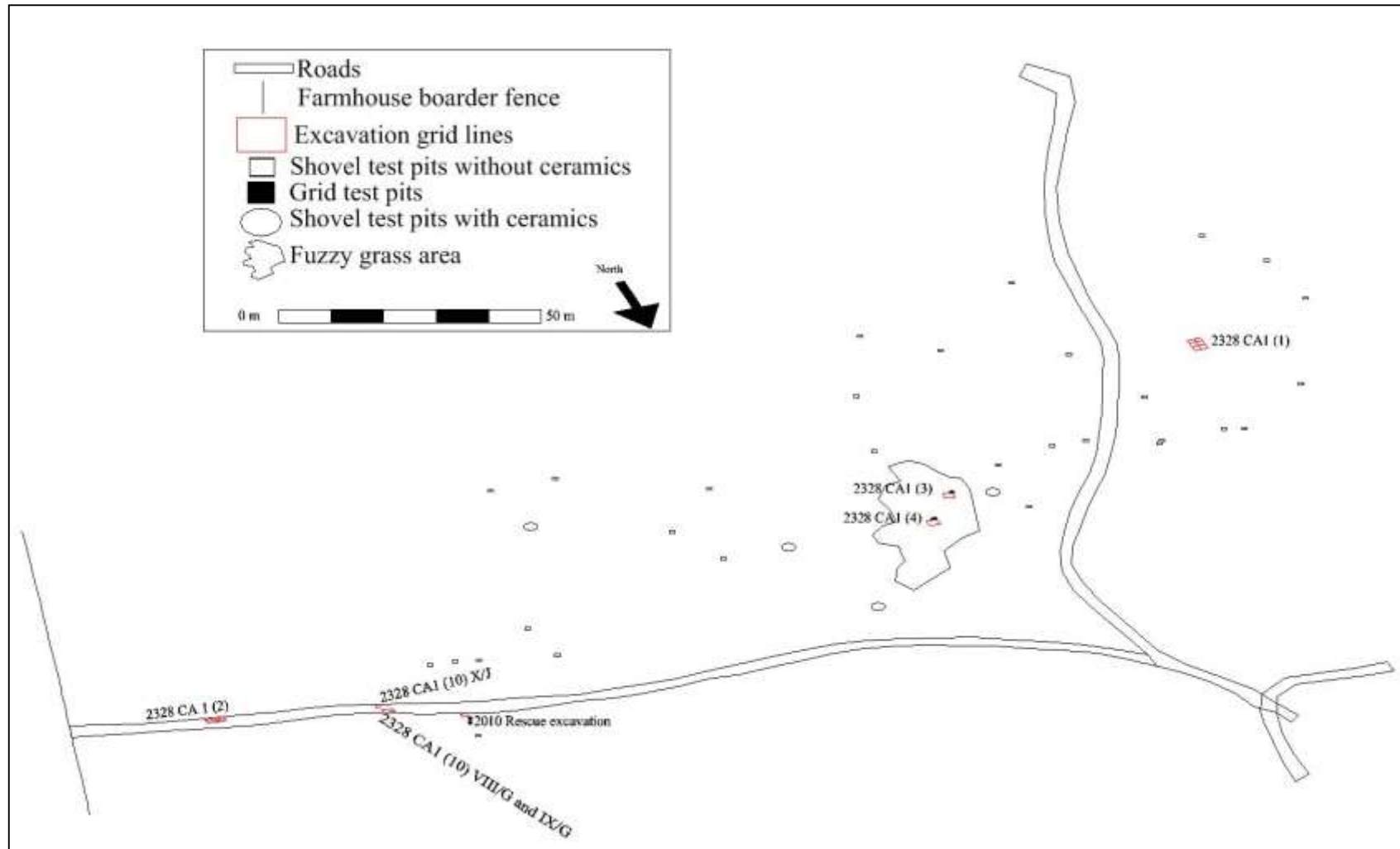


Figure 4.3: Test pits and shovel test pit locations.



Figure 4.4: Grid test pit 50cm x 50cm x ~40cm.



Figure 4.5: Shovel test pit, dug to a depth of ~40cm.



Figure 4.6: Shovel test pit with ceramic fragment.



Figure 4.7: Ceramic with Diamant decoration, found in shovel test pit hole.

4.1.3: Excavation 2328 CA1 (1)

The excavation 2328 CA1 (1) was dug, due to the presence of metal associated material culture found scattered on the surface. Figure 4.8 shows a slag covered tuyère, which was just one of numerous pieces found on the surface. As previously discussed in Chapter 3, a 2m x 3m grid was placed over the site and a checkerboard excavation began. Figure 4.9 displays the checker board pattern (used for excavating) and Figure 4.10 displays the excavation grid on the site map.



Figure 4.8: Tuyère submersed in slag on surface of 2328 CA1 (1).



Figure 4.9: 2328 CA1 (1) excavation.

Through this checkerboard pattern, the extent of the site could be covered. The three independent holes seen in Figure 4.9 represent the excavation points, XX/M (right hand side), XIX/N (far back, centre) and XX/O (left hand side). In excavation order, XIX/N was the first excavation square dug, followed by XX/O and then XX/M. Squares XIX/N and XX/O were shallow excavations, as they both were stopped at the first initial slag and tuyère layer, whereas XX/M went beyond this, to find the base layer of the slag and tuyère together.

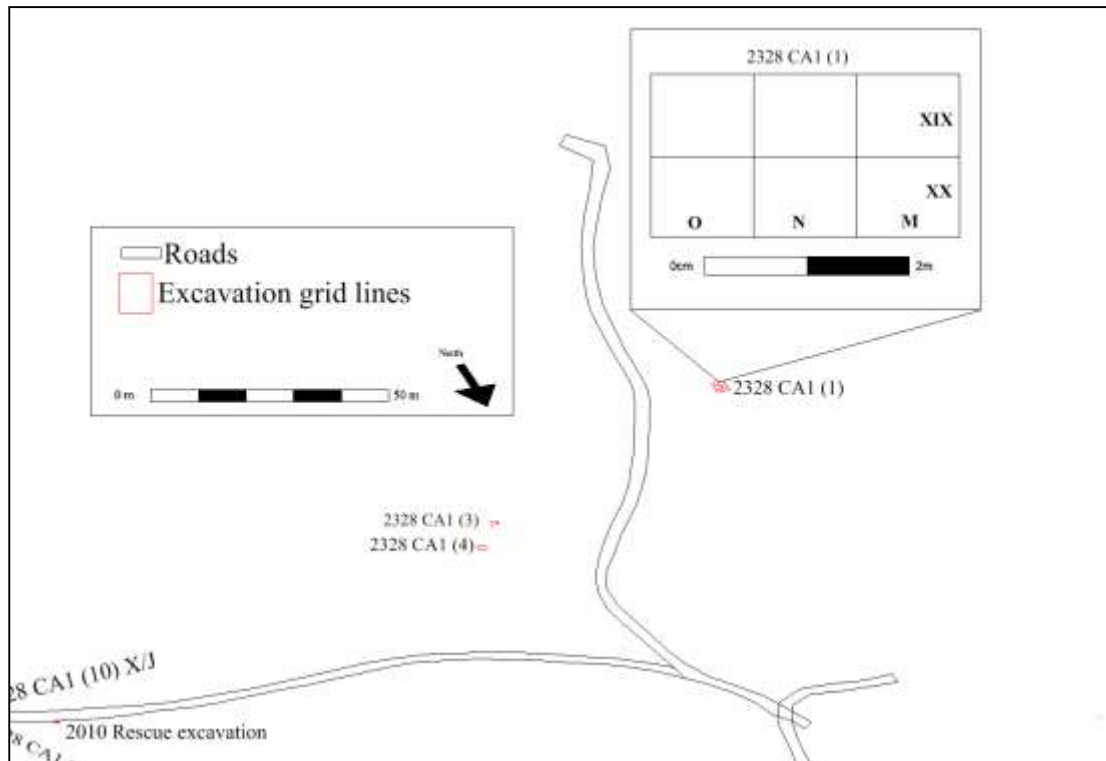


Figure 4.10: Excavation 2328 CA1 (1) location, with zoomed in grid layout.

4.1.4: Excavation 2328 CA1 (1) stratigraphy

4.1.4.1: XIX/N

Square XIX/N aided in understanding the extent of metal working debris. Although the square contained a tree and an animal hole, it was dug because it was the likely source of the scattered surface artefacts.

4.1.4.1.1: XIX/N/S

The surface layer of square XIX/N comprised loose sand, with a small tree in the grid area (Figure 4.12). On the surface, smelting and smithing associated material culture could be seen. The material on the surface was dug up from a small animal hole described in Chapter 3, displayed in Figures 4.11, and 4.12.

4.1.4.1.2: XIX/N/AD

The first level of XIX/N was labelled AD for Animal Disturbance. Due to the animal disturbance, the stratigraphy of the layer was compromised (with surface and subsurface mixing). The most disturbed section of the square was the west facing wall side, as behind it was a shrub (Figure 4.13). Animal diggings also compromised the north facing wall (Figure 4.11). In front of this was a tree (Figure 4.12). The shrub's root dispersal affected the south and west facing wall corners (seen in Figures 4.13 and 4.14).

4.1.4.1.3: XIX/N/2A

Layer 2A began revealing the small tuyère and slag pieces. The pieces were similar to those found on the surface layer, possibly the source of the surface material. The square's surface at spit 2A was covered in a collection of slag and tuyère. The layer consisted of a brown soil, with slight grey tints (Figures 4.13 to 4.14), the colour of which was attributed to the ash that came with the slag. The surface layer of the slag and tuyère was lifted, revealing that it continued further down.

4.1.4.1.4: XIX/N/2B

Square XIX/N's purpose was to determine the extent of the metal working debris, and as it revealed a surface layer of artefacts early on, this was the last layer dug of XIX/N. The layer comprised grey/red brown soil, which was consistent with the surface soil and the slag and tuyère layer. The indication of large slag and tuyère finds in this level corresponded to what was found subsequently in XX/O.

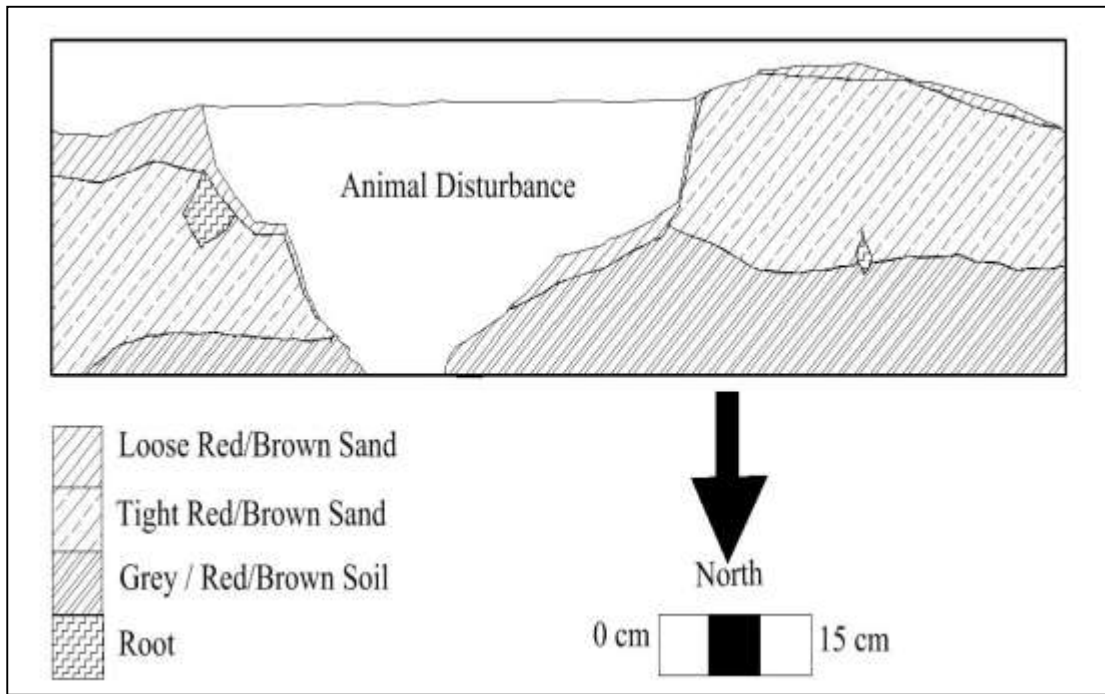


Figure 4.11: 2328 CA1 (1) XIX/N North facing wall stratigraphy.



Figure 4.12: 2328 CA1 (1) XIX/N, base layer (with tree and animal hole).

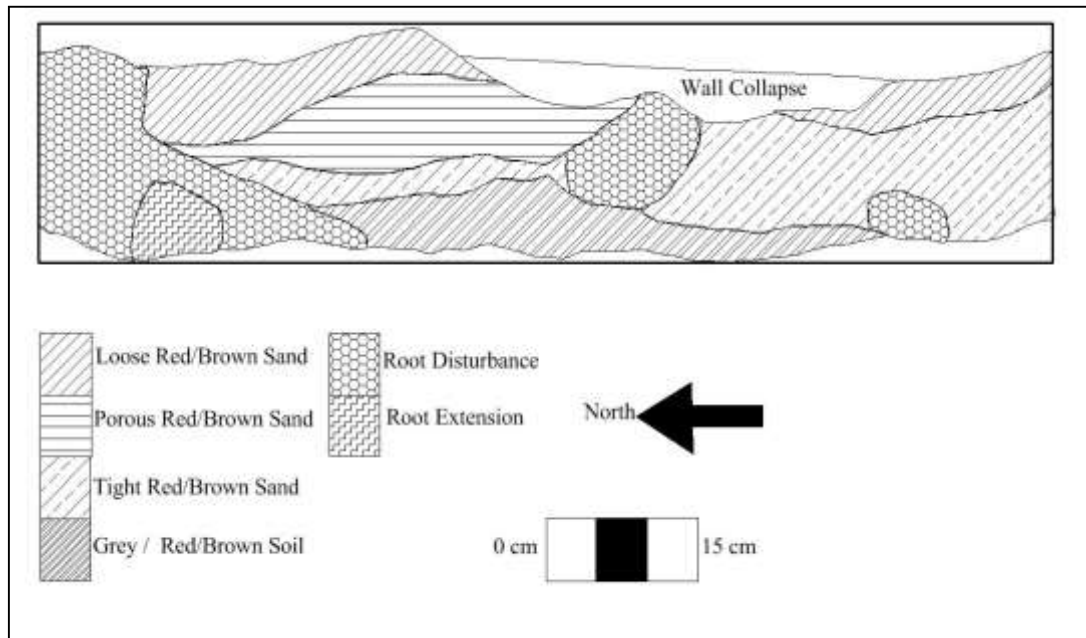


Figure 4.13: 2328 CA1 (1) XIX/N West facing wall stratigraphy.

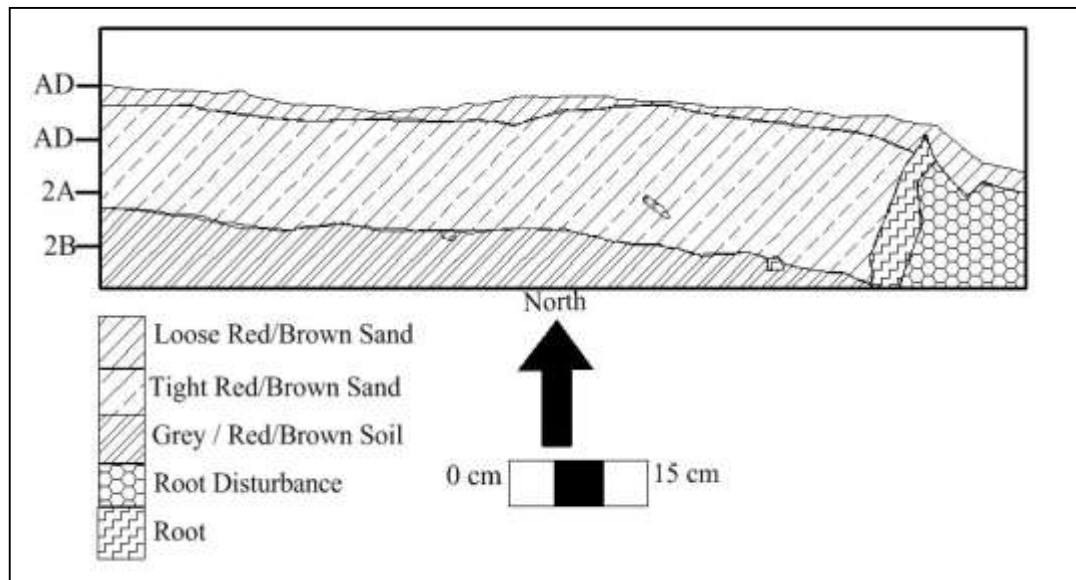


Figure 4.14: 2328 CA1 (1) XIX/N South facing wall stratigraphy, with layer indicators.

4.1.4.2: XX/O

Square XX/O represents the furthest square on the grid, and its purpose for excavation was the same as the first square (XIX/N), to understand the extent of the metal working debris. Due to a slope, however, the excavation reached the slag and tuyère layer at a shallower point than XIX/N; the slope incline is indicated in Figure 4.15.

4.1.4.2.1: XX/O/S

The surface layer of square XX/O contained small shrubs and grass. The ground was sloped, which meant that there was less loose top sand than in the other squares in this excavation. This square also contained very little surface finds.

4.1.4.2.2: XX/O/AD

Due to the contamination of archaeological material in this square, the first 5cm spit of square XX/O was labelled as animal disturbance (AD). The first 5cm spit consisted of loose red/brown sand. Figure 4.16 displays the mixing of soils on the east facing wall. This disturbance was due to a separate animal hole dug from XX/N (a non-excavated square) into XIX/N. Although the animal hole did not appear in square XX/O, its east wall was slightly contaminated. With the incline of the square's surface, very little sand was removed before the 5cm mark was reached. The slope and height of square XX/O are shown in Figure 4.15.

4.1.4.2.3: XX/O/1B

By this layer, the soil shifted from compact red/brown sand, to a red/grey soil, shown in Figures 4.17 and 4.18. The base of the layer started being covered in slag and tuyère fragments. The same effect was seen in square XIX/N, which meant that it was possible that the entire 3m x 2m grid could have the same layering. It was at this point that the decision to open square XX/M was made, to ascertain if this was the case.

4.1.4.2.4: XX/O/2A

As with XIX/N, by this layer the surface became fully enveloped in slag and tuyère fragments (Figures 4.16 and 4.18). The slag and tuyère layer was dug into for another 5cm. Ceramics sherds were discovered amongst the slag and tuyère. Their association with the slag and tuyère, however, is not understood (possibly containers for food or water, or another possibility is a container for “muti” (medicine) for the smelting process (cf. Schmidt 2009: 271)). The soil remained the compact red/grey soil, as the depth increased.

4.1.4.2.5: XX/O/2B

With the opening up of XX/M, it was decided that XX/O should be levelled off and that square XX/M would be dug to the base of the slag and tuyère. Therefore, 2B was the final spit dug in square XX/O. The last layer was dug 5cm into the slag and tuyère, however, the artefacts in layer remained densely distributed (Figure 4.18), showing the possible extent of artefact density on this excavation.

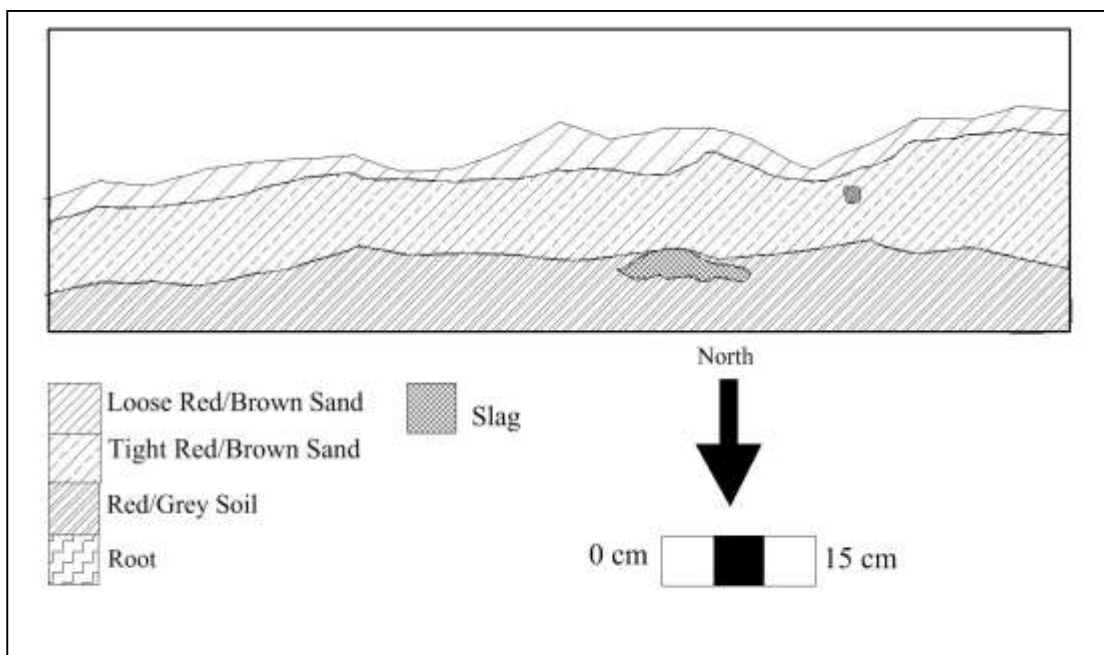


Figure 4.15: 2328 CA1 (1) XX/O North facing wall stratigraphy.

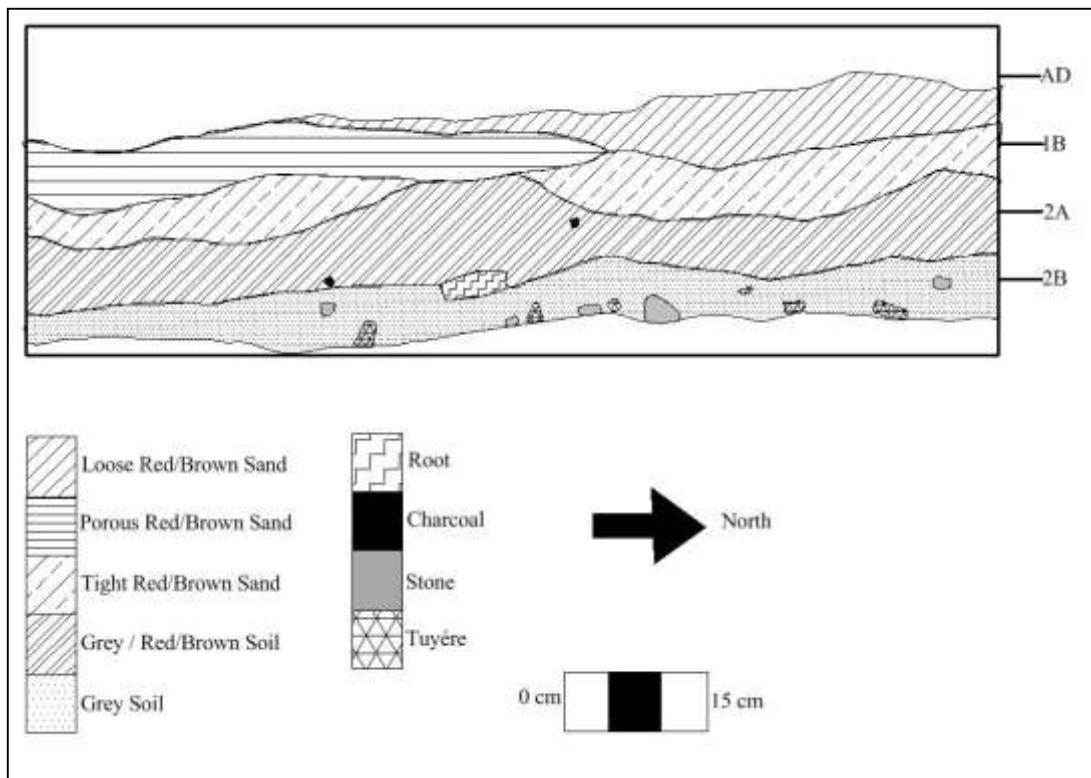


Figure 4.16: 2328 CA1 (1) XX/O East facing wall stratigraphy, with layer indicators.

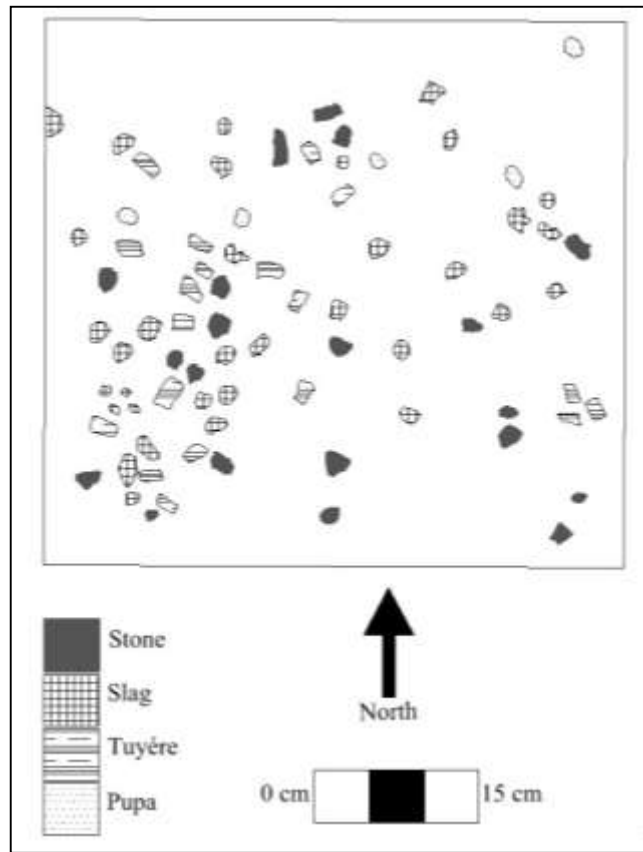


Figure 4.17: 2328 CA1 (1) XX/O Plan view.

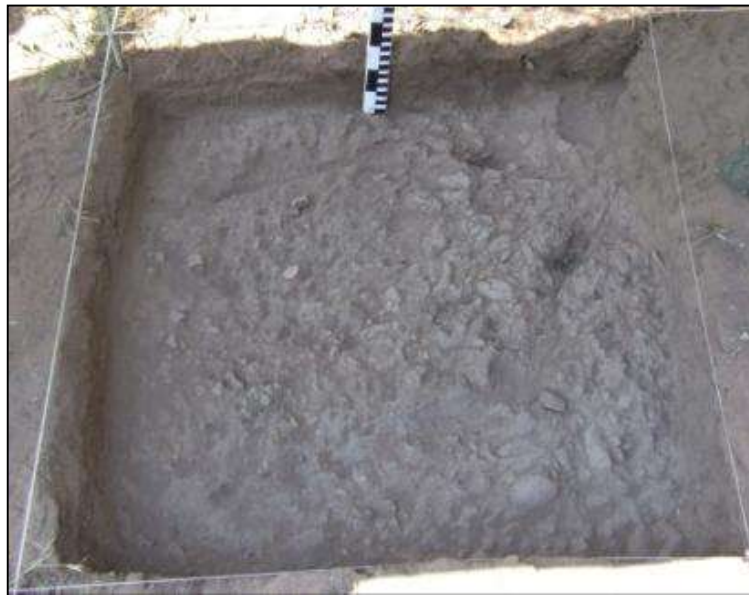


Figure 4.18: 2328 CA1 (1) XX/O at 25cm depth.

4.1.4.3: XX/M

As stated previously, square XX/M was the last square dug on excavation 2328 CA1 (1). The purpose was to discover the depth of the slag and tuyère seen in squares XIX/N and XX/O. Figure 4.19 displays the initial slag and tuyère layer seen at ~20cm depth, while Figures 4.20 and 4.21 display the base of the slag and tuyère layer.

4.1.4.3.1: XX/M/S

The surface layer of XX/M contained a small shrub bush in the south-east corner of the square. The remainder of the grid was covered in short grass, which was easily removed. The surface layer contained five slag pieces and six tuyère fragments, showing a possible spread of artefacts across the excavation grid.

4.1.4.3.2: XX/M/1A

The first layer of XX/M consisted of loose red/brown sand (Figure 4.22). The sand, however, was not loose enough to cause artefact displacement; as such, excavations were dug in 5cm spits. The south-west corner of the square appeared to have large porous holes in the soil. The large holes were due to the tree roots from XX/N, which loosened the soil causing it to fall out of the wall, the effect of which can be seen in Figures 4.19 and 4.23.

4.1.4.3.3: XX/M/1B

XX/M/1B consisted of compacted (compact) red/brown sand. This secondary level of sand was attributed to the surface being at a higher elevation than the surface of square XX/O. Within the sand, slag and daga were discovered. The discovery of daga was relatively earlier in the stratigraphy than was expected, as consistency between XIX/N and XX/O would place daga finds near the slag and tuyère layer.

4.1.4.3.4: XX/M/2A RB

Layer 2A consisted of compact red/brown sand, which continued from the layer above. This began to shift, however, at the base of the 5cm into a red/grey soil (this can be

seen in Figures 4.21 and 4.22). The change in soil was similar to the change seen in squares XX/O and XIX/N; however, due to the slope seen in Figure 4.10, the layer was deeper than previously seen. The slag discovered in this layer varied in size, and consisted of a higher number than had been found in the previous two layers.

4.1.4.3.5: XX/M/2B RG

With the previous squares (XIX/N and XX/O) as a soil guide, the 2B layer revealed a base covered in slag and tuyère fragments. Figure 4.19 displays the initial slag and tuyère layer in this square. It was decided that this square would continue being dug, in order to discover the base of the slag and tuyère layer. The soil in this layer consisted of a grey ash and red tinted soil; hence it was called red/grey soil. The mixture of the two soils was possibly due to the introduction of large amounts of slag and tuyère to the layer and layers below. In this layer, pillars of slag and tuyère in hard soil started to form around the sides of the square (Figures 4.20 - 4.23). The majority of protruding slag was seen on the East facing wall (Figure 4.22). In order to maintain stratigraphy, excavations were dug around the protrusions.

4.1.4.3.6: XX/M/3A RG

Layer 3A began the mass removal of metal production artefacts, slag, tuyère, ore, daga and stone. As this layer represented digging beneath the slag and tuyère layer, the soil changed from the red/grey to just a grey soil, due to the amounts of metal production artefacts within the square. The west-facing wall, however, changed to a brown soil, rather than a grey soil, which may have indicated that square XX/M, was placed on the edge of the slag and tuyère dump. The slag and tuyère continued throughout the 5cm and as such, excavations continued.

4.1.4.3.7: XX/M/3B RG + XX/M/3B B (Hard)

This layer was hard. Large pieces of slag covered the layer, with one weighing ~350 grams. This layer predominantly consisted of slag and tuyère, the bulk of which were large to small pieces of slag, with small tuyère fragments.

4.1.4.3.8: XX/M/4A Tuyère layer (grey)

This layer had both slag and tuyère, with more tuyère than slag. Thus, the layer was labelled as a tuyère layer, representing the large portions of tuyère discovered. The level consisted of complete tuyère pipes which had been broken, as well as tuyère fragments. The south-east corner continued to contain holes from tree roots and affected by the XX/N shrub's roots.

4.1.4.3.9: XX/M/4B Tuyère layer (grey)

XX/M/4B comprised grey soil. Undecorated ceramic sherds were discovered whilst excavating. Digging was slow due to the amount of slag and tuyère, as each piece was removed with care to prevent breaking of tuyère pipes. The base of this layer appeared to be the end of the slag dump, as there were only a few pieces of tuyère pipes which continued to deeper levels. Once these were removed, however, more were identified underneath. The breaks in the slag and tuyère density suggested that the area was used for multiple dumps.

4.1.4.3.10: XX/M/5A (grey- tuyère pipes)

The soil remained grey. At the base of the layer, in the south-east corner of the square, a rock was discovered (Figures 4.20 and 4.21). The rock was approximately 20cm x 20cm. The presence of this rock meant that there was a possibility that the base of the slag and tuyère was approaching. Whether the rock was part of the smelting material or was originally on the surface is unknown.

4.1.4.3.11: XX/M/5B B + XX/M/5B BH

The large rock had meant that most of the ground was clear of significant artefacts. Fewer large pieces of tuyère and slag remained at this level. Copious amounts of broken tuyère fragments, and a few small slag pieces still remained. By the end of the layer, almost all of the slag and tuyère appeared to have been removed, however, there were still a few artefacts going into the next layer, as such, the excavation continued further down.

4.1.4.3.12: XX/M/6A

XX/M/6A was the last layer excavated from square XX/M. The slag and tuyère density and size decreased. This indicated that the level of use has been reached, although some pieces remained. The excavation was terminated and all protruding slag and tuyère fragments in the walls were left *in situ*. Figure 4.21 shows the base of the excavation at spit 6A and, includes the rock, wall protrusions and depth of the square's excavation.



Figure 4.19: 2328 CA1 (1) XX/M first slag and tuyère layer (3A RG), with root disturbance in top right corner.

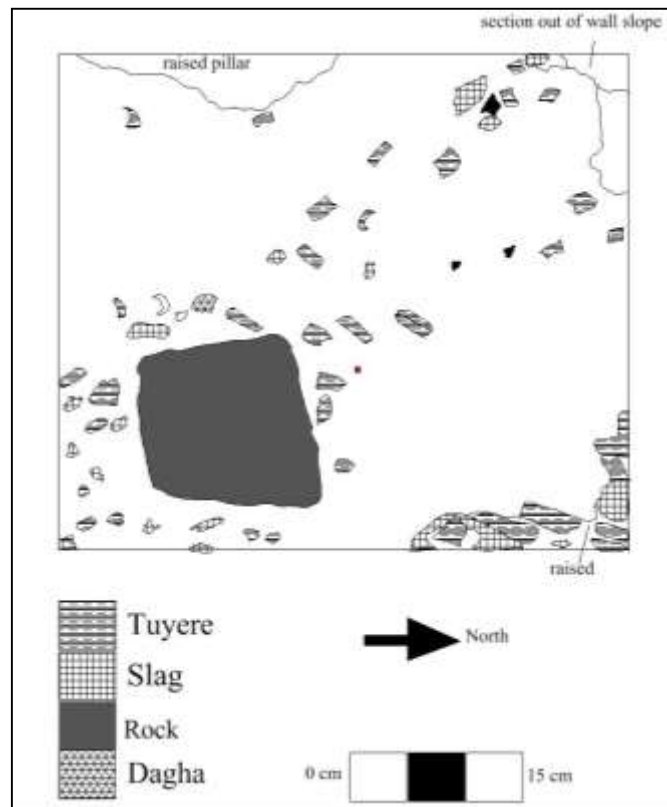


Figure 4.20: 2328 CA1 (1) XX/M Plan view.



Figure 4.21: 2328 CA1 (1) XX/M at the start of the final layer, showing the rock, slag walls and the final layer of excavation.

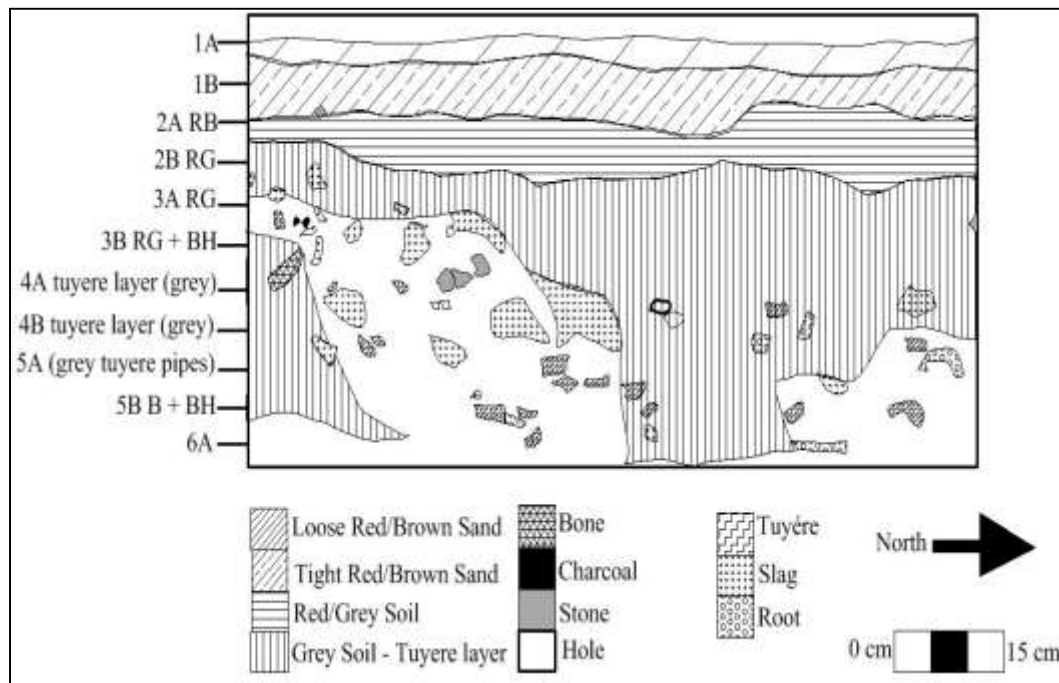


Figure 4.22: 2328 CA1 (1) XX/M East facing wall stratigraphy, with layer indicators.

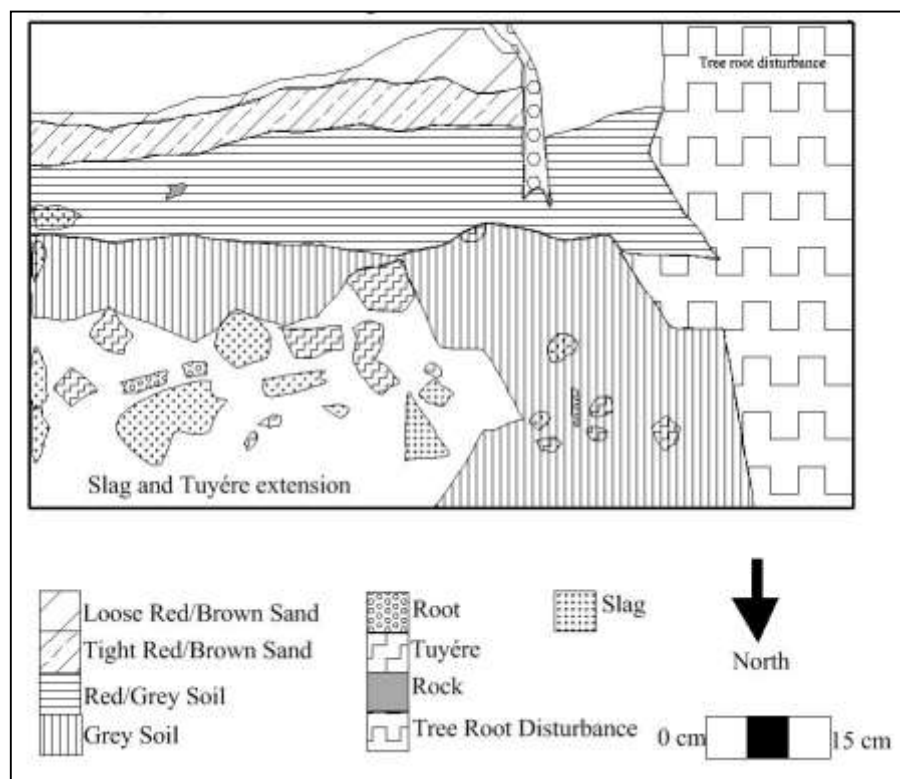


Figure 4.23: 2328 CA1 (1) XX/M North facing wall stratigraphy.

4.1.5: Excavation 2328 CA1 (2)

As stated in Chapter 3, the second excavation performed on site 2328 CA1 was excavation 2328 CA1 (2). The excavation took place on a patch of grey soil, on the old farm road surface. Figure 4.24 shows the excavation's squares row and column labels. It also shows the position of the excavation on the road to the north-east (bottom left corner of the figure).

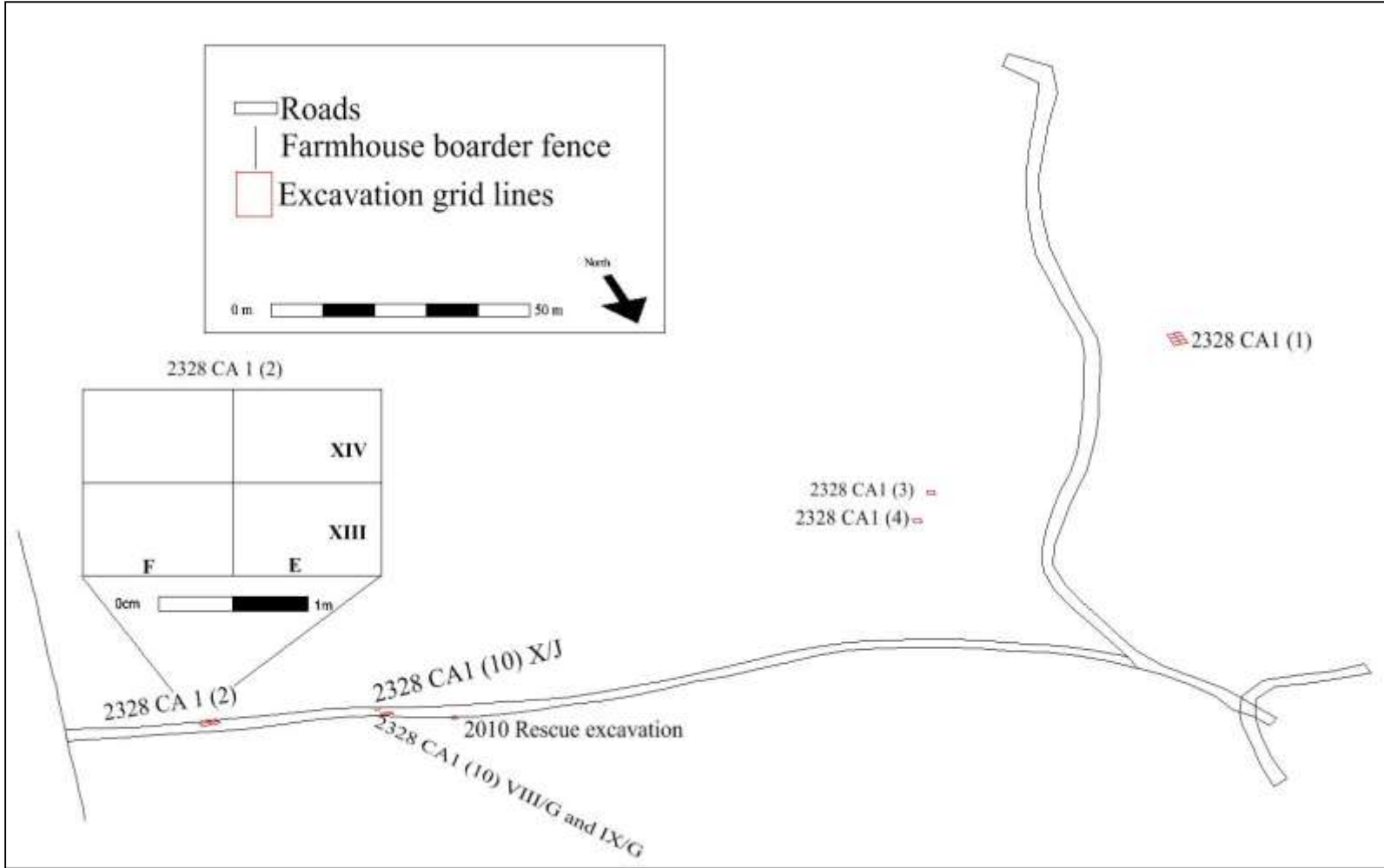


Figure 4.24: Excavation 2328 CA1 (2), with zoomed in grid layout.

4.1.6: Excavation 2328 CA1 (2) stratigraphy

4.1.6.1: XIII/E

Square XIII/E/ was situated at the highest point of excavation 2328 CA1 (2). This allowed for the tracking of erosion down slope, and aided in identifying the origin of the grey ash.

4.1.6.1.1: XIII/E/S

The surface layer of XIII/E was a hard grey soil. Due to the hardness of the road surface, very little vegetation was present. Only one small shrub grew on the surface which was trimmed, but left in the soil. The surface contained ceramic sherds, which were collected and stored. The source of the ceramic sherds was unknown.

4.1.6.1.2: XIII/E/1A

After the surface was cleared, the first 5cm was removed. Within this layer were numerous bones, undecorated ceramic sherds, stones and some charcoal. These artefacts would be typical of domestic waste, which contributed to the belief that this was a midden excavation. The ground was uneven, due to the erosion and diffusion (of material culture) on the road's surface, and as such, part of the layer was removed to achieve an even surface area. The soil was mostly grey with some red spots, and began to get harder with increased depth.

4.1.6.1.3: XIII/E/1B

The second layer of this square, much like the first, remained grey with small patches of red soil. Small rocks started to appear, but only continued another 5-10cm into the ground. The layer produced more undecorated ceramics, as well as a few pieces of slag.

4.1.6.1.4: XIII/E/2A

The third layer contained very few artefacts and a few rocks. It was at this layer that the red soil patches became more apparent and the grey layer seemed to slope more

towards square XIII/F. Excavations, however, continued to establish what was under the small rocks level.

4.1.6.1.5: XIII/E/2B

Layer XIII/E/2B, began shifting from the red and grey mixed soil to red being more dominant. The grey soil seemed to slope downwards into square XIII/F. Due to the incline of the road, not much soil had been removed on the west-facing wall. The bulk of the soil removed came from the opposite side, the east-facing wall, as it was on a higher elevation. Figure 4.25 displays the slope in soil at the last layer dug on square XIII/E. The slope is moving towards the top of the picture, whereas the bottom contains the red soil.

4.1.6.1.6: XIII/E/3A

This was the last layer of XIII/E, as it was decided to shift focus away from it and focus on XIII/F. The shift was primarily due to the amount of material being recovered from XIII/F, as well as the grey soil, seeming to stem from XIII/F. XIII/E produced bones, ceramics, a few beads, glass, slag and stones. The last layer consisted of grey soil and was cleared of all rock and roots.



Figure 4.25: 2328 CA1 (2) XIII/E, final layer.

4.1.6.2: XIII/F

Square XIII/F represented the lowest section for this excavation, and focused on the densest part of the grey ash, located on the surface soils.

4.1.6.2.1: XIII/F/S

This square contained the original grey area, which was thought to be the midden. The surface contained numerous ceramic sherds, and small faunal remains. The square was placed on a slope, which meant all finds on this surface had probably washed down, from higher up on the road.

4.1.6.2.2: XIII/F/1A

As with most excavations on this site, the first layer of XIII/F/1A was uneven, and gradually sloped downwards to the north-east corner. The surface layer was a mixture of a light and dark grey loose soil with bone and ceramic fragments protruding through the surface. Using the line level technique, the highest point of the square was used as the surface, and was dug to accommodate for the unevenness. The first layer produced

bone, charcoal, different sections of ceramic sherds, a bead and slag. There were small rocks discovered in the layer, which had probably been washed down the hill and settled in the possible midden. One rock lay above a large ceramic sherd located in the south-facing wall. Figure 4.26 shows the rock on the left-hand side of the picture, with the ceramic still protruding into the grid from the wall. Another group of rocks began protruding out of the east and west facing wall (Figure 4.27, top and bottom of the grid square).

4.1.6.3.2: XIII/F/1B

The next 5cm of grey soil changed to a new tight (compact) grain grey soil, with occasional red soil patches. The soil began to become harder at this level, possibly due to the compression, caused when the road was still open. Ceramic sherds continued to be found in this layer, however, only undecorated body sherds. Some of the bone from the previous layer had also filtered into this layer. The slope was gradually reduced to an even level. The lowest corner north-east still remained under the 5cm mark.

4.1.6.3.4: XIII/F/2A

This layer consisted mainly of the grey compact soil. It also contained the bulk of ceramic fragments found in this excavation. The ceramics varied from some with decoration, to some without. Ostrich egg shell beads, slag, copper wire, ore and bone were also discovered in this layer. The varying artefacts recovered from this layer showed that this was a rich source of archaeological information, as not only did it contain homestead associated material culture, but it also had ties with the smelting area and the finished metal products.

4.1.6.3.5: XIII/F/2B

Another 5cm down the soil became grey with red tints. Within the layer, ceramic sherds were once again found, indicating that this was a possible waste deposit with discarded homestead associated artefacts. Not only were ceramics present in this layer, but bone, charcoal, ore, slag and small stones were found as well. The two adjacent excavations

were stopped, and focus shifted to this grid, due to the grey soil seeming to originate from this square.

4.1.6.3.6: XIII/F/3A

This level remained fairly level with the layer above. The north-facing wall, however, seemed to have some contamination through erosion, as it appeared to be a grey soil with red patches. Figure 4.28 displays the red soil mixing with the grey soil on the north-facing wall. The remaining walls had very few to no red patches, and consisted of a grey compact soil. Decorated ceramic sherds began to appear more frequently in this layer, as well as slag, and charcoal.

4.1.6.3.7: XIII/F/3B

In this layer, red soil started to appear in larger patches, although the grey compact soil still dominated the stratigraphy of the excavation. As both grey and red patch soil began to appear, this layer was labelled as a mixed layer. The layer contained ceramic sherds, some decorated but the bulk was undecorated. It also contained 10 pieces of small slag, possibly smithing pieces (due to their size being smaller than those found on excavation 2328 CA1 (1)), and charcoal. Figure 4.29 displays the incline of the site, and the red soil base.

4.1.6.3.8: XIII/F/4A mixed

In this layer, the grey soil gave way to red soil. In the south-west corner of the square, however, a large circular patch of grey soil remained. The grey soil can be seen in Figures 4.26, 4.27 and 4.28. Excavations then focused on the large grey soil patch, in case it went further down. The next few layers were labelled as GA (grey ash) to indicate the shift from the 1m x 1m grid to a focus on removing the grey soil found in the south-west corner. Within this level ceramic, charcoal and slag were discovered. The shift in grey soil to a circular patch changed the belief from this being a midden excavation, to that it was a possible pit. This was due to artefacts being recovered

within the circular grey soil patch, whereas a midden would cover a large area, and contain grey soil throughout the area (due to the ash from waste being burnt).

4.1.6.3.9: XIII/F/GA 4B

The first layer of grey ash was removed at 5cm spits. The initial surface was a dark black patch surrounded by red soil. The size of the patch was significant enough to continue excavations. Within the first 5cm, bone, ceramics, ore and slag were discovered. The retrieval of homestead associated material culture meant that this was the possible source of the artefacts retrieved in the previous layers.

4.1.6.3.10: XIII/F/GA 5A

The grey ash continued down a further 5cm, whilst the diameter (Figure 4.27) of the pit remained the same. Within the layer, ceramics, charcoal and slag were discovered. Unfortunately, no decorated ceramics were recovered from this layer, and thus could not be relatively dated. At this point it was clear, that excavation 2328 CA1 (2) was not a midden, but a pit excavation.

4.1.6.3.11: XIII/F/GA 5B

This level presented a decrease in ceramic finds. The grey ash proportion remained constant, and it was decided to continue digging until the base of the grey ash. Two decorated ceramic neck sherds were discovered in this layer, however, their patterns alone were not enough to discern what ceramic style they came from. They were, however, similar to the EFC ceramics found earlier.

4.1.6.3.12: XIII/F/GA 6A

Layer GA 6A consisted of grey soil with small red patches, as seen near layer XIII/F/3B. As the excavation progressed, fewer artefacts were recovered, which indicated a possible termination of the pit at 50cm from the surface height, the grey ash continued further, as shown in Figure 4.28.

4.1.6.3.13: XIII/F/GA 6B

Layer GA 6B was the last dug at 2328 CA 1 (2). By this layer, all the grey soil had been removed and artefact density and retrieval had decreased. In total 4 pieces of ceramic body sherds, bone, ore and stones. At the base of the spit, red soil started to appear showing the end of the grey soil (Figure 4.28). The base of the pit was discovered at ~55cm (Figure 4.31). Excavation 2328 CA1 (2) was closed off and backfilled at this level.



Figure 4.26: 2328 CA1 (2) XIII/F/4A red soil mix with grey soil patch (bottom right (south-west corner)).

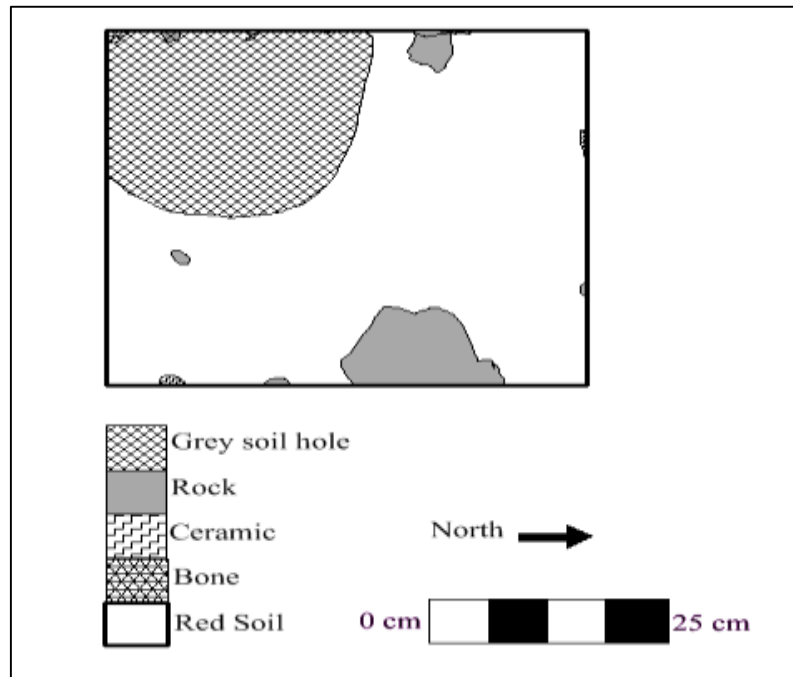


Figure 4.27: 2328 CA1 (2) XIII/F Plan View.

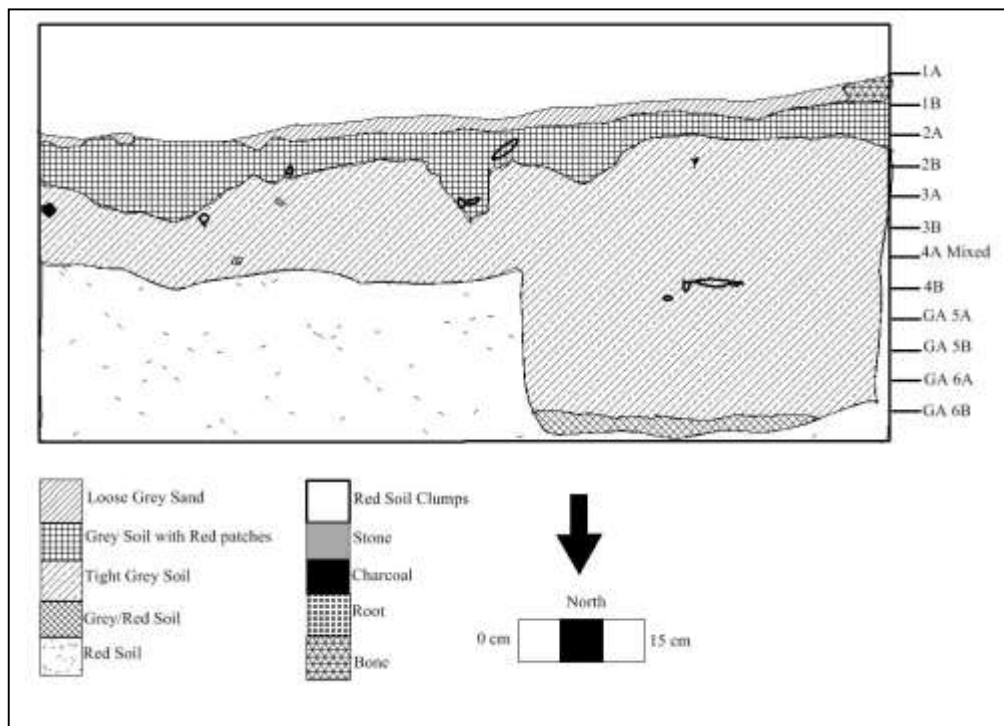


Figure 4.28: 2328 CA1 (2) XIII/F North facing wall stratigraphy, with layer indicators.

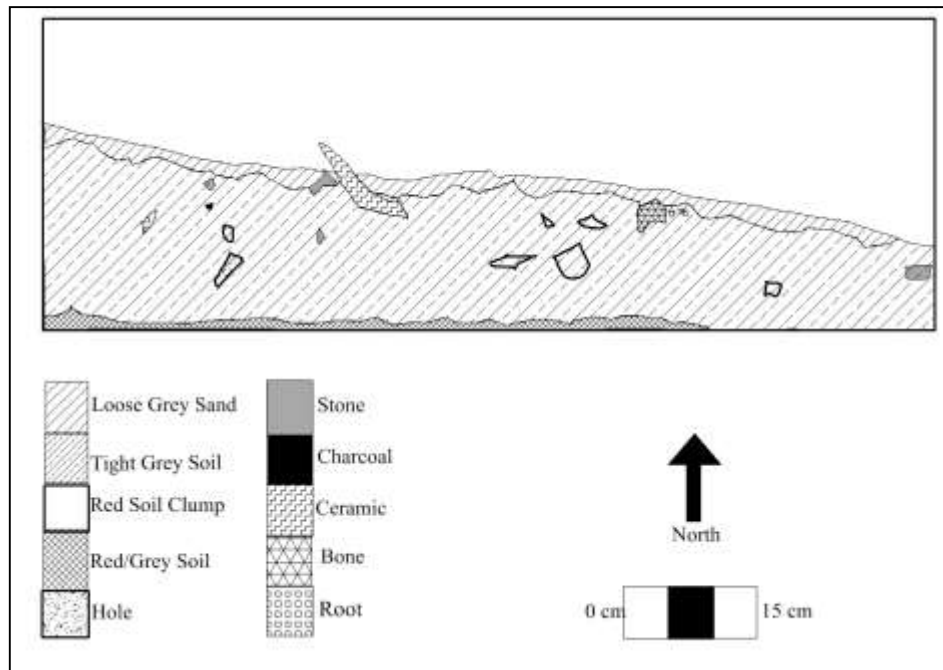


Figure 4.29: 2328 CA1 (2) XIII/F South facing wall stratigraphy.



Figure 4.30: 2328 CA1 (2) XIII/F/GA 5A final layer, showing pit base.

4.1.6.4: XIV/F

Square XIV/F was situated in an erosion prevention gully, alongside the road. This square was excavated in order to see if any material culture had washed out of the other squares, into the gully.

4.1.6.4.1: XIV/F/S

This square's surface contained a large number of ceramic shards. This was due to the south section being part of an erosion prevention gully. In this gully, numerous pieces of ceramics were retrieved and stored. The remainder of the surface was littered with stones, and some vegetation.

4.1.6.4.12: XIV/F/1A

As with the previous two squares in this area, the ground was very uneven, as the southern side sloped into a gully. This gully appears to have been formed due to water running off the side of the rocks above the excavation. The unevenness of the ground meant that not much soil was removed before the 5cm mark was reached. The surface layer was a loose grey soil, which spread across most the square; however, as the excavation proceeded down, the grey began to fade away into a red soil.

4.1.6.4.3: XIV/F/1B

By this layer, the uneven ground had almost been completely levelled, and the 5cm spit could be removed from the bulk of the grid. The grey soil began to decline and become more focused in square XIII/F. Due to this, it was decided to level off and stop excavation XIV/F, and that excavation efforts should concentrate on the grey soil in XIII/F.

4.1.7: Excavation 2328 CA1 (10)

The patterns in excavation 2328 CA1 (2) and excavation 2328 CA1 (10) were similar, thus they are discussed concurrently. A large tuyère pipe was removed from the first 5cm. The tuyère pipe, was unlike those recovered on excavation 2328 CA1 (1), as it

had a diameter of ~10cm, meaning it was possibly the proximal end of a tuyère pipe, making it the only one found on site so far. Grids X/I and VIII/G were shallow excavations (~10cm and ~15cm), whereas IX/G was dug to the end of an ash pit infill, at roughly 30cm (Figure 4.31).

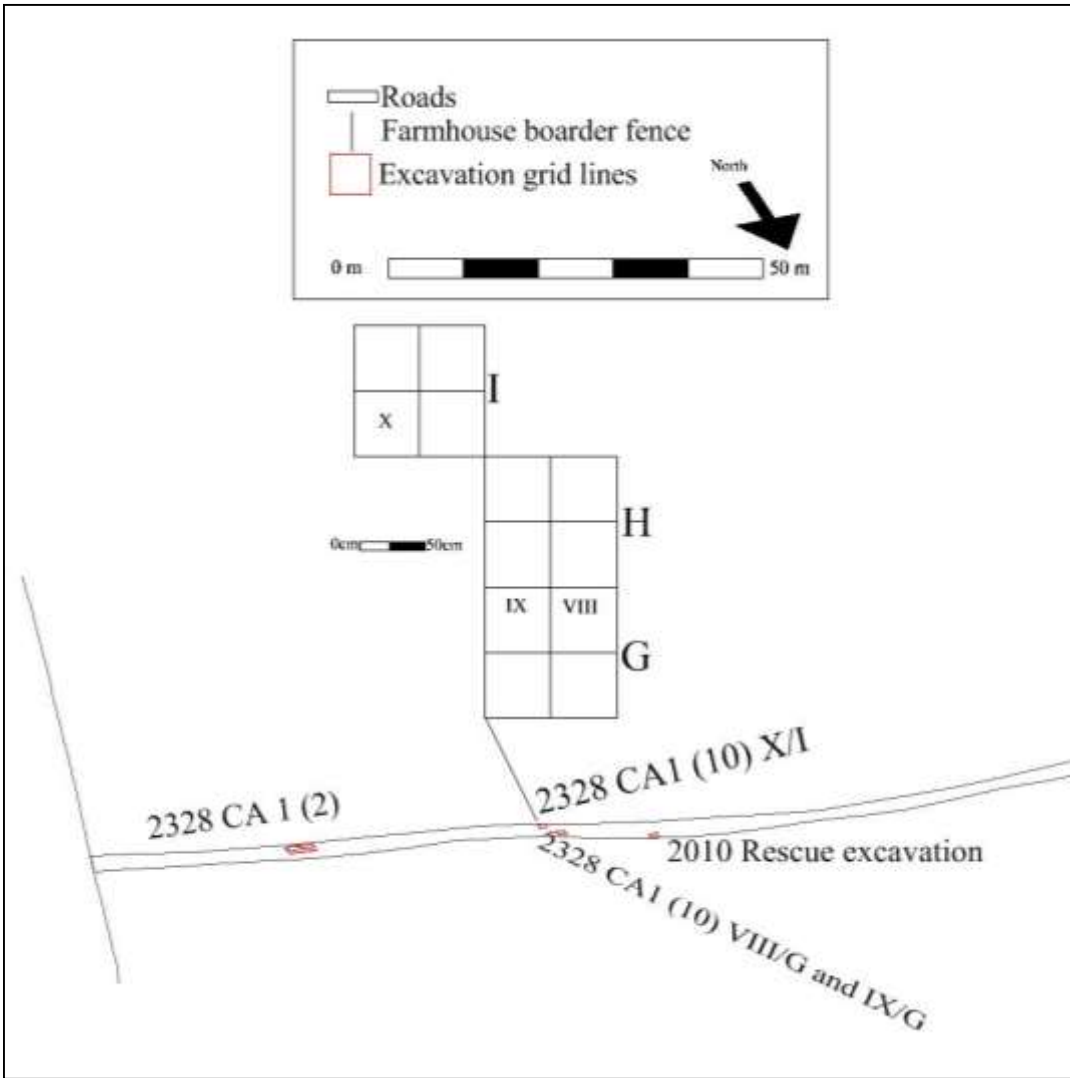


Figure 4.31: Excavation 2328 CA1 (10), with enlarged in grid layout.

4.1.8: Excavation 2328 CA1 (10) stratigraphy

4.1.8.1: Road Test X/I

As stated previously this excavation was performed to retrieve faunal remains on the road surface (Figure 4.32). The excavation was shallow, due to the main focus of retrieving the faunal remains for possible identification.

4.1.8.1.1: Road Test X/I/S

The surface of the grid was covered in small stones and loose sand (Figure 4.32). The faunal remains were visible on the surface and appeared to be a long bone, perhaps of an infant.

4.1.8.1.2: Road Test X/I/1A

The first 5cm allowed for the retrieval of ceramics, stone and most of the remains. A small part of the long bone continued deeper, as such excavations continued.

4.1.8.1.3: Road Test X/I 1B

By this layer the base of the faunal remains had been reached, as such they were lifted and Road Test X/I were terminated.



Figure 4.32: Road Test X/I, bone on surface.

4.1.8.2: VIII/G

4.1.8.2.1: VIII/G/S

The surface layer of VIII/G contained numerous stones, ceramic sherd, tuyère and slag. The focus of this grid was the retrieval of the large tuyère pipe protruding from the surface. Once the surface was cleared excavations began.

4.1.8.2.2: VIII/G/1A + 1B

Excavations began in an attempt to remove the tuyère pipe. Due to its size, both layer 1A and 1B were dug out, in order to reach the tuyère's base. Surrounding the tuyère were two medium-sized rocks, the one directly behind the tuyère (Figure 4.33), which possibly were the reason it was well preserved. The soil was a chestnut hard soil and once the base of the tuyère was reached, the soil began to change to a grey soil. Due to this soil change, excavations continued.

4.1.8.2.3: VIII/G/2A

A further 5cm contained a mixed soil type between the chestnut hard and red hard soil. This meant that pit was nearing its base. The sides of the pit began to taper towards the south-west corner of the grid and in response, the excavation focused on this corner, following the stratigraphical curve in the soil. This led to the opening of a new grid IX/G.

4.1.8.3: IX/G

4.1.8.3.1: IX/G/S

As with the previous grid VIII/G the surface was covered in a thin sand layer, with numerous stones and artefacts. The soil was chestnut colour, and no vegetation was present.

4.1.8.3.2: IX/G/1A

The initial first layer contained a chestnut hard soil. Due to the soil change recorded in grid VIII/G, the chestnut hard would soon become a red grey soil. With the amount of ceramic sherds recovered on the surface, there was a possibility that this was a pit. This would explain the appearance of the grey soil.

4.1.8.3.3: IX/G/1B

In layer 1B the ash grey focused in a circle in the centre and south-east portion of the grid. This was an indication that this layer represented the possible surface layer of the pit. The material culture recovered in this layer was consistent with the previous layer and was attributed to being domestic waste.

4.1.8.3.4: IX/G/2A

This layer was dug down following the grey ash of the pit. Instead of the entire grid's surface, only the portion of ash grey was removed. The bulk of which was removed from the south-east section of the grid. At this level the chestnut hard began to mix with red hard soil, indicating a possible past surface soil.

4.1.8.3.5: IX/G/2B

By this layer, the red hard soil covered the majority of the pits base. Hints of ash grey, however, began forming around the south-west section of the grid (Figure 4.33). As ceramic sherds were still being found in the low levels, excavations continued 5cm further down.

4.1.8.3.6: IX/G/3A+ 3B

These were the last layers of IX/G. The base of the pit was reached at 30cm, however, due to the two spits consisting of the same soil, both were dug conjointly. The soil now completely comprised of a grey ash, making this possibly the last layer of the pit. Artefacts recovered from here included: bone, charcoal and a ceramic sherd. Due to the presence of little material, the excavation was closed off on layer 3B. The identification of this secondary pit along the road led to the collection of artefacts along the road, which will be discussed later.

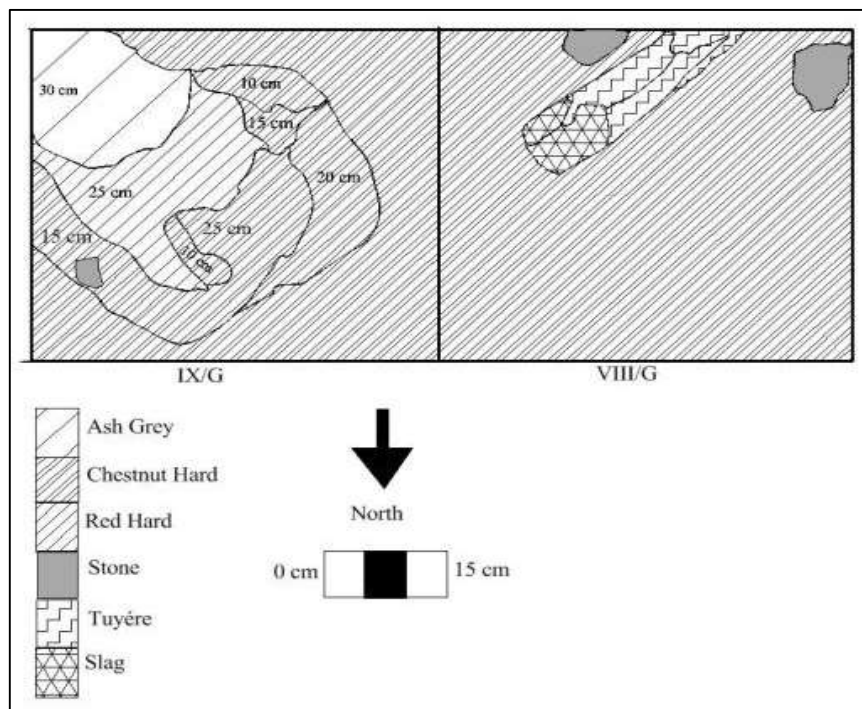


Figure 4.33: 2328 CA1 (10) Plan view, with square IX/G to the left and square VIII/G to the right.



Figure 4.34: Photo of excavation 2328 CA1 (10), at termination.

4.1.9: Excavations 2328 CA1 (3) and 2328 CA1 (4)

Excavation areas 3 and 4 were in close proximity (Figure 4.35), and thus will be discussed together. After both test pits revealed the ceramic layer spreading across the area, two 1m x 1m excavations were placed next to each test pit.

They were named 2328 CA1 (3) and 2328 CA1 (4). The first excavation 2328 CA1 (3) was labelled X/A and the second 2328 CA1 (4) was labelled XX/J. With the large amounts of ceramics excavated from the test pits, these squares were likely to expand on the source of this material. The main purpose of the excavation, however, was to attempt to identify a possible settlement structure, such as a kraal or hut floor, which would strengthen the settlement area argument.

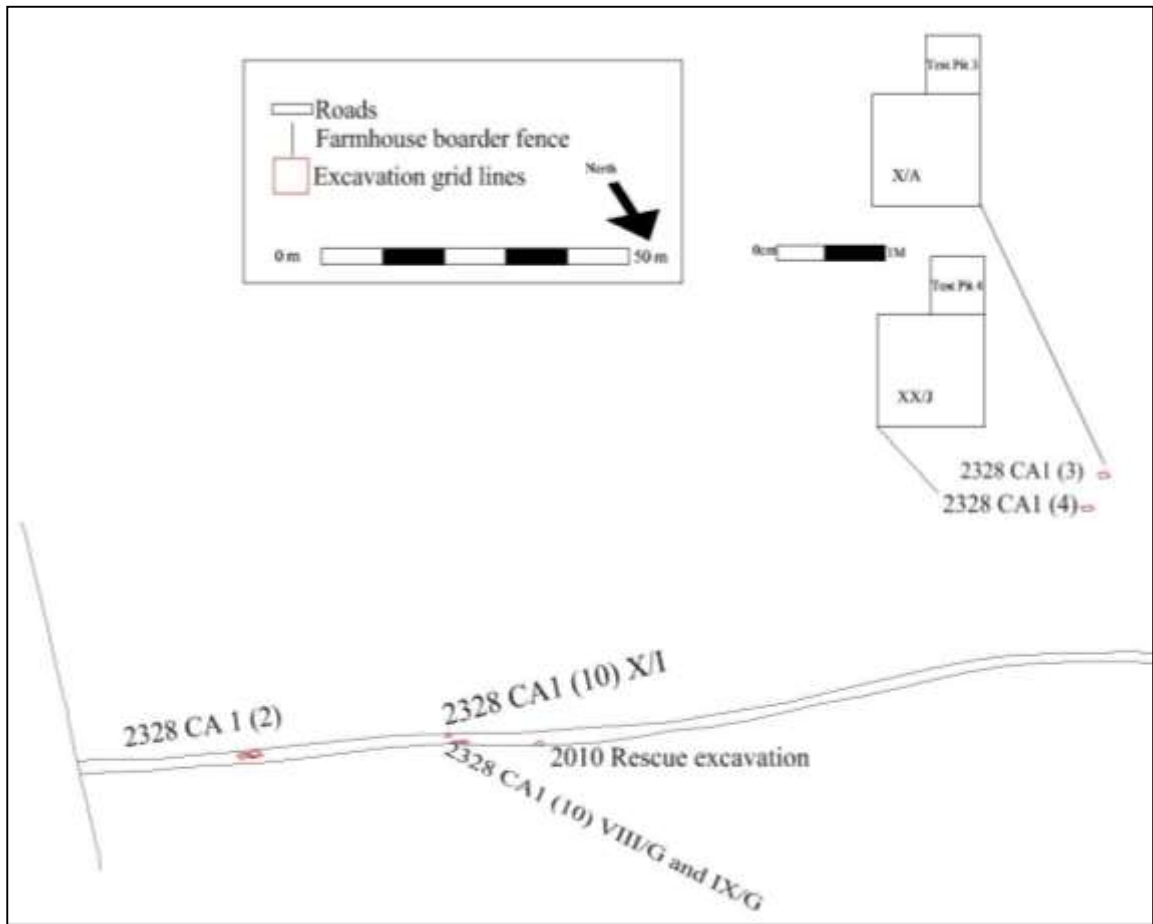


Figure 4.35: Excavation 2328 CA1 (3) and 2328 CA1 (4).

4.1.9.1: 2328 CA 1 (3) X/A

4.1.9.1.1: X/A/S

X/A's surface contained fine grained brown sand, which made clearing easier, as shrubs and grass could be removed with little effort. Figures 4.36 and 4.37 display the loose sand. On the surface, eight ceramics were discovered, one decorated body, while the remainder were undecorated bodies.

4.1.9.1.2: X/A/1A-2A

Once the fine sand was cleared off the surface level, it was decided that the first layer should be dug down to 15cm, as the test pit indicated that there would be a low possibility of artefacts at this level. The soil consisted of compact (tight) brown sand.

The compact brown sand was thinnest on the south- and west-facing walls (Figure 4.37). Some bone and three ceramic sherds were found within the 15cm spit, but only below ~10cm. As ceramics appeared, it was decided that the next levels would be dug at the usual 5cm intervals.

4.1.9.1.3: X/A/2B

Layer 2B yielded very few finds. The soil structure remained compact brown but slowly began to show slight grey tints nearing the 20cm mark (Figure 4.36). Few faunal remains and ceramics were found in this layer.

4.1.9.1.4: X/A/3A

This layer consisted of a brown grey soil, which was a good indication that the occupation layer was potentially close (Figure 4.37). As with the previous two layers, layer X/A/3A had very few artefacts. One small long piece of thick metal wire was found in this layer, which was later identified as a thick copper wire.

4.1.9.1.5: X/A/3B

Layer 3B began to shift from the compact brown soil to a grey coloured soil. This was a possible indication of an approaching occupation layer. Although numerous ceramic sherds were below 30 cm, a few appeared in this layer as well. In the south-west corner, large roots began appearing, but appeared to curl off outside the grid (Figures 4.38 and 3.39). The roots were from a baobab tree, and as seen during the grid test pit, and they had spread into this excavation as well.

4.1.9.1.6: X/A/4A

In this layer, a group of rocks appeared in the south-west corner (Figure 4.36), below the roots which had appeared in the previous layer. The rocks appeared to be in a circular pattern (Figure 4.39); and so assumed to be a possible stone circle. The surface layer of the rocks fell within the occupation layer, as the soil changed from the grey to dark brown soil patches (Figures 4.36 and 4.37).

4.1.9.1.7: X/A/4B

At layer 4B, the soil had changed from grey to a dark brown and presented numerous ceramic sherds. Ceramic sherds were found amongst the rocks, as well as spread around the grid. Their numbers had nearly doubled from what they had previously been recorded in this grid's upper layers, and thus this layer was labelled the occupation layer. At the end of the 5cm spit, the rocks still continued further down, which led to excavations continuing to discover the base of the rocks.

4.1.9.1.8: X/A/5A

This layer, as with the last, contained multiple ceramic sherds. The layer itself comprised the same dark brown soil, however, in the middle sections, long thin roots appeared, stretching across the excavation from approximately east to west (Figure 4.39). At the end of this layer, the rocks' base was discovered, however, ceramics were seen to continue further down. As such, the excavation was taken down one layer deeper.

4.1.9.1.9: X/A/5B

The last layer remained dark brown sand. The ceramics which were seen in this layer were relatively close to the layer's surface. At 50cm ceramic sherds recovered were body sections, with no distinctive decoration. The number of finds began to decrease. Due to this, it was unlikely that more would be recovered further down, and so the excavation was closed at this layer.

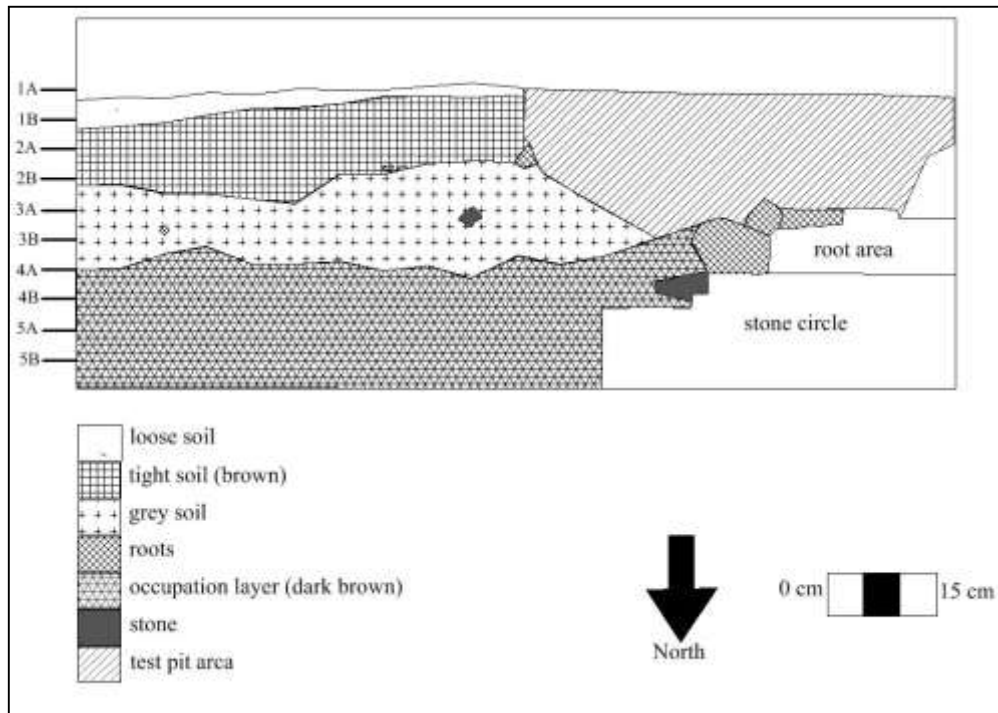


Figure 4.36: 2328 CA1 (3) X/A North facing wall stratigraphy, with layer indicators.

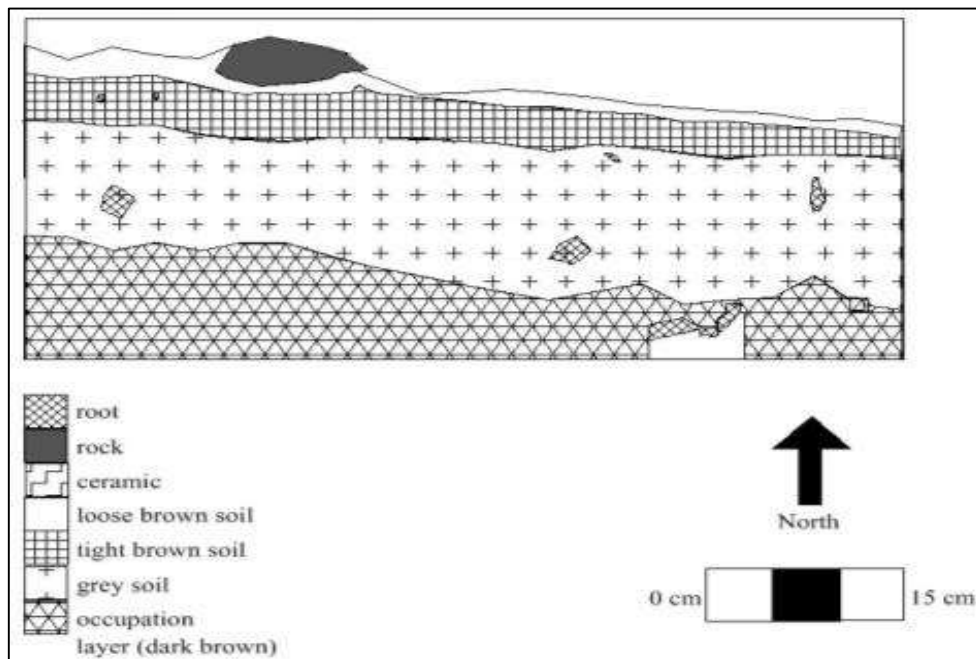


Figure 4.37: 2328 CA1 (3) X/A South facing wall stratigraphy.

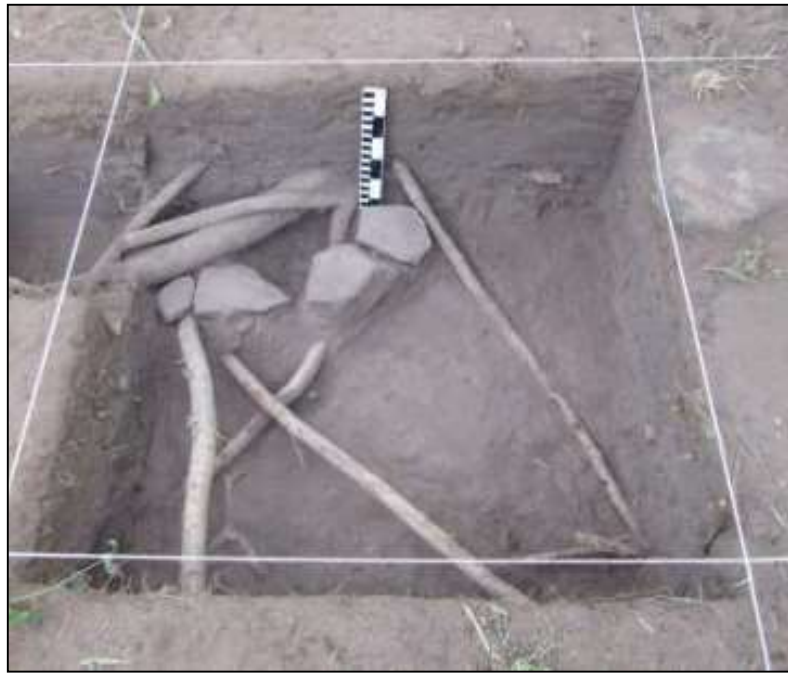


Figure 4.38: 2328 CA1 (3) with test pit 3 in top left corner.

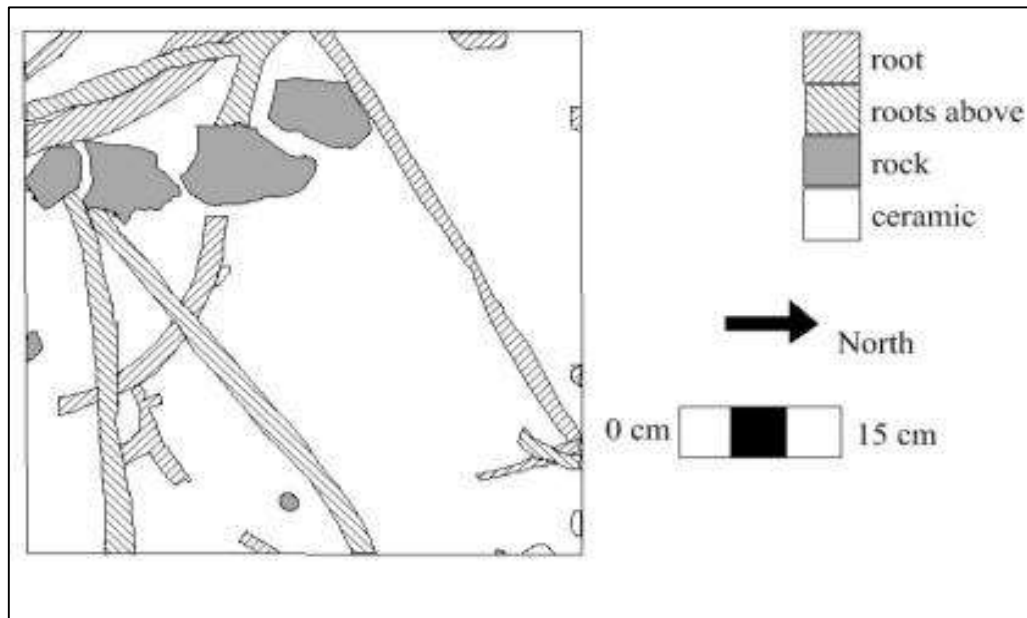


Figure 4.39: 2328 CA1 (3) Plan view.

4.1.9.2: 2328 CA 1 (4)

Excavation 2328 CA1 (4) was dug simultaneously with excavation 2328 CA1 (3). This was done in order to cover a larger part of the area. As no homestead structures had been discovered, these excavations were dug as a means of possible homestead structure discovery. This hypothesis was due to the amount of ceramics found in the test pits, which indicated the area was near the settlement structure area.

4.1.9.2.1: XX/J/S

The surface layer of this site was covered in loose brown sand, much like that seen on excavation 2328 CA1 (3)'s surface (Figure 4.40). Figure 4.41 displays the surface sand of the excavation, as well as the base at 45cm. Within the surface sand, ceramics, slag, and stones were recovered.

4.1.9.2.2: XX/J/1A + 1B

The first 10cm of 2328 CA 1 (4) revealed numerous ceramic pieces, slag, stone, bone and ore, which possibly originated from the animal hole dug just west of the excavation. The layer comprised soft brown sand, which was easy to remove, followed by a compact brown sand layer. Nearing the 10cm mark, grey soil began to appear in certain sections of the grid (Figure 4.40). Due to the ceramic discoveries, normal 5cm spits were continued at this point.

4.1.9.2.3: XX/J/2A

This layer comprised mainly grey soil, and within the layer, the bulk of artefact retrieval was ceramics body sherds. As with the previous excavation, this area seemed to be part of the homestead. The excavation itself presented no disturbances of vegetation, and as such, remained untouched and stratigraphically uncompromised.

4.1.9.2.4: XX/J/2B

This layer contained the last of the grey soil, due to it shifting to a dark brown soil, which was assumed to be the occupation layer, as it contained large amounts of ceramic

fragments. Artefacts recovered from this layer included slag and both decorated and undecorated ceramic fragments. The decorated sherds indicated that this was an EFC occupation layer, as they contained multiple bands of thick incisions creating a herringbone pattern, commonly associated with the Diamant facies (Huffman 2007).

4.1.9.2.5: XX/J/3A

Layer 3A comprised both the grey soil and the dark brown soil (occupation layer), and contained the bulk of the ceramic sherds from this excavation. The ground was easily removed and no root or rock interference had occurred. The amounts of ceramics being recovered meant that similar to the previous excavation, the area was probably within the settlement area.

4.1.9.2.6: XX/J/3B

In order to find the base of the occupation layer, the excavation continued further down. Layer 3B remained dark brown, as with the previous layer. Ceramic sherds were still being recovered in this layer, as well as charcoal, bone and ore.

4.1.9.2.7: XX/J/4A

Layer 4A indicated a possible end to the occupation layer, as artefact numbers decreased. At the base of the layer, a few pieces of ceramic and bone continued deeper (Figures 4.41 and 4.42). The soil had remained the dark brown soil at this depth.

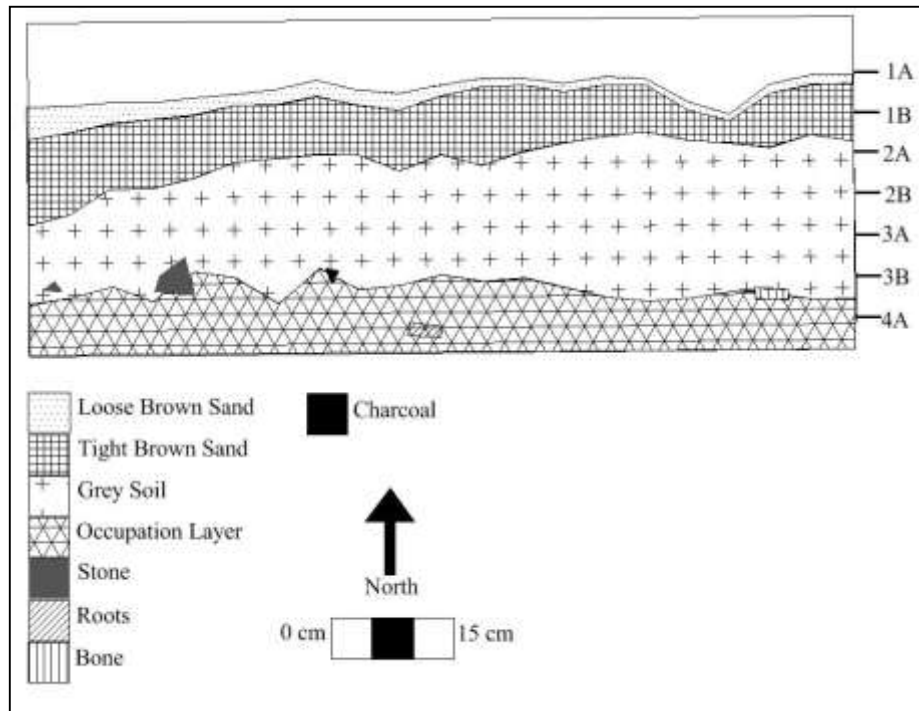


Figure 4.40: 2328 CA1 (4) XX/J North facing wall stratigraphy, with layer indicators.



Figure 4.41: 2328 CA1 (4) XX/J.

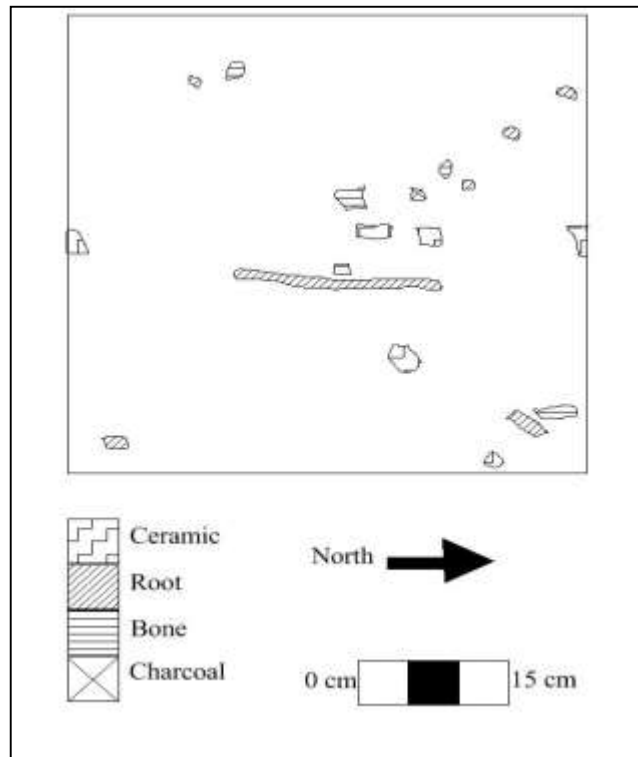


Figure 4.42: 2328 CA1 (4) Plan View.

4.1.10: 2328 CA1 Road surface Collection

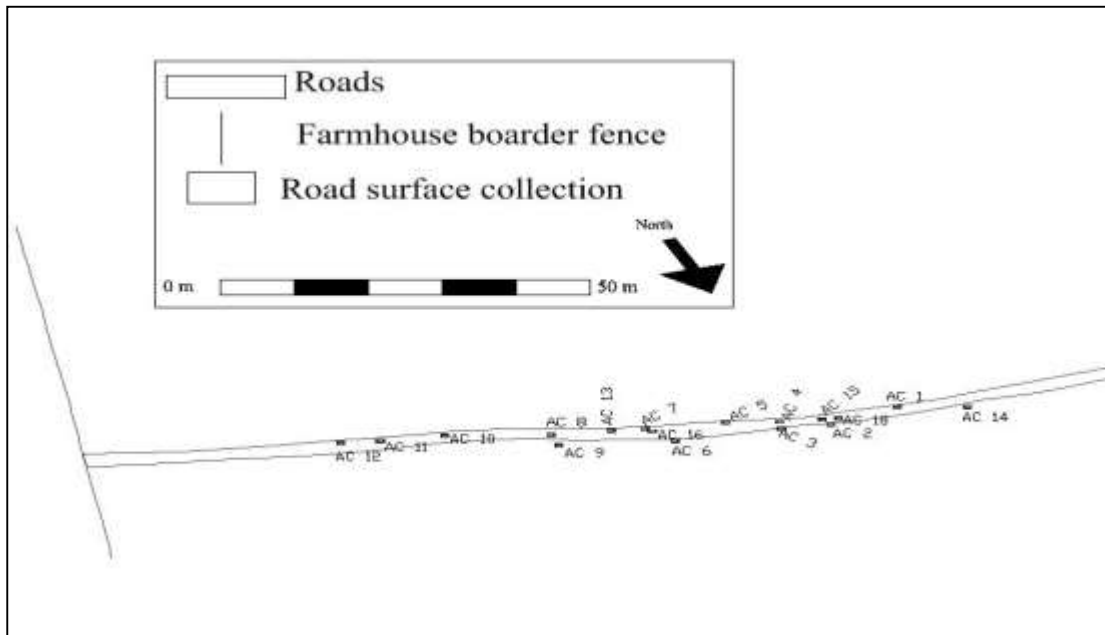


Figure 4.43: Road surface collection distribution.

The road where the 2010 rescue excavation, 2013 excavation 2328 CA1 (2) and 2328 CA1 (10) took place was littered with artefacts, e.g. ceramic scatters and surface slag (Figure 4.2). The excavation team collected 16 surface samples from the road (Figure 4.43), these included: ceramic sherds (EFC), slag, tuyère, ore, possible furnace wall and bone. The collection took place from clusters of *in situ* artefacts, eroding out of what appeared to be pits in the road (Figure 4.44). Excavations 2328 CA1 (2) and 2328 CA1 (10) both contained pits, so it was likely that these clusters could be pits whose surfaces had been eroded on the road surface.



Figure 4.44: AC 13, showing ceramics found on road surface.

4.2: Artefacts recovered

4.2.1: Artefacts recovered from each excavation

4.2.1.1: Artefacts recovered from Test pits and shovel test pits

In total, 17 pieces of slag, 10 tuyère fragments and 170 ceramic sherds were recovered from the test pits and shovel test pits (Table 4.1; Appendix A: Table A10.12.).

Table 4.1: Test pits and Spade test pit artefact summary.

Name	Slag	Total slag weight (g)	Tuyère	Ceramic	Decorated ceramic	Undecorated ceramic
Test Pits and TP shovel	17	249.85	10	170	12	158

4.2.1.2: Artefacts recovered from 2328 CA1 (1)

XIX/N yielded 2308.59g slag and 243 tuyère fragments. Square XX/O was excavated to a similar depth, and yielded similar amounts (2098.34g slag and 347 tuyère fragments). The XX/M excavation was substantially deeper and not surprisingly yielded more slag and tuyère fragments (41983.08g slag and 7171 fragments) (Table 4.2; Appendix A: Tables A10.1 - A10.3).

Table 4.2: Number of artefacts (slag and tuyère) and material culture (ceramics) recovered from each excavated square in excavation

Grid name	Slag	Total slag weight (g)	Tuyère	Ceramic	Decorated ceramic	Undecorated ceramic
2328 CA1 (1) XIX/N	802	2308.59	243	0	0	0
2328 CA1 (1) XX/M	9141	41983.08	7171	14	1	13
2328 CA1 (1) XX/O	590	2098.34	347	3	0	3
Total	10533	46390.01	7761	17	1	16

4.2.1.3: Artefacts recovered from 2328 CA1 (2)

The main focus on this excavation was the retrieval of possible EFC artefacts which could link the area to a nearby EFC settlement, or strengthen the argument for a nearby settlement or housing structures. The area yielded slag, and tuyère fragments, bone, stone, and ore, as well as decorated and undecorated ceramics (Table 4.3 and Appendix A: Tables A10.4 - A10.6).

Table 4.3: 2328 CA1 (2) Artefact breakdown.

Grid name	Slag	Total slag weight (g)	Tuyère	Ceramic	Decorated ceramic	Undecorated ceramic
2328 CA1 (2) XIII/E	32	145.90	0	153	5	148
2328 CA1 (2) XIII/F	65	293.28	0	397	26	371
2328 CA1 (2) XIV/F	8	31.34	0	34	8	26
Total	105	470.52	0	584	39	545

4.2.1.4: Artefacts recovered from 2328 CA1 (10)

Excavation 2328 CA1 (10) contained occupation, metallurgical and faunal remains, which appeared on the surface. The faunal remains were not analysed, due to the focus of this project being on metallurgy. In total 2314.40g slag, 21 tuyère fragments, one “giant” tuyère pipe (due to it having a circumference twice the size of all other tuyère collected (Figures 4.53- 4.54)) and 248 ceramic sherds were recovered (Table 4.5), each of these were classified as important artefacts to this project. A full list of artefacts recovered of both metallurgical and archaeological material from excavation 2328 CA1 (10) is provided in Appendix A: Tables A10.9 - A10.11.

Table 4.4 2328 CA1 (10) artefact breakdown.

Grid name	Slag	Total slag weight (g)	Tuyère	Ceramic	Decorated ceramic	Undecorated ceramic
Road Test 2328 CA1 (10) X/I	22	54.25	2	23	4	19
2328 CA1 (10) VIII/G	82	556.98	16	113	24	89
2328 CA1 (10) IX/G	263	1703.17	3	112	15	97
Total	367	2314.40	21	248	43	205

4.2.1.5: Artefacts recovered from 2328 CA1 (3) and 2328 CA1 (4)

The following material culture was recovered from excavations: 375.30g of slag, nine pieces of tuyère, and 546 ceramics (43 with decoration and 503 without). A circle of stones was discovered in the south-west corner of 2328 CA1 (3). Table 4.4 gives a summary of the main artefacts recovered and the full representation of the artefacts is given in Appendix A: Tables A10.7 - A10.8.

Table 4.5: 2328 CA1 (3) and 2328 CA1 (4) artefact breakdown.

Grid name	Slag	Total slag weight (g)	Tuyère	Ceramic	Decorated ceramic	Undecorated ceramic
2328 CA1 (3) X/A	15	102.64g	4	242	23	219
2328 CA1 (4) XX/J	39	272.66g	5	304	20	284
Total	54	375.30g	9	546	43	503

4.2.1.6: Artefacts recovered from the Road surface collection

This collection represents EFC artefacts, from ceramic fragments to slag, and represents the scale of artefacts and material which had been washed into the road (Appendix A: Table A10.13 and Table 4.6).

Table 4.6: Road surface collection artefact breakdown.

Name	Slag	Total slag weight (g)	Tuyère	Ceramic	Decorated ceramic	Undecorated ceramic
Alex Collection	37	872.43	6	83	32	51

4.2.2: Metal artefacts, slag and tuyère

4.2.2.1: Metal artefacts

In 2010, a metal artefact was recovered during the excavation (2328 CA1 57). During the 2013 excavations, two artefacts were recovered, one in 2328 CA1 (2) XIII/F/S and the second in 2328 CA1 (3) X/A/3A. Three more artefacts were found on the surface of Thaba Nkulu hill by the farm manager, and were handed to the excavation team. Although they were found out of context, these artefacts were still used in the analysis, as they represent artefacts from the area. In total, six metal artefacts have been recovered and analysed for this project, three of which were copper and three were iron-based. The iron artefacts recovered are: the iron arrowhead (Figure 4.45), the iron spear base (Figure 4.46), and the iron tang (Figure 4.47). The three copper artefacts retrieved consisted of 2328 CA1 (2) XIII/F/S thin wire earring (Figure 4.48), 2328 CA1 (3) X/A/3A thick copper wire (Figure 4.49) and 2328 CA1 57 copper earring (Figure 4.50).

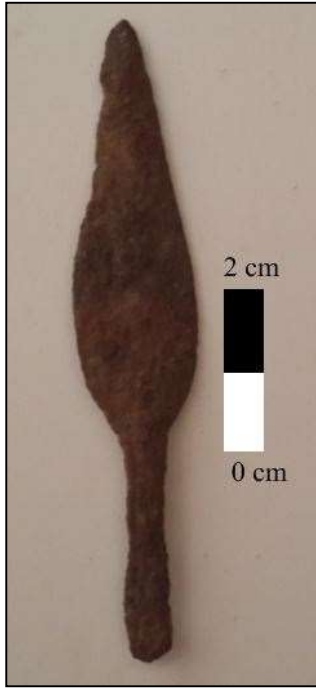


Figure 4.45: Iron arrowhead.

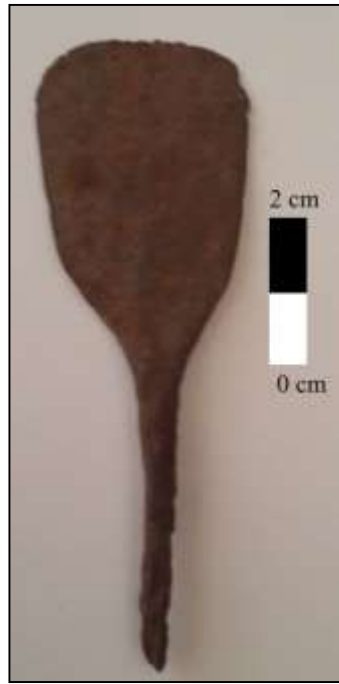


Figure 4.46: Iron spear base.



Figure 4.47 Iron tang.



Figure 4.48: Copper thin wire earring.

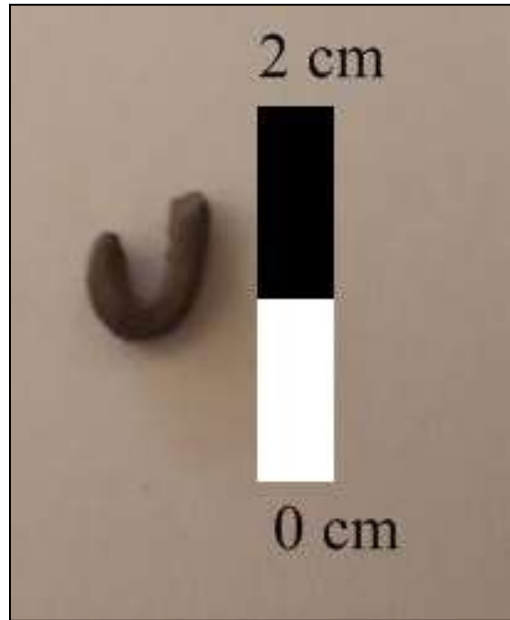


Figure 4.49: Thick copper wire.



Figure 4.50: Copper earring (2328 CA1 57).

4.2.2.2: Slag

The bulk of the analyses, however, were conducted on slag found on site. In total, 11,113 pieces of slag were found, weighing a total of 50 672.51g. The slag recovered varied in size and weight, from large chunks weighing 374.95g to small fragments weighing less than 1g. Out of the total number of slag, 196 pieces were randomly chosen and tested using XRF, and of the 196 pieces 12 were examined in the SEM. The results of both XRF and SEM are discussed in Chapter 7.

4.2.2.3: Tuyère

Tuyères were collected as they form part of the smelting or smithing process (more so smelting, as very few are needed to heat coal for hot working (smithing), and therefore, were considered metal smelting and smithing material culture. The bulk of the tuyères were recovered from excavation 2328 CA1 (1) XX/M (7171 fragments and broken pipes). The tuyère found throughout 2328 CA1 maintained an internal diameter of ~5cm (Figure 4.51), and varied in length (Figure 4.52). One tuyère found on excavation 2328 CA1 (10), however, had an internal diameter of ~10cm (Figure 4.53), and a length twice the size of other recovered tuyère pipes (Figure 4.54). The difference in diameter might be due to the different fragments coming from different parts of the tuyères, which are often tapered. In total, 7807 pieces or pipes of tuyère were recovered during excavations.



Figure 4.51: Small tuyère (viewed across the width/diameter) from excavation 2328 CA1 (1).



Figure 4.52: Small tuyère (viewed along the length) from excavation 2328 CA1 (1).

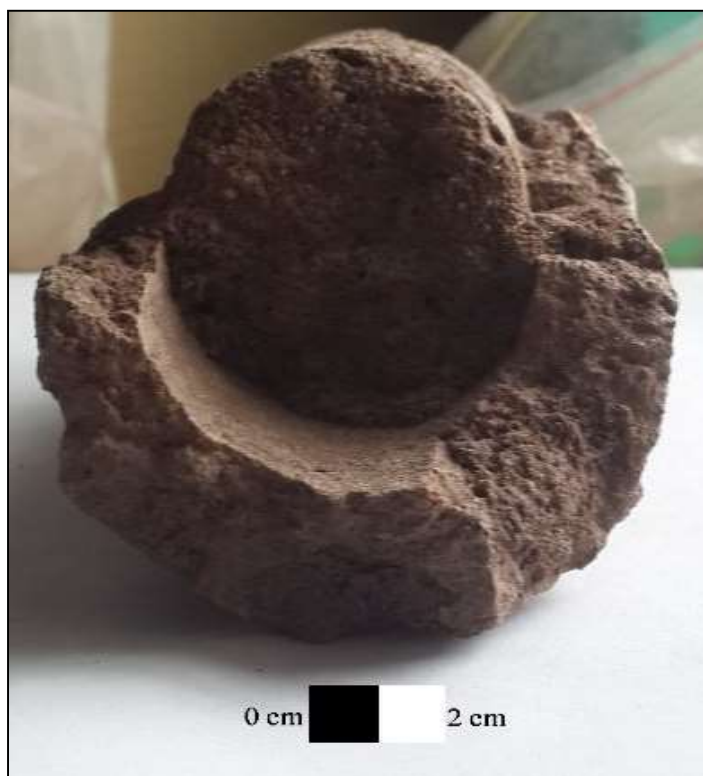


Figure 4.53: Large tuyère (viewed across the width/diameter) from excavation 2328 CA1 (10).



Figure 4.54: Large tuyère (viewed along the length) from excavation 2328 CA1 (10).

4.2.3: Ceramic fragments

Ceramics contributed the third largest artefact category from this excavation, with a total of 1648 ceramic sherds being recovered. A total of 170 were decorated, and 1478 were undecorated. The undecorated ceramics contributed 90% of the ceramics; these included rims, necks, and bodies. The decorated ceramics constituted only 10% of the total ceramics. All ceramics rim thicknesses were measured, and where less than 10mm they were considered thin, and over 10mm as thick (Appendix A: Table A10.2 – A10.13).

The ceramic decorations varied and included: punctates, incisions (Figures 4.55, 4.58, 4.62, 4.66 and 4.67), cross hatching (Figure 4.65), comb and ladder stamping (Figures 4.56, 4.57, 4.59, 4.63, 4.64 and 4.67), protrusions, ochre and black dye (Figures 4.56, 4.57), and herringbone (both impressed and incision) (Figures 4.56, 4.60, 4.61). These various decoration styles are associated with EFC communities. The ceramics can be associated to a specific style, namely Diamant (formerly known as RU 1) (cf. Hall 1981: 27-33; Huffman 2007: 223 - 230). Specifically Figures 4.61, 4.65 and 4.67, which resemble RU 1 ceramics recorded by Simon Hall (1981: 31-33). Due to Figures 4.56 and 4.60 containing herringbone designs, not associated with the broadly incised herringbone attributed to the Diamant facies (Huffman 2007: 225), there is a possibility that these fell within the transitional period between Diamant – Eiland facies.

This project focused on EFC artefacts. Thus, all LFC artefacts (which could be distinguished as such e.g. Moloko ceramic sherds) were noted as present, but not included in this dissertation. The LFC ceramics were found on the roads surface, or nearing the hill side slopes. This was to be expected, as their possible origin was likely to be the LFC site on the hill to the north of the road (Figure 1.1).

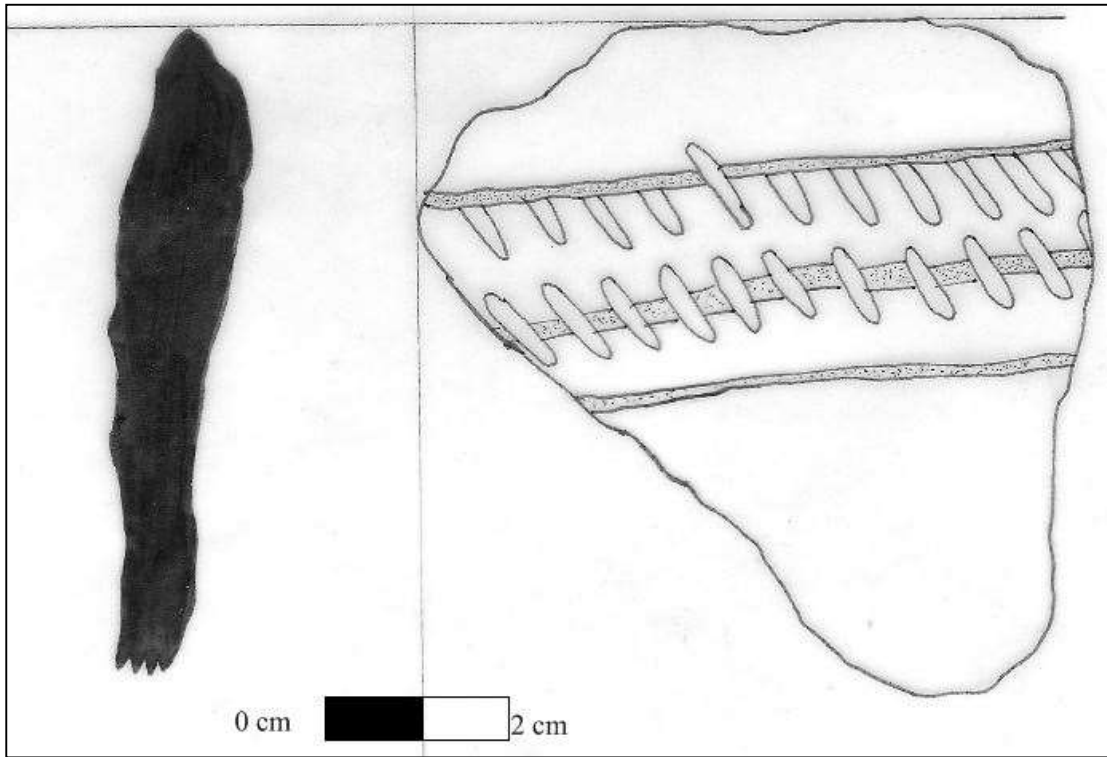


Figure 4.55: 2328 CA1 (3) X/A/3B ceramic with incision decoration.

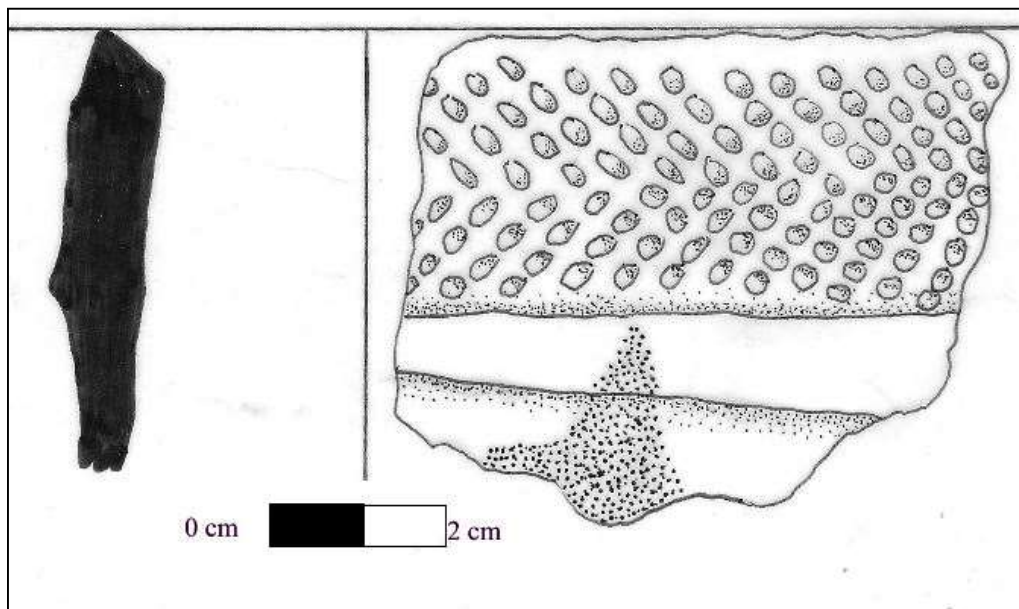


Figure 4.56: 2328 CA1 Road collection 4 ceramic with herring bone impressed decoration, burnishing on a raised surface.

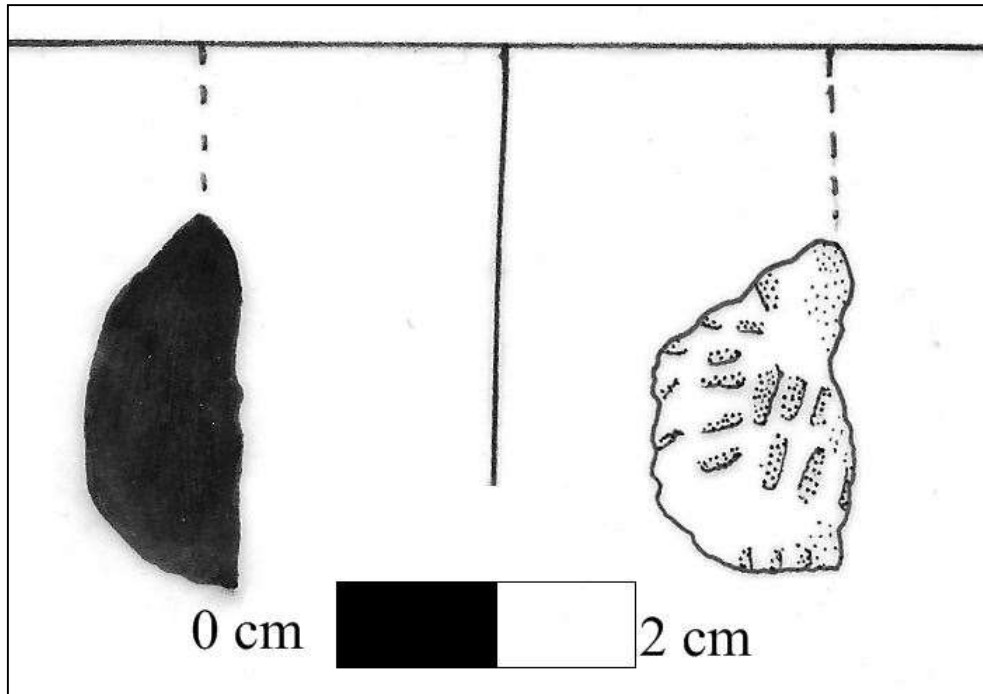


Figure 4.57: 2328 CA1 (2) XIII/E/2B raised bump with impressed decoration.

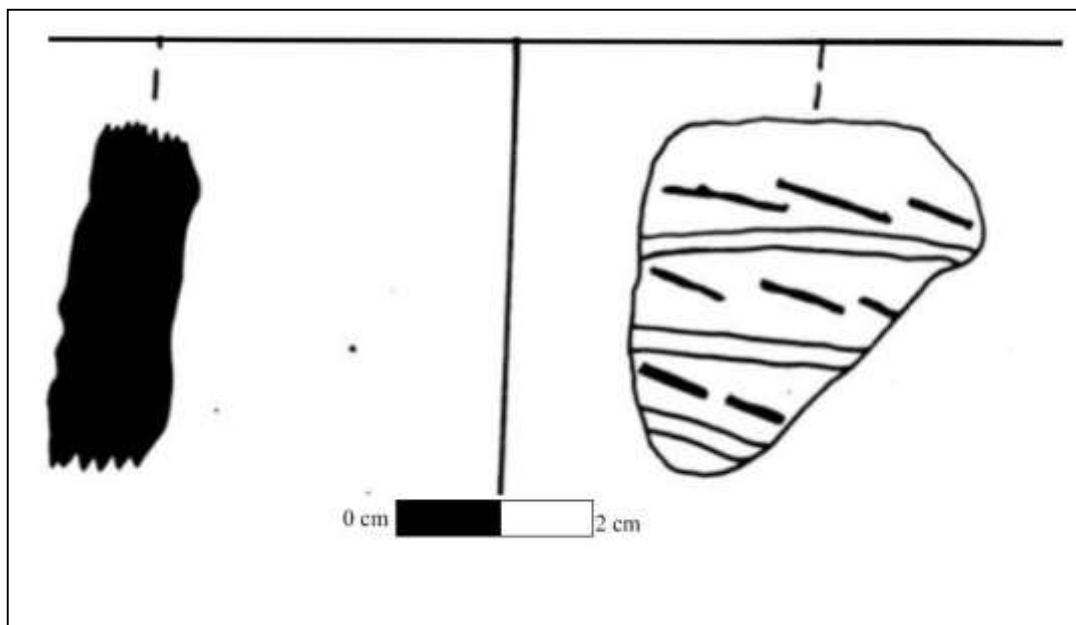


Figure 4.58: 2328 CA1 (3) X/A/5A body section, with diagonal and horizontal incision lines.

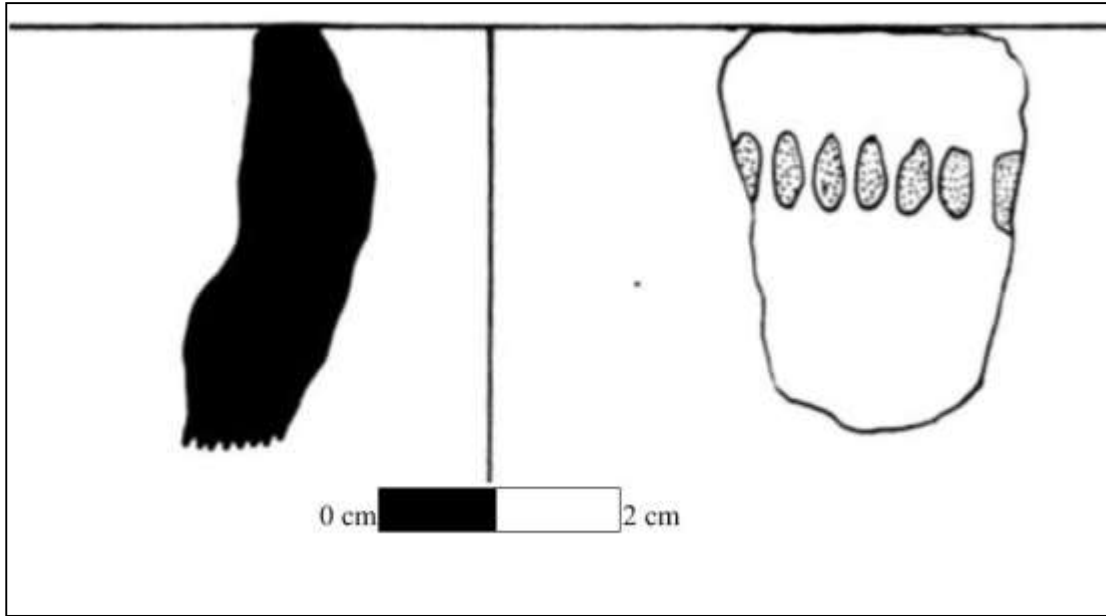


Figure 4.59: 2328 CA1 (4) XX/J/3A punctates below rim.

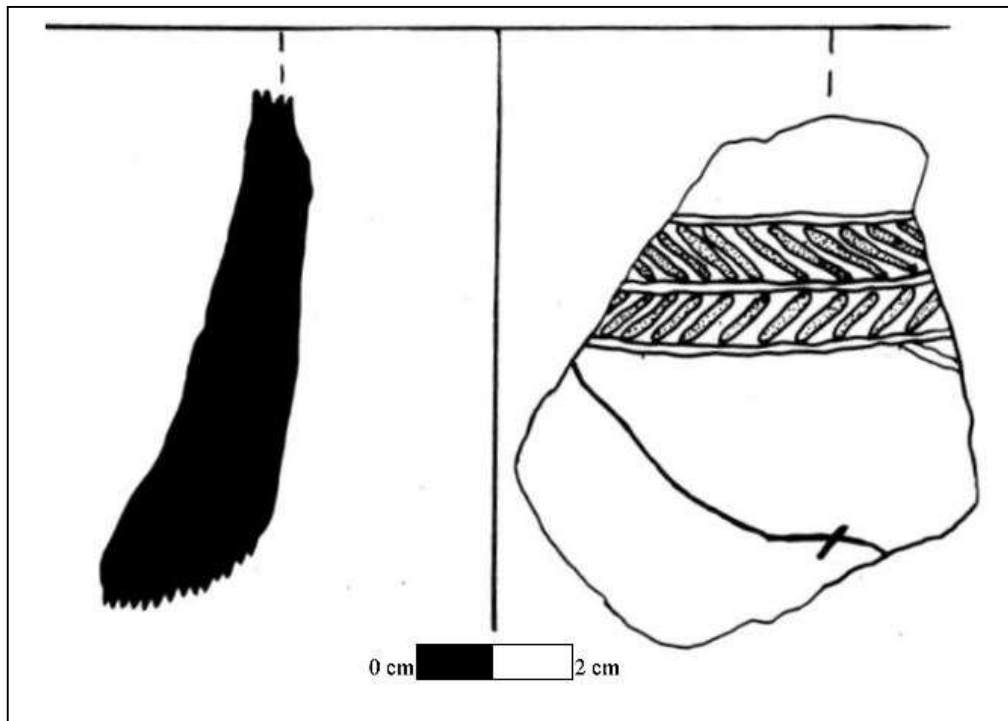


Figure 4.60: 2328 CA1 (3) X/A/3B herringbone incision with incision running diagonally down the body, with a slight incision line.

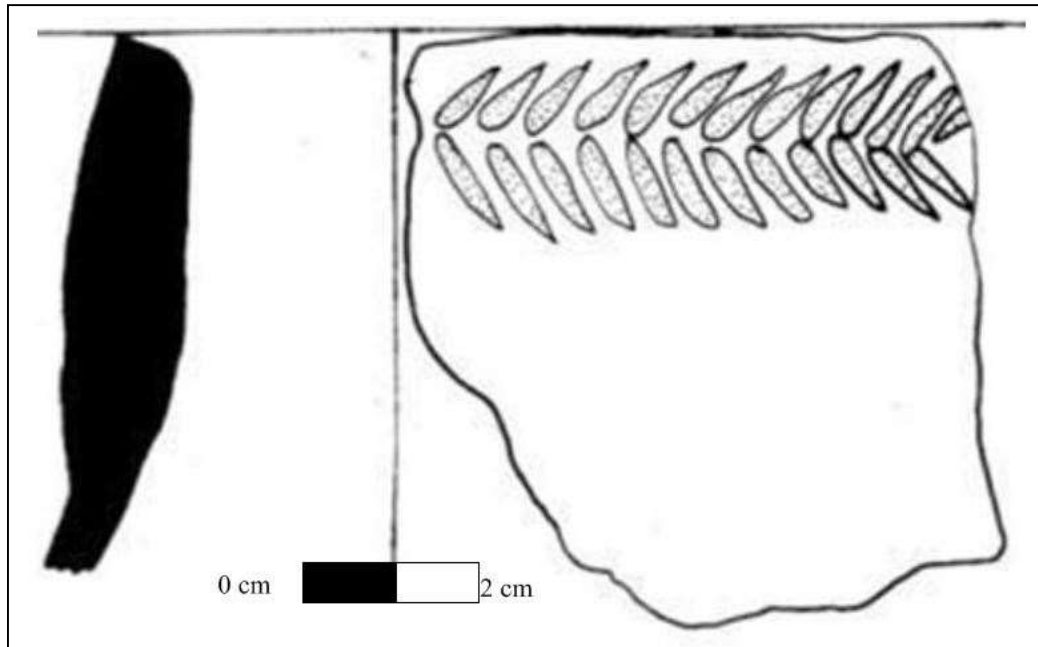


Figure 4.61: Wash down from 2328 CA1 (10) IX/G/S herringbone incisions.

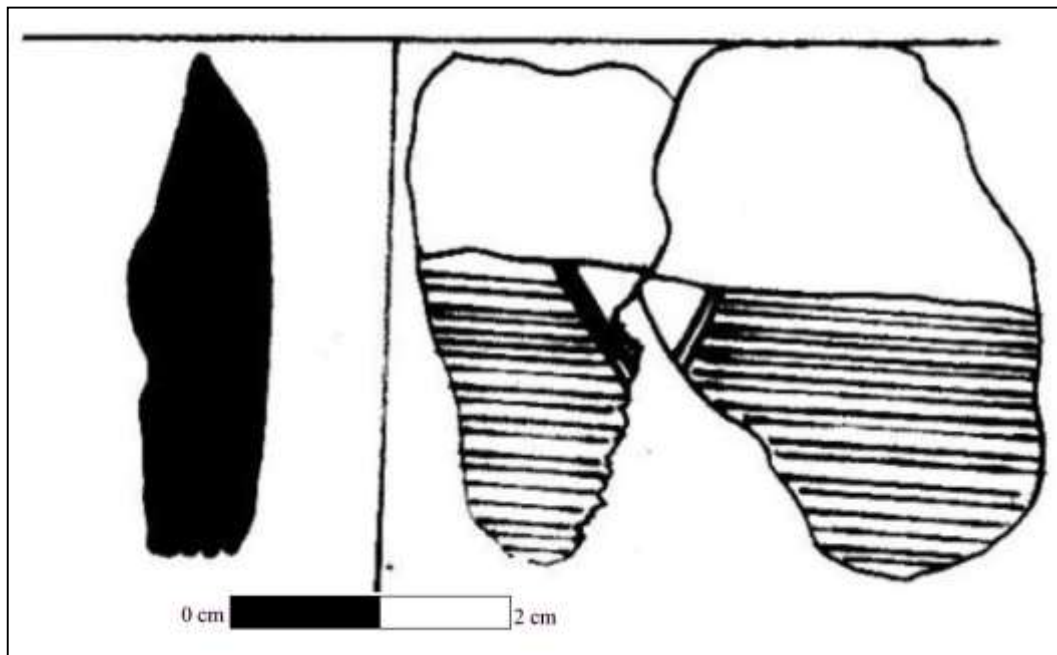


Figure 4.62: 2328 CA1 (4) XX/J/4A two pieces of ceramic, with multiple horizontal incision, with apparent V separation design between.

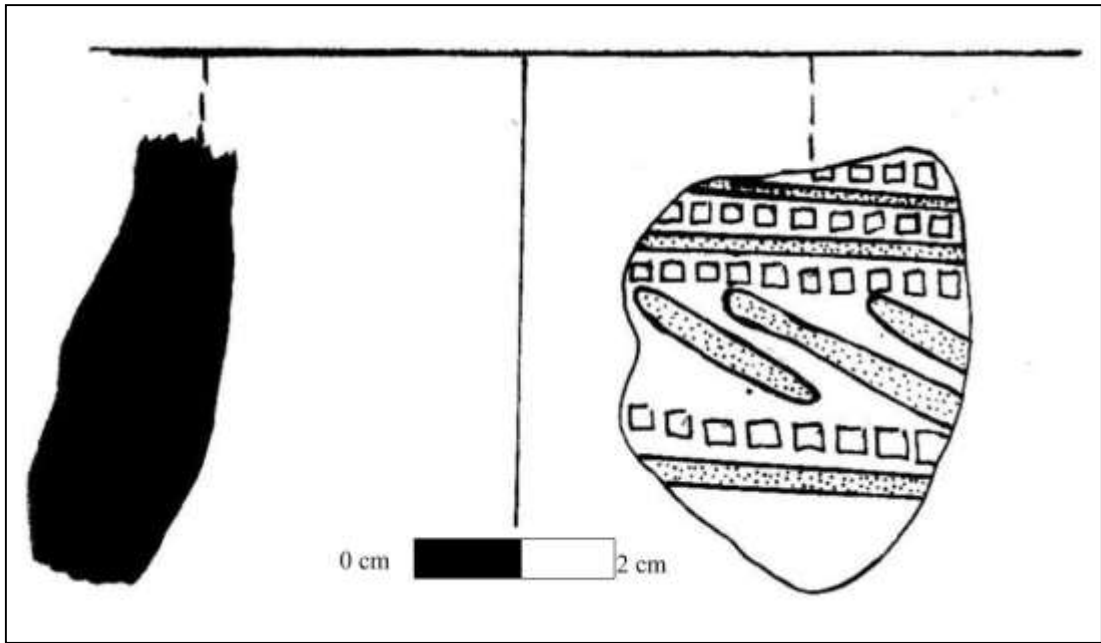


Figure 4.63: 2328 CA1 Road collection 3, comb stamping with diagonal and horizontal incisions.

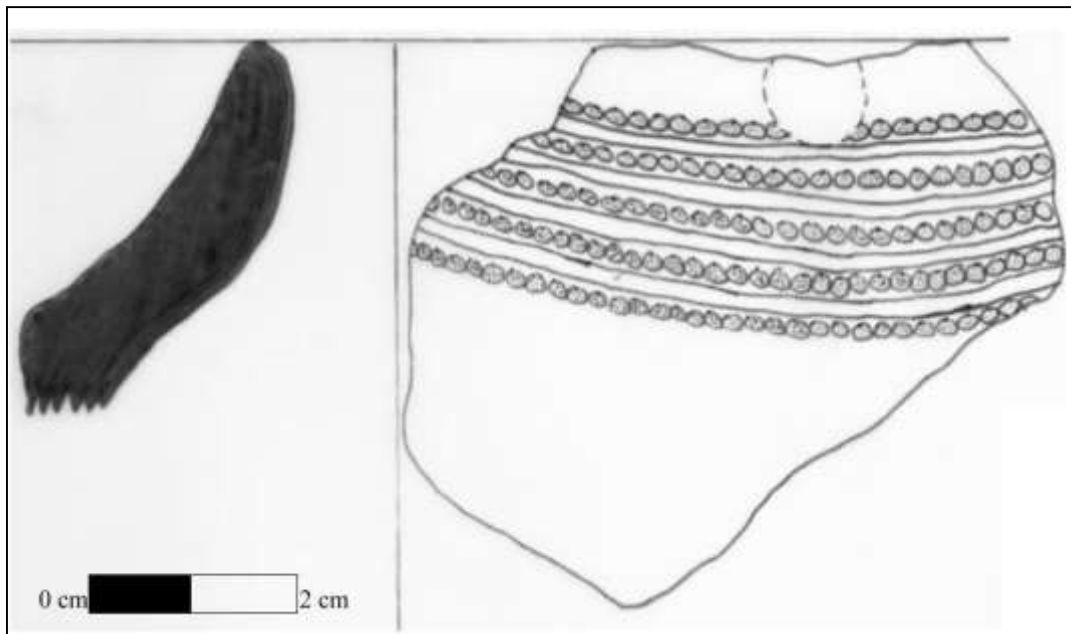


Figure 4.64: 2328 CA1 Road collection 18 multiple bands of comb stamping, separated by incisions.

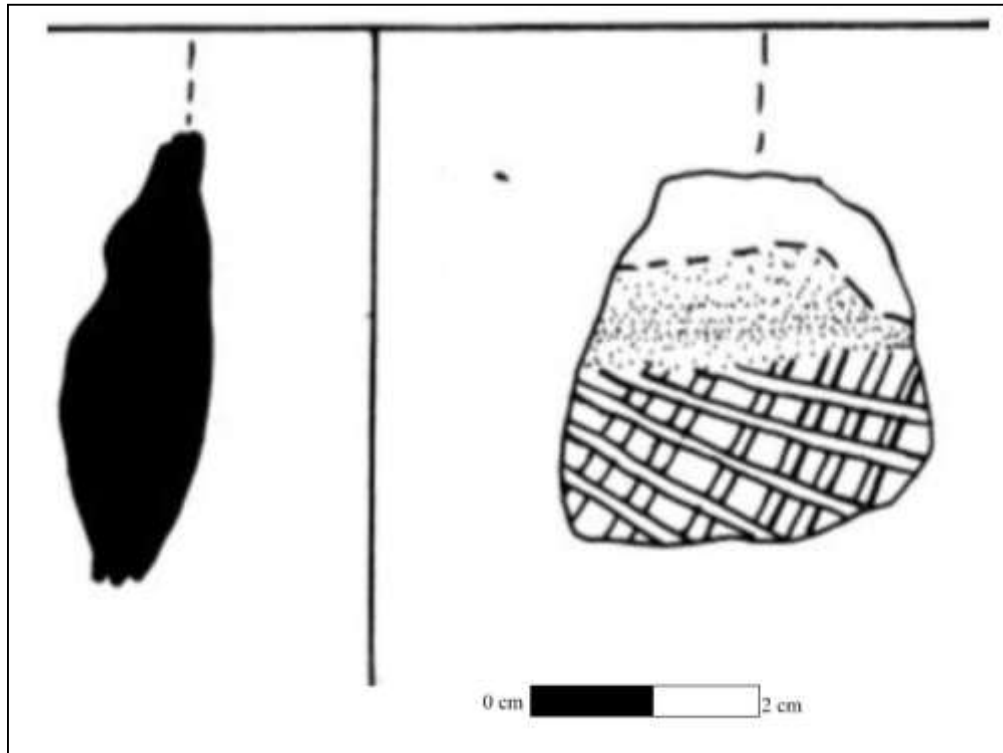


Figure 4.65: 2328 CA1 Test Pit 2 cross hatched decoration.

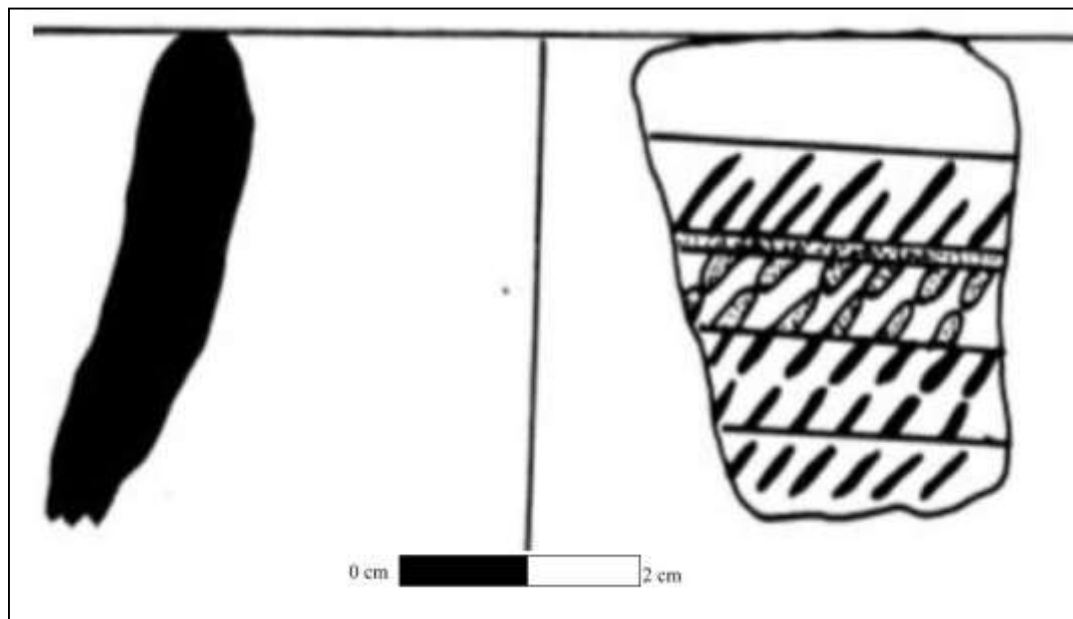


Figure 4.66: 2328 CA1 (4) XX/J/3A multiple incisions varying in width, with some containing separate diagonal slashes.

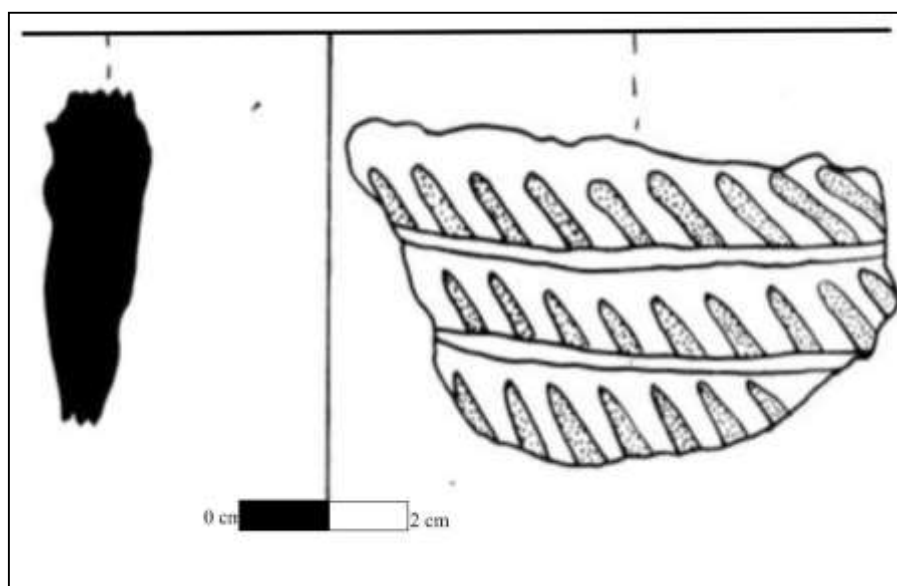


Figure 4.67: 2328 CA1 (4) XX/J/2B multiple lines of diagonal incisions, separated with horizontal incisions.

4.2.4: Charcoal

Charcoal was collected on site and was recorded from layers below ~20cm. It was then stored in tin foil, and weighed. Although charcoal was removed from most excavations, it was decided that the slag dump excavation 2328 CA1 (1) charcoal should be used for dating. The results given in Table 4.7 show that a total of 40.60g of charcoal was recovered from excavation 2328 CA1 (1).

Table 4.7: Charcoal weights.

Excavation, square and spit	Weight (g)
2328 CA1 (1) XX/M/3A RG + 3B	14.50
2328 CA1 (1) XX/M/4A Tuyère layer (grey)	10.51
2328 CA1 (1) XX/M/4B Tuyère layer (grey)	3.20
2328 CA1 (1) XX/M/5A (grey- tuyère pipes)	6.47
2328 CA1 (1) XX/M/5B + 5B BH	4.78
2328 CA1 (1) XX/M/6A	1.14

4.2.5: Other material culture

4.2.5.1: Baked sand

Although small in number, baked sand samples were recovered from excavation 2328 CA1 (1). The consistency of the sand did not match the soil in which it was discovered. Thus, it had been placed in the excavation area probably with smelting debris. As baked sand is being attributed to belonging to either the furnace wall or surrounding sand, it falls under possible smelting or smithing material.

4.2.5.2: Faunal remains

The faunal remains recovered from site 2328 CA1 varied in shape and size, scattered across the excavation sites. Faunal finds included: teeth, long bones and mandibles, although the species were not recorded, as faunal analysis did not form part of this project. The teeth were identified as coming from the family *Bovidae*, possibly antelope.

4.2.5.3: Beads

Two types of beads were recovered from the site, two glass beads and four ostrich egg shell beads. The glass beads were found near the surface levels in excavations along the road (2328 CA1 (2) and 2328 CA1 (10)). This suggests that they washed into the site, from the LFC site on the hill above the EFC site. The ostrich egg shell beads were found on the same road, although they also were found in lower levels of excavations 2328 CA1 (2) and 2328 CA1 (10). This could mean they were part of Early Farming Community deposit.

4.2.5.4: Orange compact soil/daga

Orange compact soil/daga was retrieved from excavation 2328 CA1 (1), although it was also present in the roadside excavations (2328 CA1 (2) and (10)). Whether it came from a hut floor or another possible source is not known, as too little was discovered, and only in small chunks.

4.2.6: Dating

4.2.6.1: Radiocarbon dating

Charcoal removed from the site was weighed and stored appropriately in the laboratory before analysis. For standard radiometric dating, at least 20g of charcoal is needed. Consequently, it was decided that the charcoal from 2328 CA1 (1) XX/M/3A RG + 3B and 4A should be combined, which would create the larger than 20g sample needed for dating. The charcoal from 2328 CA 1 (1) XX/M/6A was sent for AMS dating as it represented the lowest layer excavated, and only 1.14g of charcoal was recovered. In this way, the upper layers and lower layer would represent the active timeline of occupation, during which the slag dump was created. The samples were sent to Beta Analytic.

For 2328 CA1 (1) XX/M/3A RG +3B and 4A the conventional radiocarbon age was 1060 ± 30 BP = 982 – 1145 AD (2 Sigma / 95% probability (Beta – 375130)), for 2328 CA 1 (1) XX/M/6A the conventional radiocarbon age was 930 ± 30 BP = 1045 – 1220 AD (2 Sigma / 95% probability (Beta – 375131)).

Conclusion:

Excavations at Thaba Nkulu (site 2328 CA1) yielded valuable research data. The ceramic sherds recovered, indicated that the EFC occupation was aligned to the Diamant – Eiland cluster. This period was supported by the radiocarbon dates, which placed the occupation and use of the site at the end of the first millennium AD, and therefore attributed to the Eiland facies occupation (Huffman 2007; Bandama *et al.* 2015). The area and the material recovered (ore, slag, metal artefacts, ceramics, tuyère, beads and daga) showed a probable long occupational period. The amount of metal artefacts recovered implied that the site could have been independently creating their own metal artefacts.

CHAPTER 5: EXCAVATIONS AND ARTEFACTS

DISCUSSION

Introduction:

This section of the dissertation deals with the interpretation of the site and artefacts pertinent to the chemical signature analysis. The first section engages with the fieldwork results and creates an interpretation of the excavations. It then puts forward the argument for engaging in the spatial belief debate regarding smelting location on Thaba Nkulu. The second section expands on the artefacts recovered from excavations and provides some detail pertaining to what they are and where they may have fit in Thaba Nkulu's spatial configuration.

5.1: Excavations, meanings and interpretations.

5.1.1: Introduction:

In the previous chapter, the five excavations performed on Thaba Nkulu were presented in terms of what was discovered, recorded and retrieved. Using this as context for each location, the interpretation of not only the excavation areas, but also the site as a whole can be made.

5.1.2: 2328 CA1 (2) and 2328 CA1 (10) road pits, an indicator of the homestead

Excavation 2328 CA1 (2) was originally thought to be a midden, due to a patch of grey soil covering a large surface area. During excavating, the grey soil coverage decreased and became focused in one square only. As such, it was assumed that the reason for the large coverage was possibly due to erosion, and thus this was not a midden, but a pit. The second excavation, 2328 CA1 (10) started as a rescue excavation, but was expanded to include excavating a large tuyère pipe. At the base of the tuyère pipe, the ash grey surface soil, which covered the surface layers, seemed to go deeper into the stratigraphy. After the retrieval of the proximal tuyère pipe, excavations continued into a secondary grid which contained another pit.

Both excavation pits had the same stratigraphy, as both started with a red hard soil. The only difference was soil type, which contained either a grey soil or a grey ash soil. Artefacts retrieved were similar, showing that the pits came from the same occupation, and as such, were linked to the same period.

The secondary aim of this project was to understand the spatial configuration of the site. In order to do this, one would need to identify the homestead features, such as a kraal or hut floors. Neither of these, however, were discovered and alternative evidence was required. In this event, alternative homestead associated deposits, such as pits or middens (Evers *et al.* 1982) can be used to ascertain the relative position of the homestead.

The difference between the two pits was their depths. The pit in excavation 2328 CA1 (2) caused the grey ash to spread on the surface, whereas that in 2328 CA1 (10) was only discovered after ~10cm. This shows that the possible original surface had eroded away higher up on the road, which meant that all identifiable signs of huts might have been destroyed. This effect was also seen by Evers (1980) on the Klingbeil site in Lydenburg, where two truncated pits were discovered with shallow depths, which led to the belief that the village horizon had been destroyed.

Both excavation pits 2328 CA1 (2) and (10) had no full ceramic vessels within them, but such vessels were rescued by Schoeman and Wadley in 2010. Similar with the pits recorded by Evers *et al.* (1982), the Thaba Nkulu pits circumferences were narrow, unlike grain pits (Hall & Maggs 1979), suggesting that these were not grain storage pits. Instead due to the mixed contents both domestic and metal associated material culture, these pits were likely the waste deposits of homes (Greenfield & Miller 2004). With the limited circumference, these pits were most probably used by individual houses and not the entire homestead.

Evers *et al.* (1982: 29) showed that without direct evidence of structures, the contents and relative position of pits can be used to determine where the pits were situated in the homestead area. With the large scattering of domestic material across the road's surface (both EFC and LFC ceramics), it is possible that some of this material may have washed out from these pits. Due to the dense concentration, however, not all material on the road's surface could have washed out from the pits alone. Instead, it is proposed that these pits were created within the homestead area, and this is the reason for the dense concentration of material culture and artefacts on the road surface.

Furthermore, small portions of *in situ* ceramic clusters were identified and mapped across the road's surface, and as with the excavations 2328 CA1 (2) and (10), these scatterings are presented as possible pits. This indicates that the road area was previously based on the periphery of the huts, within the homestead, due to the amount of identified clusters, and the discovery of two pits in close proximity to one another. The pits discovered in excavations 2328 CA1 (2) and (10), as well as the possible pits along the road, all indicate the homestead position on site. The artefacts retrieved were of mixed material culture, which indicates that the pits were not used as storage pits (Maggs & Michael 1976; Evers *et al.* 1982), but instead were likely small waste disposals for houses. In combination with the sheer amount of domestic artefacts in the vicinity of these pits, the pits were likely to be within close proximity to the homes, or based on the homestead periphery.

The presence of LFC ceramics, however, can be used as an indicator of the spread of artefacts on the road. The nearest LFC settlement is on the hill to the north of the road. This is the probable origin of the LFC material. The LFC material was scattered and found on the surface, unlike most of the EFC ceramics found *in situ*. The presence of the LFC artefacts gives an indicator as to how much material could have shifted over time.

5.1.3: The occupation layer

Excavations 2328 CA1 (3) and (4) represented the occupation layer of this project. The first excavation, 2328 CA1 (3), contained a possible rock circle or cluster of rocks in the north-west corner of the grid. The use of the circle is unknown. No ash or charcoal was recovered within the circumference or along the parameter, ruling out its use as a fireplace. Ceramic sherds, however, were found at the base of the rocks, suggesting its possible use as an elevated storage area (Huffman 1990b: 8, 2000: 16).

A large amount of ceramic sherd artefacts were retrieved from both excavations. The sheer quantity of which was greater than seen on any of the other excavations, 2328 CA1 (1), (2), and (10). The concentration of domestic material is the key to explaining this area. Within the pits described earlier, the link between the pits being near homestead house was made due to the material found within (cf. Maggs & Michael 1976; Evers *et al.* 1982). Excavations 2328 CA1 (3) and (4) contained large amounts of domestic material. The material culture, however, was not situated in “pit” like holes on these excavations. Instead, they were scattered across each layer and were found in specific stratigraphic layers below ~20cm, indicating the original ground on which settlements were built. This indicates a possible settlement horizon.

Due to both social and ritualistic meaning of ceramics (Hall 1987), they are more likely to be recovered within the settlement area, than elsewhere. If they were broken, the pieces were sometimes placed into pits or middens near settlement huts, or on the periphery of the homestead area (Evers *et al.* 1982). As the bulk of ceramics were recovered from the last few layers in both excavations, they were probably left on the surface. A metal artefact (one copper thick wire) and metal smelting or smithing associated material culture (slag) was retrieved as well. The slag was smaller than those found in excavation 2328 CA1 (1), perhaps this was due to it being smithing slag, as smithing has been considered to take place within the homestead area, and in most cases amongst houses (cf. Huffman 1990b; Miller & Whitelaw 1994; Miller 2002; Hall *et al.* 2006).

5.1.4: The site overall

With three zones recognised as individual sections of a homestead, a hypothetical map was made (Figure 5.1). This map shows the possible boundaries of the homestead, and surrounding areas. If the domestic zones are mapped, and a circumference is placed around them, they fall within a circular zone. This zone comprises the domestic area, which includes houses, pits and domestic associated material culture, and can be claimed part of the homestead. Following this, the results of the test pit and surface finds were mapped. These create a buffer zone and allow for the possible tracing of erosion or the wash down of artefacts across the site. These zone areas indicate that the homestead could have been situated east of the smelting area. When the smelting area is mapped, it appears to fall on the outskirts of the domestic zone, which is not uncommon (cf. Maggs 1980a; Miller & Whitelaw 1994; Hall *et al.* 2006).

The area where the pits were discovered had a large concentration of homestead associated material culture. The material found had indicators of belonging to EFC occupants. The ceramic styles found on site are recorded and presented in Figures 4.9 - 4.21, Chapter 4. The radiocarbon dates collected from excavation 2328 CA1 (1) showed that the area falls within 1060 ± 30 BP = 982 – 1145 AD (2 Sigma (Beta – 375130)), and 930 ± 30 BP = 1045 – 1220 AD (2 Sigma (Beta – 375131)). These dates correspond with the end of the Diamant phase and start of Eiland phase (Huffman 2007: 223-230). The ceramic styles, however, correspond with mainly Diamant traditions (Hall 1981; Huffman 2007; Bandama *et al.* 2015).

Thus, the interpretation of the site is that of an EFC settlement. Based on the radiocarbon dates, as well as the ceramic styles recovered, the site was occupied during the later part of the EFC period. The artefacts and pits reveal the possible periphery of the homestead area. Surrounding these areas were a few ceramic clusters, however, these were all based on the surface, and could be attributed to washouts or erosion.

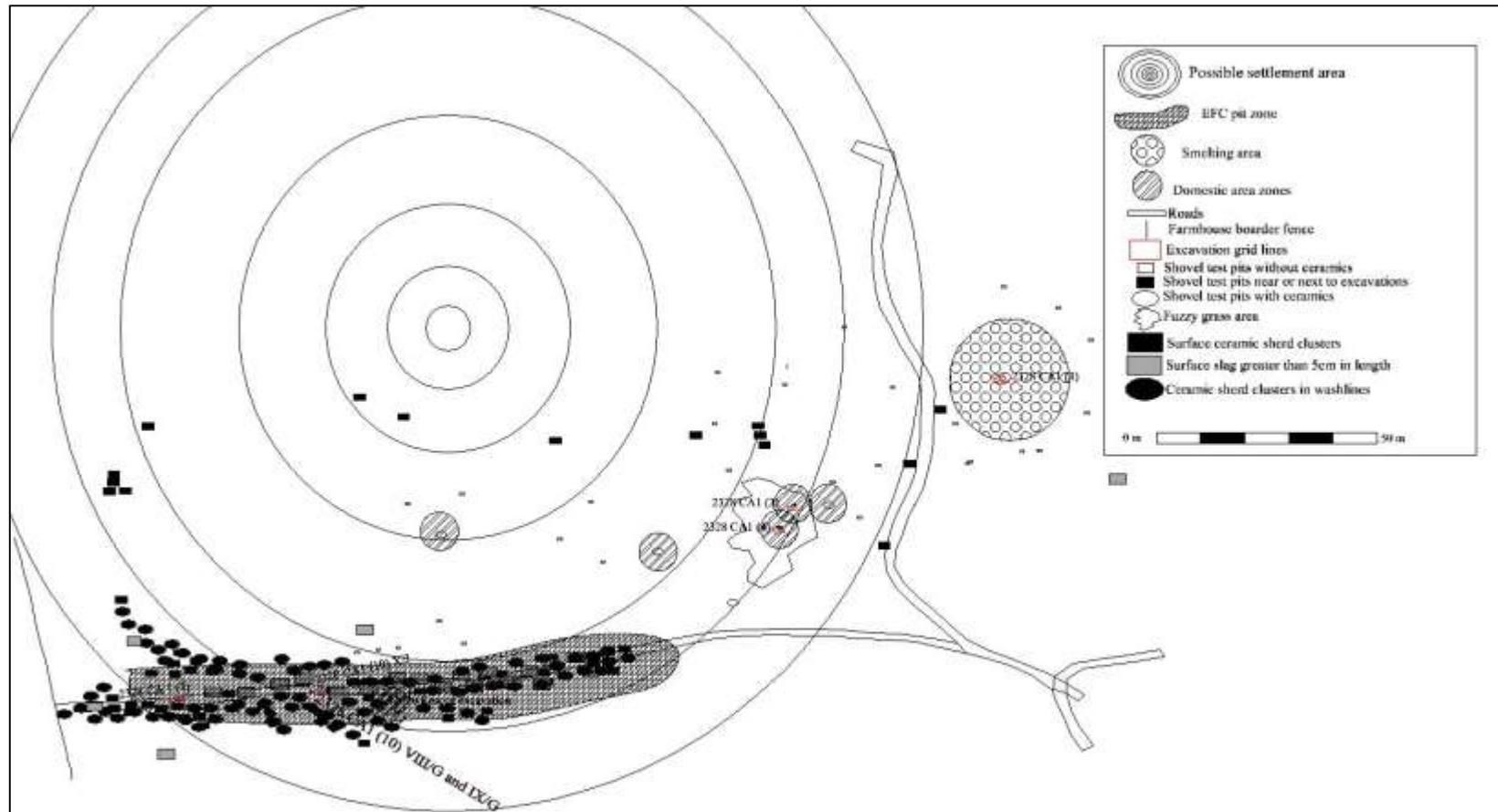


Figure 5.1: Possible area zones, indicating homestead area relative to smelting site.

While it is not possible to conclusively state that the slag dump represent the smelting area, it is likely that the smelting site excavated was placed just beyond the confines of the housing area.

This counters views that smelting was performed in seclusion away from the homestead, due to ritualistic beliefs (cf. Huffman 1990b, 1993). It also, however, showed that the smelting area did not necessarily fall within the domestic portions of the homestead (cf. Maggs 1980a, 1992), as no evidence was found which could directly link smelting within the domestic zones. Instead, the smelting area appears to be situated on the edges of the homestead (cf. Hall et al. 2006).

5.1.5: Excavation 2328 CA1 (1), the slag and tuyère dump

As described in the previous chapter, excavation 2328 CA1 (1) recovered numerous material associated with EFC metal production. With the presence of slag and tuyère discovered in all excavated squares, the extent of the material was assumed to expand beyond at least a 3m x 2m area. Within the excavation, very little homestead associated material culture was discovered, whilst the majority of artefacts recovered were associated to metal smelting or smithing. The artefacts recovered included slag, tuyère, furnace wall, ore and daga. Of these, slag comprised the most recovered artefact, which led to the excavation being termed a “slag dump”. Although other artefacts such as tuyère, daga and baked sand (furnace wall) were recovered as well, they were lower in number than the slag.

Contextually, archaeologists have used different terms to describe piles of slags, such as “slag dump” (Greenfield & Miller 2004), “slag mounds” (Goucher 1981), and “slag heaps” (Maggs 1980a, 1992; Maggs & Ward 1984; Rehren *et al.* 2007). These definitions are used to describe metal smelting or smithing waste collected and / or placed in specific areas. Unlike pits or middens, where mixed waste or domestic waste was placed (ceramics, fauna, beads, slag and tuyère), slag dumps contain mainly metal smelting or working and very little homestead associated material, such as ceramic

sherds. There is a debate, however, over whether these large piles are associated with smelting activity (Maggs 1992:66), or whether they can belong to smithing (Miller & Whitelaw 1994). With the large amount of slag and tuyère being discovered during excavating, the excavation area was likely to have been used repeatedly as a dump site. The main argument for this debate centres on furnace discovery. The furnace allows for definitive evidence in support of the smelting argument, however, when no furnace is discovered, the argument becomes a debate. On Thaba Nkulu, no furnace was discovered during the excavation process. The sheer amount of material recovered, however, suggests that smelting took place in the nearby area. The possible reason for lack of a furnace discovery could stem from the fact that during the EFC period furnaces were destroyed after smelting (Miller 2002; Greenfield & Miller 2004). This destruction is another reason why very little is known about metal working practices, during the EFC period.

Maggs (1980a: 121) discovered large heaps of slag in the Msuluzi Confluence, and as with Thaba Nkulu, no furnace was discovered. Due to slag and ore heaps discovered, Maggs (1980a) associated the area to being a smelting site, without the use of a furnace. Some archaeologists, however, such as Duncan Miller and Gavin Whitelaw (1994: 80) have experienced lack of furnace discovery, but state that without evidence of a furnace, no direct evidence can be used to verify if the debris are of smelting or smithing in nature.

With these two opposing arguments, a secondary method is needed to back up claims of whether sites without furnaces can be smelting or smithing sites. Through the examination and identifying of materials recovered, the argument for this excavation belonging to a smelting area can be strengthened.

Using the materials recovered such as slag, tuyère, daga and furnace wall, the argument for the support of interpreting excavation 2328 CA1 (1) as being part of a smelting site can be made. Although these materials can be found on both smelting and smithing

sites, there are differences which separate them. The slag recovered was large in both size and quantity. Maggs (1992: 66) suggests that smelting sites can be identified through “large blocks of fired clay from the walls of furnaces, often showing vitrification on the inner surface, large quantities of slag including some of fist size or larger as well as iron ore”. The slag recovered comprised varying sizes, from some only a few centimetres in length, to some greater than 10cm. Baked sand was also recovered, which could possibly have been furnace wall, as it was recovered amongst the slag, as well as ore. The ore would not be required on a smithing site, although it could be found within a general dumping area.

One artefact type not mentioned in Maggs’ (1992) list are tuyères. Tuyères are present on both smelting and smithing sites, although there are differences found amongst them. Tuyère fragments and broken pipes were recovered during the excavation, with some tuyères having slag filling the inner core and outer surface of the tuyères. If this slag dump was a smithing area, there would be no need to re-heat iron to the point of liquidation, to work on the metal (Miller 2001: 96). Numerous pieces and pipes of tuyère were recovered with slag coatings from Thaba Nkulu’s 2328 CA1 (1) excavation area. This suggests that the tuyère came from a smelting site, and not smithing.

Most of the slag recovered was identified as being wüstite (discussed in Chapter 8), and thus poor quality, as large amounts of iron remained in the slag (Miller *et al.* 1995: 41). This could possibly be the reason why large amounts of slag were recovered (large amounts needed to ensure the necessary iron quantities). Another interpretation for the large amounts of slag could be due to the production requirements for the settlement area (cf. Chirikure *et al.* 2010: 80). If Thaba Nkulu was part of a trade network, which is suggested by the copper artefacts, perhaps they produced more iron than was needed locally, and the balance was traded. Unfortunately, due to the presence of very few metallic artefacts, the production related questions could not be addressed at present. This, however, still does not indicate as to why the large amounts of slag were recovered in this specific area.

One possible explanation could be that the slag was carried in substantial quantities to this location post smelt (Miller 2002). Although if it was a general metal associated dump or smithing area, there would be some form of evidence relating to smithing. In the case of Thaba Nkulu's excavation 2328 CA1 (1), there was no evidence of smithing related material recovered.

The sheer volume of waste found on excavation 2328 CA1 (1) would suggest that smelting took place relatively close by, and due to the EFC post smelting furnace break down, the furnace would be relatively hard to find. Thus, with no specific evidence of smithing material culture found in excavation 2328 CA1 (1), and although slag may be carried in substantial quantities, it does not account for all the smelting associated material recovered. As such, it can be concluded that the excavation area of 2328 CA1 (1) is probably related to the smelting zone of Thaba Nkulu, and with further excavations, the likelihood of furnace discovery or furnace bowl lining could be discovered, proving that 2328 CA1 (1) can be claimed as a smelting area.

5.2: Main artefacts recovered interpretations

5.2.1: Introduction:

Before site interpretation and a chemical signature can be discussed, it is imperative that the artefacts retrieved are interpreted and discussed, due to their chemical signature possibly being affected by what they represent or where their place was in the production line. Some archaeologists, such as Coustures *et al.* (2003), state that a chemical signature can be acquired, as long as all material is retrieved.

5.2.2: Metallic smelting and smithing materials

5.2.2.1: Slag

Slag comprised the most collected artefact and main metal smelting or smithing material culture recovered from the site. The slag retrieved, however, contained no indicators of whether it was from smelting or smithing. The identification of slag type

was problematic, as context plays an important role in the identification of slag type (Miller & Killick 2004). In Chapter 2 (Table 2.1) Miller and Killick's (2004) categories of slag identification (smelting slag, tabular slag, frothy glassy slag and indeterminate slag) were presented, however, the identification process is more complex. On a visual appearance, the slag collected from excavation 2328 CA1 (1) appeared to fall within the smelting slag category, as the majority appeared to be large chunks, with vesicular portions (Figure 5.2).

The secondary type that, by visual identification, appeared to be flow slag (Miller 2001, 2002; Miller & Killick 2004; Hall *et al.* 2006; Chirikure 2007), as the slag contained an appearance of flowing out and solidifying (Figure 5.3). Both types of slag are associated with smelting (Chirikure 2007: 92). Slag found outside of excavation 2328 CA1 (1), varied in size and some differed in structure. The size difference was most noted, as most pieces were smaller (Figure 5.2) than those recovered from excavation 2328 CA1 (1) (Figure 5.3).



Figure 5.2: Smelting slag, recovered from excavation 2328 CA1 (2).



Figure 5.3: Flow slag, recovered from 2328 CA1 (1).

Due to the lack of furnace discovery, the slag types could only be assumed based on the general categories given by Miller and Killick (2004). Alternative context, however, was used to strengthen the slag type identification. Although no furnace was discovered within excavation 2328 CA1 (1), the sheer amount of slag recovered indicates a possible smelting dumping ground (cf. Maggs 1980a: 121). Contextually, the slag found in excavation 2328 CA1 (1) was found with numerous material culture also associated with smelting (ore, tuyère and furnace lining). With this in mind, the slag recordings from both the XRF and SEM tests were analysed, to see if they could aid in the identification of the slag, as performed by Miller and Killick (2004), to see whether the argument for interpreting excavation 2328 CA1 (1) as a smelting area could be strengthened.

5.2.2.2: Iron artefacts

The three iron artefacts recovered (as discussed in the previous chapter), the iron arrowhead (Figure 4.45), the iron spear base (Figure 4.46), and the iron tang (Figure 4.47), represented the final product in the metal production *chaînes opératoires*. Due to them being handed over from the farm manager their association could not be made, however, they represent part of the metal production on site.

5.2.2.3: Copper artefacts

Of the three copper artefacts retrieved (Figures 4.48 – 4.50), the first two artefacts (the copper thin wire earring and the thick copper wire) were collected during the 2013 excavation, whereas the latter (copper earring 2328 CA1 57) was collected during the 2010 rescue excavation. Unfortunately, no copper slag was recovered during the excavation, and the copper ore retrieved was mainly recovered on the surface and shallow sub-surface levels. As such, the complete production phase of copper (if it occurred) from Thaba Nkulu could not be examined at this time, preventing any sort of chemical signature analyses of copper from Thaba Nkulu. Their presence on Thaba Nkulu, however, allows for possible connections to trade networks or future research into copper production on site (cf. Bandama *et al.* 2013).

5.2.3.1: Tuyère

The smaller tuyère pipes were similar in shape and size to those found on the Early Farming Community site of the Msuluzi Confluence (Maggs 1982: 134). These small tuyère fragments contained either a glass covering, due to high temperatures causing the clay and sand to melt and create glass, or a slag coating (Figure 4.52). The larger tuyère (Figures 4.53 and 4.54), was probably the “flare” end of the pipe, where the bellows were attached (Schmidt 1997: 63). The diameter and length matched the description of the “flare” end, as well as the lack of an iron slag coating or the presence of glass (due to heat) on this tuyère. The numerous amounts of tuyère fragments recovered from excavation 2328 CA1 (1), show the level of production on site (cf. Hall *et al.* 2006; Chirikure 2007). In order to produce such large quantities of slag, tuyères were needed for every smelt and smithing production process (Childs 2000: 213).

5.2.3.2: Ore

Two types of ore were recovered during the excavation process, iron ore (Figure 5.4) and copper ore. The copper ore, as previously stated, was commonly found on the surface, with very few or small ore stones found in excavations. Although copper

artefacts were recovered, the ore could not be associated to their creation. The iron ore, however, could be linked to the slag found on site. This gave a direct link between the source material and production phase of the material. As such, focus was placed on iron ore over copper ore, as a means to record Thaba Nkulu's chemical composition.



Figure 5.4: Iron ore from Thaba Nkulu.

Following this chapter, the dissertation will present the laboratory analysis, beginning with the methods and techniques used to identify the chemical composition of the recovered artefacts. It will then reveal the results of these analyses, followed by a discussion. Chapter 9 will then concluded on both the excavation and XRF and SEM-EDS findings.

CHAPTER 6: LABORATORY METHODOLOGY

6.1: Analysis of samples

6.1.1: XRF Analysis

In order to see which elements the metal artefacts of Thaba Nkulu comprised, the University of the Witwatersrand's Geology Department's portable X-ray Fluorescence spectrometer (XRF) was used. XRF was used since previous research had been done on identifying chemical composition, which was successful using XRF (cf. Miller & Killick 2004; Chirikure *et al.* 2010). The XRF analysis allowed for multiple testing, and provided results based on a pre-determined setting. These results would either give an element weight percentage or parts per million in terms of elemental consistency within an artefact. There were two types of XRF instruments, the first being the XRF station (unfortunately this was not available at the time) and the second the portable XRF instrument. Both would give accurate results, although the necessary artefact preparations between the two differ. The station was more destructive and time consuming, due to the process requiring the crushing of an artefact, then mounting the powder onto a pellet, and finally a longer time period for testing.

For this project, access to the XRF station was not available because this project would have taken too much time from other projects (of the researchers using the XRF). As such, the portable XRF had to be chosen, which allowed for more results in a shorter time, as well as being non-destructive (Shugar 2012: 17). The portable XRF was only able to detect elements with an atomic number of 12 (magnesium) and above. Elements with an atomic number less than 12 could not be recorded and the remaining undetected percentage was grouped together as a balance of unidentifiable elements, which gives much higher errors. The main elements which contain an atomic number less than 12 were carbon and oxygen. Concerns, however, have been identified for the accuracy of the portable XRF (cf. Shugar 2013: 180). To address these concerns, and increase the expected accuracy of the portable XRF results (Shugar 2012: 18), certain procedures were applied. These included noting of the detection limits (Aimers *et al.* 2013),

polishing important specimens to make them flat, placing the specimens on top of Mylar film (directly over the sensors) in an enclosed mount stand, so that lost x-rays were limited (because some x-ray have very small penetration distances (Pollard *et al.* 2006)). It was recognised that this was a surface technique (cf. Pollard *et al.* 2006), but the surfaces were newly-prepared (sectioned and polished on some) and did not include pottery glazes or corrosion (Aimers *et al.* 2013). Fortunately, although calibration against iron standards was not done (iron being the most common and the most major element), the instrument calibrated itself prior to each batch of samples of similar types. Calibration is especially important for samples with uneven surfaces (because the x-rays can get lost), but as some samples were ground flat, this would reduce the errors, and also render specific calibration less important (cf. Pollard *et al.* 2006). Since the samples were not ground and re-constituted for analysis using an added binder, there was no need to calculate the ROI (loss of water) in the samples (Chirikure *et al.* 2010; Bandama 2013).

6.1.1.1: XRF preparation

Before the XRF analysis was performed, and due to time constraints on the use of the equipment, 217 samples were selected from the recovered artefacts. Where possible, three samples were taken from each spit in a grid, per site. Most of the samples consisted of slag, while the rest were tuyère and ore. Another specification for samples chosen was that they should have at least one flat surface. The flat edge would allow the XRF analysis to scan a large area of the sample (without further sample preparation), thus yielding a more accurate result (Shugar 2013: 180).

When XRF analyses are performed, samples are usually ground up into a powder, and then pressed into a powder pellet or cut polished and mounted before analysis (e.g. Chirikure *et al.* 2010; Sheikh *et al.* 2010; Shugar 2013). In this investigation, however, it was decided that grinding samples and reducing them to a powder could result in cross-contamination (cf. Eivindson & Mikkelsen 2001), so the samples were left intact. The mounting, grinding and polishing of samples would prevent large sample groups,

and as such this too was decided against (except for some). Therefore, most samples were not prepared with what is being recommended as a standard preparation when using XRF. It is also stated, however, that this method is costly and would require destructive methods on artefacts (which was avoided intentionally), but the standard would produce sufficiently accurate results for qualitative and quantitative analysis (cf. Pollard *et al.* 2006; Shugar 2013). The samples, however, would still produce results that could be used in the identification of a chemical signature, but would include some contaminants, which would have to be identified and removed during the results phase of testing. Instead, all samples were washed in water and the surface soils removed with a nail brush. The removal of the soils and other sediments was pivotal, as the XRF would identify these elements and corrupt the data (Sheikh *et al.* 2010). Following this, the samples were then placed into plastic containers with dividers to separate them and create an effective sorting system.

6.1.1.2: XRF testing

The XRF used for analysis was the Niton handheld portable XRF XL3 GOLDD+ edition. Prior to each analysis, a system check was performed. The device performs its own check and calibrates itself for testing. There are various types of testing methods, soils, minerals and a mixture of both. For the discovery of trace elements, all types can be used. The soil analysis would present the recording in parts per million (ppm), whereas the minerals would present the recordings in a percentage base.

Using the soils and minerals test, with mining element specifications, the mining copper and zinc (Cu/Zn) test was chosen. It was the best suited to identify the trace elements and represent elements found as a percentage of the entire sample.

Each sample was analysed for 200 seconds. This allowed for the various high, medium and low angle beams of X-rays to penetrate the sample, and record both the micro-elements and macro-elements within the sample. Micro being elements under 2% of a sample, and macro being greater than 2%.

The beam was a 10mm diameter circle, meaning samples less than 10mm would incur a high balance reading, because there would be signals collected from the region surrounding the sample (cf. Pollard *et al.* 2006). A balance reading also occurred when samples contained large pores, or uneven surfaces instead of flat ones, since the body of the sample would not be directly on top of the beam section. A possible source of contamination, although minor, was the silica transfer from hands to sample. This is also a form of cross-contamination and although it impacts on the recorded data, it is not enough to alter the results significantly. It would add a minor increase to the silica percentage (Sheikh *et al.* 2010).

6.1.2: Scanning Electron Microscope Analysis

The XRF data was supplemented by Scanning Electron Microscope (SEM) data. In this study, the University of the Witwatersrand's Faculty of Engineering and the Built Environment, Sigma Zeiss field emission SEM was used. Within archaeology, there are numerous ways to test for a material's chemical composition, the most common of which are XRF and SEM (Miller *et al.* 1993; Miller & Killick 2004; Koursaris *et al.* 2007; Chirikure *et al.* 2010). Through the use of the Energy Dispersive X-ray Spectrometer (EDX) inside the SEM, further evidence of chemical composition would be recorded and added to the results, recording further chemical compositions of metal manufacturing materials from Thaba Nkulu. The combined analysis of XRF and SEM allowed for the detection of all elements in a sample.

The EDX functions in a manner similar to the XRF: both instruments analyse and bombard samples with electrons, which cause the emission of X-rays which are captured and analysed to allow for the chemical composition to be obtained (Miller & Hall 2008). The SEM's ability of detection, however, does not allow for the detection of trace elements, whereas the XRF does (Pollard *et al.* 2006: 111-113). Thus, the combination of the two instruments was paramount.

6.1.2.1: SEM preparation

Before the SEM analysis could take place, the samples had to be prepared. Unfortunately, size and shape of samples have to be uniform for SEM analysis (cf. Pollard *et al.* 2006). Samples had to be small enough to fit inside the specimen chamber. With the possibility of sand or dust particles still remaining on the samples, there were concerns about contaminating the instrument. This meant that some of the samples had to have sections cut off. For these artefacts, small areas were cut off using a steel blade hacksaw. As the blade was steel, this would help in identifying any cross-contamination, if any occurred. The sections were then mounted for analysis in the SEM. For other artefacts, crushing was used as a secondary method. By crushing a sample, a fraction of a piece could be taken, instead of a small cut off section. Both cut and crushed samples were then blown with compressed air. This could lower the chances of small loose particles remaining and allow for the samples to be placed into the SEM without further preparation.

The main concern with crushed samples being placed directly into the SEM was the risk of charging. Due to the nonconductive nature of some materials, normally a conductive coating is placed on them to prevent charging and the potential loss of data through radiation or thermal damage (cf. Goldstein *et al.* 1981: 461). It was decided that the cut samples should be mounted (cf. Buchwald & Wivel 1998) and prepared, following standard metallographic standards.

The second step of preparation was finishing, grinding and the polishing. As the sample had just been mounted, the samples surface was covered with Bakelite, so the Bakelite, was ground back, which removes some of the samples' surface.

A Rockwell delta finishing belt with a grit of 80 was used. As the belt spun, the sample was placed on the surface and rotated 90 degrees at a time until it was fully rotated. This left the surface of the Bakelite removed, leaving a Bakelite and artefact surface.

The third step was grinding, which was done sequentially on three different grades of grinding paper. The first had a grit of 200, the second 600 and finally 1000, until the surface was fully smoothed. Whilst grinding to create the smooth surface, the paper was washed with water (to remove the debris) and grinding was done in a clockwise movement.

Following the grinding, came the polishing. In order to obtain a smooth surface, polishing was performed using a rotating wheel and a slushy mixture of still water and 1 micron thick aluminium powder, placed on it. The mounted sample was then firmly rotated on the wheel in the opposite direction from the wheel direction until most of the slush was gone. Finally, the sample was removed, any excess slush rinsed off, and dried with high powered compressed air or ethanol.

6.1.2.2: Etching

The final stage of preparation is known as etching, which is the reaction of an etchant with the sample to view the differences in chemical composition under a microscope. Through etching, the different components (with different chemical compositions) become visible under a microscope (Miller & Killick 2004; Koursaris *et al.* 2007; Miller & Hall 2008; Chirikure *et al.* 2010). In this way, materials can be identified pre-SEM by optical microscopy. Etching was not performed on all the samples, but only on the metal artefacts and a few pieces of slag and ore.

Through drawing on the XRF data, separating the material was easier, since each element requires a different solution to etch it. For iron/steel based material, 3% Nital was used. For iron/steel, the artefact was dipped into the 3% Nital for a few seconds (~5 seconds).

The copper alloy artefacts needed a polish attack in order for etching to take place. The FeCl_3 was mixed with 1 micron aluminium powder and a small amount of water on

emery paper, and then the artefact was placed on this and polished in a clockwise direction making small circular motions.

Once metallographic preparation was finished, the samples were placed on a digital light microscope, to check if sufficient etching had occurred.

6.1.2.3: Optical microscopy

For the optical microscopy, a Leica DM 6000 M was used. This in combination with the Leica DFC 490 camera enabled the identification of microstructures, as well as to allow for the captured image to be further analysed. This project used 5x to 50x magnification.

6.1.2.4: SEM analyses

The working distance for the EDX had to be 8.5mm, as any higher would not produce accurate results. This meant that the specimen samples had to be small enough to be moved around and positioned inside the SEM, as different height specimens would risk damaging the internal lens. The EDX was used to determine the elements of the sample. The working distance was the machine manufacturer's optimal working distance.

During analysis, a few samples began charging, due to them not being covered in a conductive coating. Coating had been decided against, in order to achieve accurate sample data. Due to the charging, it was suggested that the samples could be tested by using a different SEM, an EDAX SEM, under the same conditions as the Sigma Zeiss. The same testing was performed on the initial charging or charged samples. This time, however, charging was reduced and the EDX analysis could be performed. The results of which were similar to the Sigma Zeiss systems results.

6.1.3: Conversion of results

In order to identify possible chemical signatures, the XRF and SEM results were compared to selected research results (cf. Miller & Killick 2004) from around southern Africa. Results may vary in output description, e.g. in oxides such as FeO, and this dissertation's results were recorded in terms of elements, e.g. Fe. The results, both current and other researchers', needed to be compatible for comparison. Consequently, the results were converted using a factor conversion, when necessary.

The factor conversion followed Molecular weight and conversion factors (<http://www.geol.umd.edu/~piccoli/probe/molweight.html>). When necessary, this project's element results were multiplied by their respective factor to determine their oxide results, whereas other researchers' oxide results were divided by their respective factors, to obtain non-oxide element percentages. This conversion to oxides was performed on the XRF results, shown in Appendix C.

CHAPTER 7: XRF AND SEM RESULTS

7.1: XRF findings

7.1.1: Introduction

For X-ray fluorescence (XRF), the elements detected in the metallurgical analysis were separated into low percentage proportions and higher percentage proportions. Any element above 2% in the sample was considered a higher percentage element, whereas <2% but >0.01% was considered a low percentage element. In total, 220 samples were analysed using XRF. The XRF results were then separated into 5 sections of artefact type: slag (Tables 7.1-7.2 and Figures 7.1-7.2), tuyère (Tables 7.3-7.4 and Figures 7.3-7.4), ore (Tables 7.5-7.6 and Figures 7.5-7.6), iron artefacts (Tables 7.7-7.8 and Figures 7.7-7.8), and copper artefacts (Tables 7.9-7.10 and Figures 7.9-7.10). Appendix B: Tables B11.1 – B11.28 contain a full and detailed list of each excavation and layer samples. Appendix B: Figures B11.1 - B11.40 contain bar charts of the low and high proportion percentage elements from XRF of each excavation's grid. The tables in the appendix section contain the unaltered percentages, and include contaminants not usually associated with furnace thermodynamics. The tables and figures represented in this section were created using elements associated with furnace thermodynamics, as well as, elements seen to be considered trace elements (cf. Coustures *et al.* 2003: 603; Miller & Killick 2004: 36-45; Blakelock *et al.* 2009: 1747-1751; Chirikure *et al.* 2010: 1659-1661; Bandama 2013: 149, 274-277; Bandama *et al.* 2013: 255).

Appendix C: Tables C12.1 – C12.10 contain the converted oxide and normalised results of these elements. Appendix C: Figures C12.1 – C12.10 contain bar charts of each sections converted oxides and normalised XRF's low and high proportion percentage elements. In the discussion section (Chapter 8), selected elements were used to put forward arguments, it is from the non-normalised results that the arguments were created. Where necessary, the elements were converted into oxides, to create or match other researchers' results.

The purpose of these tables is to present the elements found within the different metal associated material culture. At the end of each table, the average and standard deviation are given. The range of variation in testing is shown, and the lower the standard deviation, the more consistent were the sample recordings. The dash symbol (-) in the tables represents elements either too low to detect, or values of zero. Elements which could not be recorded by the XRF were all placed into a percentage group called Bal (Balance), which was included in the non-normalised sections.

7.1.2: Slag

The slag samples were the largest sample group, with 196 samples. From the collection of slag, approximately three slag samples from each excavation layer were analysed. The elements detected in the slag samples were constant, with very little deviation. Table 7.1 displays the low proportion percentages of elements found in the Thaba Nkulu slags. The minimum elements were: barium (Ba), strontium (Sr), copper (Cu), nickel (Ni), cobalt (Co), iron (Fe), manganese (Mn), chromium (Cr), vanadium (V), titanium (Ti), calcium (Ca), potassium (K), phosphorus (P), sulphur (S), and magnesium (Mg). Elements such as Ba, Sr, Co, Ni, and Cr are considered by Coustures *et al.* (2003: 605) as trace elements not commonly associated to the main compositional elements found in slag. Some archaeologists such as Miller and Killick (2004) consider Cr to form part of the main composition. The tabulated results were then placed in a bar chart Figure 7.1.

The high proportion elements discovered were: Fe, Ca, K, aluminium (Al), P, silicon (Si) and Mg, as well as the balance (Bal), and are represented in Table 7.2. These too are represented on a bar chart in Figure 7.2, which shows the high proportion elements. From the graph the number of samples containing an element can be seen as well. Some elements, such as Fe, Ca, K, P, and Mg, were recorded in both the low proportion and high proportion percentages. These elements, however, were either high values in the low proportion sections or low values in the low proportion sections, e.g. Fe, and so could be in either group.

Mention must be made about three artefacts: 2328 CA1 (1) XX/M/4B, 2328 CA1 (2) XIII/F/S (2) and 2328 CA1 (4) XX/J/2A 35-40 (2). Due to physical appearance, texture and in some cases weight, it was assumed that these three artefacts were slag, and they were tested together with the slag samples. It was only after their compositions were recorded that these three artefacts were identified as being slag-like material (cf. Miller and Killick 2004: 24), due to them containing small amounts of slag < 10%, and high silicon amounts, making these artefacts non slag. They are included in Table 7.1, but will not be included in the XRF and SEM discussion chapter.

Table 7.1: XRF slag results, low proportion percentages in wt%.

Artefact slag	Bal	Ba	Sr	Cu	Ni	Co	Fe	Mn	Cr	V	Ti	Ca	K	P	S	Mg	Total
2328 CA1 (1) XIX/N/S	-	0.04	-	-	-	-	-	0.03	0.06	0.02	0.07	0.28	1.08	0.11	0.07	-	1.76
2328 CA1 (1) XIX/N/S (2)	-	0.03	-	-	0.02	-	-	-	0.05	0.04	0.06	0.16	0.75	0.08	0.1	-	1.29
2328 CA1 (1) XIX/N/S (3)	-	0.05	-	-	0.03	-	-	0.02	0.07	0.06	0.14	0.36	0.82	0.1	0.04	1.45	3.14
2328 CA1 (1) XIX/N/AD	-	0.05	-	-	0.02	-	-	0.06	0.06	0.05	0.08	0.56	1.05	0.17	0.07	-	2.17
2328 CA1 (1) XIX/N/AD (2)	-	0.04	-	-	-	0.08	-	-	0.06	0.03	0.09	0.21	1.14	0.12	0.11	1.67	3.55
2328 CA1 (1) XIX/N/AD (3)	-	0.05	-	-	-	-	-	0.07	0.04	0.06	0.16	0.61	1.82	0.27	0.09	1.76	4.93
2328 CA1 (1) XIX/N/2A	-	0.05	-	-	-	0.16	-	0.06	0.03	0.04	0.26	1.13	-	0.24	0.27	1.55	3.79
2328 CA1 (1) XIX/N/2A (2)	-	0.04	-	-	-	-	-	0.05	0.05	0.09	0.24	0.98	-	0.21	0.05	1.22	2.93
2328 CA1 (1) XIX/N/2A (3)	-	0.11	0.02	-	0.01	-	-	0.13	0.04	0.05	0.22	1.74	-	0.45	0.13	1.71	4.61
2328 CA1 (1) XIX/N/2B	-	0.06	-	-	0.01	-	-	0.06	0.04	0.06	0.27	-	1.55	0.45	0.1	0.88	3.48
2328 CA1 (1) XIX/N/2B (2)	-	0.04	-	-	-	0.17	-	0.09	0.04	0.04	0.25	0.54	-	0.57	0.08	1.99	3.81
2328 CA1 (1) XIX/N/2B (3)	-	0.13	0.04	-	0.02	-	-	0.07	0.03	0.02	0.26	-	-	0.14	0.15	1.75	2.61
2328 CA1 (1) XX/M/PERIMETER	1.14	0.07	0.01	-	-	0.05	-	0.11	0.07	0.04	0.16	-	1.33	0.26	0.1	-	3.34
2328 CA1 (1) XX/M/PERIMETER (2)	-	0.07	0.01	-	0.01	-	-	0.13	0.04	0.05	0.28	0.95	-	0.57	0.12	-	2.23
2328 CA1 (1) XX/M/PERIMETER (3)	-	0.09	-	-	0.04	-	-	0.05	0.05	0.04	0.11	0.36	1.37	0.4	0.14	1.17	3.82
2328 CA1 (1) XX/M/S	-	0.06	-	-	-	0.09	-	0.07	0.05	0.04	0.15	1.04	-	0.51	0.1	1.22	3.33
2328 CA1 (1) XX/M/S (2)	-	0.11	0.02	-	0.01	0.03	-	0.1	0.04	0.03	0.2	0.62	-	0.76	0.06	1.89	3.87
2328 CA1 (1) XX/M/S (3)	-	0.09	0.02	-	0.03	-	-	0.04	0.05	0.04	0.09	0.92	1.35	0.44	0.11	1.31	4.49
2328 CA1 (1) XX/M/1A	-	0.09	-	-	0.01	0.05	-	0.07	0.05	0.05	0.18	1.25	1.44	0.45	0.05	1.91	5.6
2328 CA1 (1) XX/M/1A (2)	-	0.07	-	-	0.03	-	-	0.06	0.05	0.03	0.11	1.29	1.62	0.26	0.08	-	3.6
2328 CA1 (1) XX/M/1A (3)	-	0.07	-	-	0.03	-	-	0.05	0.05	0.07	0.19	1.43	1.01	0.55	0.07	-	3.52
2328 CA1 (1) XX/M/1B	-	0.07	0.01	-	-	0.04	-	0.07	0.04	0.04	0.4	-	-	0.28	0.07	-	1.02
2328 CA1 (1) XX/M/1B (2)	-	0.08	0.01	-	0.01	-	-	0.07	0.07	0.09	0.49	1.7	-	0.78	0.08	1.71	5.09
2328 CA1 (1) XX/M/1B (3)	-	0.04	-	-	-	-	-	0.08	0.04	0.05	0.14	0.79	1.8	0.52	0.07	1.34	4.87

Artefact slag	Bal	Ba	Sr	Cu	Ni	Co	Fe	Mn	Cr	V	Ti	Ca	K	P	S	Mg	Total
2328 CA1 (1) XX/M/2A RB	-	0.06	-	-	-	-	-	0.04	0.06	0.08	0.15	0.78	1.24	0.24	0.07	-	2.72
2328 CA1 (1) XX/M/2A RB(2)	-	0.05	-	-	0.03	-	-	0.03	0.07	0.07	0.21	0.31	0.78	0.18	0.07	-	1.8
2328 CA1 (1) XX/M/2A RB(3)	-	0.05	-	-	-	-	-	0.07	0.04	0.05	0.25	1.13	1.81	0.31	0.08	1.85	5.64
2328 CA1 (1) XX/M/2B RG	-	0.06	-	-	0.01	-	-	0.03	0.07	0.11	0.32	0.61	0.72	0.16	0.04	1.83	3.96
2328 CA1 (1) XX/M/2B RG (2)	-	0.06	-	-	0.02	-	-	0.04	0.06	0.12	0.35	0.65	0.72	0.17	0.04	1.55	3.78
2328 CA1 (1) XX/M/2B RG (3)	-	0.06	-	-	0.04	-	-	0.05	0.05	0.03	0.07	-	0.81	0.09	0.1	1.84	3.14
2328 CA1 (1) XX/M/3A RG	-	0.04	-	-	-	-	-	0.02	0.05	0.03	0.01	0.22	0.61	0.21	0.24	0.79	2.22
2328 CA1 (1) XX/M/3A RG (2)	-	0.05	0.01	-	0.02	-	-	0.06	0.04	0.05	0.14	-	0.68	0.1	0.07	1.77	2.99
2328 CA1 (1) XX/M/3A RG (3)	-	0.05	-	-	0.02	-	-	0.04	0.07	0.08	0.1	0.93	0.49	0.14	0.05	1.52	3.49
2328 CA1 (1) XX/M/3B RG + BH	-	0.05	-	-	0.02	-	-	0.04	0.06	0.06	0.13	1.67	0.64	0.04	0.06	-	2.77
2328 CA1 (1) XX/M/3B RG + BH (2)	-	0.05	-	-	0.04	-	-	0.03	0.07	0.12	0.14	0.38	0.46	0.11	0.02	1.27	2.69
2328 CA1 (1) XX/M/3B RG + BH (3)	-	0.06	-	-	-	-	-	0.05	0.03	0.03	0.15	1.49	1.58	0.12	0.05	1.55	5.11
2328 CA1 (1) XX/M/4A tuyère layer (grey)	-	0.03	-	-	0.01	-	-	0.05	0.08	0.07	0.13	0.13	0.57	0.05	0.02	1.06	2.2
2328 CA1 (1) XX/M/4A tuyère layer (grey) (2)	-	0.06	-	-	-	-	-	0.05	0.03	0.05	0.13	0.72	1.54	0.15	0.06	1.83	4.62
2328 CA1 (1) XX/M/4A tuyère layer (grey) (3)	-	0.05	-	-	0.03	-	-	0.05	0.06	0.08	0.08	0.96	0.37	0.05	0.09	1.91	3.73
2328 CA1 (1) XX/M/4B tuyère layer (grey)	-	0.04	-	-	0.01	-	-	0.05	0.07	0.11	0.15	1.15	0.84	0.08	0.06	-	2.56
2328 CA1 (1) XX/M/4B tuyère layer (grey) (2)	-	0.06	0.02	-	0.03	-	-	0.03	0.06	0.07	0.06	0.49	0.83	0.19	0.12	1.25	3.21
2328 CA1 (1) XX/M/4B tuyère layer (grey) (3)	-	0.11	-	-	-	-	-	-	0.04	-	0.13	-	0.67	0.72	-	-	1.67
2328 CA1 (1) XX/M/5A (grey tuyère pipes)	-	0.06	-	-	-	-	-	0.04	0.05	0.1	0.29	-	1.16	0.07	0.06	1.12	2.95
2328 CA1 (1) XX/M/5A (grey tuyère pipes) (2)	-	0.08	0.01	-	-	0.15	-	0.08	0.04	0.03	0.25	1.05	-	0.15	0.07	-	1.91
2328 CA1 (1) XX/M/5A (grey tuyère pipes) (3)	-	0.04	-	-	-	-	-	0.05	0.04	0.08	0.18	1.02	-	0.15	0.06	-	1.62
2328 CA1 (1) XX/M/5B B + BH	-	0.07	0.02	-	-	0.13	-	0.07	0.04	0.05	0.19	1.42	-	0.12	0.08	-	2.19
2328 CA1 (1) XX/M/5B B + BH (2)	-	0.08	0.01	-	0.03	-	-	0.11	0.04	0.03	0.1	-	1.13	0.13	0.05	-	1.71
2328 CA1 (1) XX/M/5B B + BH (3)	-	0.05	-	-	0.02	-	-	0.04	0.06	0.08	0.13	-	0.97	0.08	0.05	-	1.48
2328 CA1 (1) XX/M/6A	-	0.09	0.01	-	0.01	-	-	0.09	0.05	0.1	0.15	1.57	1.93	0.16	0.08	1.01	5.25

Artefact slag	Bal	Ba	Sr	Cu	Ni	Co	Fe	Mn	Cr	V	Ti	Ca	K	P	S	Mg	Total
2328 CA1 (1) XX M 6A (2)	-	0.07	0.02	-	0.03	-	-	0.05	0.06	0.06	0.1	-	0.33	-	0.04	1.62	2.38
2328 CA1 (1) XX M 6A (3)	-	0.07	0.02	-	0.02	-	-	0.06	0.05	0.12	0.24	-	0.51	0.1	0.04	-	1.23
2328 CA1 (1) XX/O/S	-	0.06	-	-	-	-	-	0.08	0.05	0.07	0.07	0.58	1.36	0.13	0.06	-	2.46
2328 CA1 (1) XX/O/S (2)	-	0.08	0.01	-	0.03	-	-	0.05	0.06	0.07	0.18	-	1	0.31	0.06	-	1.85
2328 CA1 (1) XX/O/S (3)	-	0.05	-	-	0.03	-	-	0.06	0.06	0.05	0.14	0.7	1.52	0.18	0.11	1.58	4.48
2328 CA1 (1) XX/O/AD	-	0.1	0.01	-	0.02	-	-	0.1	0.05	0.09	0.11	1.12	1.45	0.68	0.14	0.83	4.7
2328 CA1 (1) XX/O/AD (2)	-	0.05	-	-	0.02	-	-	0.04	0.04	0.03	0.05	0.33	0.72	0.24	0.07	1.18	2.77
2328 CA1 (1) XX/O/AD 1	-	0.05	-	-	-	0.11	-	0.07	0.05	0.07	0.16	1.21	-	0.07	0.07	1.99	3.85
2328 CA1 (1) XX/O/AD 1 (2)	-	0.11	0.02	-	-	-	-	0.12	0.04	0.04	0.25	1.07	-	0.18	0.08	1.72	3.63
2328 CA1 (1) XX/O/AD 1 (3)	-	0.12	0.02	-	-	-	-	0.09	0.03	0.04	0.23	0.89	-	0.22	0.12	1.18	2.94
2328 CA1 (1) XX/O/AD 2	-	0.03	-	-	-	-	-	0.02	0.07	0.09	0.02	1.02	0.62	0.11	0.07	1.71	3.76
2328 CA1 (1) XX/O/AD 2 (2)	-	0.06	0.01	-	0.03	-	-	0.05	0.05	0.13	0.22	-	1.71	0.18	0.06	1.28	3.78
2328 CA1 (1) XX/O/AD 2 (3)	-	0.06	0.01	-	0.03	-	-	0.07	0.05	0.03	0.12	-	1.27	0.14	0.08	-	1.86
2328 CA1 (1) XX/O/IB	-	0.06	-	-	0.02	-	-	0.04	0.06	0.07	0.15	0.8	0.61	0.3	0.04	1.64	3.79
2328 CA1 (1) XX/O/IB (2)	-	0.06	0.01	-	-	0.19	-	0.08	0.04	0.04	0.33	1.21	-	0.29	0.11	-	2.36
2328 CA1 (1) XX/O/IB (3)	-	0.03	-	-	0.02	-	-	-	0.05	0.03	0.07	0.14	0.67	0.16	0.06	1.9	3.13
2328 CA1 (1) XX/O/2A	-	0.04	-	-	-	-	-	0.04	0.05	0.07	0.11	0.53	0.78	0.28	0.07	-	1.97
2328 CA1 (1) XX/O/2A (2)	-	0.05	-	-	0.02	-	-	0.05	0.05	0.07	0.13	0.84	0.85	0.42	0.09	1.59	4.16
2328 CA1 (1) XX/O/2A (3)	-	0.04	-	-	0.02	-	-	0.03	0.04	0.05	0.14	0.7	0.87	0.2	0.09	1.81	3.99
2328 CA1 (1) XX/O/2B	-	0.07	0.01	-	-	0.04	-	0.1	0.03	0.04	0.26	-	-	0.22	0.1	-	0.87
2328 CA1 (1) XX/O/2B (2)	-	0.16	0.03	-	0.01	-	-	0.1	0.04	0.04	0.33	0.96	-	0.4	0.14	1.64	3.85
2328 CA1 (1) XX/O/2B (3)	-	0.05	-	-	0.02	-	-	0.09	0.04	0.03	0.12	-	1.57	0.35	0.09	1.74	4.1
2328 CA1 (2) XIII/E/S	-	0.06	-	-	0.01	-	-	0.05	0.05	0.08	0.06	0.53	0.76	0.62	0.11	1.26	3.59
2328 CA1 (2) XIII/E/S (2)	-	0.14	0.02	-	0.01	-	-	0.12	0.06	0.09	0.06	-	0.87	1.69	0.19	-	3.25
2328 CA1 (2) XIII/E/S (3)	-	0.08	-	-	0.02	-	-	0.13	0.05	0.06	0.09	0.58	1.08	0.74	0.1	-	2.93

Artefact slag	Bal	Ba	Sr	Cu	Ni	Co	Fe	Mn	Cr	V	Ti	Ca	K	P	S	Mg	Total
2328 CA1 (2) XIII/E/1A	-	0.08	-	-	0.02	-	-	0.06	0.05	0.05	0.08	-	0.45	-	0.08	1.73	2.6
2328 CA1 (2) XIII/E/1B	-	0.34	0.03	-	-	-	-	0.21	0.02	0.02	0.09	-	1.29	-	0.1	1.13	3.23
2328 CA1 (2) XIII/E/1B (2)	-	0.06	-	-	0.01	-	-	0.04	0.05	0.08	0.07	0.71	1.43	0.31	0.37	1.78	4.91
2328 CA1 (2) XIII/E/1B (3)	-	0.1	-	-	0.02	-	-	0.11	0.05	0.05	0.17	1.21	1.57	1.01	0.1	1.42	5.81
2328 CA1 (2) XIII/E/2A	-	0.05	-	-	-	0.1	-	0.09	0.05	0.03	0.18	1.12	1.62	0.69	0.12	1.14	5.19
2328 CA1 (2) XIII/E/2B	-	0.07	-	-	0.02	-	-	0.12	0.05	0.06	0.11	1.97	1.57	0.66	0.14	1.3	6.07
2328 CA1 (2) XIII/E/2B(2)	-	0.1	-	-	-	0.08	-	0.24	0.05	0.07	0.2	1.35	1.71	0.75	0.09	-	4.64
2328 CA1 (2) XIII/E/2B(3)	-	0.04	-	-	-	-	-	0.06	0.06	0.05	0.22	0.37	1.08	-	0.04	1.92	3.84
2328 CA1 (2) XIII/E/3A	-	0.09	-	-	0.01	0.1	-	0.06	0.05	0.08	0.23	1.21	1.77	0.8	0.05	-	4.45
2328 CA1 (2) XIII/F/S	-	0.07	-	0.01	0.01	-	-	0.07	0.05	0.09	0.1	0.56	1.67	0.39	0.06	-	3.08
2328 CA1 (2) XIII/F/S (2)	-	0.12	0.05	0.01	-	-	0.33	0.21	-	-	0.04	-	0.54	-	0.31	-	1.61
2328 CA1 (2) XIII/F/S (3)	-	0.04	-	-	0.01	-	-	0.03	0.07	0.05	0.04	0.4	0.76	0.38	0.03	-	1.81
2328 CA1 (2) XIII/F/1A	-	0.05	-	-	-	-	-	0.04	0.03	0.06	0.13	1.1	1.38	0.49	0.26	1.54	5.08
2328 CA1 (2) XIII/F/1A (2)	-	0.05	-	-	0.02	-	-	0.06	0.05	0.08	0.17	1.04	1.29	0.53	0.09	-	3.38
2328 CA1 (2) XIII/F/1A (3)	-	0.05	-	-	0.02	-	-	0.05	0.05	0.09	0.15	0.77	1.88	0.35	0.05	1.73	5.19
2328 CA1 (2) XIII/F/2A	-	0.11	0.02	-	-	0.11	-	0.11	0.05	0.03	0.04	-	1.44	-	0.25	-	2.16
2328 CA1 (2) XIII/F/2A (2)	1.6	0.07	-	-	-	0.08	-	0.17	0.04	0.05	0.26	1.55	-	0.65	0.28	-	4.75
2328 CA1 (2) XIII/F/2A (3)	-	0.05	-	-	0.01	-	-	0.05	0.05	0.11	0.1	0.45	0.37	0.59	0.05	1.68	3.51
2328 CA1 (2) XIII/F/2B	-	0.06	-	-	-	-	-	0.06	0.05	0.05	0.1	0.84	1.94	0.56	0.1	1.05	4.81
2328 CA1 (2) XIII/F/2B (2)	-	0.04	-	-	0.02	-	-	0.05	0.07	0.07	0.05	0.37	0.62	0.26	0.09	2	3.64
2328 CA1 (2) XIII/F/2B (3)	-	0.04	-	-	0.02	-	-	0.04	0.07	0.19	0.17	0.4	0.61	0.34	0.04	-	1.92
2328 CA1 (2) XIII/F/3A	-	0.1	-	-	-	-	-	0.04	0.03	0.04	0.13	0.86	1.38	0.44	0.06	1.17	4.25
2328 CA1 (2) XIII/F/3A (2)	-	0.09	-	-	0.01	0.04	-	0.19	0.04	0.04	0.16	1.28	-	0.52	0.05	-	2.42
2328 CA1 (2) XIII/F/3A (3)	-	0.11	0.02	-	0.02	-	-	0.13	0.05	0.05	0.09	-	1.63	1.57	0.07	1.2	4.94
2328 CA1 (2) XIII/F/3B	-	0.05	-	-	-	-	-	0.04	0.06	0.09	0.14	0.54	1.62	0.21	0.05	-	2.8

Artefact slag	Bal	Ba	Sr	Cu	Ni	Co	Fe	Mn	Cr	V	Ti	Ca	K	P	S	Mg	Total
2328 CA1 (2) XIII/F/3B (2)	-	0.04	-	-	0.03	-	-	0.02	0.07	0.08	0.07	0.21	0.45	0.15	-	1.6	2.72
2328 CA1 (2) XIII/F/3B (3)	-	0.05	-	-	0.01	-	-	0.1	0.05	0.05	0.11	1.06	1.19	1.11	0.07	1.97	5.77
2328 CA1 (2) XIII/F/4A Mixed	-	0.07	-	-	0.02	-	-	0.06	0.05	0.08	0.11	0.61	1.19	0.41	0.05	1.82	4.47
2328 CA1 (2) XIII/F/GA 4B	-	0.04	-	-	0.01	-	-	0.04	0.05	0.14	0.1	0.43	0.79	-	0.05	1.93	3.58
2328 CA1 (2) XIII/F/GA 4B (2)	-	0.05	-	-	0.02	-	-	0.04	0.06	0.09	0.19	0.86	1.87	0.42	0.06	-	3.66
2328 CA1 (2) XIII/F/GA 4B (3)	-	0.05	-	-	0.01	-	-	0.04	0.06	0.14	0.1	0.69	0.91	0.83	0.07	-	2.9
2328 CA1 (2) XIII/F/GA 5A	-	0.03	-	-	-	0.07	-	0.03	0.06	0.07	0.08	0.57	-	0.21	0.07	-	1.19
2328 CA1 (2) XIV/F/1A	-	0.07	-	-	0.01	0.07	-	0.13	0.05	0.05	0.15	1.65	1.95	0.99	0.11	-	5.23
2328 CA1 (2) XIV/F/1A (2)	-	0.06	-	-	-	0.09	-	0.09	0.06	0.05	0.07	0.62	1.09	0.57	0.05	-	2.75
2328 CA1 (2) XIV/F/1A (3)	1.32	0.07	-	-	0.02	-	-	0.06	0.07	0.05	0.13	0.68	1.15	0.58	0.11	-	4.24
2328 CA1 (2) XIV/F/1B	-	0.07	-	-	-	0.11	-	0.05	0.05	0.06	0.16	1.39	1.82	1.86	0.1	1.81	7.48
2328 CA1 (2) XIV/F/1B (2)	-	0.05	-	-	-	-	-	0.05	0.05	0.07	0.1	0.49	1.69	0.28	0.06	1.73	4.57
2328 CA1 (2) XIV/F/1B (3)	-	0.05	-	-	0.01	-	-	0.04	0.05	0.07	0.09	0.58	0.6	0.34	0.05	-	1.88
2328 CA1 (3) X/A/S	-	0.12	0.01	-	-	0.12	-	0.09	0.05	0.03	0.1	1.56	1.03	-	0.11	1.66	4.88
2328 CA1 (3) X/A/3B	-	0.07	-	-	-	0.1	-	0.04	0.04	0.02	0.22	1.19	1.62	1.23	0.05	1.43	6.01
2328 CA1 (3) X/A/4A	-	0.04	-	-	0.02	-	-	0.04	0.04	0.02	0.09	0.46	0.9	0.29	0.06	1.65	3.61
2328 CA1 (3) X/A/4B	-	0.04	-	-	-	0.04	-	0.05	0.03	0.02	0.16	1.51	-	1.37	0.1	1.53	4.85
2328 CA1 (3) X/A/4B (2)	-	0.12	0.02	-	0.01	-	-	0.08	0.04	0.03	0.15	1.53	1.67	1.02	0.1	-	4.77
2328 CA1 (3) X/A/5A	1.51	0.05	-	-	-	0.07	-	0.06	0.05	0.13	0.15	0.68	1.97	0.56	0.07	1.92	7.22
2328 CA1 (3) X/A/5A (2)	-	0.1	0.02	-	0.02	-	-	0.05	0.05	0.02	0.1	1.38	1.32	1.22	0.06	-	4.34
2328 CA1 (3) X/A/5B	-	0.09	0.02	-	0.01	-	-	0.04	0.04	0.03	0.1	-	1.88	0.84	0.1	-	3.15
2328 CA1 (3) X/A/5B (2)	-	0.19	0.02	-	0.02	-	-	0.08	0.05	0.04	0.13	-	0.92	0.58	0.12	-	2.15
2328 CA1 (3) X/A/5B (3)	-	0.08	-	-	0.01	-	-	0.07	0.04	0.03	0.15	0.7	1.79	0.52	0.06	0.95	4.4
2328 CA1 (4) XX/J/S	-	0.08	-	-	0.01	-	-	0.12	0.07	0.07	0.1	0.76	1.01	0.84	0.08	-	3.14
2328 CA1 (4) XX/J/S (2)	1.59	0.04	-	-	0.02	-	-	0.03	0.07	0.06	0.07	0.76	0.5	0.17	0.05	-	3.36

Artefact slag	Bal	Ba	Sr	Cu	Ni	Co	Fe	Mn	Cr	V	Ti	Ca	K	P	S	Mg	Total
2328 CA1 (4) XX/J/S (3)	-	0.08	-	-	0.04	-	-	0.12	0.06	0.06	0.11	0.49	0.6	0.86	0.15	-	2.57
2328 CA1 (4) XX/J/1A + 1B	-	0.06	-	-	-	-	-	0.06	0.05	0.13	0.12	-	0.63	0.75	0.07	1.78	3.65
2328 CA1 (4) XX/J/1A + 1B (2)	-	0.1	-	-	0.02	-	-	0.07	0.04	0.04	0.2	-	1.51	0.59	0.07	1.07	3.71
2328 CA1 (4) XX/J/1A + 1B (3)	-	0.06	-	-	0.02	-	-	0.05	0.05	0.12	0.18	0.74	0.93	0.53	0.08	-	2.76
2328 CA1 (4) XX/J/2A	-	0.08	-	-	0.01	-	-	0.06	0.06	0.07	0.16	1.47	1.18	1.05	0.07	-	4.21
2328 CA1 (4) XX/J/2A (2)	-	0.08	0.02	-	0.02	-	-	0.07	0.05	0.03	0.09	1.88	1.37	0.87	0.09	1.58	6.15
2328 CA1 (4) XX/J/2A (3)	-	0.05	-	-	0.03	-	-	0.06	0.05	0.06	0.25	0.86	1.29	1.09	0.11	1.87	5.72
2328 CA1 (4) XX/J/2B	-	0.04	-	-	-	-	-	0.03	0.08	0.07	0.08	0.14	0.37	0.06	0.05	1.12	2.04
2328 CA1 (4) XX/J/2B (2)	1.93	0.04	-	-	0.03	-	-	0.03	0.08	0.1	0.11	0.27	0.48	0.23	0.06	1.83	5.19
2328 CA1 (4) XX/J/2B (3)	-	0.12	0.02	-	0.03	-	-	0.12	0.04	0.05	0.23	1.36	-	0.93	0.11	1.81	4.82
2328 CA1 (4) XX/J/3A	-	0.04	0.01	-	-	-	-	0.08	0.08	0.05	0.02	1.39	0.54	0.56	0.05	-	2.82
2328 CA1 (4) XX/J/3B	-	0.07	-	0.02	-	-	-	0.03	0.05	0.03	0.1	1.76	1.27	1.8	0.08	1.4	6.61
2328 CA1 (4) XX/J/3B (2)	-	0.09	-	-	-	-	-	0.16	0.02	0.02	0.45	0.78	-	0.44	0.04	1.34	3.34
2328 CA1 (4) XX/J/3B (3)	-	0.08	-	-	-	-	-	0.06	0.05	0.04	0.22	1.48	-	1.44	0.1	1.49	4.96
2328 CA1 (4) XX/J/4A	-	0.04	-	0.06	-	0.04	-	0.05	0.04	0.02	0.14	1.56	1.66	0.54	0.09	1.36	5.6
2328 CA1 (4) XX/J/4A (2)	-	0.03	-	-	0.01	-	-	0.04	0.05	0.03	0.07	0.29	0.67	0.3	0.05	-	1.54
2328 CA1 (10) VIII/G/S	-	0.06	-	-	-	-	-	0.06	0.04	0.05	0.08	0.71	0.89	0.7	0.06	1.45	4.1
2328 CA1 (10) VIII/G/S (2)	-	0.04	-	-	0.02	-	-	0.03	0.07	0.07	0.09	0.17	0.31	0.2	0.05	1.7	2.75
2328 CA1 (10) VIII/G/S (3)	-	0.04	-	-	0.02	-	-	0.03	0.06	0.06	0.07	0.43	0.56	0.83	0.13	0.8	3.03
2328 CA1 (10) VIII/G/1A + 1B	-	0.05	-	-	-	0.1	-	0.06	0.05	0.06	0.09	1.73	1.46	1.23	0.14	-	4.97
2328 CA1 (10) VIII/G/1A + 1B (2)	-	0.16	0.02	-	-	-	-	0.24	0.05	0.05	0.16	1.66	1.86	-	0.26	1.92	6.38
2328 CA1 (10) VIII/G/1A + 1B (3)	-	0.12	0.02	-	-	-	-	0.04	0.03	0.03	0.09	1.97	1.58	1.54	0.13	1.49	7.04
2328 CA1 (10) VIII/G/1A + 1B 2	-	0.04	-	-	-	-	-	0.04	0.07	0.08	0.14	0.26	0.29	0.12	0.03	1.46	2.53
2328 CA1 (10) VIII/G/1A + 1B 2 (2)	-	0.08	-	-	0.02	-	-	0.03	0.04	0.03	0.04	-	1.01	0.96	0.3	-	2.51
2328 CA1 (10) VIII/G/1A + 1B 2 (3)	-	0.06	-	-	0.02	-	-	0.05	0.04	0.04	0.05	1.89	1.19	0.51	0.1	-	3.95

Artefact slag	Bal	Ba	Sr	Cu	Ni	Co	Fe	Mn	Cr	V	Ti	Ca	K	P	S	Mg	Total
2328 CA1 (10) IX/G/S	-	0.04	-	-	-	-	-	0.04	0.07	0.07	0.04	0.35	0.43	0.24	0.06	-	1.34
2328 CA1 (10) IX/G/S (2)	-	0.05	-	-	0.03	-	-	0.03	0.06	0.07	0.06	0.36	0.49	0.24	0.09	-	1.48
2328 CA1 (10) IX/G/S (3)	-	0.05	-	-	0.02	-	-	0.02	0.07	0.06	0.06	0.25	1.18	0.11	0.07	1.22	3.11
2328 CA1 (10) IX/G/1A	-	0.04	-	-	-	0.21	-	0.07	0.05	0.06	0.06	-	1.07	0.28	0.08	-	1.92
2328 CA1 (10) IX/G/1A (2)	-	0.07	-	-	-	-	-	0.06	0.03	0.03	0.05	-	1.16	0.53	0.1	1.81	3.84
2328 CA1 (10) IX/G/1B	-	0.05	-	-	-	0.1	-	0.05	0.05	0.08	0.08	-	0.97	0.57	0.1	1.68	3.73
2328 CA1 (10) IX/G/1B (2)	-	0.06	0.01	-	0.01	0.05	-	0.05	0.05	0.03	0.04	-	1.37	0.7	0.21	-	2.58
2328 CA1 (10) IX/G/2A	-	0.08	0.01	-	-	0.07	-	0.12	0.04	0.05	0.13	1.95	-	0.88	0.08	1.86	5.27
2328 CA1 (10) IX/G/2A (2)	-	0.06	0.01	-	-	0.12	-	0.07	0.06	0.02	-	-	0.87	0.55	0.26	-	2.02
2328 CA1 (10) IX/G/2A (3)	-	0.04	0.01	-	-	0.08	-	0.04	0.05	0.04	0.03	-	0.89	0.31	0.14	1.73	3.36
2328 CA1 (10) Road Test X/I/S	-	0.04	-	-	-	-	-	0.05	0.03	0.01	0.04	0.55	1.33	0.39	0.14	0.75	3.33
2328 CA1 (10) Road Test X/I/S (2)	-	0.06	-	-	0.02	-	-	0.05	0.05	0.03	-	0.65	1.31	0.76	0.18	-	3.11
2328 CA1 (10) Road Test X/I/S (3)	-	0.1	0.01	-	0.01	-	-	0.34	0.05	0.05	0.11	1.54	1.24	1.9	0.09	1.71	7.15
2328 CA1 (10) Road Test X/I/1A	-	0.03	-	-	-	0.07	-	0.04	0.05	0.06	0.36	0.42	1.1	-	-	1.75	3.88
2328 CA1 TP 4	-	0.03	-	-	-	-	-	0.05	0.02	-	0.13	-	1.77	0.8	0.09	1.09	3.98
2328 CA1 TP 4 (2)	-	0.06	0.01	-	0.02	-	-	0.04	0.05	0.11	0.16	-	0.93	0.85	0.06	-	2.29
2328 CA1 TP 4 (3)	-	0.08	0.01	-	0.02	-	-	0.06	0.04	0.03	0.13	1.83	1.21	0.72	0.11	-	4.24
2328 CA1 TP 5	-	0.02	-	-	-	-	-	0.18	0.06	0.08	0.04	0.38	0.75	0.4	0.02	-	1.93
2328 CA1 TP 5 (2)	-	0.06	0.01	-	0.02	-	-	0.05	0.06	0.03	0.08	1.41	1.21	1.32	0.1	1.69	6.04
2328 CA1 TP 5 (3)	-	0.03	-	-	0.02	-	-	0.21	0.06	0.07	0.07	0.44	0.89	0.42	0.04	-	2.25
2328 CA1 AC 4	-	0.08	-	-	0.02	-	-	0.13	0.03	0.03	0.05	1.08	1.12	0.8	0.09	0.75	4.18
2328 CA1 AC 4 (2)	-	0.04	-	-	0.03	-	-	0.02	0.06	0.04	0.06	0.25	0.75	0.15	0.03	-	1.43
2328 CA1 AC 4 (3)	-	0.04	-	-	0.02	-	-	0.04	0.05	0.08	0.08	0.53	1.13	0.41	0.05	-	2.43
2328 CA1 AC 5	-	0.06	-	-	0.03	-	-	0.06	0.06	0.05	0.06	0.33	0.76	0.2	0.13	-	1.74
2328 CA1 AC 5 (2)	-	0.06	-	-	0.01	-	-	0.08	0.05	0.05	0.17	0.51	1.07	0.31	0.06	1.29	3.66

Artefact slag	Bal	Ba	Sr	Cu	Ni	Co	Fe	Mn	Cr	V	Ti	Ca	K	P	S	Mg	Total
2328 CA1 AC 7	-	0.04	-	-	0.03	-	-	0.04	0.07	0.11	0.1	0.11	0.22	0.09	0.04	1.07	1.92
2328 CA1 AC 7 (2)	-	0.05	-	-	0.03	-	-	0.19	0.06	0.02	0.03	0.31	0.5	0.31	0.05	-	1.55
2328 CA1 AC 8	-	0.04	-	-	0.03	-	-	0.04	0.07	0.1	0.1	0.22	0.41	0.15	0.04	-	1.2
2328 CA1 AC 8 (2)	-	0.08	-	-	0.02	-	-	0.08	0.04	0.04	0.07	0.97	1.14	0.62	0.15	-	3.21
2328 CA1 AC 8 (3)	-	0.05	-	-	0.03	-	-	0.07	0.06	0.07	0.06	0.23	0.56	0.26	0.07	1.3	2.76
2328 CA1 AC 9	-	0.06	-	-	0.02	-	-	0.03	0.07	0.06	0.1	0.63	0.61	0.2	0.05	-	1.83
2328 CA1 AC 9 (2)	-	0.11	-	-	0.02	-	-	0.24	0.05	0.1	0.33	0.9	-	0.81	0.1	1.61	4.27
2328 CA1 AC 9 (3)	-	0.07	-	-	0.02	-	-	0.13	0.04	0.04	0.07	0.73	0.69	1.1	0.22	0.86	3.97
2328 CA1 AC 10	-	0.05	-	-	0.02	-	-	0.05	0.05	0.06	0.08	0.45	0.97	1.29	0.11	1.97	5.1
2328 CA1 AC 10 (2)	1.29	0.05	-	-	0.02	-	-	0.04	0.08	0.15	0.14	0.4	1.61	0.17	0.12	-	4.07
2328 CA1 AC 10 (3)	-	0.04	-	-	0.03	-	-	0.03	0.07	0.07	0.05	0.07	0.26	0.11	0.04	1.38	2.15
2328 CA1 AC 11	-	0.06	-	-	0.03	-	-	0.05	0.06	0.04	0.07	0.23	1.62	0.19	0.05	-	2.4
2328 CA1 AC 12	-	0.07	-	-	0.02	-	-	0.09	0.04	0.12	0.21	1.03	1.28	0.38	0.09	1.26	4.59
2328 CA1 AC 13 B	-	0.07	-	-	0.02	-	-	0.11	0.06	0.07	0.07	0.73	0.84	1.25	0.17	1.76	5.15
2328 CA1 AC 13 B (2)	-	0.06	-	-	0.02	-	-	0.06	0.06	0.18	0.22	0.69	-	0.48	0.06	1.25	3.08
2328 CA1 AC 13 s	-	0.03	-	-	0.03	-	-	0.02	0.07	0.07	0.13	0.13	0.27	0.14	0.04	-	0.93
2328 CA1 AC 13 s (2)	-	0.04	-	-	0.03	-	-	0.04	0.07	0.13	0.1	0.17	0.52	0.13	0.04	-	1.27
2328 CA1 AC 16	-	0.07	-	-	-	-	-	0.12	0.04	0.07	0.08	1.18	0.77	1.31	0.12	1.56	5.32
2328 CA1 AC 16 (2)	-	0.04	-	-	0.03	-	-	0.02	0.06	0.08	0.07	0.88	0.79	0.15	0.04	-	2.16
2328 CA1 AC 18	-	0.07	-	-	0.02	-	-	0.06	0.05	0.04	0.07	0.54	1.65	0.58	0.1	1.5	4.68
2328 CA1 AC 18 (2)	-	0.07	-	-	0.03	-	-	0.11	0.05	0.07	0.17	0.73	0.96	1.13	0.12	1.12	4.56
2328 CA1 AC 18 (3)	-	0.04	-	-	0.03	-	-	0.02	0.05	0.04	0.06	0.11	0.64	0.12	0.04	1.11	2.26
Average	1.48	0.06	0.02	0.03	0.02	0.09	0.33	0.07	0.05	0.06	0.14	0.83	1.07	0.49	0.09	1.5	
Standard Deviation	0.28	0.03	0.01	0	0.01	0.04	0.02	0.05	0.01	0.03	0.08	0.54	0.57	0.4	0.06	0.78	

Table 7.2: XRF slag results, higher proportion percentages in wt%.

Artefact slag	Bal	Fe	Ca	K	Al	P	Si	Mg	Total
2328 CA1 (1) XIX/N/S	-	66.63	-	-	14.31	-	15.19	2.03	98.16
2328 CA1 (1) XIX/N/S (2)	-	67.77	-	-	14.3	-	14.1	2.49	98.66
2328 CA1 (1) XIX/N/S (3)	23.14	55.05	-	-	7.45	-	11.06	-	96.7
2328 CA1 (1) XIX/N/AD	8.89	53.9	-	-	15.91	-	16.76	2.3	97.76
2328 CA1 (1) XIX/N/AD (2)	-	62.63	-	-	15.57	-	18.11	-	96.31
2328 CA1 (1) XIX/N/AD (3)	19.79	39.98	-	-	13.51	-	21.73	-	95.01
2328 CA1 (1) XIX/N/2A	18.07	27.22	-	2.89	19.52	-	28.46	-	96.16
2328 CA1 (1) XIX/N/2A (2)	-	47.71	-	2.09	25.26	-	21.94	-	97
2328 CA1 (1) XIX/N/2A (3)	25.15	27.15	-	2.4	14.47	-	26.19	-	95.36
2328 CA1 (1) XIX/N/2B	20.9	35.22	2.34	-	14.78	-	23.23	-	96.47
2328 CA1 (1) XIX/N/2B (2)	-	41.94	-	2.58	22.84	-	28.78	-	96.14
2328 CA1 (1) XIX/N/2B (3)	29.37	15.59	9.43	2.54	15.77	-	24.69	-	97.39
2328 CA1 (1) XX/M/PERIMETER	-	52.73	6.53	-	15.09	-	19.71	2.53	96.59
2328 CA1 (1) XX/M/PERIMETER (2)	18.72	30.14	-	2.25	15.7	-	28.94	2	97.75
2328 CA1 (1) XX/M/PERIMETER (3)	7.58	52.69	-	-	16.83	-	18.96	-	96.06
2328 CA1 (1) XX/M/S	13.97	33.31	-	2.2	17.56	-	29.6	-	96.64
2328 CA1 (1) XX/M/S (2)	11.58	34.36	-	2.86	18.36	-	28.95	-	96.11
2328 CA1 (1) XX/M/S (3)	20.21	47.18	-	-	12.76	-	15.29	-	95.44
2328 CA1 (1) XX/M/1A	7.02	50.77	-	-	16.99	-	19.54	-	94.32
2328 CA1 (1) XX/M/1A (2)	6.32	49.85	-	-	17.68	-	20.48	2	96.33
2328 CA1 (1) XX/M/1A (3)	7.09	54.24	-	-	15.81	-	17.05	2.23	96.42
2328 CA1 (1) XX/M/1B	22.63	19.37	4.56	2.35	15.66	-	34.38	-	98.95
2328 CA1 (1) XX/M/1B (2)	6.99	41.73	-	2.34	19.93	-	23.87	-	94.86
2328 CA1 (1) XX/M/1B (3)	22.89	36.85	-	-	11.78	-	23.55	-	95.07

Artefact slag	Bal	Fe	Ca	K	Al	P	Si	Mg	Total
2328 CA1 (1) XX/M/2A RB	-	54.75	-	-	21.45	-	20.33	-	96.53
2328 CA1 (1) XX/M/2A RB (2)	-	68.17	-	-	13.74	-	14.08	2.14	98.13
2328 CA1 (1) XX/M/2A RB (3)	24.96	30.02	-	-	12.3	-	27.04	-	94.32
2328 CA1 (1) XX/M/2B RG	3.99	62.46	-	-	16.61	-	12.87	-	95.93
2328 CA1 (1) XX/M/2B RG (2)	3.31	62.81	-	-	16.71	-	13.3	-	96.13
2328 CA1 (1) XX/M/2B RG (3)	16.46	57.66	2.82	-	9.44	-	10.38	-	96.76
2328 CA1 (1) XX/M/3A RG	25.23	55.65	-	-	8.15	-	8.63	-	97.66
2328 CA1 (1) XX/M/3A RG (2)	25.86	44.37	2.57	-	8.03	-	16.11	-	96.94
2328 CA1 (1) XX/M/3A RG (3)	9.06	64.77	-	-	10.29	-	12.25	-	96.37
2328 CA1 (1) XX/M/3B RG + GH	32.16	46.7	-	-	5.7	-	12.5	-	97.06
2328 CA1 (1) XX/M/3B RG + GH (2)	7.72	72.76	-	-	8.64	-	8.13	-	97.25
2328 CA1 (1) XX/M/3B RG + GH (3)	8.88	36.5	-	-	15.83	-	33.64	-	94.85
2328 CA1 (1) XX/M/4A tuyère layer (grey)	12.77	65.77	-	-	10.29	-	8.94	-	97.77
2328 CA1 (1) XX/M/4A tuyère layer (grey) (2)	27.64	33.05	-	-	11.35	-	23.3	-	95.34
2328 CA1 (1) XX/M/4A tuyère layer (grey) (3)	29.19	56.73	-	-	4.84	-	5.4	-	96.16
2328 CA1 (1) XX/M/4B tuyère layer (grey)	3.84	59.01	-	-	16.03	-	16.31	2.16	97.35
2328 CA1 (1) XX/M/4B tuyère layer (grey) (2)	18.53	55.13	-	-	9.75	-	13.31	-	96.72
2328 CA1 (1) XX/M/4B tuyère layer (grey) (3)	-	9.13	3.85	-	25.64	-	50.97	8.71	98.3
2328 CA1 (1) XX/M/5A (grey tuyère pipes)	12.35	47.82	2.59	-	13.28	-	20.92	-	96.96
2328 CA1 (1) XX/M/5A (grey tuyère pipes) (2)	-	33.35	-	3.35	26.76	-	32.11	2.49	98.06
2328 CA1 (1) XX/M/5A (grey tuyère pipes) (3)	-	44.8	-	2.35	24.06	-	25.07	2.03	98.31
2328 CA1 (1) XX/M/5B B + BH	15.4	30.78	-	3.34	19.83	-	27.74	-	97.09
2328 CA1 (1) XX/M/5B B + BH (2)	20.22	43.86	2.94	-	11.53	-	16.63	3.04	98.22
2328 CA1 (1) XX/M/5B B + BH (3)	-	59.98	2.91	-	17.07	-	15.47	2.99	98.42
2328 CA1 (1) XX/M/6A	16.52	40.21	-	-	15.73	-	22.24	-	94.7

Artefact slag	Bal	Fe	Ca	K	Al	P	Si	Mg	Total
2328 CA1 (1) XX/M/6A (2)	38.71	44.95	5.41	-	3.47	-	4.96	-	97.5
2328 CA1 (1) XX/M/6A (3)	28.74	38.36	7.17	-	8.79	-	13.18	2.42	98.66
2328 CA1 (1) XX/O/S	8.98	56.71	-	-	14.88	-	14.72	2.19	97.48
2328 CA1 (1) XX/O/S (2)	25.29	37.65	3.79	-	12.09	-	18.45	-	97.27
2328 CA1 (1) XX/O/S (3)	6.1	51.28	-	-	17.86	-	20.24	-	95.48
2328 CA1 (1) XX/O/AD	29.12	37.14	-	-	10.22	-	18.78	-	95.26
2328 CA1 (1) XX/O/AD (2)	17.26	56.56	-	-	9.82	-	13.49	-	97.13
2328 CA1 (1) XX/O/AD 1	-	45.4	-	2.22	21.95	-	26.55	-	96.12
2328 CA1 (1) XX/O/AD 1 (2)	24.95	26.92	-	2.58	16.37	-	25.52	-	96.34
2328 CA1 (1) XX/O/AD 1 (3)	23.27	21.33	-	3.21	15.49	-	33.75	-	97.05
2328 CA1 (1) XX/O/AD 2	13.06	67.89	-	-	7.95	-	7.25	-	96.15
2328 CA1 (1) XX/O/AD 2 (2)	-	46.61	2.62	-	24.62	-	22.36	-	96.21
2328 CA1 (1) XX/O/AD 2 (3)	11.39	45.5	2.78	-	15.73	-	20.58	2.1	98.08
2328 CA1 (1) XX/O/1B	10.6	56.67	-	-	14.16	-	14.71	-	96.14
2328 CA1 (1) XX/O/1B (2)	8.85	27.15	-	3.58	25.18	-	30.61	2.23	97.6
2328 CA1 (1) XX/O/1B (3)	-	68.51	-	-	14.11	-	14.15	-	96.77
2328 CA1 (1) XX/O/2A	13.5	54.82	-	-	12.33	-	16.54	-	97.19
2328 CA1 (1) XX/O/2A (2)	6.68	55.75	-	-	14.58	-	18.75	-	95.76
2328 CA1 (1) XX/O/2A (3)	21.19	43.74	-	-	10.33	-	20.72	-	95.98
2328 CA1 (1) XX/O/2B	25.54	25.63	2.23	2.31	13.75	-	28.99	-	98.45
2328 CA1 (1) XX/O/2B (2)	21.02	20.89	-	2.98	17	-	34.2	-	96.09
2328 CA1 (1) XX/O/2B (3)	-	52.53	2.43	-	17.98	-	22.91	-	95.85
2328 CA1 (2) XIII/E/S	19.37	52.15	-	-	8.24	-	16.55	-	96.31
2328 CA1 (2) XIII/E/S(2)	18.89	51.11	2.59	-	6.47	-	15.22	2.31	96.59
2328 CA1 (2) XIII/E/S(3)	19.67	54.26	-	-	8.58	-	13.76	-	96.27

Artefact slag	Bal	Fe	Ca	K	Al	P	Si	Mg	Total
2328 CA1 (2) XIII/E/1A	16.96	47.17	5.49	-	7.17	4.67	15.81	-	97.27
2328 CA1 (2) XIII/E/1B	43.25	16.01	3.37	-	5.38	4.13	24.6	-	96.74
2328 CA1 (2) XIII/E/1B (2)	11.28	53.7	-	-	11.73	-	18.31	-	95.02
2328 CA1 (2) XIII/E/1B (3)	17	43.14	-	-	12.34	-	21.63	-	94.11
2328 CA1 (2) XIII/E/2A	7.75	52.84	-	-	14.37	-	19.31	-	94.27
2328 CA1 (2) XIII/E/2B	13.69	46.98	-	-	13.11	-	20.07	-	93.85
2328 CA1 (2) XIII/E/2B (2)	3.47	47.21	-	-	18.15	-	23.56	2.88	95.27
2328 CA1 (2) XIII/E/2B (3)	-	60.76	-	-	16.86	-	18.48	-	96.1
2328 CA1 (2) XIII/E/3A	2.29	42.37	-	-	19.81	-	28.09	2.92	95.48
2328 CA1 (2) XIII/F/S	13.16	46.15	-	-	11.56	-	23.98	2.01	96.86
2328 CA1 (2) XIII/F/S (2)	37.05	-	33.27	-	4.46	15.36	8.1	-	98.24
2328 CA1 (2) XIII/F/S (3)	-	69.91	-	-	12.43	-	13.34	2.44	98.12
2328 CA1 (2) XIII/F/1A	26.66	36.49	-	-	10.44	-	21.19	-	94.78
2328 CA1 (2) XIII/F/1A (2)	8.2	48.79	-	-	15.1	-	21.34	3.16	96.59
2328 CA1 (2) XIII/F/1A (3)	-	59.53	-	-	17.06	-	18.19	-	94.78
2328 CA1 (2) XIII/F/2A	14.91	49.99	4.54	-	6.93	7.2	10.24	3.91	97.72
2328 CA1 (2) XIII/F/2A (2)	-	42.79	-	2.6	20.61	-	26.6	2.6	95.2
2328 CA1 (2) XIII/F/2A(3)	15.99	59.24	-	-	6.94	-	14.24	-	96.41
2328 CA1 (2) XIII/F/2B	10.39	50.87	-	-	14.3	-	19.51	-	95.07
2328 CA1 (2) XIII F 2B (2)	4.77	71.79	-	-	9.9	-	9.77	-	96.23
2328 CA1 (2) XIII F 2B (3)	-	69.43	-	-	12.77	-	13	2.8	98
2328 CA1 (2) XIII/F/3A	36.95	31.31	-	-	7.62	-	19.83	-	95.71
2328 CA1 (2) XIII/F/3A (2)	16.69	35.77	-	2.26	15.25	-	24.73	2.82	97.52
2328 CA1 (2) XIII/F/3A (3)	17.25	45.32	2.21	-	13.19	-	17.06	-	95.03
2328 CA1 (2) XIII/F/3B	2.08	60.89	-	-	15.35	-	16.75	2.01	97.08

Artefact slag	Bal	Fe	Ca	K	Al	P	Si	Mg	Total
2328 CA1 (2) XIII/F/3B (2)	-	78.41	-	-	9.83	-	8.31	-	96.55
2328 CA1 (2) XIII/F/3B (3)	9.13	56.66	-	-	12.54	-	15.79	-	94.12
2328 CA1 (2) XIII/F/4A Mixed	9.13	56.37	-	-	11.61	-	18.36	-	95.47
2328 CA1 (2) XIII/F/GA 4B	10.8	57.44	-	-	10.1	-	17.57	-	95.91
2328 CA1 (2) XIII/F/GA 4B (2)	-	46.31	-	-	22.52	-	24.45	3.03	96.31
2328 CA1 (2) XIII/F/GA 4B (3)	-	64.41	-	-	12.64	-	17.44	2.41	96.9
2328 CA1 (2) XIII/F/GA 5A	-	53.76	-	2.1	21.69	-	18.94	2.3	98.79
2328 CA1 (2) XIV/F/1A	5.3	47.74	-	-	16.92	-	21.71	3.02	94.69
2328 CA1 (2) XIV/F/1A (2)	-	53.33	-	-	17.88	-	22.89	3.14	97.24
2328 CA1 (2) XIV/F/1A (3)	-	59.22	-	-	17.76	-	16.56	2.14	95.68
2328 CA1 (2) XIV/F/1B	13.32	44.35	-	-	11.33	-	23.43	-	92.43
2328 CA1 (2) XIV/F/1B (2)	6.27	60.48	-	-	12.93	-	15.63	-	95.31
2328 CA1 (2) XIV/F/1B (3)	-	56.8	-	-	15.45	-	22.85	2.96	98.06
2328 CA1 (3) X/A/S	21.25	48.46	-	-	7.61	2.73	15.02	-	95.07
2328 CA1 (3) X/A/3B	19.33	33.47	-	-	12.02	-	29.11	-	93.93
2328 CA1 (3) X/A/4A	8.54	57.15	-	-	11.48	-	19.09	-	96.26
2328 CA1 (3) X/A/4B	26.13	23.45	-	2.55	10.49	-	32.49	-	95.11
2328 CA1 (3) X/A/4B (2)	23.51	43.83	-	-	10.89	-	16.13	-	94.36
2328 CA1 (3) X/A/5A	-	51.49	-	-	18.16	-	23.03	-	92.68
2328 CA1 (3) X/A/5A (2)	-	55.34	-	-	18.48	-	19.25	2.52	95.59
2328 CA1 (3) X/A/5B	23.03	42.19	3.34	-	10.32	-	16.98	-	95.86
2328 CA1 (3) X/A/5B (2)	29.94	43.39	2.59	-	6.45	-	13.37	2.03	97.77
2328 CA1 (3) X/A/5B (3)	21.17	27.7	-	-	17.53	-	29.17	-	95.57
2328 CA1 (4) XX/J/S	19.51	52.89	-	-	9.23	-	12.71	2.36	96.7
2328 CA1 (4) XX/J/S (2)	-	73.22	-	-	11	-	9.64	2.67	96.53

Artefact slag	Bal	Fe	Ca	K	Al	P	Si	Mg	Total
2328 CA1 (4) XX/J/S (3)	18.33	54.65	-	-	9.37	-	14.04	-	96.39
2328 CA1 (4) XX/J/1A + 1B	18.52	49.29	2.73	-	10	-	15.61	-	96.15
2328 CA1 (4) XX/J/1A + 1B (2)	20.17	40.74	2.44	-	11.98	-	20.91	-	96.24
2328 CA1 (4) XX/J/1A + 1B (3)	3.31	52.91	-	-	15.35	-	22.92	2.7	97.19
2328 CA1 (4) XX/J/2A	-	53.89	-	-	18.27	-	20.92	2.62	95.7
2328 CA1 (4) XX/J/2A (2)	20.22	48.06	-	-	10.73	-	14.74	-	93.75
2328 CA1 (4) XX/J/2A (3)	8.01	51.88	-	-	15.12	-	19.13	-	94.14
2328 CA1 (4) XX/J/2B	12.74	71.74	-	-	7.16	-	6.16	-	97.8
2328 CA1 (4) XX/J/2B (2)	-	71.39	-	-	12.09	-	11.28	-	94.76
2328 CA1 (4) XX/J/2B (3)	14.72	37.13	-	2.29	16.29	-	24.68	-	95.11
2328 CA1 (4) XX/J/3A	7.26	66.13	-	-	13.16	-	9.84	-	96.39
2328 CA1 (4) XX/J/3B	18.71	50.77	-	-	8.17	-	15.66	-	93.31
2328 CA1 (4) XX/J/3B (2)	42.98	8.24	-	2.3	11.77	-	31.33	-	96.62
2328 CA1 (4) XX/J/3B (3)	14.14	34.78	-	2.55	17.43	-	26.02	-	94.92
2328 CA1 (4) XX/J/4A	20.38	33.18	-	-	11.41	-	29.37	-	94.34
2328 CA1 (4) XX/J/4A (2)	-	61.14	-	-	12.79	-	21.88	2.58	98.39
2328 CA1 (10) VIII/G/S	19.41	50.78	-	-	9.57	-	16.01	-	95.77
2328 CA1 (10) VIII/G/S (2)	12.66	71.49	-	-	6.81	-	6.16	-	97.12
2328 CA1 (10) VIII/G/S (3)	27.11	56.3	-	-	5.24	-	8.22	-	96.87
2328 CA1 (10) VIII/G/1A + 1B	7.42	54.43	-	-	14.58	-	16.12	2.38	94.93
2328 CA1 (10) VIII/G/1A + 1B (2)	13.04	46.88	-	-	13.56	2.48	17.51	-	93.47
2328 CA1 (10) VIII/G/1A + 1B (3)	25.93	36.11	-	-	12.52	-	18.36	-	92.92
2328 CA1 (10) VIII/G/1A + 1B 2	16.64	67.27	-	-	5.97	-	7.45	-	97.33
2328 CA1 (10) VIII/G/1A + 1B 2 (2)	24.18	47.54	2.24	-	9.39	-	13.34	-	96.69
2328 CA1 (10) VIII/G/1A + 1B 2 (3)	7.78	56.27	-	-	14.45	-	15.37	2.17	96.04

Artefact slag	Bal	Fe	Ca	K	Al	P	Si	Mg	Total
2328 CA1 (10) IX/G/S	10	72.73	-	-	7.16	-	6.52	2.13	98.54
2328 CA1 (10) IX/G/S (2)	7.13	73.15	-	-	9.01	-	8.15	-	97.44
2328 CA1 (10) IX/G/S (3)	6.18	73.9	-	-	9.26	-	7.39	-	96.73
2328 CA1 (10) IX/G/1A	-	60.75	11.44	-	12.26	-	11.56	2.03	98.04
2328 CA1 (10) IX/G/1A (2)	18.5	50.37	3.15	-	10.4	-	13.68	-	96.1
2328 CA1 (10) IX/G/1B	3.65	62.86	5.05	-	10.91	-	13.75	-	96.22
2328 CA1 (10) IX/G/1B (2)	11.62	56.26	7.22	-	8.29	-	10.9	3.04	97.33
2328 CA1 (10) IX/G/2A	14.99	38.69	-	3.33	14.03	-	23.61	-	94.65
2328 CA1 (10) IX/G/2A (2)	11.61	56.88	13.65	-	5.62	-	7.44	2.69	97.89
2328 CA1 (10) IX/G/2A (3)	7.26	64.46	8.12	-	7.55	-	9.14	-	96.53
2328 CA1 (10) Road Test X/I/S	40.41	36.66	-	-	7.2	-	12.35	-	96.62
2328 CA1 (10) Road Test X/I/S (2)	21.49	53.1	-	-	9.54	-	10.56	2.04	96.73
2328 CA1 (10) Road Test X/I/S (3)	10.82	52.15	-	-	13.31	-	16.48	-	92.76
2328 CA1 (10) Road Test X/I/1A	-	59.2	-	-	16.13	-	20.64	-	95.97
2328 CA1 TP 4	38.94	16.13	2.09	-	5.46	-	33.34	-	95.96
2328 CA1 TP 4 (2)	17.72	45.97	2.76	-	10.49	-	18.15	2.58	97.67
2328 CA1 TP 4 (3)	10.08	48.84	-	-	13.15	-	21.05	2.55	95.67
2328 CA1 TP 5	-	64.45	-	-	16.76	-	14.05	2.69	97.95
2328 CA1 TP 5 (2)	11.75	51.32	-	-	12.24	-	18.55	-	93.86
2328 CA1 TP 5 (3)	-	59.21	-	-	17.81	-	18.09	2.63	97.74
2328 CA1 AC 4	28.76	48.36	-	-	7.44	-	11.19	-	95.75
2328 CA1 AC 4 (2)	-	69.55	-	-	14.25	-	11.7	3	98.5
2328 CA1 AC 4 (3)	2.35	63.95	-	-	14.3	-	13.5	3.39	97.49
2328 CA1 AC 5	2.71	66.85	-	-	13.3	-	13.08	2.23	98.17
2328 CA1 AC 5 (2)	17.51	53.67	-	-	8.66	-	16.42	-	96.26

Artefact slag	Bal	Fe	Ca	K	Al	P	Si	Mg	Total
2328 CA1 AC 7	18.56	70.72	-	-	4.09	-	4.54	-	97.91
2328 CA1 AC 7 (2)	11.4	68.93	-	-	9.42	-	8.58	-	98.33
2328 CA1 AC 8	11.84	70.13	-	-	8.53	-	8.19	-	98.69
2328 CA1 AC 8 (2)	22.85	50.55	-	-	9.13	-	13.48	-	96.01
2328 CA1 AC 8 (3)	7.34	71.64	-	-	9.28	-	8.87	-	97.13
2328 CA1 AC 9	13.98	65.74	-	-	8.37	-	7.9	2.03	98.02
2328 CA1 AC 9 (2)	3.53	45.9	-	2.14	21.64	-	22.5	-	95.71
2328 CA1 AC 9 (3)	23.48	57.22	-	-	5.77	-	9.43	-	95.9
2328 CA1 AC 10	10.74	60.1	-	-	10.13	-	13.82	-	94.79
2328 CA1 AC 10 (2)	-	65.57	-	-	14.31	-	14.93	-	94.81
2328 CA1 AC 10 (3)	12.18	73.49	-	-	6.24	-	5.77	-	97.68
2328 CA1 AC 11	-	64.43	-	-	17.36	-	13.15	2.62	97.56
2328 CA1 AC 12	24.53	47.49	-	-	9.47	-	13.85	-	95.34
2328 CA1 AC 13 B	13.39	56.23	-	-	8.88	-	16.31	-	94.81
2328 CA1 AC 13 B (2)	6.8	51.64	-	4	16.98	-	17.4	-	96.82
2328 CA1 AC 13 S	16.1	70.16	-	-	6.96	-	5.75	-	98.97
2328 CA1 AC 13 S (2)	3.14	71.35	-	-	11.72	-	12.42	-	98.63
2328 CA1 AC 16	22.82	54.64	-	-	6.25	-	10.87	-	94.58
2328 CA1 AC 16 (2)	27.12	57.57	-	-	4.67	-	6.01	2.29	97.66
2328 CA1 AC 18	24.47	49.69	-	-	7.54	-	13.5	-	95.2
2328 CA1 AC 18 (2)	16.04	53.46	-	-	11.81	-	13.75	-	95.06
2328 CA1 AC 18 (3)	-	72.41	-	-	12.53	-	11.58	-	96.52
Average									
	16.36	50.86	5.15	2.64	12.86	6.1	17.7	2.61	
Standard Deviation									
	8.98	13.91	5.55	0.5	4.73	4.84	7.24	0.9	

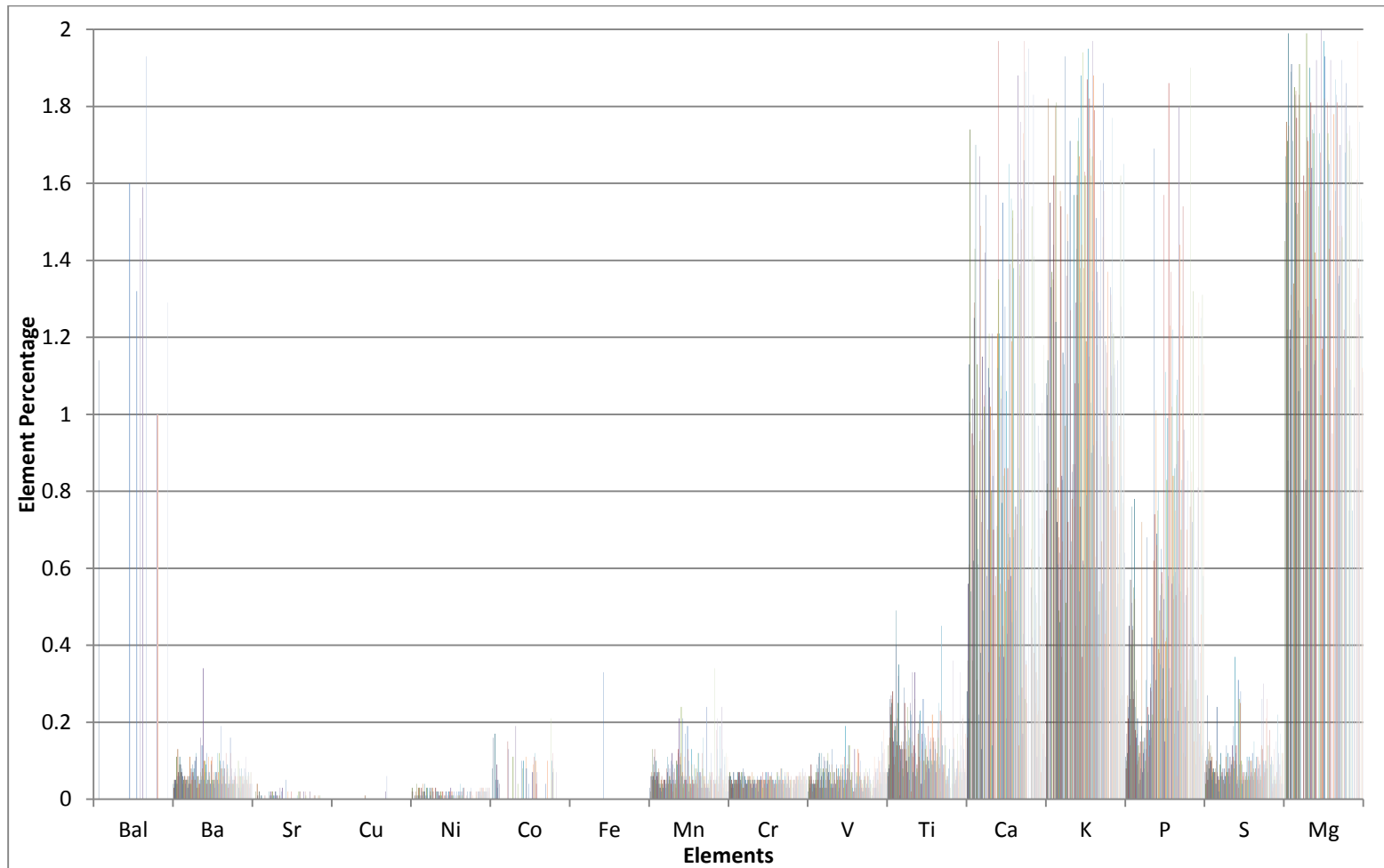


Figure 7.1: Thaba Nkulu slag XRF low percentage element proportions (each colour represents one slag sample).

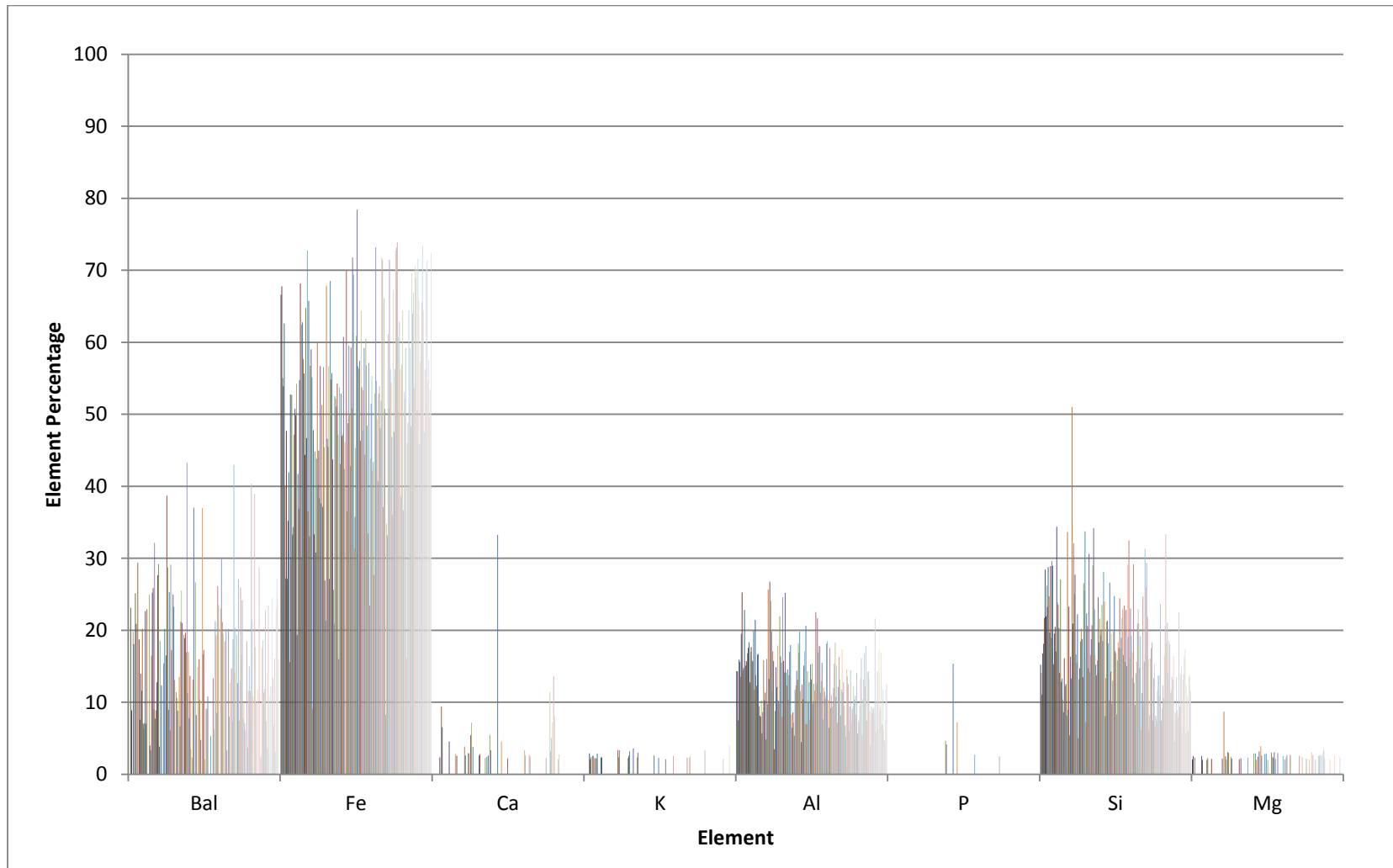


Figure 7.3: Thaba Nkulu slag XRF higher percentage element proportions (each colour represents one slag sample).

7.1.3: Tuyère fragments

Out of the 220 XRF samples, only four tuyère pieces were analysed. From these samples, elements such as: Ba, zirconium (Zr), Sr, Ni, Mn, Cr, V, Ti, Ca, P, S, and Mg were detected in the low proportion percentages. Zirconium was a new element detected in the tuyère samples; it was detected in only one other sample outside of the tuyères, the iron tang. Ba, Zr, and Sr were considered as trace elements recorded in the tuyères. The other elements found in the tuyère low proportion percentages were seen in the slag results as well. Within the high proportion percentages: Fe, Ca, K, Al and Si, as well as the unrecognised elements (balance) were recorded. The iron found in the tuyères possibly came from the iron slag inside the furnace. It must be noted that some tuyère fragments contained a slag covering, or had slag inside (Figure 4.8). In the case of the former, both inner and outer surfaces were analysed, to record all possible elements.

Table 7.3 displays the low proportion elements detected in the tuyère samples, and Table 7.4 displays the high proportion percentages. As with the slag samples, the data were then plotted as bar charts, to display which elements were predominant within each section. These results can be seen in Figure 7.3 for the low proportion percentages, and Figure 7.4 for the high proportion percentages. The averages and the standard deviations for the low proportion percentages were low (under 1%, except for Mg with an average of 1.19%), whereas the averages for the high proportion percentages were high, above 10%, except for Ca and K.

Table 7.3: XRF tuyère results, low proportion percentages in wt%.

Artefact tuyère	Ba	Zr	Sr	Ni	Mn	Cr	V	Ti	Ca	P	S	Mg	Total
2328 CA1 (1) XIX/N/AD tuyère	0.11	0.01	0.02	0.02	0.11	0.04	0.04	0.27	1.66	0.15	0.11	1.83	4.37
2328 CA1 (1) XX/M/4A tuyère layer (grey) glass tuyère	0.14	0.01	0.06	0.01	0.05	0.02	0.02	0.23	-	0.32	0.05	1.53	2.44
2328 CA1 (10) VIII/G/1A + 1B Giant tuyère	0.06	0.02	0.01	-	0.12	0.01	0.02	0.26	-	0.48	0.12	0.74	1.84
2328 CA1 (10) VIII/G/1A + 1B Giant tuyère Core	0.05	0.02	-	-	0.07	-	-	0.22	-	0.47	0.11	0.67	1.61
Average	0.09	0.01	0.02	0.01	0.09	0.02	0.02	0.25	0.42	0.36	0.09	1.19	
Standard Deviation	0.04	0	0.02	0.01	0.03	0.02	0.02	0.02	0.83	0.15	0.03	0.58	

Table 7.4: XRF tuyère results, higher proportion percentages in wt%.

Artefact tuyère	Bal	Fe	Ca	K	Al	Si	Total
2328 CA1 (1) XIX/N/AD tuyère	8.93	32	-	3.1	23.06	28.51	95.6
2328 CA1 (1) XX/M/4A tuyère layer (grey) glass tuyère	29.88	4.24	15.73	4.23	13.81	29.66	97.55
2328 CA1 (10) VIII/G/1A + 1B Giant tuyère	46.62	4.61	5.85	3.56	12.32	25.2	98.16
2328 CA1 (10) VIII/G/1A + 1B Giant tuyère Core	56.69	2.26	2.02	2.68	8.98	25.74	98.37
Average	35.53	10.78	5.9	3.39	14.54	27.28	
Standard Deviation	20.9	14.18	6.99	0.66	6.02	2.15	

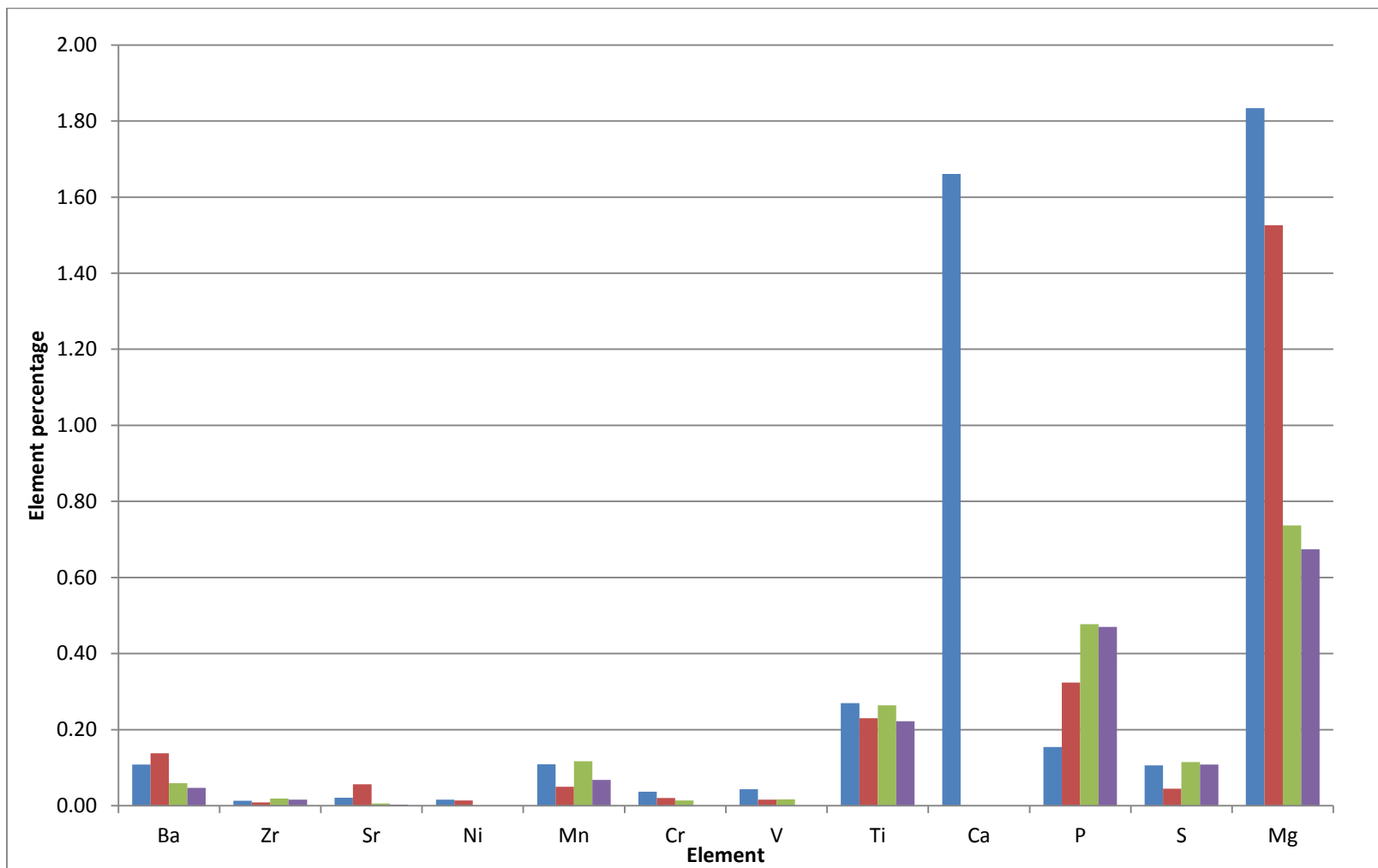


Figure 7.3: Thaba Nkulu tuyère XRF low percentage element proportions (colours represent individual samples).

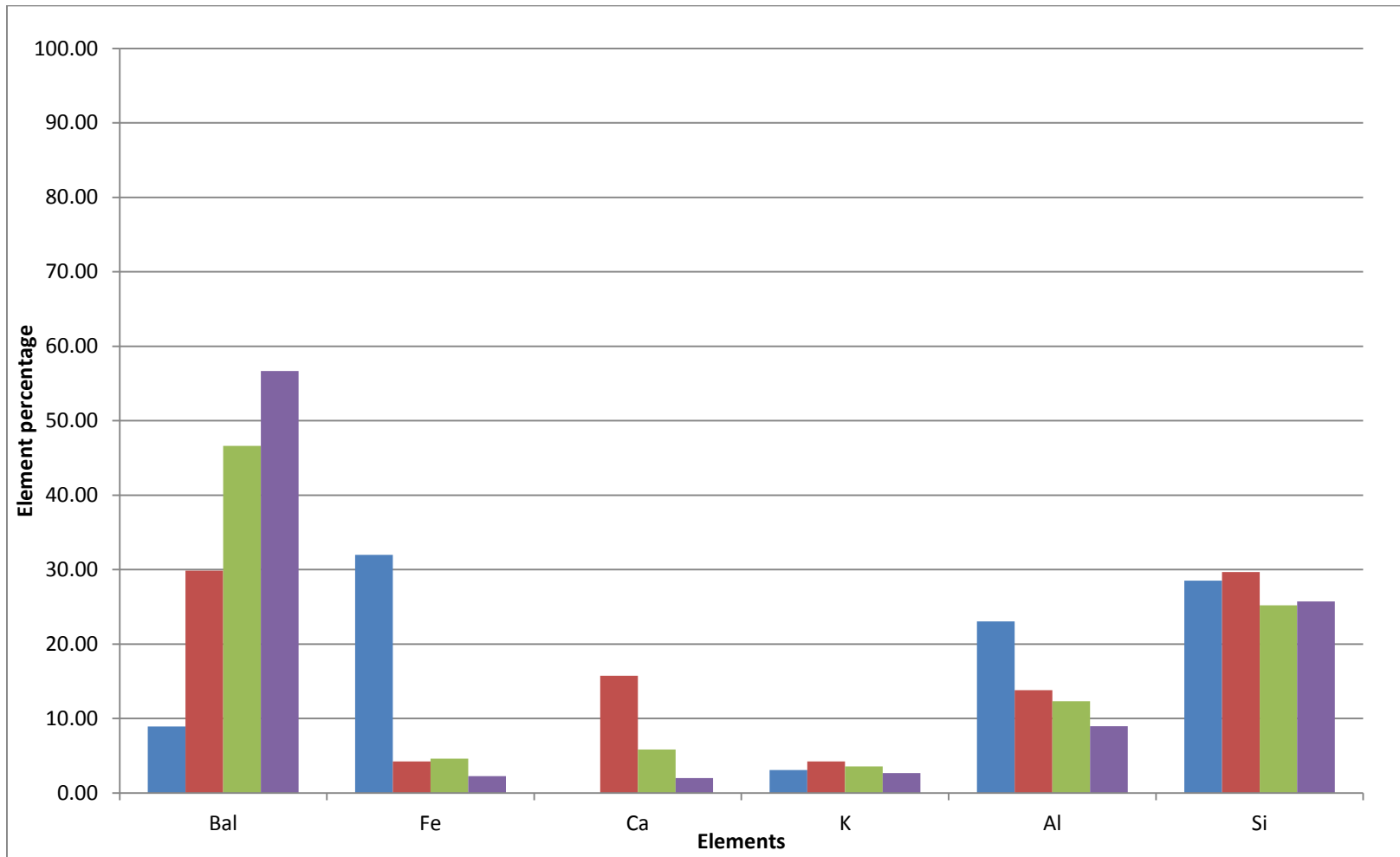


Figure 7.4: Thaba Nkulu tuyère XRF higher percentage element proportions (colours represent individual samples).

7.1.4: Ore

The ore samples consisted of fourteen samples. These samples were analysed and sorted using the same techniques as before, and are displayed in the same way, with the low proportion percentages being given in Table 7.5, and a bar chart display in Figure 7.5. The high proportion percentages are given in Table 7.6, and displayed in Figure 7.6. The elements detected in the low proportion percentages were: Ba, niobium (Nb), Ni, Co, Mn, Cr, V, Ti, Ca, K, P, S, and Mg. The high proportion percentages were: Fe, Ca, Al, Si and Mg and balance. The trace elements recorded were Ba, Nb, and Co.

As the ore samples represent the natural form of elements, being unaltered, they represented the base of elements, which should be discovered in metal and metal associated material culture. All artefacts after the smelting process would contain similar elements, with varying additive elements due to the smelting and smithing process. In the case of the ores found on Thaba Nkulu, one sample contained a low proportion percentage of niobium, although, the remaining elements recorded were seen in both the tuyère and slag samples. The averages and standard deviations of the samples were reasonable for both high (mostly under 10%) and low (less than 1%) proportions, with no element containing a large variation, other than those with a single element count. The higher variation in the higher proportion elements would be expected from the natural inhomogeneity of the ores. As most of the “-” records meant zero, the standard deviation is based on these and not an empty slot.

Table 7.5: XRF ore results, low proportion percentages in wt%.

Artefact ore	Ba	Nb	Ni	Co	Mn	Cr	V	Ti	Ca	K	P	S	Mg	Total
2328 CA1 (2) XIII/F/S ORE	0.04	-	-	0.26	0.04	0.06	0.03	0.08	0.64	1.02	0.54	0.08	1.89	4.68
2328 CA1 (2) XIII/F/1A ORE	0.06	0.03	0.03	-	0.09	0.05	0.11	0.05	0.42	1.03	0.54	0.05	-	2.46
2328 CA1 (2) XIII/F/1A ORE (2)	0.04	-	-	-	0.08	0.05	0.04	0.08	1.07	1.12	0.75	0.14	1.8	5.17
2328 CA1 (2) XIII/F/2B ORE	0.07	-	-	-	0.09	0.05	0.06	0.07	1.17	1.34	0.61	0.17	1.82	5.45
2328 CA1 (2) XIII/F/2B ORE (2)	0.03	-	0.01	-	0.04	0.05	0.06	0.03	0.25	0.65	0.15	0.04	1.52	2.83
2328 CA1 (4) XX/J/S ORE	0.02	-	-	0.05	0.08	0.06	0.08	0.21	0.53	1.3	0.46	0.1	1.27	4.16
2328 CA1 (10) IX/G/S ORE	0.04	-	-	-	-	0.05	0.07	0.04	0.21	0.3	0.09	0.05	1.81	2.66
2328 CA1 (10) IX/G/S ORE (2)	0.03	-	0.01	-	0.05	0.05	0.12	0.09	0.48	1.07	0.34	0.07	1.36	3.67
2328 CA1 (10) IX/G/S ORE (3)	0.03	-	0.02	-	0.02	0.05	0.06	0.05	0.32	0.39	0.14	0.04	1.63	2.75
2328 CA1 (10) IX/G/2B ORE	0.03	-	-	0.27	0.1	0.05	0.03	0.1	-	1.6	0.57	0.15	-	2.9
2328 CA1 AC 4 ORE	0.01	-	0.01	-	0.03	0.03	0.09	0.07	0.23	0.5	0.16	0.05	1.07	2.25
2328 CA1 AC 5 ORE	0.04	-	0.02	-	0.02	0.06	0.13	0.22	0.13	0.7	0.16	0.11	1.66	3.25
2328 CA1 AC 11 ORE	0.03	-	0.03	-	-	0.06	0.06	0.06	0.1	0.34	0.11	0.05	1.03	1.87
2328 CA1 AC 16 ORE	0.04	-	0.02	-	0.02	0.05	0.04	0.05	0.49	0.5	0.27	0.05	1.59	3.12
Average	0.04	0.01	0.02	0.19	0.05	0.05	0.07	0.08	0.46	0.85	0.35	0.08	1.54	
Standard Deviation	0.01	0.02	0.01	0.12	0.03	0.01	0.03	0.06	0.33	0.42	0.22	0.04	0.3	

Table 7.6: XRF ore results, high proportion percentages in wt%.

Artefact ore	Bal	Fe	Ca	Al	Si	Mg	Total
2328 CA1 (2) XIII/F/S ORE	4.84	37.74	-	10.82	41.83	-	95.23
2328 CA1 (2) XIII/F/1AORE	-	63.46	-	13.87	17.64	2.43	97.4
2328 CA1 (2) XIII/F/1AORE (2)	-	59.32	-	18.01	17.43	-	94.76
2328 CA1 (2) XIII/F/2B ORE	10.89	54.21	-	13.41	15.65	-	94.16
2328 CA1 (2) XIII/F/2B ORE (2)	-	68.1	-	12.32	16.05	-	96.47
2328 CA1 (4) XX/J/S ORE	-	55.33	-	16.88	23.58	-	95.79
2328 CA1 (10) IX/G/S ORE	16.64	70.26	-	5.5	4.87	-	97.27
2328 CA1 (10) IX/G/S ORE (2)	-	65.26	-	16.73	14.32	-	96.31
2328 CA1 (10) IX/G/S ORE (3)	12.61	69.61	-	7.83	7.12	-	97.17
2328 CA1 (10) IX/G/2B ORE	-	54.13	8.06	17.84	16.04	-	96.07
2328 CA1 AC 4 ORE	30.43	43.01	-	6.31	17.97	-	97.72
2328 CA1 AC 5 ORE	4.52	69.16	-	11.74	11.27	-	96.69
2328 CA1 AC 11 ORE	15.12	67.25	-	8.69	7	-	98.06
2328 CA1 AC 16 ORE	7.03	68.94	-	11.78	9.08	-	96.83
Average	7.29	60.41	0.58	12.27	15.7	0.17	
Standard Deviation	9.02	10.34	2.15	4.16	9.15	0.65	

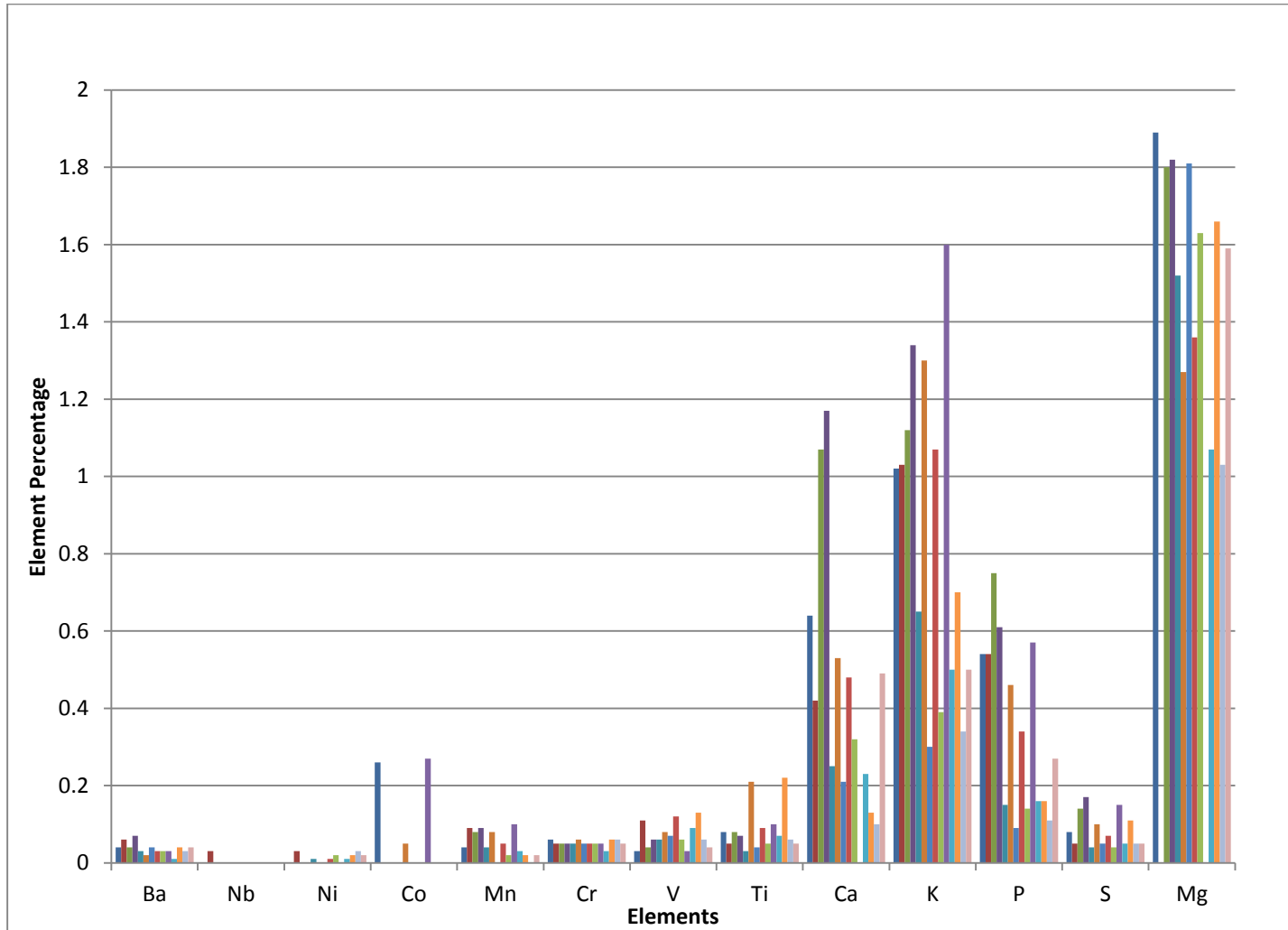


Figure 7.5: Thaba Nkulu ore XRF low percentage element proportions (colours represent individual samples).

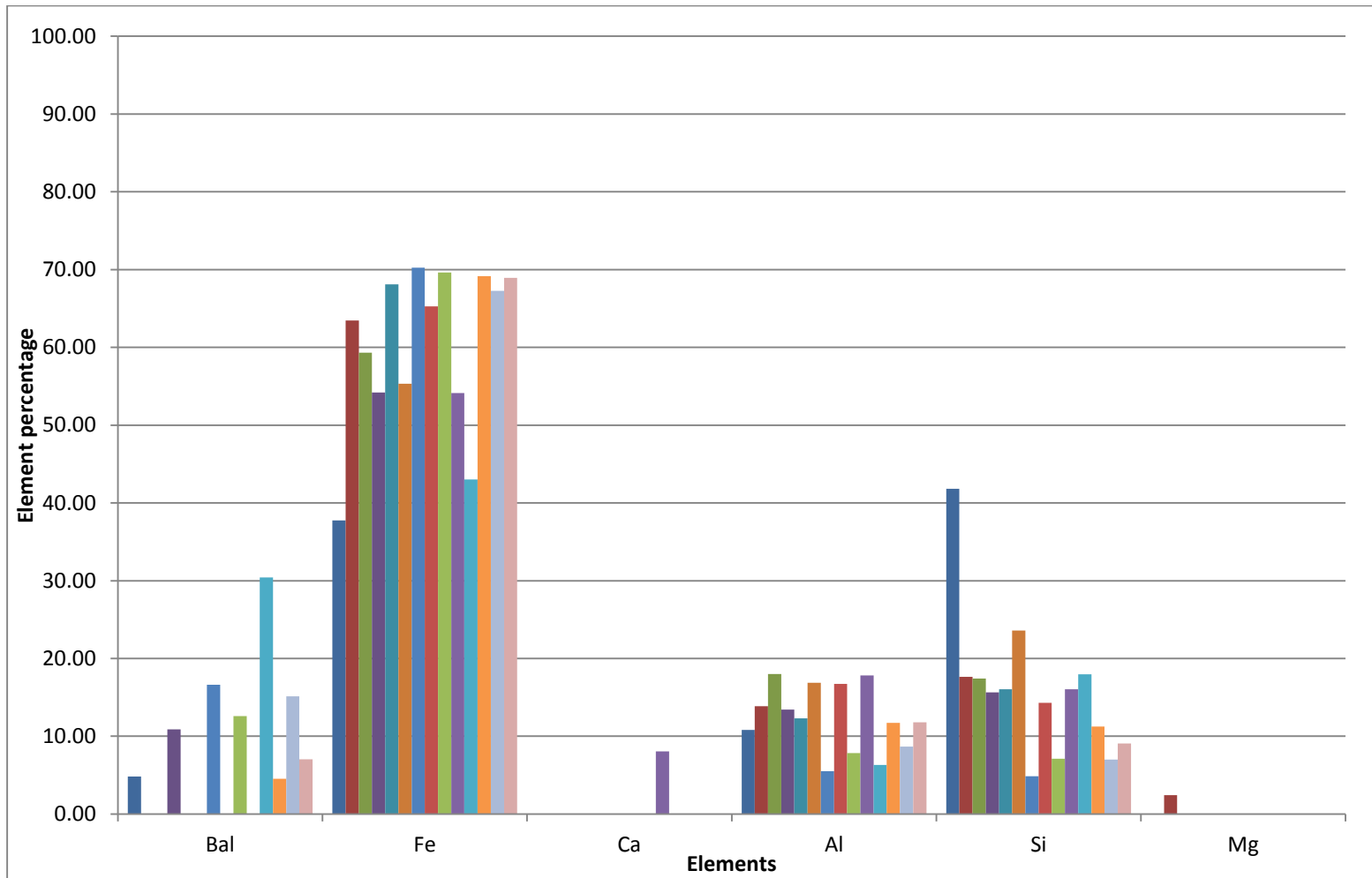


Figure 7.6: Thaba Nkulu ore XRF higher percentage element proportions (colours represent individual samples).

7.1.5: Iron artefacts

The iron artefacts are represented first, as the majority of artefacts found comprised or contained iron, making these artefacts the final result of the smelting and smithing process. The standard deviations for iron artefacts were similar to those in the slag, with low percentages in the low proportion results, and high (but acceptable ranges) in the higher proportion percentage section.

The elements found in the low proportion percentages are presented in Table 7.7, and contained the elements: Ba, tin (Sn), Zr, arsenic (As), Cu, Co, Mn, Cr, V, Ti, Ca, K, P, S, and Mg. The trace elements discovered in the iron artefacts were Ba, Zr, As, and Co. The high proportion percentages contained Fe, K, Al, Si, and Mg, seen in Table 7.8, as well as the unidentified (balance Bal) elements. The results are displayed in Figures 7.7 and 7.8. The previously unreported elements which appeared in the iron artefacts only appeared in one sample, the spear base, whereas, copper appeared in one sample as well, sample 2328 CA1 Tang. This was the only iron artefact which contained copper.

Table 7.7: XRF iron artefacts results, low proportion percentages in wt%.

Artefact iron	Ba	Sn	Zr	As	Cu	Co	Mn	Cr	V	Ti	Ca	K	P	S	Mg	Total
Tang Thaba Nkulu (iron)	0.04	-	0.02	0.02	0.01	0.41	0.15	0.05	0.02	0.3	0.64	-	1.14	0.18	-	2.98
Arrow head (iron)	0.03	-	-	-	-	0.12	0.04	0.06	0.03	0.07	0.19	1.12	1.74	0.23	1.66	5.29
Spear base (iron)	0.02	0.11	-	0.03	-	0.14	0.1	0.06	0.02	0.12	0.37	1.4	1.97	0.25	-	4.59
Average	0.03	0.04	0.01	0.02	0	0.22	0.1	0.05	0.02	0.16	0.4	0.84	1.62	0.22	0.55	
Standard Deviation	0.01	0.06	0.01	0.02	0.01	0.16	0.05	0.01	0	0.12	0.23	0.74	0.43	0.04	0.96	

Table 7.8: XRF iron artefacts results, higher proportion percentages in wt%.

Artefact iron	Bal	Fe	K	Al	Si	Mg	Total
Tang Thaba Nkulu (iron)	2.37	43.04	3.13	21.37	26.36	-	96.27
Arrow head (iron)	5.21	62.68	-	13.99	12.7	-	94.58
Spear base (iron)	-	62.44	-	15.28	15.15	2.25	95.12
Average	2.53	56.05	1.04	16.88	18.07	0.75	
Standard Deviation	2.61	11.27	1.8	3.94	7.28	1.3	

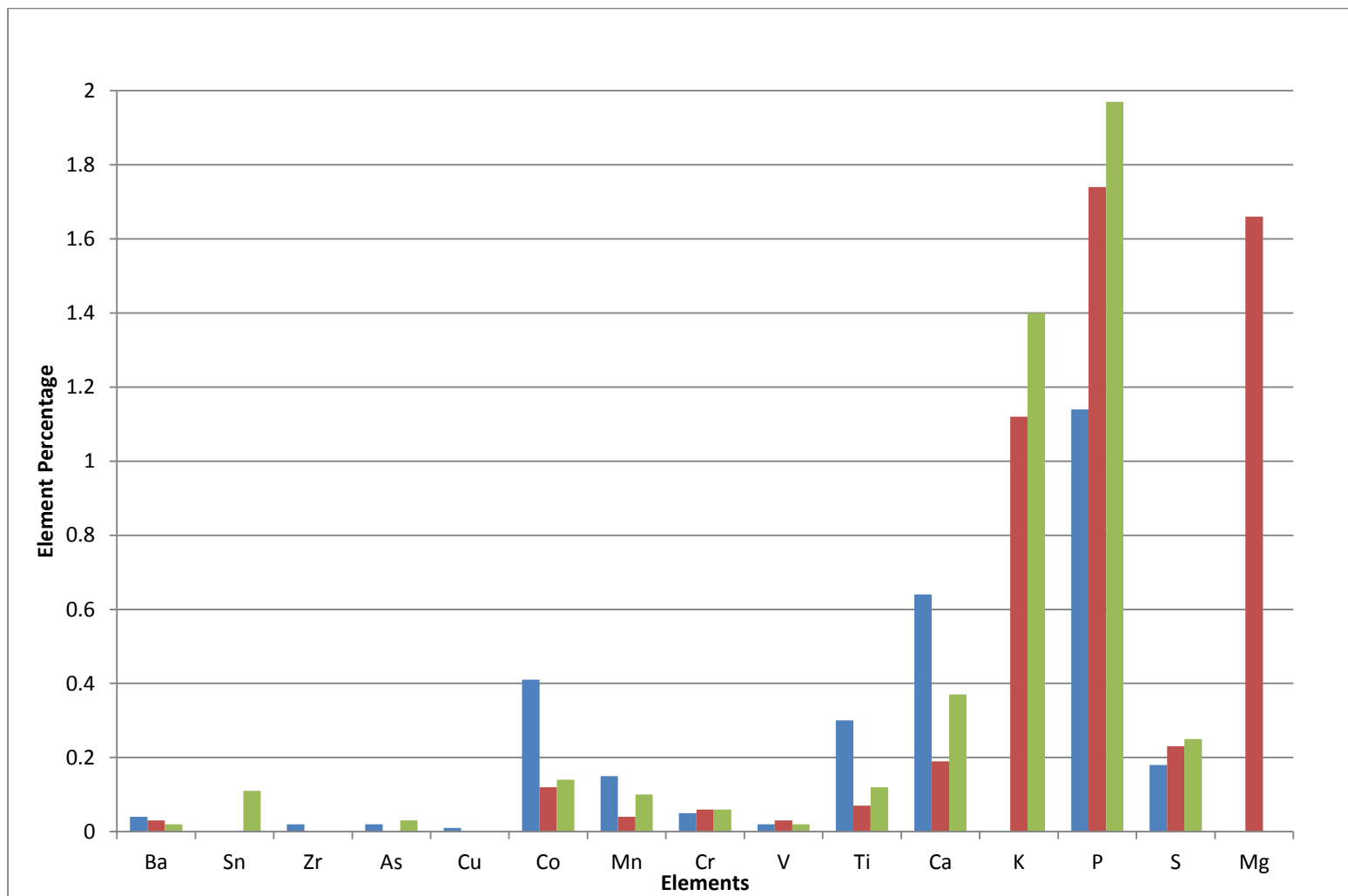


Figure 7.7: Thaba Nkulu iron artefacts XRF low percentage element proportions (colours represent individual samples).

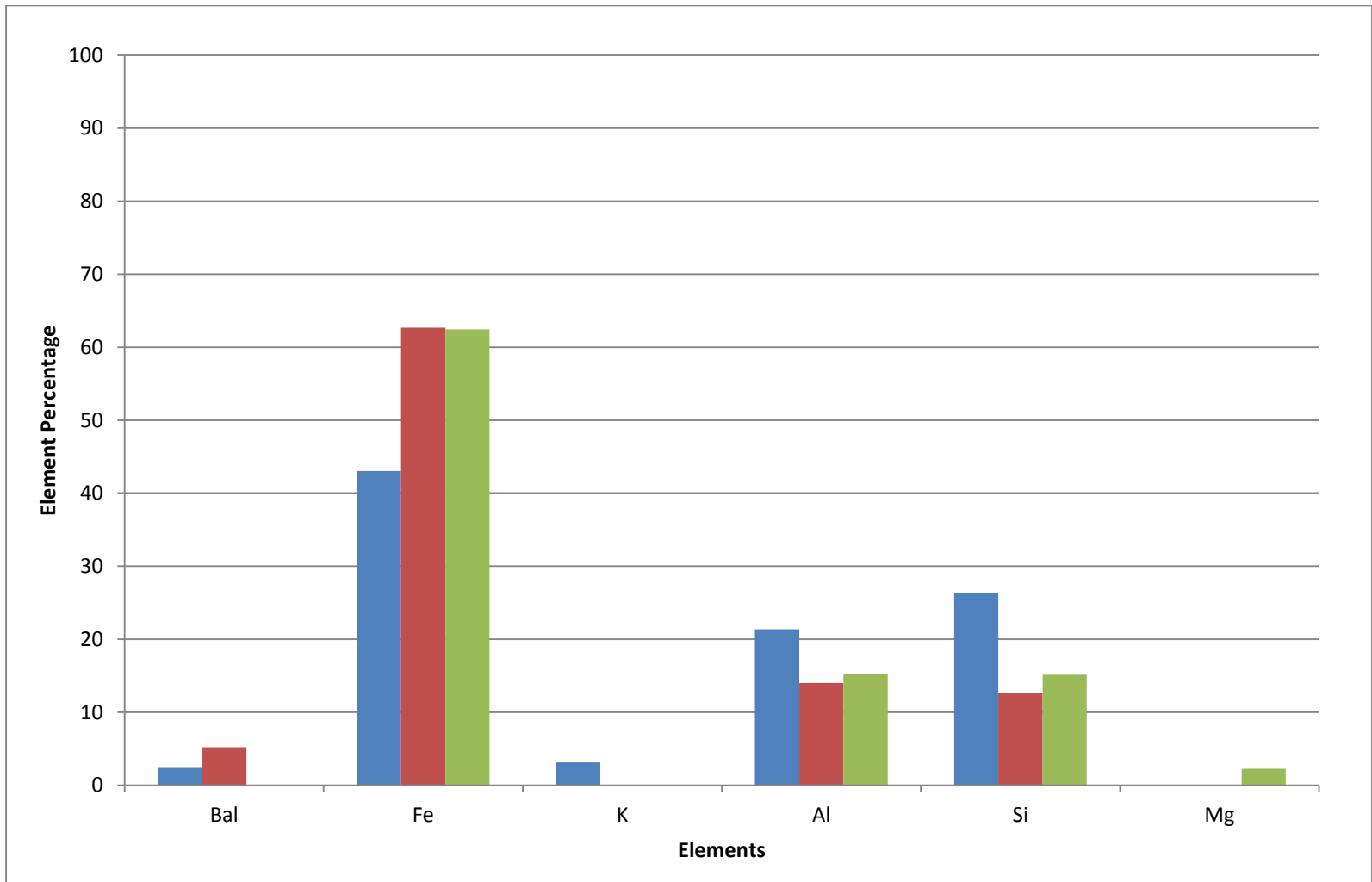


Figure 7.8: Thaba Nkulu iron artefacts XRF higher percentage element proportions (colours represent individual samples).

7.1.6: Copper artefacts

The copper artefacts contained similar elements, but differed in proportions especially Cu and Fe. The elements detected in the low proportion percentage range were: Ba, silver (Ag), Sr, As, lead (Pb), Zn, Ni, Fe, Mn, V, Ti, Ca, K, P, S and Mg, shown in Table 7.9. Trace elements differed in the copper artefacts as: Ag, As, Pb were now present, as well as Ba, Sr, and Zn. The high proportion elements detected were: Sn, Cu, K, Al and Si, given in Table 7.10. As these were copper artefacts, the main element detected was copper.

The averages and standard deviations were in acceptable ranges, as recorded within the previous XRF results. The two artefacts retrieved in 2013 (2328 CA1 (2) XIII/F/S and 2328 CA1 (3) X/A/3A) were similar in composition, whereas that recovered from the 2010 (2328 CA1 57) excavation differed slightly in the low proportion range, as it had a higher arsenic recording than the other two. Figure 7.9 displays the three artefacts in a bar chart. In the high proportion percentage range, the elements recovered were similar across all three artefacts, except for tin (Sn) as 2328 CA1 57 contained none, as Figure 7.10 shows.

Table 7.9: XRF copper artefacts results, low proportion percentages in wt%.

Artefact copper	Ba	Ag	Sr	As	Pb	Ni	Fe	Mn	V	Ti	Ca	K	P	S	Mg	Total
2010 copper earring 2328 CA1 57	0.06	-	0.01	0.3	-	-	1	0.03	0.02	0.13	1.56	1.92	1.04	0.19	-	6.26
2328 CA1 (2) XIII/F/S copper thin wire earring artefact	0.09	0.01	-	0.02	0.01	0.04	0.9	0.06	-	0.11	1.61	1.6	1.37	0.2	-	6.02
2328 CA1 (3) X/A/3A thick copper wire artefact	0.04	0.01	-	0.01	-	-	1.3	0.03	-	0.19	1.43	-	0.74	0.11	1.68	5.54
Average	0.06	0.01	-	0.11	-	0.01	1.07	0.04	0.01	0.14	1.53	1.17	1.05	0.16	0.56	
Standard Deviation	0.03	0.01	0.01	0.16	0.01	0.02	0.21	0.02	0.01	0.04	0.09	1.03	0.31	0.05	0.97	

Table 7.10: XRF copper artefacts results, higher proportion percentages in wt%.

Artefact copper	Sn	Cu	K	Al	Si	Total
2010 copper earring 2328 CA1 57	-	49.21	-	18.1	25.02	92.33
2328 CA1 (2) XIII/F/S copper thin wire earring artefact	8.23	45.96	-	17.77	21.44	93.4
2328 CA1 (3) X/A/3A thick copper wire artefact	5.86	34.34	2.14	20.58	31.35	94.27
Average	4.7	43.17	0.71	18.82	25.93	
Standard Deviation	4.24	7.82	1.23	1.53	5.02	

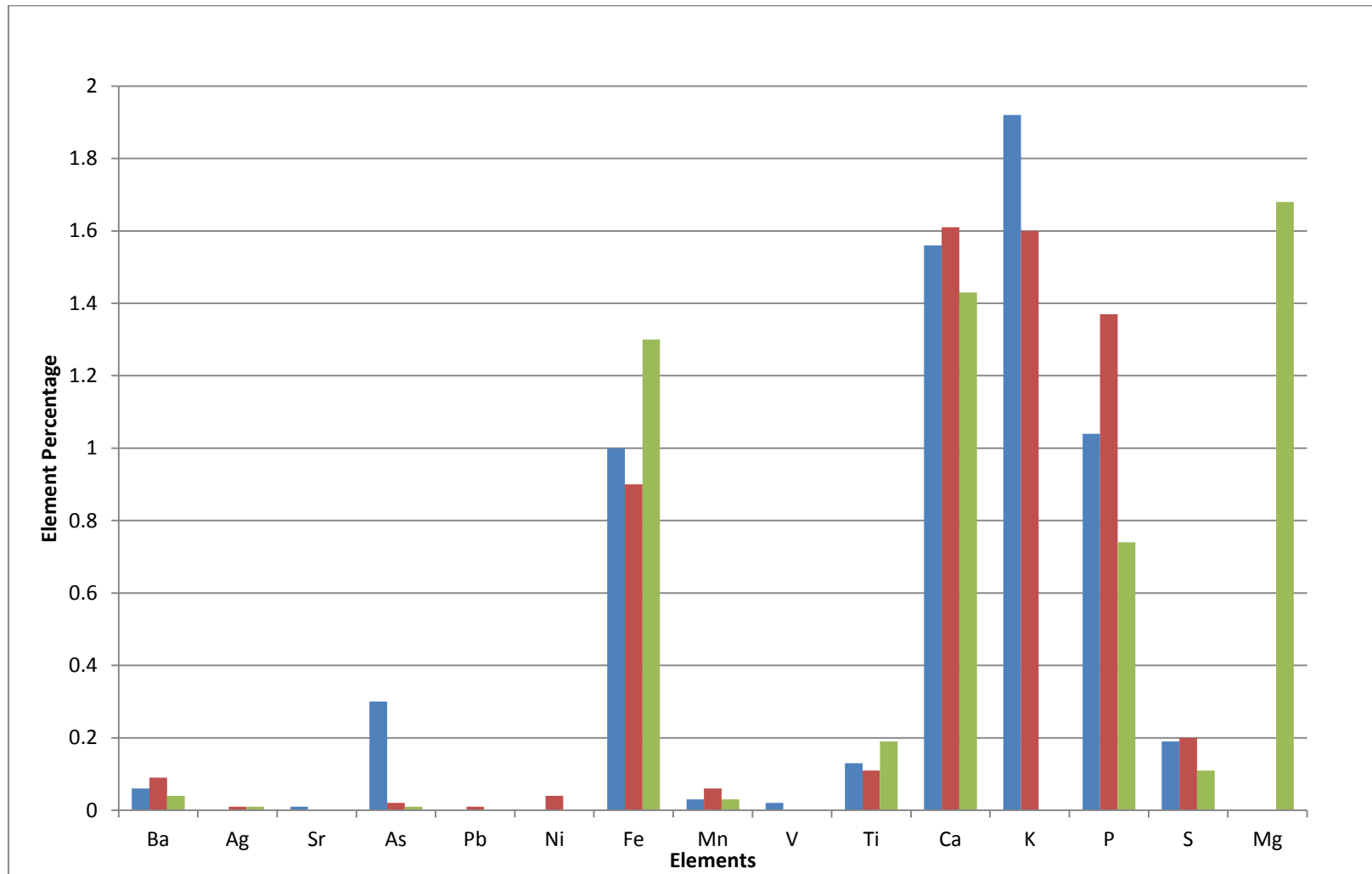


Figure 7.9: Thaba Nkulu copper artefacts XRF low percentage element proportions. The blue column represents 2328 CA1 57.

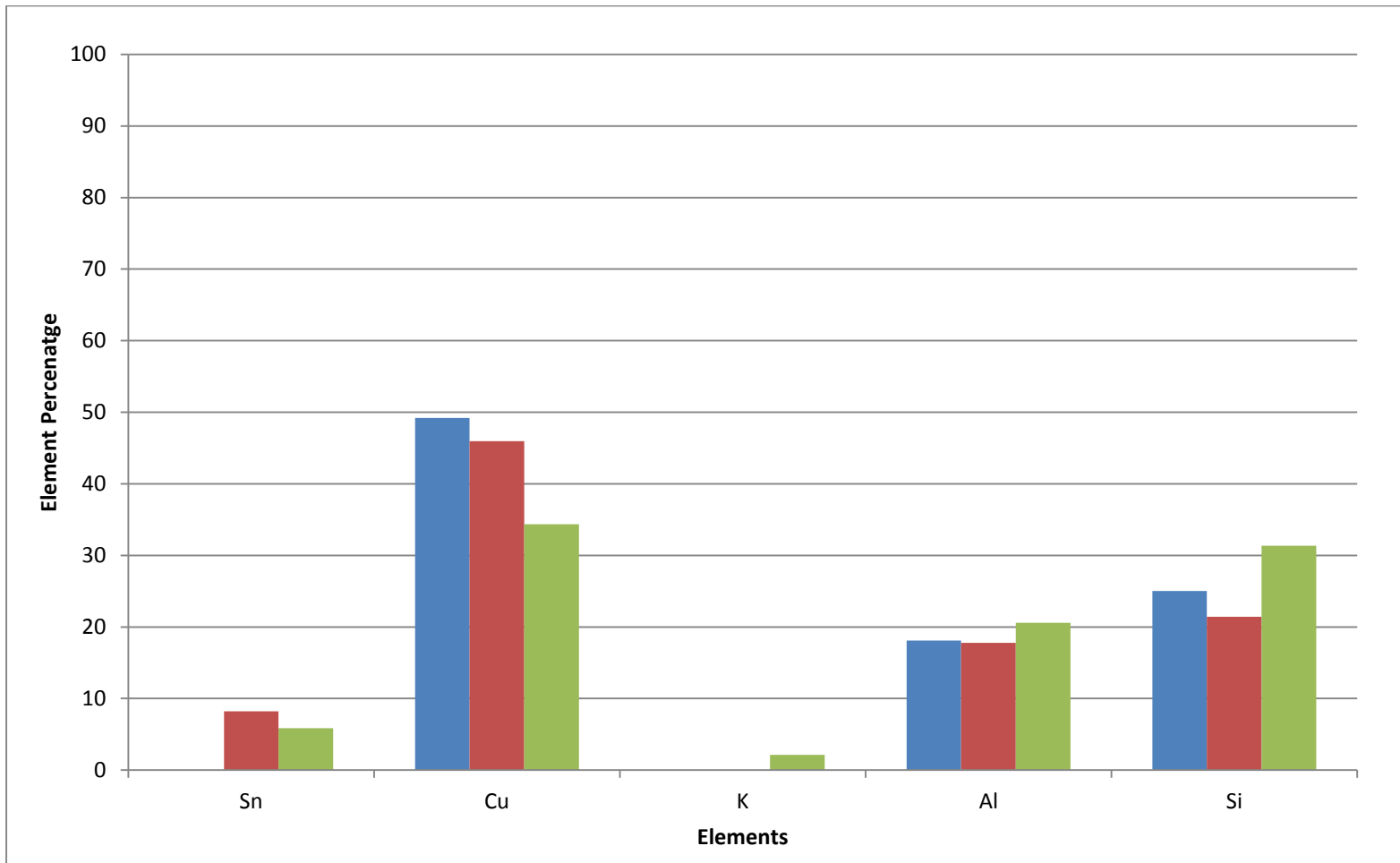


Figure 7.10: Thaba Nkulu copper artefacts XRF higher percentage element proportions. The blue column represents 2328 CA1
57.

7.2: Metallography

7.2.1: Copper artefacts

Figure 7.11 shows the microstructure of a copper artefact. Within the grains, the lighter shades were annealing twins, which have parallel straight sides (indicated by arrow 1). These and the mainly equiaxed grains show that the artefact was annealed, heated up to soften it after working, and this process was probably repeated. Other identified structures were the aligned and elongated stringers (which are either oxides or sulphides) throughout the artefact surface (indicated by arrow 2). These indicate that the artefact was worked, probably by hammering or drawing.

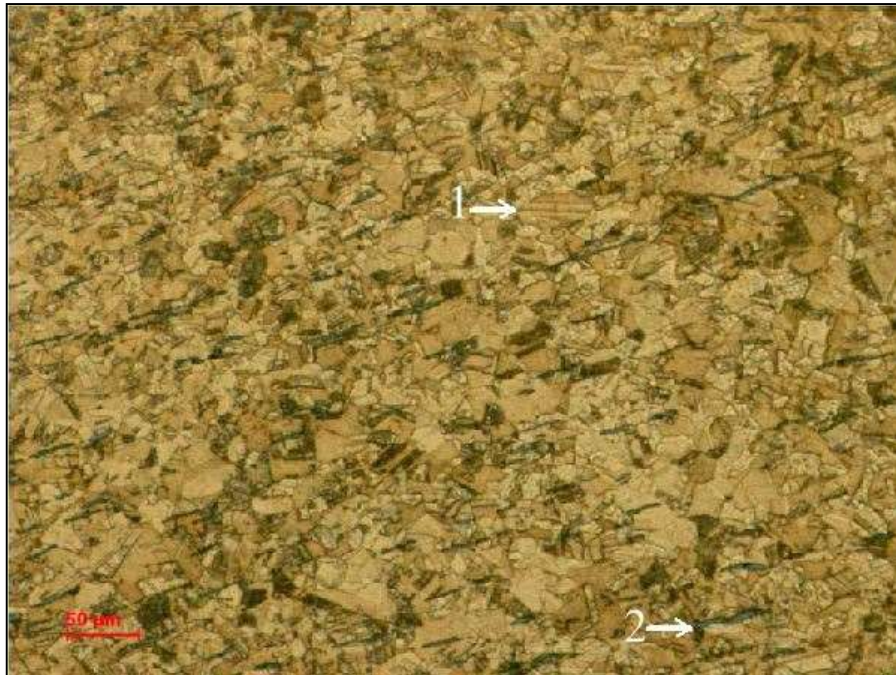


Figure 7.11: Optical micrograph of 2328 CA1 (3) X/A/3A copper artefact after sectioning and etching showing: grains (of different shades) with annealing twins (parallel sides (arrow 1)) and stringers of inclusions (grey (arrow 2)). Bar (bottom left) represents 50 microns.

The second copper artefact recovered, an earring, had a similar microstructure to the artefact discussed above. There were aligned and elongated stringers (which are either

oxides or sulphides) (Figures 7.12, 7.13), across the artefact. These show that the artefact was worked, probably by hammering or drawing. It also had equiaxed grains with annealing twins (Figure 7.14), showing that the artefact was heated up to soften it during working. This working and annealing process was probably repeated.

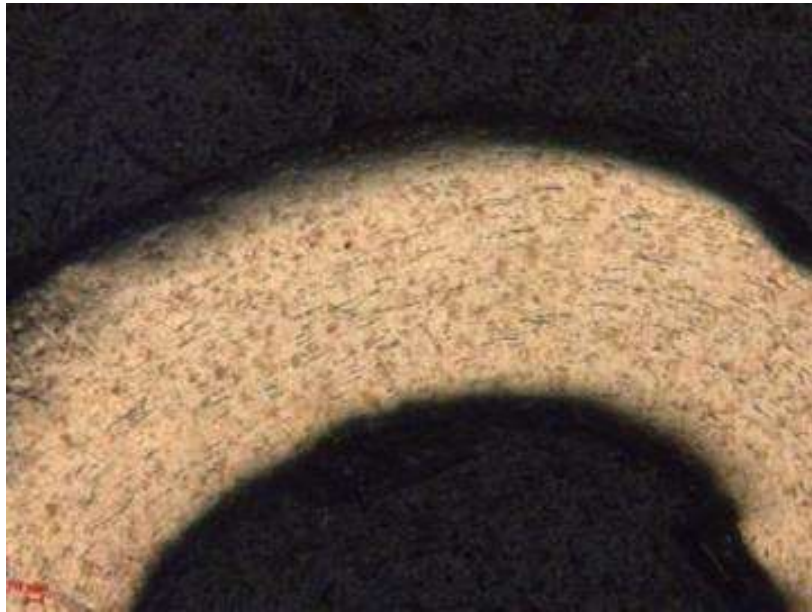


Figure 7.12: Optical micrograph at lower magnification micrograph of 2328 CA1 (2) XIII/F/S a thin copper earring after etching showing: grains with annealing twins (parallel sides) and aligned stringers of inclusions (grey). Bar represents 50 microns.



Figure 7.13: Optical micrograph at intermediate magnification of 2328 CA1 (2) XIII/F/S, a thin copper earring after etching, showing: mainly equiaxed grains with annealing twins (parallel sides) and aligned stringers of inclusions (grey). Bar represents 50 microns.



Figure 7.14: Optical micrograph at higher magnification of 2328 CA1 (2) XIII/F/S, a thin copper earring after etching, showing: mainly equiaxed grains with annealing twins (parallel sides) and aligned stringers of inclusions (grey). Bar represents 50 microns.

7.2.2: Iron artefacts

Figures 7.15 and 7.16 are micrographs of the arrow head handed over by the farm manager. The artefact was heavily oxidised and had high proportions of oxides on the boundaries of the ferrite grains throughout the artefacts' surface, and small amounts of pearlite between the ferrite grains.



Figure 7.15: Low magnification of 2328 CA1 iron arrow head, showing: ferrite grains (light), pearlite (darker) and sulphide stringers (very dark), and high proportion of oxides in the bottom right hand corner, grey. Red bar represents 50 microns.



Figure 7.16: High magnification of 2328 CA1 iron arrow head microstructure, showing ferrite grains (light), pearlite (darker) and sulphide stringers (grey). Red bar represents 50 microns.

The next iron artefact analysed was the spear head (collected by the farm manager, and classified as a surface find). This had large ferrite grains (light in Figures 7.17, and 7.18), with the decomposed carbides of the pearlite having now formed irregular graphite nodules (dark grey in Figures 7.17, and 7.18). This microstructure suggests heating to fairly high temperatures.



Figure 7.17: Optical micrograph of 2328 CA1 iron spear head, showing mainly equiaxed ferrite grains (lighter) and irregular graphite (very dark). Bar represents 50 microns.



Figure 7.18: Optical micrograph of 2328 CA1 iron spear head, showing ferrite grains (light) with graphite (dark).

The last iron artefact the iron tang (Figures 7.19, and 7.20) also had large ferrite grains (with a bainitic-like morphology), being less regular, and the carbon was the graphite nodules. The bainitic morphology usually only occurs after heating to fairly high temperatures and cooling rapidly.

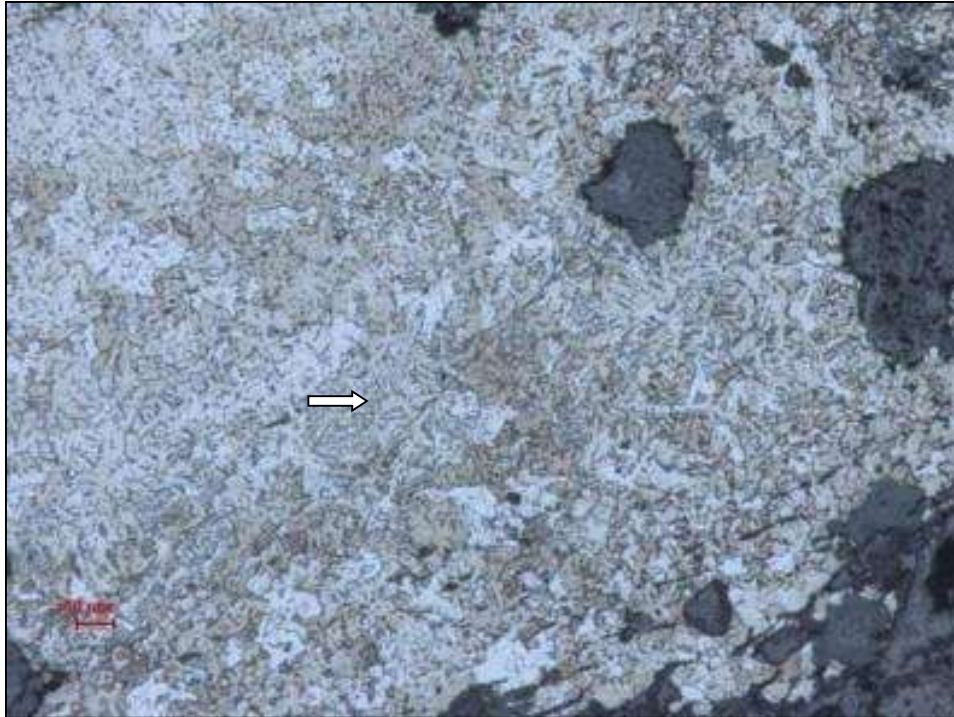


Figure 7.19: 2328 CA1 iron tang showing ferrite grains, needle like structure (arrow) and carbides, red bar equals 50 microns.



Figure 7.20: 2328 CA1 iron tang, showing ferrite grains and carbides, red bar represents 50 microns.

7.3: SEM-EDX findings

7.3.1: SEM-EDX slag

SEM-EDX results were similar to those recorded by XRF, although “Balance” was split between oxygen, nitrogen and carbon (Table 7.11). These new elements were those that the XRF could not detect, having atomic numbers below 11, and therefore were placed in the “balance” i.e. unidentified elements. The totals were not included in these tables, as the totals were all equal 100, due to the SEM normalising it automatically.

Although the XRF analyses identified more elements, the SEM-EDX identified the elements detected by the XRF in higher proportions. Elements such as Fe, Al, Si, and Mg were all present in the high percentage proportion ranges in XRF. In total, 12 elements were detected in the slag samples by SEM analysis. The elements were:

carbon, nitrogen, indium, oxygen, aluminium, magnesium, silicon, phosphorus, potassium, calcium, iron and bromine.

The averages and the standard deviations of the slag elements were acceptable for those within the high proportion percentages and low proportion percentages. The highest standard deviation amongst the slag samples was 22.9 for iron, and the lowest was 0.5 for phosphorus.

The microstructure of a typical dendrite-rich slag is shown in Figure 7.21, and there were pores lined with a thin layer of iron, iron-rich wüstite dendrites, pores, and different inclusions in a needle-like matrix. Interestingly, the slag appeared to nucleate on the iron droplet and the inclusion formed between the needles of the matrix of the slag. The microstructure in Figure 7.21 was similar to one from another archaeological site Ndongondwane (Miller & Killick 2004), located in KwaZulu-Natal, except there was a higher proportion of dendrites in the Thaba Nkulu slags. Other slag fragments contained no pure iron, lower dendrite proportions, and also inclusions that had high nitrogen content. The compositions of the Thaba Nkulu slags themselves varied considerably, and there was variation in the analyses of the different phases. The slag Fe compositions varied by more than 20% for iron, and they had different microstructures, indicating that there was a range of slag compositions. The full SEM-EDX results, in both figures (areas scanned) and elemental recordings can be seen in Appendices D and E, for both the Sigma Zeiss and EDAX SEM-EDX results. Due to the variation in the Fe, this would make identifying a chemical signature for Thaba Nkulu difficult. Thus, alternative methods and hypothesis were explored, in order to determine a chemical signature. These will be presented in the next chapter.

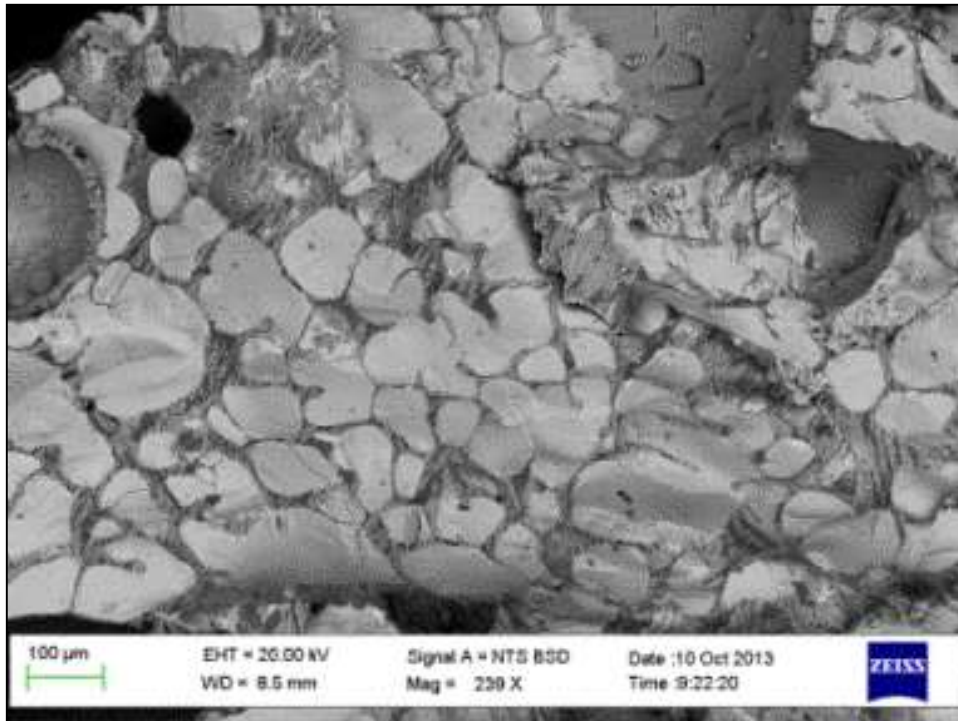


Figure 7.21: Slag 2328 CA1 (10) Road Test X/I/S SEM-BSE of a section through a slag fragment, showing a round hole with iron lining at the left hand side (dark), iron-aluminium silicate dendrites (light), iron-aluminium silicate needles (medium).

Table 7.11: SEM-EDX slag results in wt%.

Slag samples WITS SEM	Element											
	C	N	In	O	Al	Mg	Si	P	K	Ca	Fe	Br
2328 CA1 (1) XIX/N/2B 1	-	-	-	51.8	6.3	-	19.7	-	2.9	12.0	7.3	-
2328 CA1 (1) XIX/N/2B 2	-	-	-	46.6	6.4	1.8	14.1	-	-	18.1	13.0	-
2328 CA1 (1) XIX/N/2B 3	-	-	-	66.6	5.3	5.3	16.9	-	0.8	5.1	-	-
2328 CA1 (1) XX/M/1B 1	16.1	-	-	45.2	4.4	-	9.1	-	1.2	-	23.9	-
2328 CA1 (1) XX/M/1B 2	8.9	-	-	58.5	8.9	-	17.1	-	2.8	0.6	3.3	-
2328 CA1 (1) XX/M/1B 3	-	-	-	45.9	4.4	-	9.4	-	1.1	-	39.3	-
2328 CA1 (1) XX/M/2A RB 1	-	-	6.4	-	32.0	-	12.1	-	-	-	37.4	12.1
2328 CA1 (1) XX/M/2A RB 2	-	-	-	-	-	-	7.8	-	7.0	-	75.3	9.9
2328 CA1 (1) XX/M/2A RB 3	-	-	-	43.4	9.5	-	25.6	-	4.4	-	17.0	-
2328 CA1 (1) XX/O/AD 1 (1)	-	-	-	49.5	4.0	-	10.5	-	-	14.8	21.2	-
2328 CA1 (1) XX/O/AD 1 (2)	-	30.1	-	26.3	-	-	3.8	-	-	10.6	29.2	-
2328 CA1 (1) XX/O/AD 1 (3)	-	-	-	40.8	3.9	-	11.1	-	1.3	11.4	31.5	-
2328 CA1 (1) XX/O/2B 1	-	-	-	49.7	6.9	-	19.6	-	2.3	-	21.5	-
2328 CA1 (1) XX/O/2B 2	6.0	-	-	56.4	7.1	-	22.3	-	2.9	-	5.3	-
2328 CA1 (10) Road Test X/I/S 1	9.0	-	1.0	35.1	2.1	-	3.3	-	-	-	49.4	-
2328 CA1 (10) Road Test X/I/S 2	7.6	14.8	-	35.1	-	-	-	-	-	42.5	-	-
Slag samples EDAX SEM												
2328 CA1 (4) XX/J/3B Area 1 20kV	-	-	-	45.2	5.9	0.8	31.6	0.9	2.4	1.9	11.2	-
2328 CA1 (10) IX/G/1B Area 1 Spot 1 20kV	9.6	-	-	51.4	-	1.4	8.7	-	1.8	19.3	2.0	-
2328 CA1 (10) IX/G/1B Area 1 Spot 2 20kV	-	-	-	22.8	0.7	-	0.3	-	0.1	-	76.1	-
2328 CA1 (10) IX/G/1B Area 1 30kV	-	-	-	24.9	4.9	1.2	7.5	0.3	0.8	5.2	55.3	-
Average	9.53	22.47	3.69	44.19	7.03	2.10	13.18	0.61	2.27	12.87	28.85	11.01
Standard deviation	3.48	10.84	3.76	11.78	7.03	1.82	8.07	0.45	1.78	11.60	22.92	1.53

7.3.2: SEM-EDX tuyère and ore

Only two tuyère fragments and two ore pieces were analysed by SEM-EDX (Table 7.12). The elements detected in the tuyère were: carbon, oxygen, aluminium, magnesium, silicon, phosphorus, potassium, calcium, titanium, and iron. Of these samples, only one contained phosphorus and titanium. The two pieces yielded different results. Only one section of the tuyère from 2328 CA1 (3) X/A/3C contained carbon, whereas the other tuyère piece from 2328 CA1 (1) XIX/N/AD contained carbon in all sample groups.

It is likely that the difference in the SEM tuyère results is due to different sections of tuyère being sampled. As explained in the XRF tuyère section each of the tuyère pieces contained an inner and outer surface, these surfaces were the slag covered exterior of the tuyère, and the clay interior. They had different compositions due to the different materials associated with them.

In the ore samples, the detection ratios varied greatly. One sample (2328 CA1 Road collection) tested in the Wits SEM only contained carbon. The piece, however, contained micro-sand particles, and was consequently removed, due to fear of contaminating the SEM. Two more pieces, of similar grain structure, were analysed in the EDAX (non-WITS) SEM-EDX and contained: oxygen, aluminium, silicon, calcium, and one (2328 CA1 (4) XX/J/1D) contained manganese, whereas both contained iron.

Table 7.12: SEM-EDX tuyère and ore results in wt%.

Tuyère sample WITS SEM	Element										
	C	O	Al	Mg	Si	P	K	Ca	Ti	Mn	Fe
2328 CA1 (1) XIX/N/AD 1	15.6	55.9	7.5	-	14.1	-	2.0	3.1	-	-	1.8
2328 CA1 (1) XIX/N/AD 2	16.1	62.0	6.7	-	10.0	-	1.4	2.1	-	-	1.7
2328 CA1 (1) XIX/N/AD 3	13.9	59.2	4.9	-	14.1	-	1.8	4.4	-	-	1.8
Tuyère sample EDAX SEM											
2328 CA1 (3) X/A/5B Bottom 20kV	-	45.0	-	0.7	32.2	-	3.4	-	-	-	4.9
2328 CA1 (3) X/A/5B Top 20kV	-	43.6	12.9	-	33.9	-	-	1.3	-	-	4.9
2328 CA1 (3) X/A/5B Bottom 30kV	7.4	44.9	12.2	0.9	-	-	4.4	1.8	-	-	7.3
2328 CA1 (3) X/A/5B Top 30kV	-	41.6	13.1	0.9	25.3	0.9	3.9	1.8	0.4	-	12.2
Ore sample WITS SEM											
2328 CA1 Road Collection 16 Ore	100.0	-	-	-	-	-	-	-	-	-	
Ore sample EDAX SEM											
2328 CA 1 (10) VIII/G/S Ore 20kV	-	30.5	3.6	-	4.4	-	-	0.6	-	-	61.0
2328 CA1 (4) XX/J/3A Area 1 20kV	-	28.3	5.4	-	6.7	-	-	1.1	-	1.0	57.5
Average	30.58	45.66	8.28	0.81	17.59	0.88	2.80	2.02	0.42	1.01	17.01
Standard deviation	38.97	11.78	3.87	0.14	11.42	-	1.24	1.23	-	-	24.21

7.3.3: SEM-EDX iron artefacts

Eight elements were detected in the iron artefacts. They were: carbon, oxygen, aluminium, magnesium, silicon, potassium, calcium, and iron (Table 7.13). The two main elements detected within the iron artefact samples were oxygen and iron; both were detected 12 times, out of 13 total sample areas, across the three artefacts. Only one sample, the 2328 CA1 tang, contained magnesium and calcium, so it had no standard deviation. The remaining elements, however, were detected in two or more of the sample areas. This detection does not represent the entire artefact, as only a small sample area was analysed each time, as discussed previously.

Table 7.13: SEM-EDX iron artefacts results in wt%.

Iron artefact samples WITS SEM	Element							
	C	O	Al	Mg	Si	K	Ca	Fe
2328 CA1 Arrowhead 1	-	16.3	-	-	-	-	-	83.7
2328 CA1 Arrowhead 2	-	35.1	-	-	-	-	-	64.9
2328 CA1 Arrowhead 3	-	-	-	-	-	-	-	100.0
2328 CA1 Arrowhead 4	-	45.3	-	-	-	-	-	54.7
2328 CA1 Arrowhead 5	-	15.5	-	-	-	-	-	84.5
2328 CA1 Spear base 1	-	50.2	4.2	-	35.1	2.1	-	8.4
2328 CA1 Spear base 2	-	45.3	-	-	29.3	-	-	8.2
2328 CA1 Spear base 3	17.2	32.3	2.4	-	3.9	-	-	61.4
2328 CA1 Spear base 4	-	15.5	-	-	-	-	-	84.4
2328 CA1 Tang 1	-	45.4	1.8	-	3.6	-	-	49.3
2328 CA1 Tang 2	7.9	37.6	13.6	-	-	-	-	40.9
2328 CA1 Tang 3	-	46.1	6.8	-	12.1	2.4	-	32.6
2328 CA1 Tang 4	60.3	37.1	-	0.8	1.1	-	0.7	-
Average	28.46	35.15	5.76	0.79	14.18	2.23	0.71	56.07
Standard deviation	27.97	12.81	4.82	-	14.56	0.25	-	29.86

7.3.4: SEM-EDX copper artefacts

In total, six different elements were detected in the copper artefacts: carbon, oxygen, aluminium, chlorine, copper and tin (Table 7.14). Two of the copper artefacts, 2328 CA1 (2) XIII/F/1A and 2328 CA1 (3) X/A/3C, presented similar results, which also was the case in their XRF results. The main elements recorded in the first two artefacts were: carbon, oxygen, copper and tin.

Conversely, artefact 2328 CA1 57, exhibited a different set of elements including aluminium and chlorine, which were not present in the samples discussed above. 2328 CA1 57 contained no tin, indicating a possible different origin of the artefact or a different manufacturing method. The averages and standard deviations within the copper samples were in acceptable ranges. The deviations varied, with the highest being 24% for Cu and the lowest being 1.5% for Sn.

Table 7.14: SEM-EDX copper artefacts results in wt%.

Copper artefact samples WITS SEM	Element					
	C	O	Al	Cl	Cu	Sn
2328 CA1 (2) XIII/F/S thin wire earring 1	-	-	-	-	92.3	7.7
2328 CA1 (2) XIII/F/S thin wire earring 2	32.4	10.6	-	-	51.8	5.3
2328 CA1 (3) X/A/3Athick copper wire 1	-	-	-	-	92.1	7.9
2328 CA1 (3) X/A/3Athick copper wire 2	30.3	11.0	-	-	53.7	5.1
2328 CA1 57 Copper Earring 1	-	-	-	-	100.0	-
2328 CA1 57 Copper Earring 2	36.5	6.3	-	-	57.2	-
2328 CA1 57 Copper Earring 3	-	32.0	22.9	8.1	36.9	-
2328 CA1 57 Copper Earring 4	-	5.7	-	10.4	84.0	-
Average	33.05	13.12	22.91	9.24	70.99	6.50
Standard deviation	3.17	10.85	-	1.57	23.69	1.53

7.4: Overall SEM-EDX analysis

All the samples used in the SEM-EDX analysis were present in the XRF analysis, however, a few new artefacts were introduced and analysed with SEM-EDX such as: a tuyère (2328 CA1 (3) X/A/3C), and two ore pieces 2328 CA1 (4) XX/J/1D and 2328 CA1 (10) VIII/G/S. These newer artefacts were introduced as they would give a single sample group test perspective, whereas all other samples would have both the XRF and SEM-EDS recordings. The results from the SEM-EDX differed slightly from those recorded by XRF analyses, as not only were fewer elements detected, but four previously undetected were now detected: carbon, oxygen, bromine, and nitrogen. Many of the low proportion element percentages recorded by the XRF were not present in the SEM-EDX results. Those that were present fell within the dominant elements present in the samples. The patterns of similarity and differences were due to the element detection difference between the instruments, as well as the different surface areas analysed. As the SEM-EDX analyses a few microns in area (although the area measured can be larger if required), the element detection is limited to these selected small areas and multiple analyses are needed to be statistically representative, whereas XRF analyses an area of 1cm², meaning a greater percentage of the sample is analysed and more elements can be recorded simultaneously.

The results displayed homogenous elements amongst those in the higher proportion percentage groups, with very little differences amongst those found in the low proportion percentages. Further methods of determining a chemical signature, however, were used and will be addressed in the next chapter.

Conclusions:

The metal artefacts and metal smelting and smithing associated material culture, proved to comprise homogenous elements. This meant that a chemical signature could not be recorded based on the chemical compositions alone. The homogeneity was caused by the major elements being recorded across all sample groups. The trace elements, however, proved to vary in element detection, these could possibly lead to a chemical signature when compared to other sites results. For this to be plausible, however, the comparative results need to have the same elements, or indicate whether or not they could be detected. These possibilities will be discussed in the next chapter, and the chemical signature of Thaba Nkulu, will be explored as well.

CHAPTER 8: CHEMICAL SIGNATURE

DISCUSSION

Introduction:

This chapter will expand on the proposed plausible chemical signatures for the metal and metal associated material culture found on site Thaba Nkulu. Which is then followed by the final chapter, which concludes on both the site and analysis outcomes.

8.1: Artefacts chemical signatures

8.1.1: Metallic smelting and smithing material

8.1.1.1: Slag chemical composition and signature

The chemical composition of the slags returned results that were homogenous within the high proportion elements. However, this was to be expected (cf. Miller *et al.* 1995; Coustures *et al.* 2003: 600; Miller & Killick 2004; Blakelock *et al.* 2009: 1752). The homogenous elements detected in the slag were: Ba, Ni, Mn, Fe, Al, Si, Cr, V, Ti, Ca, K, P, S, and Mg. These elements were detected in more than 50% of the slag samples analysed, and represent the foundation elements within Thaba Nkulu slag. Most of these elements, however, are commonly found in slag (Buchwald & Wivel 1998: 74). The slag composition suggests a similar origin, which could indicate that the ores used may have been local.

The element ratios between slags were heterogeneous and varied by more than 5%, which made it impossible to distinguish slag types based on chemical composition alone. Although Miller and Killick (2004: 34) state that “it is often impossible to distinguish smelting and smithing slags on chemical and micro-structural criteria”, from the context of materials found within excavation 2328 CA1 (1), it can be suggested that the majority of slag recovered from there can be associated to smelting slag. This corresponds to the visual appearance of the slag found on site. The smaller pieces of slag found on other excavations will need further analyses, in order to distinguish if any of these can be categorized as smithing slag.

Following this, another attempt to identify the slag type was made. For this, the slag samples were taken and identified into slag metal type (constitution). This experiment was based on Miller (1995) and Miller and Killick's (2004) work on slag identification. After identifying through XRF and SEM that the slag samples had little or no calcium (majority (160) had percentages under 2%, with 36 samples having carbon above 2% (the highest one just over 30%)), and were not visually considered as glassy slag, it was decided that they would not be plotted on a $\text{SiO}_2\text{-CaO}\cdot\text{Al}_2\text{O}_3\cdot 2\text{SiO}_2\text{-FeO}$ liquidus surface projection, which incorporates anorthite, and measures both CaO and Al_2O_3 as seen in Miller and Killick (2004: 28-29). Instead, they were Al, Si and Fe rich (Table 8.1), and as such, it was determined that they should be plotted on an $\text{Al}_2\text{O}_3\text{-FeO-SiO}_2$ liquidus surface projection (which shows the onset of melting for different compositions). The slags' Al-Fe-Si results were converted into oxides and were normalised into Al_2O_3 , FeO and SiO_2 proportions and plotted in Figure: 8.1. This would indicate their melting points, as well as constitution (cf. Miller *et al.* 1995; Miller & Killick 2004).

Table 8.1: Averages and standard deviations of slag samples.

	Fe	Al	Si
Average Slag (XRF)	50.9	12.9	17.7
Standard Deviation Slag (XRF)	13.9	4.7	7.2
Average Slag (EDX)	28.9	7.0	13.2
Standard Deviation Slag (EDX)	22.9	7.0	8.1

The normalising was done assuming that all the selected elements Al, Fe, Si and O formed the oxides. Based on this H_2O was not calculated. Chirikure *et al.* (2010: 1659) suggests that H_2O should always be calculated, otherwise the analytical totals would fall short. As it was assumed that the elements would equal 100, this was avoided, as well as the fact that the samples had not been ground and re-constructed in pellets (cf. Chirikure *et al.* 2010).

The plotted slag samples indicated that the majority of the slags were wüstite, with five samples falling in the fayalite phase (Figure 5.4). The bulk of the slags fell within the higher end of the wüstite section, and so was melted at a temperature mainly exceeding 1300°C, but less than 1400°C. According to Miller *et al.* (1995: 41) the presence of wüstite indicates that the smelting was not efficient, due to a high iron content remaining in the slag.

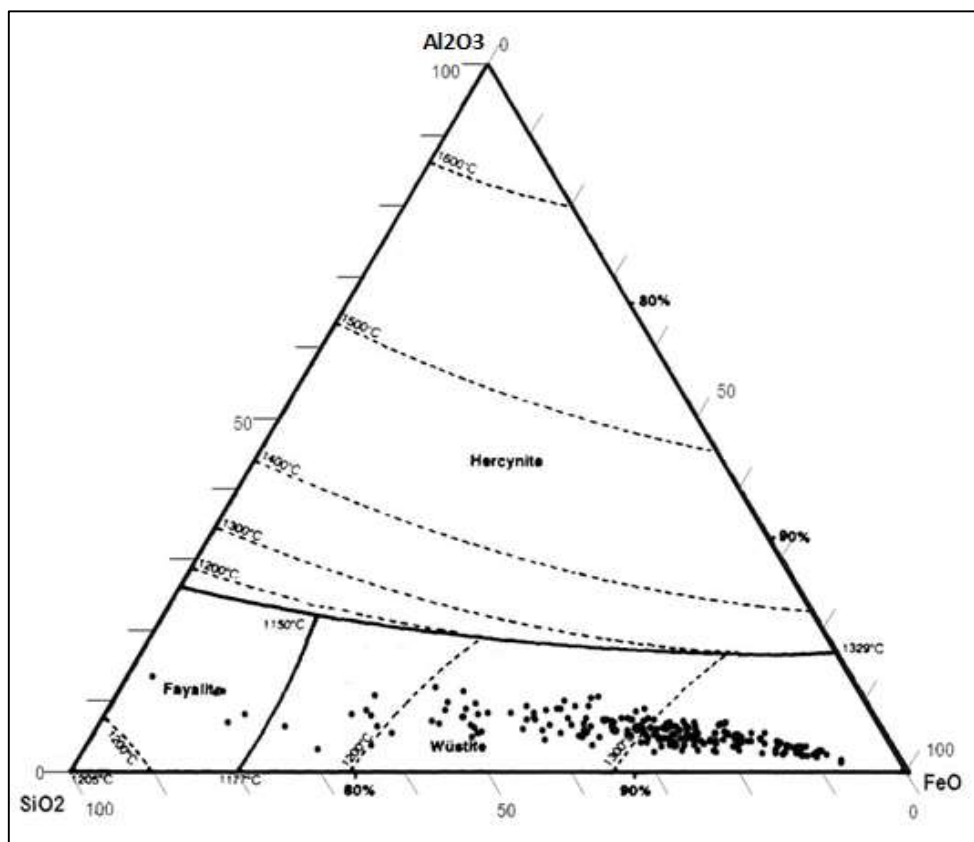


Figure 8.1: Recalculated compositions of slag, plotted using FeO-SiO₂-Al₂O₃ (Redrawn from Miller *et al.* 1995: Fig. 4).

Figure 8.1 shows that the slag composition fell on a line with a SiO₂ : Al₂O₃ ratio of about 85 : 15. Unlike the results seen in Miller *et al.* (1995) and Miller and Killick (2004), which plotted mainly in the lower portion of the wüstite/fayalite region, and

some in Hercynite, the Thaba Nkulu results remained in this linear pattern. This could indicate a constant $\text{SiO}_2 : \text{Al}_2\text{O}_3$ ratio for the slags, and hence a possible signature. It is likely that the linear relationship is due the proportions of the phases varying, which draws a single point into a line.

8.1.1.2: Iron artefacts chemical composition and signature

The iron artefacts' chemical compositions obtained from the XRF and SEM-EDX analyses followed closely those recorded in the slag samples, with the higher proportion percentages elements Fe, Al and Si constituting the majority elements detected (Table 8.2), and Ba, Co, Mn, Cr, V, Ti, Ca, P, and S in the low proportion percentage group. The similarities in element detection between the artefacts and the slags could represent their connection with the site (cf. Buchwald & Wivel 1998; Coustures *et al.* 2003).

Although the element compositions are similar, the direct link between artefacts and slag stems from the slag inclusions found within the artefact. Due to the artefacts being created from the iron bloom, their Fe ratios should consist of a greater percentage than the Fe ratio recorded in the slag, this can be compared in Table 8.2. During the artefact creation process, the chemical composition is affected by the use of flux, which would cause a lack of distinction between a sites' slag and the product created from the smelting and smithing process (Blakelock *et al.* 2009). Although this may be the case in terms of Thaba Nkulu's artefacts, their main compositions comprised the same as slag.

Table 8.2: Averages and standard deviations of slag and iron artefact samples.

	Fe	Al	Si
Average artefact (XRF)	56.1	16.9	18.1
Standard Deviation artefact (XRF)	11.3	3.9	7.3
Average Slag (XRF)	50.9	12.9	17.7
Standard Deviation Slag (XRF)	13.9	4.7	7.2
Average artefact (EDX)	56.1	5.8	14.2
Standard Deviation artefact (EDX)	29.9	4.8	14.6
Average Slag (EDX)	28.9	7.0	13.2
Standard Deviation Slag (EDX)	22.9	7.0	8.1

Again, the Si, Al and Fe were converted into oxides and plotted on the Al_2O_3 -FeO-SiO₂ composition triangle, and the results corresponded to those from the slag results, with a SiO₂ : Al₂O₃ ratio of around 85 : 15 (Figure 8.2). Although this diagram could not represent possible changes in the chemical composition, due to the adding of flux, or temperature difference (cf. Miller *et al.* 1995; Miller & Killick 2004; Blakelock *et al.* 2009), it does represent a continuing trend amongst the metal artefacts and associated material culture found on Thaba Nkulu, and hence strengthens the argument for this being a possible signature. It must be stated however, that although there is a linear relationship, it is possible for other sites' slag and metal artefacts to fall within this linear relationship, although the values with higher SiO₂ had lower Al₂O₃. Future research would be required to see if this concept carries throughout different sites' results.

Unfortunately, as only three iron artefacts were recovered, this only represents a fraction of the Thaba Nkulu iron artefacts. Without larger numbers of artefacts to compare, this artefact result is based on an assumption and does not represent an absolute chemical signature of Thaba Nkulu. As the artefacts, however, fell within the same ratio, the likelihood that other artefacts (if retrieved) would follow this pattern is

high. In order to present and strengthen the argument for possible chemical signatures of Thaba Nkulu, further research was done, which is discussed later in this section.

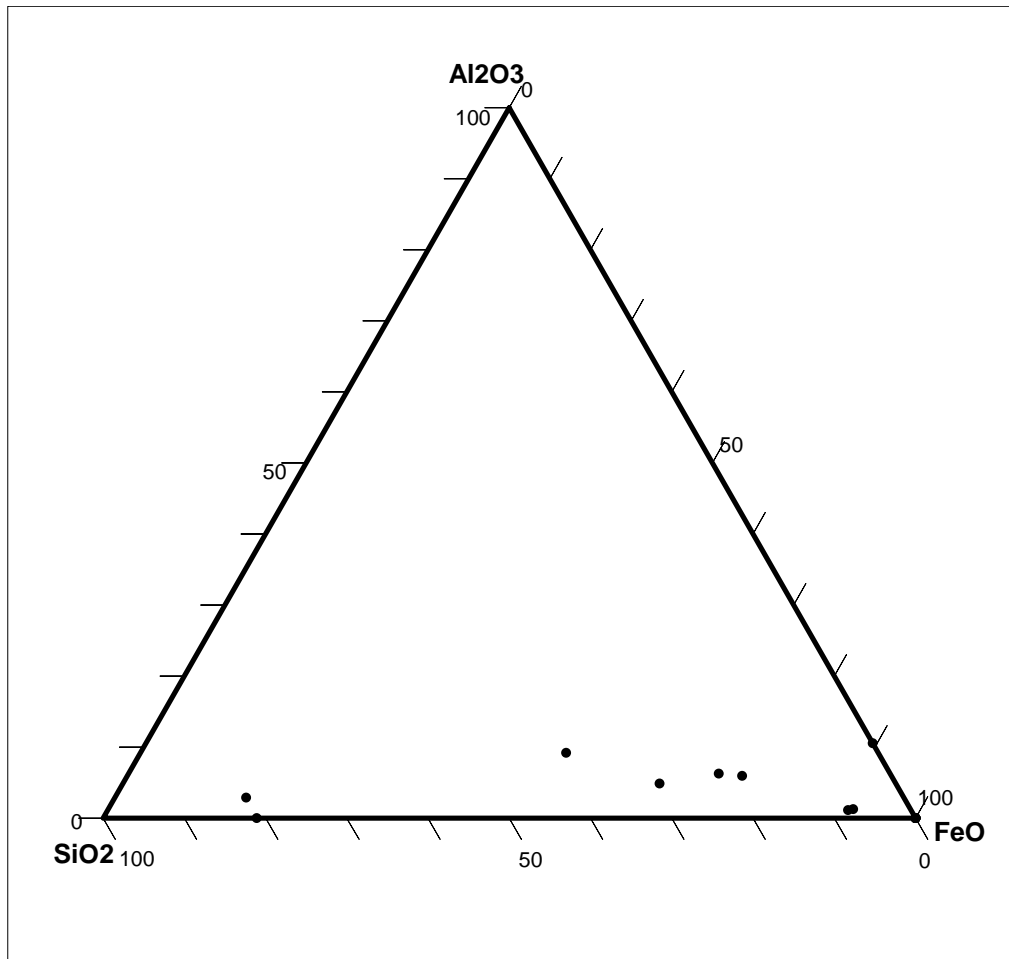


Figure 8.2: Iron artefacts plotted on the composition triangle for FeO - SiO_2 - Al_2O_3 .

8.1.1.3: Copper artefact chemical composition and signature

The chemical compositions retrieved from the artefacts, however, gave some insight into their production. The copper earring (2328 CA1 57 (Figure 4.50)) contained variations in the elements detected, compared to the other two copper artefacts. These variations were recorded in both the XRF and SEM-EDX results. In the XRF data, the copper earring (2328 CA1 57) contained a higher ratio of As (arsenic) than the other two artefacts (Figures 4.48 and 4.49). The ratio, however, was still less than one

percent, unlike other arsenic copper artefacts seen in the area (cf. Grant 1994; Grant & Huffman 2007; Chirikure *et al.* 2010; Thondhlana 2012). The other two artefacts both contained Sn (tin), whereas the copper earring (2328 CA1 57) did not.

The XRF results, however, did coincide with the element ratio seen in the slag and iron artefacts, with the main elements comprising Cu, Al and Si. The SEM-EDX result only recorded aluminium within the copper earring (2328 CA1 57). The SEM results, revealed the main composition elements to be Cu and Sn for the copper thin wire earring and the thick copper wire, and Cu and Al for the copper earring (2328 CA1 57).

The reason for the chemical composition difference could be due to their retrieval, as well as possible origins (cf. Hammel *et al.* 2000; Hall *et al.* 2006). The two copper artefacts, 2328 CA1 (2) XIII/F/1A thin wire earring and 2328 CA1 (3) X/A/1C thick copper wire, were both retrieved during the 2013 excavation, whereas the copper earring (2328 CA1 57) was acquired from the 2010 rescue excavation and was a surface discovery. The two 2013 copper artefacts have a similar chemical composition as artefacts found on Marothodi, a 19th century Tswana town, in the Rustenburg district, roughly around 100km away from Rooiberg (Hall *et al.* 2006: 26). Due to their chemical composition consisting mainly of Cu and Sn (therefore bronze), the artefacts' origins were attributed as belonging to Rooiberg (Hall *et al.* 2006: 26). In a more recent study Bandama *et al.* (2013) introduce the possibility of early second millennium AD, tin, copper and tin bronze production in the Southern Waterberg (cf. Bandama 2013; Bandama *et al.* 2013: 264; Bandama *et al.* 2015). The tin bronze artefacts from Thaba Nkulu, may have originated on site during this time or been introduced from the Southern Waterberg to the site. With the radiocarbon dates recording during the early second millennium, the artefact appearance has a possible connection with bronze production in the Waterberg region.

The dates recovered from Thaba Nkulu place it around 1060 ± 30 BP = 982 – 1145 AD (2 Sigma (Beta – 375130)), and 930 ± 30 BP = 1045 – 1220 AD (2 Sigma (Beta –

375131)). This corresponds to the possible trade of “bronze” out of Rooiberg (cf. Miller 2002; Hall et al. 2006; Bandama *et al.* 2013) and could imply that they were traded into the site during this period. It, however, should be noted that these objects could also originate from the LFC occupation on the hill. The physical appearance of 2328 CA1 (2) XIII/F/1A thin wire earring, is the same as those recovered at Marothodi, which indicates a long history of design, and spread throughout the country (Hall *et al.* 2006). Conversely, the copper earring (2328 CA1 57) matches the physical appearance of a spiral wire recovered at Mapungubwe (cf. Koleini 2012:21).

8.1.2: Non-metallic smelting and smithing material

8.1.2.1: Tuyère

The tuyère main element compositions were homogenous, as the high proportion elements were similar to those recorded from tuyères on other sites (cf. Chirikure *et al.* 2010). Most of the tuyère recovered from Thaba Nkulu, however, contained some slag coating (seen in Figure 4.52), which influences the chemical composition, and from this, the high percentages of Al, Si and in some cases Fe were recorded (Table 8.3). The Al ratio remained constant when compared with the Al ratio in the slag, although the Si and Fe ratios differed. The difference in Si can be attributed to the tuyères being made from clay, whereas the Fe ratio could have been from the slag coating or Fe in the clays used to create the tuyère pipes.

The Fe, Al, Si ratio, however, was recorded in the tuyère samples as well. This gave greater validity that this constant ratio may be a plausible signature of both the metal and metal smelting and smithing associated material culture. It must be said that although these three elements were recorded in the high percentage proportion groups, other elements recorded higher percentages. These were found in the balance (Bal) of the XRF results and in carbon and oxygen in the SEM-EDX results.

Table 8.3: Averages and standard deviations between tuyère and slag samples.

	Fe	Al	Si
Average tuyère (XRF)	10.8	14.5	27.3
Standard Deviation tuyère (XRF)	14.2	6.0	2.2
Average Slag (XRF)	50.9	12.9	17.7
Standard Deviation Slag (XRF)	13.9	4.7	7.2
Average tuyère (EDX)	4.9	8.2	21.6
Standard Deviation tuyère (EDX)	3.8	4.9	10.2
Average Slag (EDX)	28.9	7.0	13.2
Standard Deviation Slag (EDX)	22.9	7.0	8.1

8.1.2.2: Ore

The iron ore (Figure 5.4), contained high levels of Fe, Al and Si, which indicated a correlation to the slag compositions. Table 8.4 displays the averages between the slag and ore, from both XRF and SEM-EDX results. Although Coustures *et al.* (2003) theory of ore ratios neglected the changes made during the smelting and smithing phases of production (Blakelock *et al.* 2009), there was a correlation between the high proportion element ratios. The three elements which constantly ranged in high percentages were transmitted to the slag, and even the finished products. As discussed previously, the slag ratio between FeO, Al₂O₃ and SiO₂ created a plausible ratio between SiO₂ : Al₂O₃, and this ratio remained constant. The elements recorded represent homogenous elements detected in all of Thaba Nkulu's artefacts.

Table 5.4: Averages and standard deviations between ore and slag samples.

	Fe	Al	Si
Average Ore (XRF)	60.4	12.3	15.7
Standard Deviation Ore (XRF)	10.3	4.2	9.2
Average Slag (XRF)	50.9	12.9	17.7
Standard Deviation Slag (XRF)	13.9	4.7	7.2
Average Ore (EDX)	59.3	4.5	5.6
Standard Deviation Ore (EDX)	2.5	1.3	1.6
Average Slag (EDX)	28.9	7.0	13.2
Standard Deviation Slag (EDX)	22.9	7.0	8.1

8.1.3: Thaba Nkulu's chemical signatures

Although the $\text{SiO}_2 : \text{Al}_2\text{O}_3$ ratio allows for a plausible chemical signature, further analyses were required. This is due to only partial collection of artefacts from Thaba Nkulu, and as such, further experimentation was done. Following on past research (cf. Killick 1991; Buchwald & Wivel 1998; Coustures *et al.* 2003; Miller & Killick 2004; Blakelock *et al.* 2009; Chirikure *et al.* 2010), two further experiments were performed. These were done in order to either strengthen the argument of a possible signature, or try and determine a universal method in order to establish a chemical signature analysis.

Research focusing on chemical signatures has been in practice for more than two decades, although the ideas relating to methods and means of achieving accurate results have continuously been questioned (cf. Buchwald & Wivel 1998; Coustures *et al.* 2003; Blakelock *et al.* 2009). With the recovery of the ore, slag and artefacts, a complete production phase was available for analysis (cf. Coustures *et al.* 2003). This would allow for understanding what elements were removed or added during the production phase (Blakelock *et al.* 2009). The purpose of such additions or subtractions may indicate a chemical signature, through the consistency of alterations in general or site specific alterations. This method has proven to be effective, as seen with the Tin Lerale from Rooiberg (cf. Killick 1991; Grant 1999; Miller & Hall 2008).

In the case of tin, however, there are very few areas in southern Africa which contain tin deposits, and Rooiberg is the only place found so far with evidence for tin production (Friede & Steel 1976; Chirikure *et al.* 2010). With this said, it still took decades of research before this could be proven (cf. Friede & Steel 1976; Killick 1991; Grant 1994, 1999; Miller & Hall 2008; Chirikure *et al.* 2010).

In the case of iron artefacts, there is one main difference between the sourcing of iron and tin. This difference is the scale of production. In the case of iron, there are numerous sources, as well as artefacts produced across southern Africa (cf. Stuiver & van der Merwe 1968; Miller & Killick 2004). This leaves multiple origin points, as well as a large lacuna when it comes to determining the chemical signature of iron-based artefacts. With that said, and what research is currently known, a hypothetical chemical signature may be presented, which can be compared and justified with current research.

With the possible link between ore and slag, the theory of Coustures *et al.* (2003) of ratio comparisons was attempted. This theory was chosen as it proposed that by using ore to finished product, one could identify a chemical signature. This theory is the same as gold fingerprinting (see Grigorova *et al.* 1998a; Grigorova *et al.* 1998b). Although Blakelock *et al.* (2009) states that the theory would not work, as the ratios would be altered during the smelting process, and therefore, the link between ore and slag through element transfer would be impossible. It was noted, however, that only one set of ratios was detected, and as such, Coustures *et al.* (2003) theory could not be used to detect a chemical signature. It should also be realised that the ore, slag and completed artefact are not in the same composition sequence because both the slag and the artefact contain some elements removed from the ore, as well as some added by the flux addition, but that the combination of them should be related.

8.1.3.1: Ratio analysis

Following the unsuccessful attempt to use Coustures *et al.* (2003) theory, Blakelock *et al.* (2009)'s theory was used instead. As with the previous attempts, it was noted that only three of the ratios could be compared from the Thaba Nkulu results. The comparable ratios were MgO : CaO, MgO : K₂O and Al₂O₃ : SiO₂. As there were no traces of Mn found within the SEM-EDX results, although Mn was recorded in the XRF results, the SiO₂ : MnO ratio was not used in this experiment, as Blakelock *et al.* (2009)'s theory uses SEM-EDX results only. Although not all ratios could be used, the three that could be used, would allow for some insight into a possible chemical signature.

The SEM-EDX slag and artefact results were normalised and converted to oxides. They were then plotted on a scatter graph representing the selected ratios. Figure 8.3 represents the Thaba Nkulu MgO: CaO ratio, whereas Figure 8.4 represents the Blakelock *et al.* (2009) experiment MgO: CaO ratio. The next set of figures (Figures 8.5 and 8.6) represent the MgO : K₂O ratios, and Figures 8.7 and 8.8 represent Al₂O₃ : SiO₂.

The first set of figures representing MgO : CaO had a linear pattern stemming from 2% to 4%, falling within the same pattern as experiment bar 3 from Blakelock *et al.* (2009). There, however, were higher ratios of MgO in the Thaba Nkulu slag, and nearly double the CaO, when compared to the Blakelock results (Figures 8.3 and 8.4). Using the MgO : K₂O ratios, compared to Blakelock *et al.* (2009) there was much more MgO than K₂O, and the current results agreed with only the lower K₂O values (Figures 8.5 and 8.6). The MgO levels varied between just above 2% to just below 14%, whereas the K₂O, remained under 2%. Blakelock *et al.* (2009: 1756) state that two ratio comparison systems allow for the identification of some smelting systems; these ratios were MgO : K₂O and SiO₂ : MnO. Although the Thaba Nkulu slags contained no MnO, the MgO : K₂O ratio was present. This ratio showed a distinctive difference compared to Blakelock *et al.* (2009)'s data results, however, as no artefact results could be recorded

for the MgO : K₂O ratio, a correlation between slag and artefact could not be made. It does, however, indicate a difference in slag production areas (Figure 8.5).

The final ratio, Al₂O₃ : SiO₂, created a cluster grouping for the slag, but a linear relationship for the artefacts. This indicates that during the smithing process, the slags' chemical composition was altered, possibly by the use of a flux. This change is noted by Blakelock *et al.* (2009: 1751-1752) in which they state that the slag inclusion compositions were more affected by the fuel ash chemistry, than ore composition. This is why they claim Coustures *et al.* (2003) proposed theory does not include compositional changes. Originally, the Al₂O₃ : SiO₂ ratio was used to indicate a possible signature. Blakelock *et al.* (2009), however, recorded that this ratio could cause two different sites' slag and artefacts to appear as though they came from one site and not two.

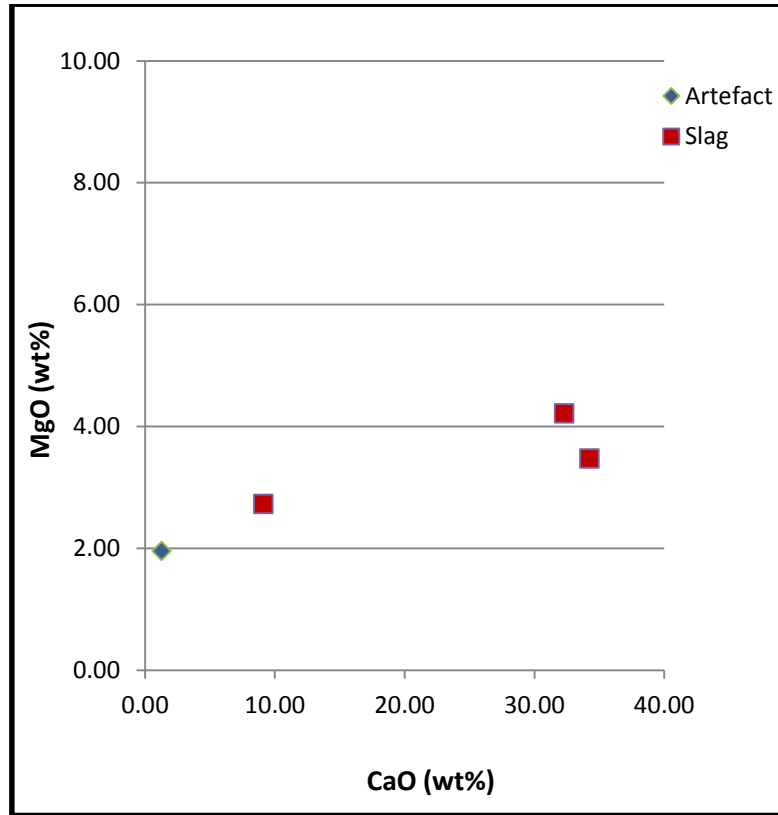


Figure 8.3: Thaba Nkulu MgO (wt%) to CaO (wt%).

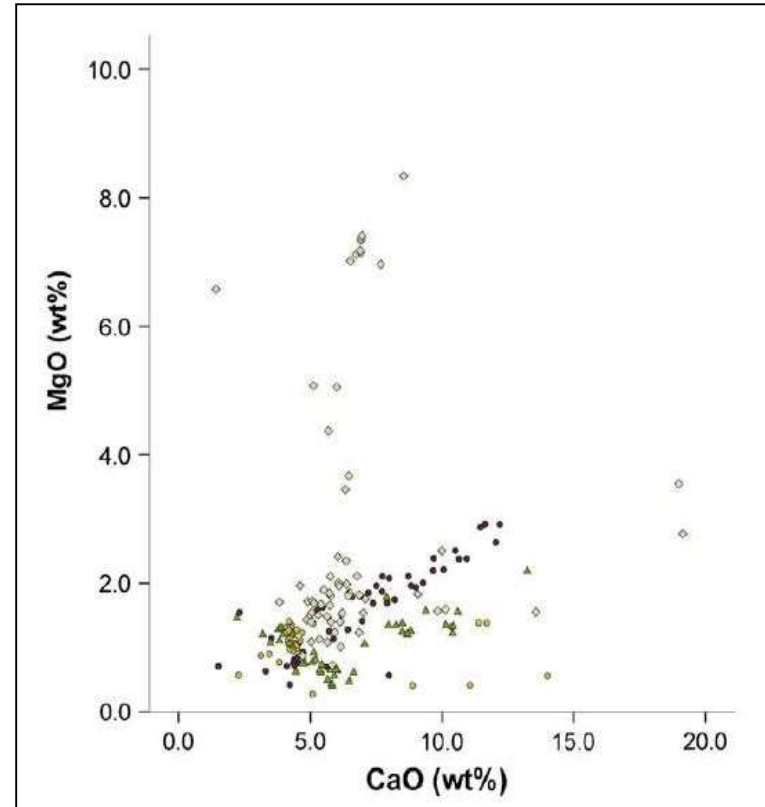


Figure 8.4: Blakelock *et al.* (2009: 1750) MgO (wt%) to CaO (wt%).

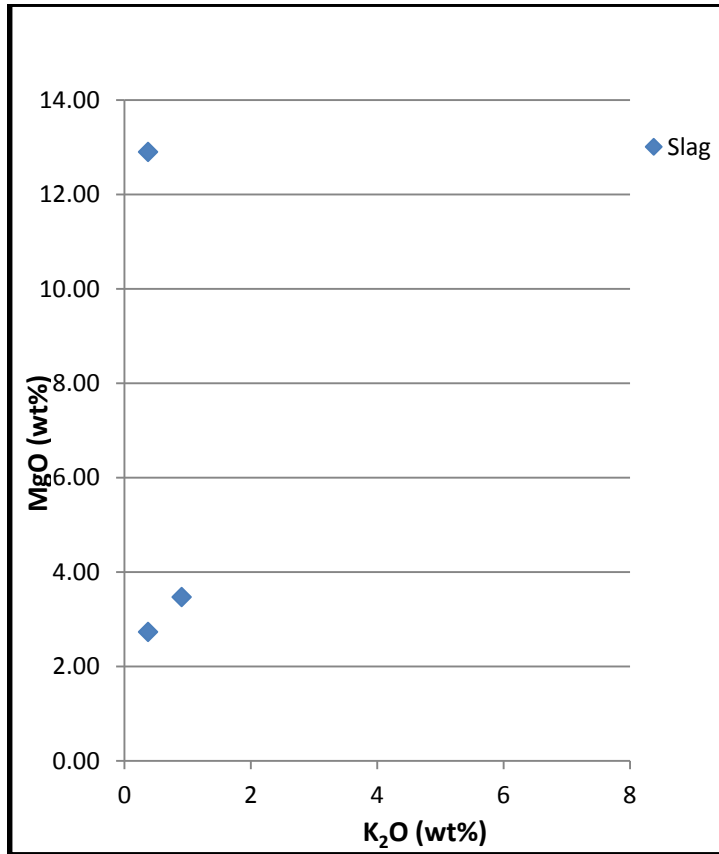


Figure 8.5: Thaba Nkulu MgO (wt%) to K₂O (wt%).

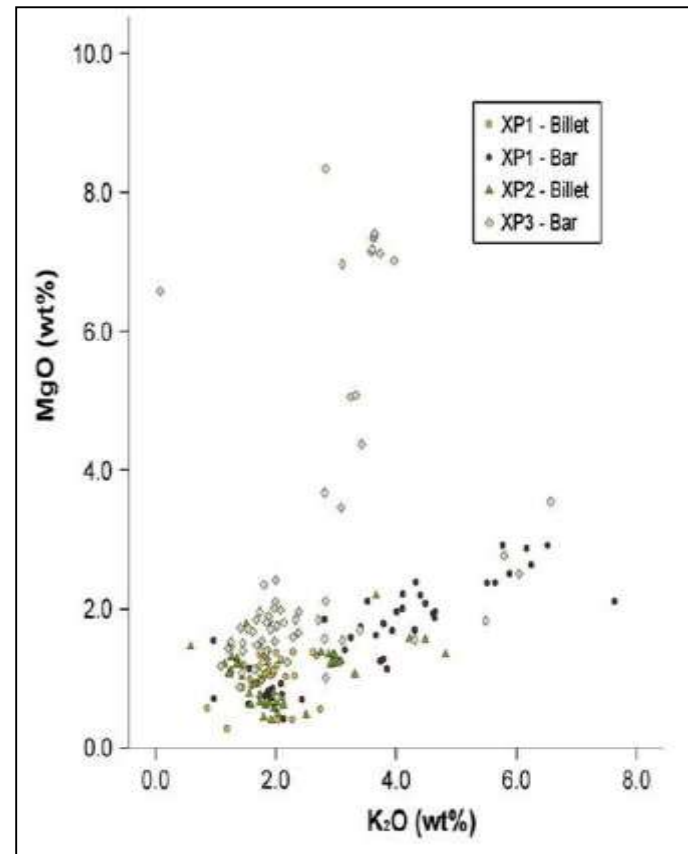


Figure 8.6: Blakelock *et al.* (2009: 1750) MgO (wt%) to K₂O (wt%).

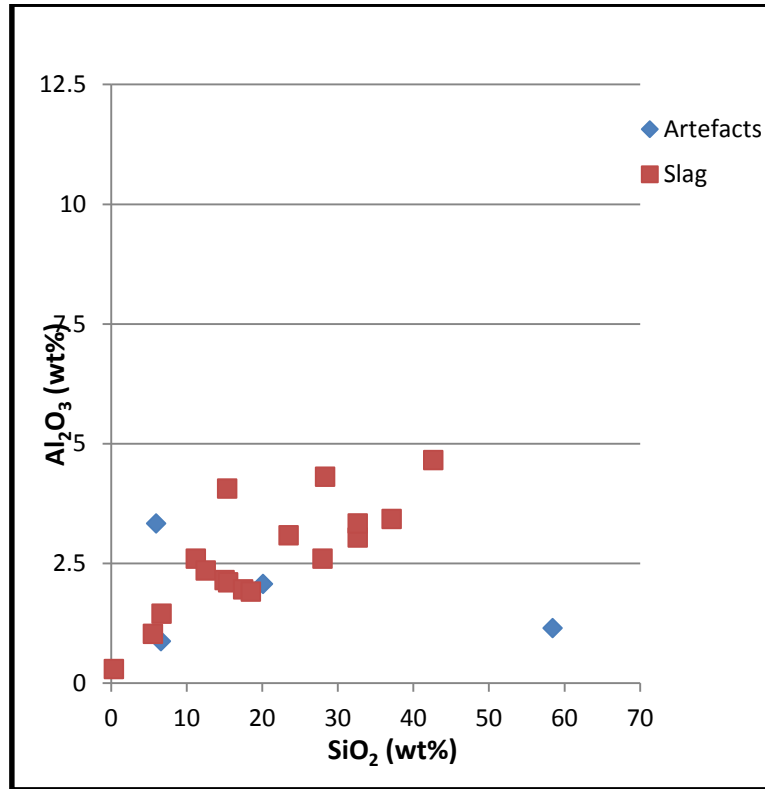


Figure 8.7: Thaba Nkulu Al₂O₃ (wt%) to SiO₂ (wt%).

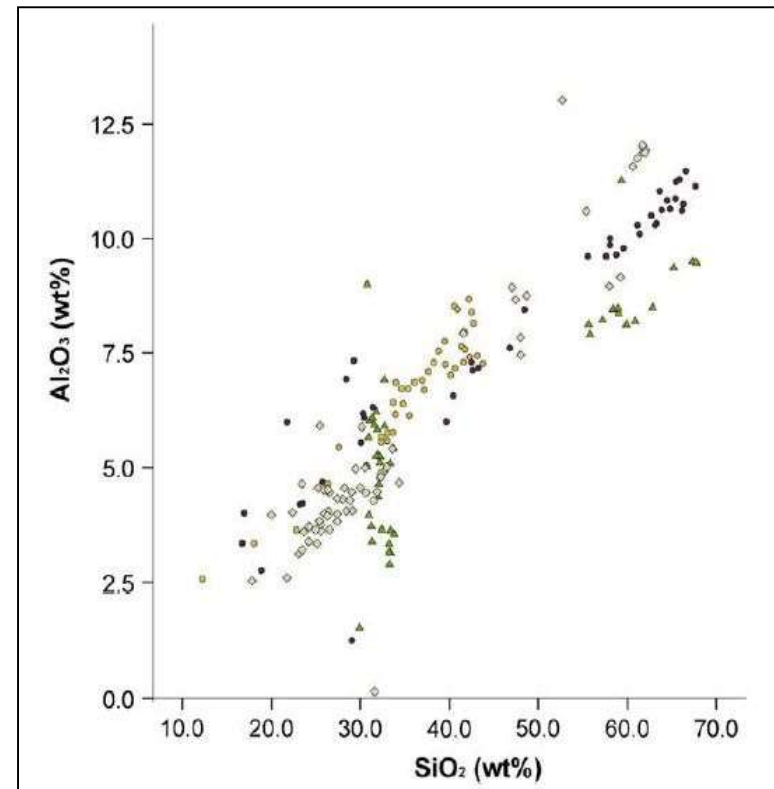


Figure 8.8: Blakelock *et al.* (2009: 1750) Al₂O₃ (wt%) to SiO₂ (wt%).

Using these results, some of the Thaba Nkulu slag and artefacts fell within experiment 1 and 2 results from Blakelock *et al.* (2009), and the latter used a high-grade ore (Sishen ore). This ore has a high iron content, and is very homogeneous, which is why it is still used commercially today. With archaeology, the ores used would not have been of such high grade (cf. Miller 2002: 1100). The second type of ore used, however, was Blaenavon ore (Blakelock *et al.* (2009)), this ore would be a more typical archaeological ore. This is due to it originating from a specific area; as with most ore used, the ore was either collected locally or traded from the nearest source. The quality of ore used in the EFC period is based on the quality in the area, and from this smelters and smiths would produce a variety of artefacts, based on a variety of different ores (cf. Miller & Van der Merwe 1994b; Miller 2002). The Thaba Nkulu slags, which fell within the parameters of Blakelock *et al.* (2009) experiment 1 and 2, correspond to a high-grade ore. Those that fell within experiment 3 parameters, however, would be more consistent with archaeological findings.

The Thaba Nkulu slag and artefacts fell within the same groupings as the Blakelock results, except for the MgO : K₂O category. These comparisons, however, are based on visual representation, as there are far too little data to do any of the “data cleaning” of Dillmann and L’Héritier (2007), which was used by Blakelock *et al.* (2009). In Figures 8.3 and 8.7, the Thaba Nkulu artefacts have been included and indicate a correspondence to the slag results, except for one recording seen in Figure 8.7. This artefact had a single result that placed its SiO₂ at a high level. All other recordings from this artefact, however, fell within normal parameters, and matched the two other artefacts recordings. Unfortunately due to the limited number of artefacts, the results were unable to reveal a full list of potential changes, which may have occurred during the smithing process. Blakelock *et al.* (2009) were able to record these, due to the experiment being done under a controlled environment, whereas artefacts recovered in the field vary and are limited in quantity.

Blakelock *et al.* (2009), however, do indicate a possible chemical signature or means of recording one. This is indicated by the MgO : K₂O ratio, as the slag from Thaba Nkulu could be differentiated from slag and artefacts found in Blakelock *et al.* (2009) MgO : K₂O ratio. Unfortunately, no artefacts could give an MgO : K₂O ratio, thus these could not be compared. This is similar for the SiO₂ : MnO ratio; neither the slag nor the artefacts produced a matching comparative ratio, as such, this test could not be performed. This was a setback, as Blakelock *et al.* (2009), states that this ratio could distinguish and possibly provenance metal based artefacts and material culture. As such, for future testing, the ratio system must be taken into account, and although Mn was recorded in the XRF results, it was not recorded by the SEM-EDX which indicates possible limitations to its use.

8.1.3.2: Comparison analysis

In order to record which elements or element ratios can distinguish these samples from any other sample within South Africa (as seen with the Rooiberg tin (Killick 1991; Grant 1994, 1999; Chirikure *et al.* 2010), all elements need to be taken into account. The elemental composition of all artefact types comprises low proportion elements and high proportion elements. The low proportion element percentages are often called trace elements, as their percentages fall within 0.01 and 2% of the entire sample (see Coustures *et al.* 2003; Miller & Killick 2004; Chirikure *et al.* 2010). Conversely, the higher proportion percentages, or major elements consist of elements above 2% of a sample. In the previous chemical signature experiments, the trace elements, as well as the major elements, have been used to propose possible chemical signatures.

The first attempt, recorded through the Al₂O₃, FeO and SiO₂ ternary, led to the discovery of the SiO₂ : Al₂O₃ ratio of 85 : 15. These oxides constitute major elements, which were prominent throughout all metal and metal smelting and smithing associated material culture. The second attempt identified a possible ratio system using trace and major elements. In the second analysis, trace elements found in slag led to the plausible

identifying of slag from Thaba Nkulu, whereas the major elements could not be used to link artefacts to Thaba Nkulu. As such, further experimentation was required.

This analysis considered both trace and major elements, as well as, incorporating a comparison system. Although ratio systems are commonly incorporated in order to perceive plausible signatures (cf. Buchwald & Wivel 1998; Coustures *et al.* 2003; Blakelock *et al.* 2009), this analysis incorporated all elements detected. As before, the iron slag was used in this analysis, as it constituted the majority artefact collected and studied, and both the XRF and SEM-EDX results were compared with other sites' XRF and SEM results (cf. Miller & Killick 2004), in order to see if any elements or element percentage ratios could distinguish site materials.

Using the same types of graphs used to present the XRF results (Chapter 7), the XRF and SEM-EDX results were plotted representing their low proportion percentages and higher proportion percentages. Following this, multiple sites' slag recordings presented in Miller and Killick (2004) were converted into standard elements from oxides, and plotted alongside the Thaba Nkulu slag results. The XRF results are presented in Figures 8.9 and 8.10, and the SEM-EDX results are presented in Figures 8.11 and 8.12. Due to the XRF not being able to detect oxygen, carbon or nitrogen, these and any other possible undetectable elements were placed under the balance column, for both XRF and SEM results. They were calculated as the remaining percentage left, after the converted elements were added up, all of which equalled 100.

Within the figures (Figures 8.9 – 8.12), the homogenous elements can be identified, however, from a ratio perspective, differences between site results can be determined. The XRF low proportion percentages (Figure 8.9) recorded heterogeneous elements, with some elements not being recorded in the Thaba Nkulu samples and *vice versa*. This, however, could be due to detection limits or purely site specific elements. These elements were Na, Cu, S, Br, and Sr in the low proportion percentage groups. Although these elements are trace amounts, they separate results from one site to another. Such

examples were seen in the Cu detection, as only the Matsepe slags from Phalaborwa (Killick & Miller in press) contained Cu (Figure 8.9 (green)), or the high trace amounts of Mn (red) seen in the northern province slags (Miller *et al.* 1995). These trace amount differentiations may be used to distinguish sites, should the majority of the sites' sample group contain similar results.

As for the higher proportion percentages (Figure 8.10), these too produced separate ratio systems amongst the homogenous results. In the case of Thaba Nkulu, the aluminium percentages were greater than all other sites' aluminium recordings (Figure 8.10 (black)). Other higher proportion percentages were seen in the Mn values with Miller *et al.* (1995) and Greenfield and Miller (2004) containing higher recordings than the other sites. In some cases, sites' chemical compositions contained neither exceptionally high or low percentages, as seen with Rehoboth in Namibia (Miller 1994; Miller & Sandelowsky 1999 (yellow)). In these cases, the slag could not be differentiated amongst the groups present. It must be stated, however, that in Miller and Killick (2004), the results contained both Fe and Fe₂O₃ (Killick & Miller in press) or Fe₂O₃ only (Miller 1994; Miller & Sandelowsky 1999; Greenfield & Miller 2004). Those results containing Fe₂O₃ only were not converted into Fe. This was due to the format in which they were represented in Miller and Killick (2004: 36-44).

Unlike the XRF data, the SEM-EDX results displayed multiple variations in the elements. The SEM-EDX results, however, could not distinguish site differences as determined by the XRF comparison analysis. This is likely due to the recording methods. As stated in the previous chapter (Chapter 7), the SEM-EDX recorded microscopic areas of a sample (to ensure flat areas with reduced errors), whereas XRF recorded a greater area/whole sample. This meant the SEM-EDX recordings were not recording the same areas as the XRF, and thus some elements may not have been identified. For the Thaba Nkulu results, these recording differences were significant. This was due to only a handful of elements detected during the XRF testing, being recorded during the SEM-EDX testing. The SEM-EDX results, however, contained

elements not previously recorded as well. For the sites' slag results represented in Miller and Killick (2004), the element detections tended to correlate with those recorded through the XRF testing (Figures 8.11 and 8.12). In the case for both the Thaba Nkulu and other sites' slag, however, the SEM-EDX results no longer created ratio clusters, instead the ratios varied by more than 5% for certain elements. This meant that certain possible signatures recorded in the XRF experiment were no longer confirmed (see Thaba Nkulu Al ratio (Figure 8.10 vs. Figure 8.12)).

In the higher proportion percentage group (Figure 8.12), certain sites' samples contained elements either not detected by the XRF (e.g. Ni Miller (2001) medium blue) or samples which contained higher proportions than other sites' samples (e.g. Mn for Maggs & Miller (1995) yellow and Miller *et al.* (1995) red). This link to specific site only element detection or upper percentage ratios were seen in both the XRF and SEM-EDX results. Unfortunately, the comparison was limited to only a portion of the sites used in this analysis.

From the element detection issues recorded by the SEM-EDX, as with the XRF, the oxides were converted and all unknown elements were placed in a balance (Bal) column. The elements positively identified were not part of the balance, and were placed in individual columns. Some elements, however, were unique to specific sites. For Thaba Nkulu, these elements were: Br and In. Whether these elements were present in the other sites recordings is not clear, as they were not represented in Miller and Killick (2004). The other sites' results contained elements not recorded on the Thaba Nkulu; these were: S, Cl, Na, Cu and Ni.

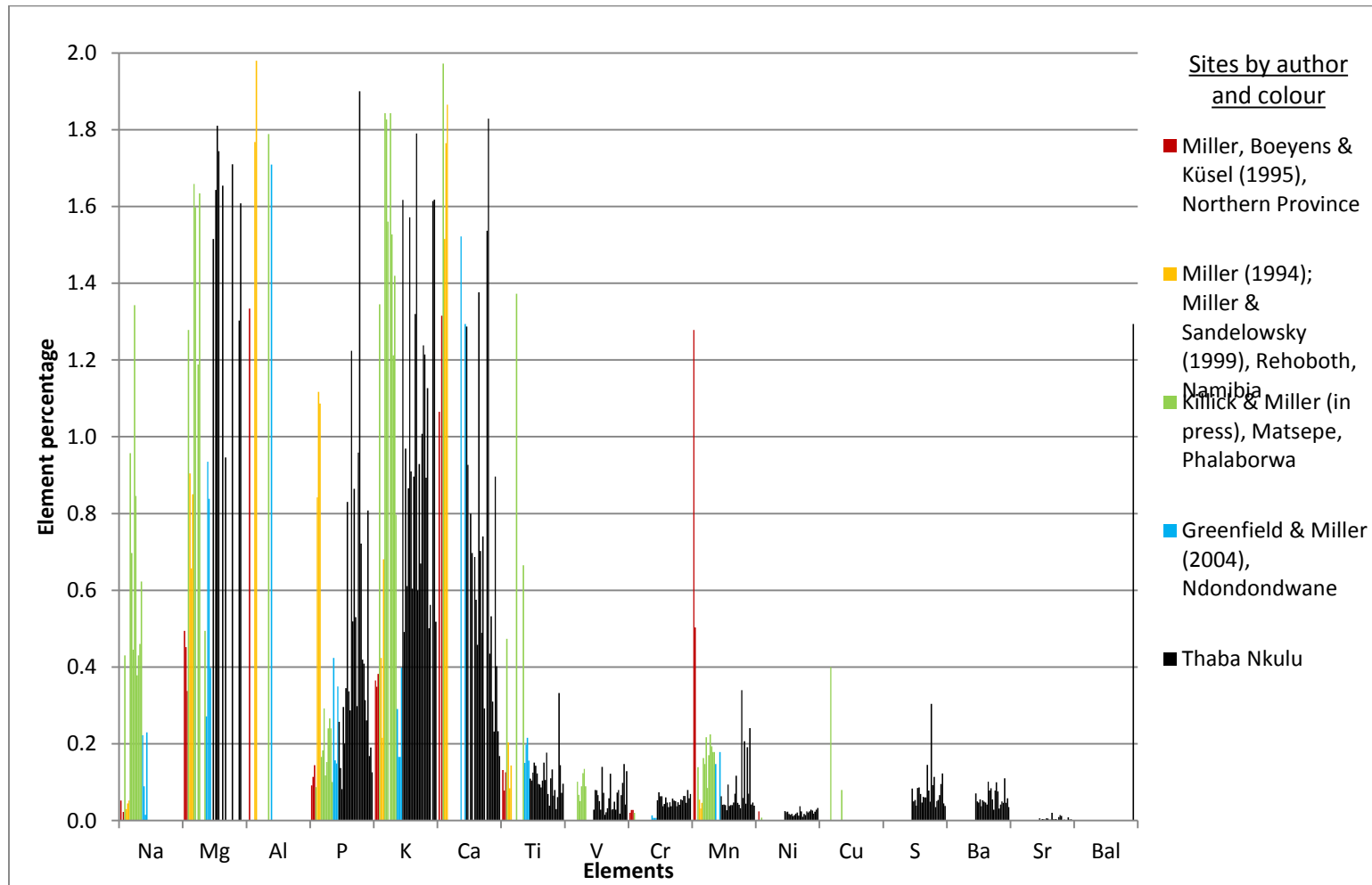


Figure 8.9: Various sites' slag, XRF analyses low proportion percentages (from Miller & Killick 2004) compared with Thaba Nkulu slag.

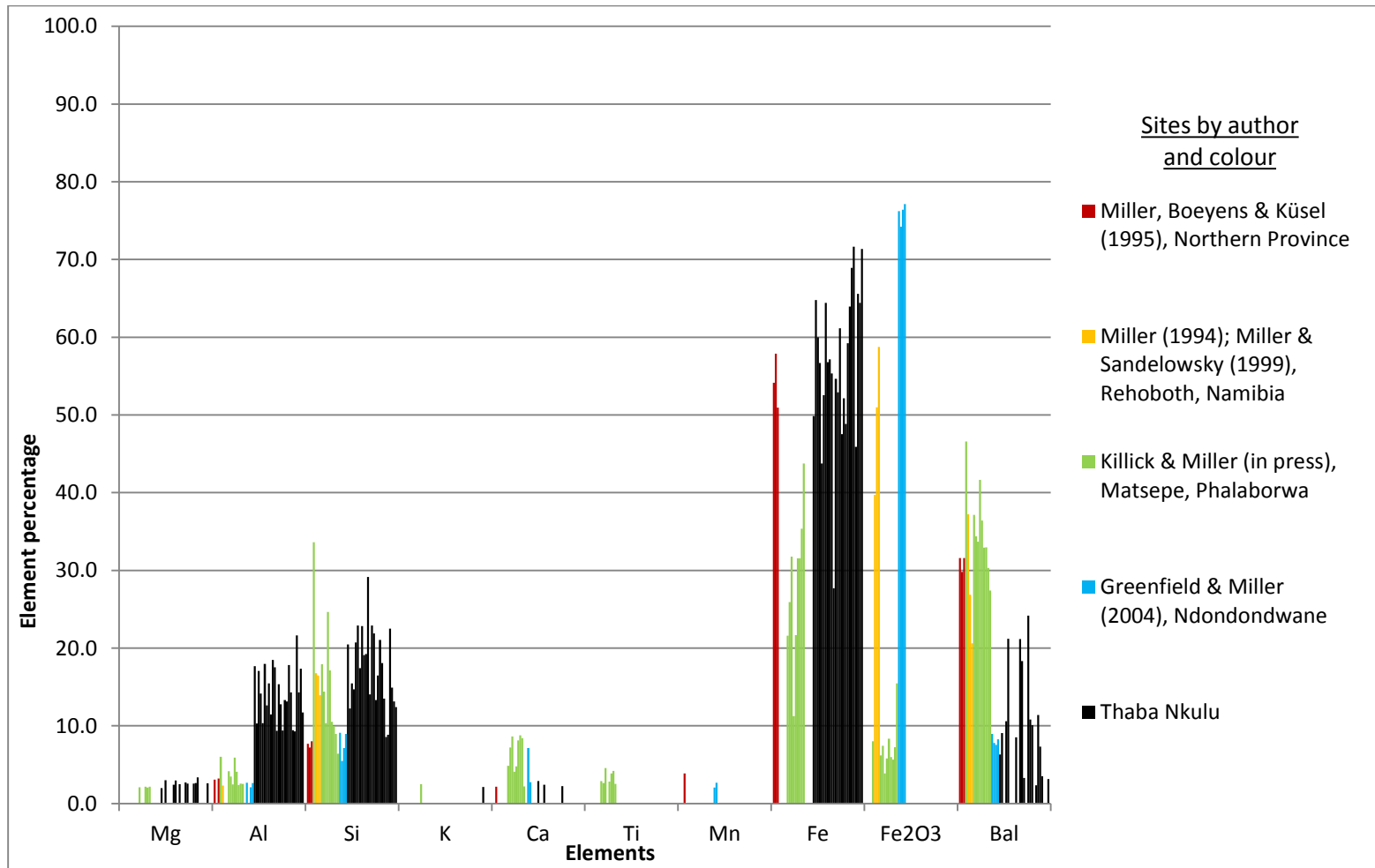


Figure 8.10: Various sites' slag, XRF analyses higher proportion percentages (from Miller & Killick 2004) compared with Thaba Nkulu slag.

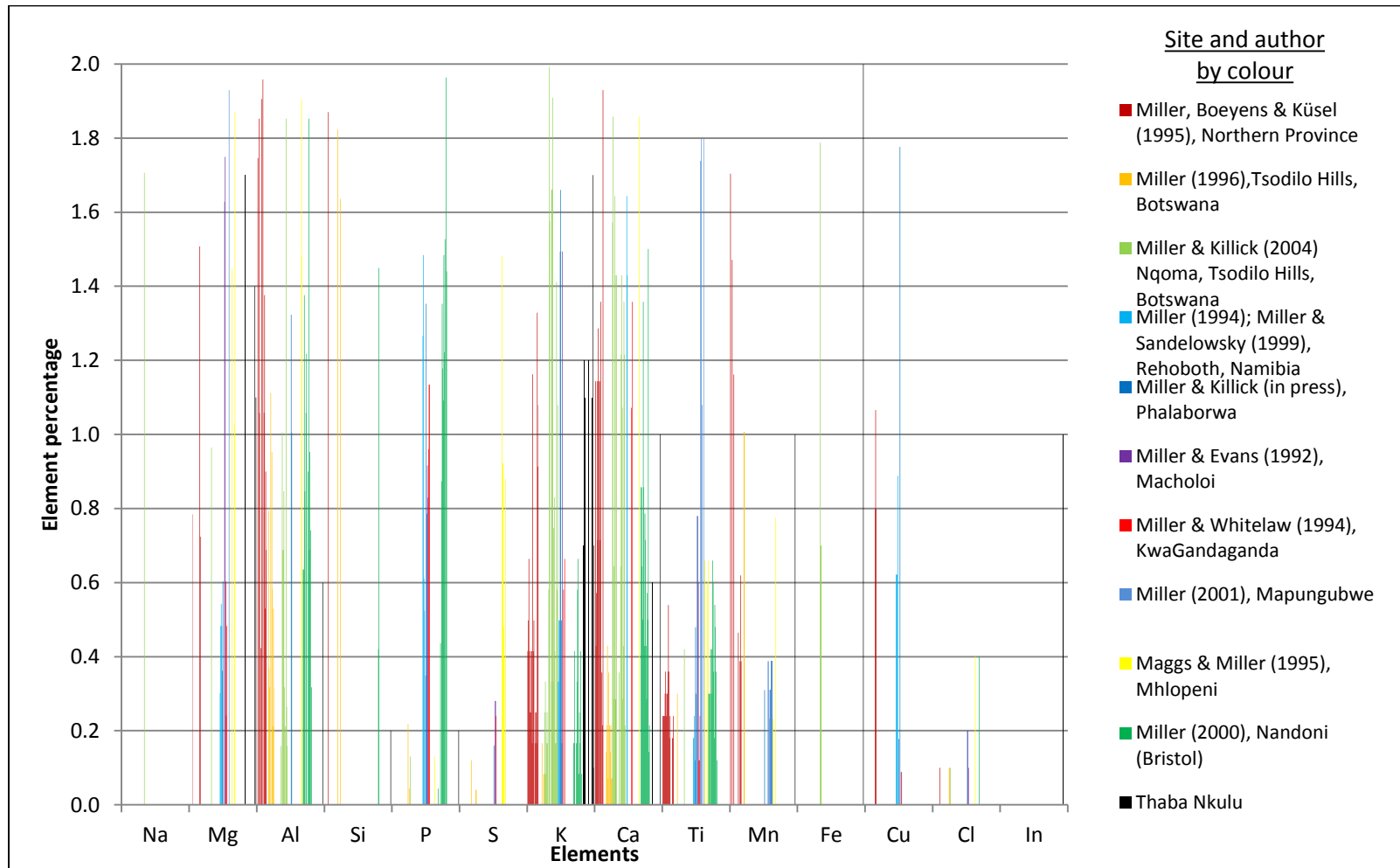


Figure 8.11: Various sites slag, SEM-EDS analyses low proportion percentages (from Miller & Killick 2004) compared with Thaba Nkulu slag.

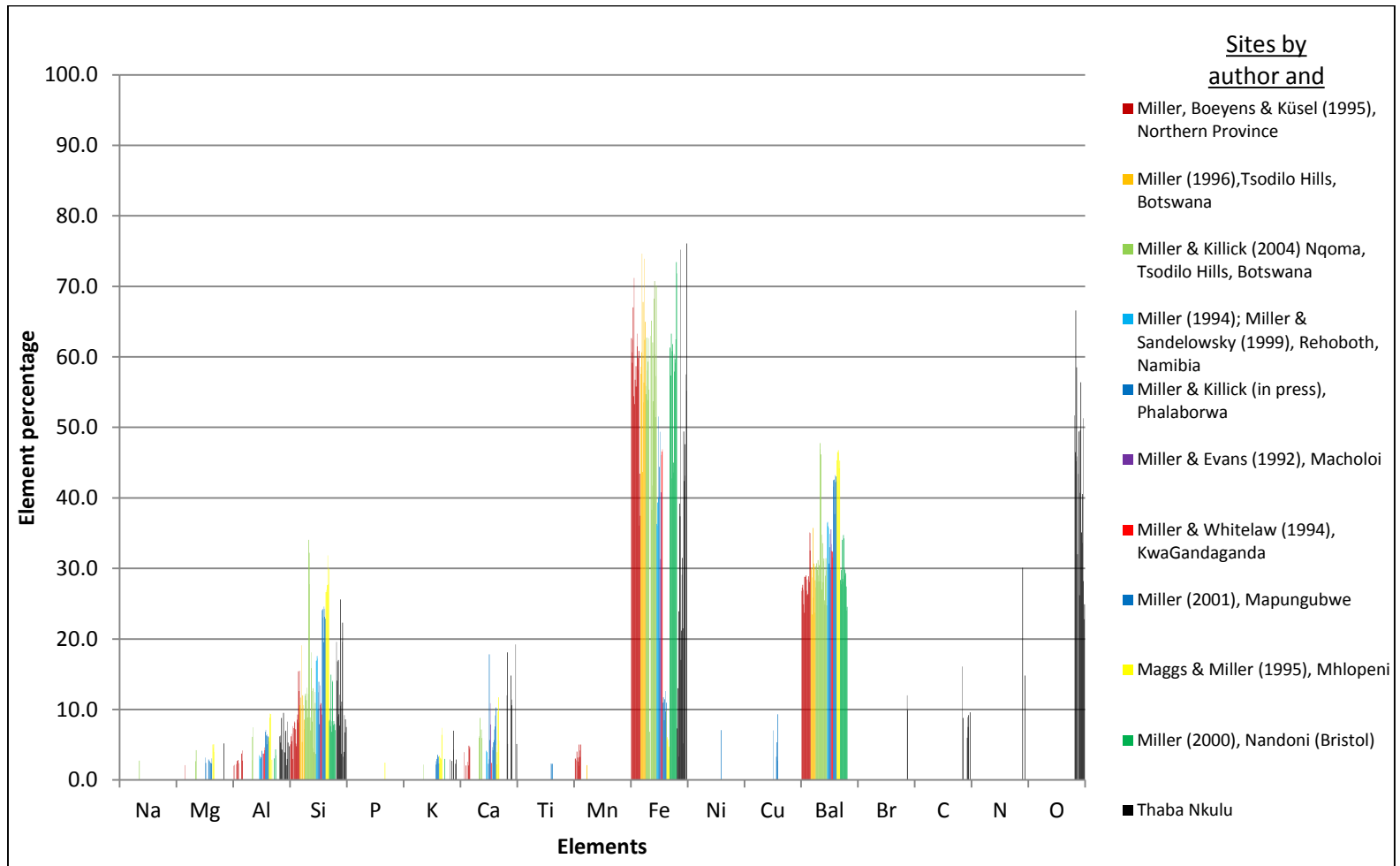


Figure 8.12: Various sites slag, SEM-EDS analyses higher proportion percentages (from Miller & Killick 2004) compared with Thaba Nkulu slag.

The XRF results indicated numerous possible chemical signatures, whereas the SEM-EDX results displayed numerous variations in the ratio detections, and thus a chemical signature based on these results could not be determined. Although elements which may single out specific slag from sites were present in the SEM-EDX results, without comparative results, the ratio variations prevent multi-site separation. The XRF comparative results, however, enabled a possible chemical signature for Thaba Nkulu, through the high ratio of Al, even though these results were not reinforced by the SEM-EDX results

This leaves a gap in research, as finding a chemical signature through SEM analysis would be problematic if not all samples are recorded at 100% of the surface covered by the XRF. Unless the same areas are analysed, elements may not be present when comparing results. In order to ascertain a true chemical signature, all samples should be recorded in the same manner, and all specimens prepared for SEM-EDX should be prepared metallographically to ensure flat surfaces and reduced errors. When compared, the averages of the samples should be taken into account, so as to avoid variations when using a comparison analysis. The XRF results showed mass groups and very little variations, which may be due to the results representing a more accurate composition of the sample, thus plausible signatures. Since iron's chemical signature tracing is still in its infancy, and these results only represent a fraction of iron-based material recovered, further analyses will be required to substantiate these results, as well as allow for further testing and comparisons to be made.

CHAPTER 9: CONCLUSIONS

Introduction:

Thaba Nkulu is located in a relatively under explored region. Over an eleven day period, five areas were excavated at Thaba Nkulu. These excavations subsequently contributed to the spatial configuration of EFC sites in the area.

The evidence collected and analysed allowed for the chemical compositions of ore, slag, and artefacts to be recorded, through the use of XRF and SEM-EDX. These results were then subjected to experimental theories in order to deduce possible chemical signatures. Subsequently, the materials and evidence found on site were used in order to interpret the site and determine the location of smelting upon Thaba Nkulu.

9.1: Excavation outcomes

This research found that Thaba Nkulu was occupied by EFC occupants during the turn of the first millennium AD. This was confirmed by ceramic styles (those belonging to the Diamant and possibly Eiland facies (Hall 1981; Huffman 2007; Bandama *et al.* 2015)), and radiocarbon dating place the site in the EFC period, 1060 ± 30 BP = 982 – 1145 AD (2 Sigma (Beta – 375130)), and 930 ± 30 BP = 1045 – 1220 AD (2 Sigma (Beta – 375131)).

These dates point to a late Diamant or early Eiland association. The dates and ceramics, raise the question of whether or not the slag dump could be related to an episode or occupation postdating the main EFC settlement, as the ceramics tended to appear more within the Diamant facies (Huffman 2007: 223-225), than the Eiland facies (Huffman 2007: 227-229). This can only be established through further research on the site.

Excavations identified two zones. The first zone was a possible smelting area (2328 CA1 (1)), which was identified and labelled such, due to large amounts of slag, tuyère, as well as other associated material such as ore, furnace lining and daga being

recovered there. The second zone was identified as the possible domestic area. Excavations in two separate areas recovered pits (along a road) and evidence of a cultural horizon (east of the smelting site).

If contemporaneous, the relationship between these areas suggests that the smelting area was located on the periphery of the homestead. The view and interpretation of this project placed a smelting area (2328 CA1 (1)) not in seclusion. The findings of this project, however, were based solely on recovered evidence, and possible interpretations. In order to fully and conclusively state whether the areas indicated are domestic zones and a smelting area, further excavations are required to add substantial backing to these claims. As without a furnace, these claims can be countered, as seen with Miller and Whitelaw (1994).

9.2: Thaba Nkulu's chemical signature

With the recovery of ore, slag, tuyère and iron and copper artefacts, the full line of metal production was recovered. These were then analysed using a combination of XRF and SEM-EDX, which recorded the chemical compositions of these artefacts. Following this, the artefacts were then subjected to three analyses in order to determine the possible chemical signatures.

Through these analyses, three possible signatures were determined. The first was seen in the $\text{SiO}_2\text{-FeO-Al}_2\text{O}_3$ system. When the slag and artefacts were converted to $\text{SiO}_2\text{-FeO-Al}_2\text{O}_3$ and plotted, following Miller *et al* (1995)'s slag identification, a chemical composition, as well as the slag constitution were recorded. This identified the slag as wüstite. Within the ternary plot, $\text{SiO}_2 : \text{Al}_2\text{O}_3$ formed a constant ratio, across all slag samples, which was approximately 85 : 15. When performed on the iron artefacts, these ratios appeared again, strengthening the argument for this being a chemical signature for Thaba Nkulu artefacts.

The second possible chemical signature recorded could only be determined for slag. This analysis was based on the Blakelock *et al.* (2009) theory of set ratios being able to determine site specific slag and artefacts. In this analysis, the MgO : K₂O ratio allowed for the distinguishing of Thaba Nkulu slags, compared to Blakelock *et al.* (2009). Unfortunately, due to the lack of artefact recoveries (only three were found), the artefact MgO and K₂O ratios could not be determined. Another possible link would have been the SiO₂ : MnO ratio, however, due to composition detection differences in this projects' SEM-EDX analyses and Blakelock *et al.* (2009)'s, no MnO and SiO₂ could be compared. This was one of the limitations found during this dissertation, as the methods used were the same as other researchers, but the results differed.

The final plausible chemical signature was derived from comparative analyses. For this, Thaba Nkulu's XRF and SEM-EDX slag results were compared to XRF and SEM-EDX slag results presented in Miller and Killick (2004). The XRF results indicated plausible signatures, due to element ratio proportions and elemental differences. The SEM-EDX results, however, had variations in the element ratios, as sampling recorded ratios were based on sample area, not the artefacts as a whole, and also, not all the analysed surfaces were metallographically flat. Thus, the XRF ratios could not be reproduced by the SEM-EDX results. Further problems of individual element detections were recorded in the SEM-EDX results. For some sites, the slag recorded high proportion ratios in some elements, or the slag contained specific elements, not found on other sites. In the case of Thaba Nkulu, too few samples contained high proportions or specific elements, thus preventing plausible SEM-EDX chemical signature identifiers.

Thus in the cross-comparison of the SEM-EDX results, very few sites could be distinguished, and as such, the SEM-EDX data could not produce satisfactory signatures. The XRF results, however, allowed for the cross-comparison analyses to identify possible signatures, one of which was the higher proportion ratio of Al in the Thaba Nkulu slag.

The signatures were based mainly on two types of artefacts; iron artefacts and slag. For slag, a large number of samples were used, and this allowed chemical signatures retrieved to be plausible based on their representative amounts, and relative to what was recovered on site. The iron artefacts, however, only consisted of three samples. These three samples, unfortunately, do not represent a significant number to represent the sites' entire production range. The $\text{SiO}_2 : \text{Al}_2\text{O}_3$ ratio artefact chemical signature agreed with the ratio recorded from the slag data, and thus, if further artefacts are recovered, they are likely to follow this chemical signature. The $\text{SiO}_2 : \text{Al}_2\text{O}_3$ ratio seems to be the most likely accurate chemical signature for Thaba Nkulu's metal and metal smelting and smithing associated material culture.

Overall, three possible signatures were determined, the first being the $\text{SiO}_2 : \text{Al}_2\text{O}_3$ ratio, second the $\text{MgO} : \text{K}_2\text{O}$ SEM ratio for the slag of Thaba Nkulu, and finally the different elements and ratios determined by the XRF results, when compared with other sites' results. These three chemical signatures, individually reflect possible chemical signatures, however if combined they allowed for the distinction of Thaba Nkulu artefacts (ore, slag or artefact). The first chemical signature encompassed all artefacts relating to iron production on Thaba Nkulu, and as such, is determined to be the closest link for an absolute single signature.

The second aim of this dissertation was achieved when excavation 2328 CA1 (1) was determined to be a smelting associated area, rather than just a typical dump or smithing area. This evidence, when combined with the four other excavations, led to the 2328 CA1 (1) being positioned on the periphery of the EFC homestead, which would then follow the pattern of non-ritualistic belief, and thus follow Tim Maggs' (1980a, 1992, 1993) proposed settlement structure for some EFC communities.

9.3: Future research options

9.3.1: Future site options

Although evidence allowed for the site interpretation of being an EFC occupation, with a smelting area on the periphery, further finds could be sought. One such find would be the furnace area. As the debate regarding the identification of slag centres on both the chemical signature, as well as the context, furnace discovery plays a pivotal role in identifying slag types (Miller 2002; Greenfield & Miller 2004; Miller & Killick 2004). Furnace discovery would aid in the differentiation between smelting and smithing slag, and although slag was discovered in the domestic areas, without further research, the assumption is that they fall under smithing slag (due to visual appearance and description (cf. Miller 2002; Miller & Killick 2004).

With regards to copper, no copper slag or furnace was discovered during excavating. Copper was usually worked amongst houses within the homestead (Hall *et al.* 2006). The discovery of copper working may have ties with the iron smithing area as well (cf. Hall *et al.* 2006; Chirikure 2007; Grant & Huffman 2007), but due to no formal structures (hut floors or kraals) being found, the specific areas of Thaba Nkulu involved remain unknown, but extensive future excavations could shed light on this. Further research at Thaba Nkulu could explain the relationship with Rooiberg, with regards to the copper artefact chemical signature.

9.3.2: Future analysis options

Although XRF was performed on samples, the standards for sample preparation and testing according to Pollard *et al.* (2006: 107) and Shugar (2013: 180) were not performed in this research. They suggest sample preparation must be performed before testing. This preparation may include milling, grinding, sectioning or cutting samples, before mounting or pressing into a disk. These methods should force sample homogeneity and testing can be performed on flat surfaces, with the same degree of testing for all samples. This was not done for the XRF analyses, due to the attempt at keeping the samples as close to their original state as possible. Pollard *et al.* (2006),

however, suggests that some sample grains can be placed on plastic film such as Mylar. This was done during the XRF analyses and samples with flat surfaces were chosen for standardisation. Unfortunately, due to the surfaces not being ground or cut flat (although as flat as possible within their original context), this limited the accuracy of the results. Thus, it is realised that although these standards are time consuming and somewhat costly, for this type of analysis, the preparation of samples and use of the XRF station is recommended as a standard to guarantee accurate results, and also allows for better comparison to other reported results.

Relevant elements identified by other researchers (cf. Coustures *et al.* 2003: 603; Miller & Killick 2004: 36-45; Blakelock *et al.* 2009: 1747-1751; Chirikure *et al.* 2010: 1659-1661; Bandama 2013: 149, 274-277; Bandama *et al.* 2013: 255) were selected for further comparison and analysis. Unfortunately, the portable XRF does have limitations and is better suited to more homogenous samples (cf. Aimers *et al.* 2013; Shugar 2013), and hence less so for archaeological samples (which are not homogenous). In this investigation, many analyses were done because of the inhomogeneity (cf. Shugar 2013: 183). One example for the cause of inhomogeneity is given by Aimers *et al.* (2013) and is concerned with corroded areas on metals, however, corroded areas were avoided for this study, yet inhomogeneity still factored in the results. Currently for archaeological samples, there is very little one can do to avoid destructive preparation, if accurate results are required, but having many analyses does help (cf. Shugar 2013).

The experiments performed on the metal and metal smelting and smithing associated material culture led to the finding of these artefacts' chemical composition, as well as possible chemical signatures. Although the general use of XRF or SEM-EDX is accepted for the attempted discovery of chemical signatures, the methods and instruments vary between researchers (cf. Miller 2002; Coustures *et al.* 2003; Miller & Killick 2004; Hall *et al.* 2006; Blakelock *et al.* 2009; Chirikure *et al.* 2010; Bandama 2013; Bandama *et al.* 2013; Bandama *et al.* 2015). The Thaba Nkulu element results

needed to be converted before being compared to other researchers' oxide results (cf. Miller & Killick 2004).

A standard method for the cross comparison research, would aid future research into chemical signatures. Although equipment may differ, the results (within errors) can be compared, and perhaps one day a complete list of chemical compositions from all South African iron production sites may be recorded. For future research, it is suggested that the standards suggested above be used when using XRF and that more samples be analysed using reflected light microscopy and the SEM-EDX.

Another possible instrument to use would be X-ray Diffraction (XRD). The use of XRD in future research would not only provide information attaining to possible changes, (e.g. between ore to slag), but also indicate hardness tests, allowing for the distinction of smelting and smithing slags.

REFERENCES:

Aimers, J.J., Farthing, D.J. & Shugar, A.N. 2013. Handheld XRF analysis of Maya ceramics: a pilot study presenting issues related to quantification and calibration. In: Shugar, A.N., & Mass, J.L. (eds.) *Studies in archaeological science Vol. 3: Handheld XRF for art and archaeology*: 17-36. Leuven: Leuven University Press.

Anderson, M.S. 2009. *Marothodi: The Historical Archaeology of an African Capital*. Northamptonshire: Atikkam Media Limited.

Aukema, J. 1988. Lephalala: 'n Argeologiese Opname. Department Report, Dept Anthropology and Archaeology UNISA.

Aukema, J. 1989. Rain-making: A thousand year-old ritual? *The South African Archaeological Bulletin* 44(150): 70-72.

Avery, D.H. & Schmidt, P. 1979. A metallurgical study of iron bloomery particularly as practised in Buhaya. *Journal of Metals* 31: 14-20.

Balme, J. & Paterson, A. 2006. Chapter 4: Stratigraphy. In Balme, J. & Paterson, A. (eds.) *Archaeology in Practice: A student guide to archaeological analyses*, pp. 97-116. Oxford: Blackwell Publishing.

Bandama, F. 2013. The archaeology and technology of metal production in the Late Iron Age of the southern Waterberg, Limpopo Province, South Africa. Unpublished PhD thesis. Cape Town: University of Cape Town.

Bandama, F., Chirikure, S. & Hall, S. 2013. Ore sources, smelters and archaeometallurgy: exploring Iron Age production in the Southern Waterberg, South Africa. *Journal of African Archaeology* 11(2): 243-267.

Bandama, F., Hall, S., Chirikure, S., Eiland crucibles and the earliest relative dating for tin and bronze working in southern Africa, *Journal of Archaeological Science* (2015), doi:10.1016/j.jas.2015.07.007.

Blakelock, E., Martínón-Torres, M., Veldhuijzen, H.A. & Young, T. 2009. Slag inclusions in iron objects and the quest for provenance an experiment and case study. *Journal of Archaeological Science* 36: 1745-1757.

Boeyens, J.C.A. & Küsel, M.M. 1992. Current research in the Waterberg. *The Digging Stick* 9(1): 2-4.

Boeyens, J., Van der Ryst, M., Coetzee, F., Steyn, M. & Loots, M. 2009. From uterus to jar: the significance of an infant pot burial from Melora Saddle, an early nineteenth-century African farmer site on the Waterberg Plateau. *Southern African Humanities* 21: 213–238.

Bradfield, J., Holt, S. & Sadr, K. 2009. The last of the LSA on the Makgabeng Plateau, Limpopo Province. *The South African Archaeological Bulletin* 64(190): 176-183.

Buchwald, V.F. & Wivel, H. 1998. Slag analysis as a method for the characterization and provenancing of ancient iron objects. *Materials Characterization* 40(2): 73–96.

Calabrese, J.A. 2005. Ethnicity, Class, and Polity: The emergence of social and political complexity in the Shashi-Limpopo valley of southern Africa, AD 900 to 1300. Unpublished PhD thesis. Johannesburg: University of the Witwatersrand.

Childs, S.T. 2000. Traditional Iron Working: A Narrated Ethnoarchaeological Example. In: Bisson, M.S., Childs, S.T., De Barros, P. & Holl, A.F.C. (eds.) *Ancient*

African Metallurgy: The Socio-Cultural Context, pp. 199–255. Walnut Creek: Altamira Press.

Chirikure, S. 2007. Metals in society: Iron production and its position in Iron Age communities of southern Africa. *Journal of Social Archaeology* 7(1): 72-100.

Chirikure, S., Heimann, R.B. & Killick, D. 2010. The technology of tin smelting in the Rooiberg Valley, Limpopo Province, South Africa, ca. 1650–1850 CE. *Journal of Archaeological Science* 37: 1656–1669.

Chirikure, S. & Bandama, F. 2014. Indigenous African furnace types and slag composition – Is there a correlation? *Archaeometry* 56(2): 296-312.

Coustures, M.P., Béziat, D., Tollon, F., Domergue, C., Long, L. & Rebiscoul, A. 2003. The use of trace element analysis of entrapped slag inclusions to establish ore – bar iron links: examples from two Gallo-Roman iron-making sites in France (Les Martyrs, Montagne Noire, and Les Ferrys, Loiret). *Archaeometry* 45(3): 599-613.

Crew, P. 2001. Review Article: Iron in archaeology: the European bloomery smelters by Radomír Pleiner. *Historical Metallurgy* 35(2): 99-102.

David, A. 2006. Chapter 1: Finding sites. In Balme, J. & Paterson, A. (eds.) *Archaeology in Practice: A student guide to archaeological analyses*, pp. 1-38. Oxford: Blackwell Publishing.

Delegorgue, A. 1990. *Travels in Southern Africa*. 1 Durban: Killie Campbell Africana Library & Pietermaritzburg: University of Natal Press.

Denbow, J. 1979. *Cenchrus ciliaris*: an ecological indicator of Iron Age middens using aerial photography in eastern Botswana. *South African Journal of Science* 75: 405–408.

Dillmann, P. & L'Héritier, M. 2007. Slag inclusion analyses for studying ferrous alloys employed in French medieval buildings: supply of materials and diffusion of smelting processes. *Journal of Archaeological Science* 34: 1810–1823.

Edgeworth, M. 2013. Chapter 2: The clearing: archaeology's way of opening the world. In Ruibal, A.F. (ed.) *Reclaiming Archaeology: Beyond the Tropes of Modernity*, pp. 33-43. London: Routledge.

Eivindson, T. & Mikkelsen Ø. 2001. Problems by using pressed powder pellets for XRF analysis of ferrosilicon alloys. *CPDS-International Centre for Diffraction Data, Advances in X-ray Analysis* 4: 409-418.

Environmental Management Framework for the Waterberg District. 2010. Environmental Management Framework for the Waterberg District - Draft Environmental Management Framework Report. (Consulted April 2012): http://www.metrogis.co.za/docs/WDEMF_Draft_EMF_Report_Cover.pdf.

Evers, T.M. 1975. Recent Iron Age Research in the Eastern Transvaal, South Africa. *The South African Archaeological Bulletin* 30(119/120): 71-83.

Evers, T.M. 1980. Klingbeil Early Iron Age Sites, Lydenburg, Eastern Transvaal, South Africa. *The South African Archaeological Bulletin* 35(131): 46-57.

Evers, T.M., Voigt, E.A. & de Villiers, H. 1982. Excavations at the Lydenburg Heads Site, Eastern Transvaal, South Africa. *The South African Archaeological Bulletin* 37(135): 16-33.

Friede, M.H. 1979. Iron-smelting furnaces and metallurgical traditions of the South African Iron Age. *Journal of the South African Institute of Mining and Metallurgy* 79:372-382.

Friede, M.H. & Steel, R.H. 1976. Tin mining and smelting in the Transvaal during the Iron Age. *Journal of the South African Institute of Mining and Metallurgy* 76: 461-470.

Friede, H. & Steel, R. 1985. Iron Age iron smelting furnaces of the western/central Transvaal: their structure, typology and affinities. *The South African Archaeological Bulletin* 40(141): 45-49.

Goldstein, J.I., Newbury, D.E., Echlin, P., Joy, D.C., Fiori, C. & Lifshin, E. 1981. *Scanning Electron Microscopy and X-Ray Microanalysis: A text for biologists, materials scientists, and geologists*. New York: Plenum

Goucher, C.L. 1981. Iron is iron 'til it is rust: trade and ecology in the decline of West African Iron-Smelting. *The Journal of African History* 22(2): 179-189.

Grant, M.R. 1994. Iron in ancient tin from Rooiberg, South Africa. *Journal of Archaeological Science* 21: 455-460.

Grant, M.R. 1999. The sourcing of southern African tin artefacts. *Journal of Archaeological Science* 26: 1111-1117.

Grant, M. & Huffman, T.N. 2007. The extractive metallurgy of copper at Iron Age Madikwe. *South African Journal of Science* 103: 403-408.

Greenfield, H., van Schalkwyk, L.O. & Jongsma, T. 1997. Preliminary Results of the 1995 Research at the Early Iron Age site of Ndongondwane, KwaZulu-Natal, South Africa. *Nyame Akuma* 47: 42-52.

Greenfield, H.J. & Miller, D. 2004. Spatial patterning of Early Iron Age metal production at Ndongondwane, South Africa: the question of cultural continuity between the Early and Late Iron Ages. *Journal of Archaeological Science* 31: 1511-1532.

Grigorova, B., Anderson, S., de Bruyn, J., Smith, W., Stülpner, K. & Barzev, A. 1998a. The AARL gold fingerprinting technology. *Gold Bulletin* 31(3): 26-29.

Grigorova, B., Smith, W., Stülpner, K., Tumilt, J.A. & Miller, D. 1998b. Fingerprinting of gold artefacts from Mapungubwe, Bosutswe and Thulamela. *Gold Bulletin* 31(3): 99-102.

Hall, M. 1984. Pots and Politics: Ceramic interpretations in southern Africa. *World Archaeology* 15(3): 262-273.

Hall, M. 1987. Archaeology and modes of production in pre-colonial southern Africa. *Journal of Southern African Studies* 14(1): 1-17.

Hall, M. & Maggs, T. 1979. Nqabeni, a later Iron Age site in Zululand. *South African Archaeology Society Goodwin Series* 3: 159-176.

Hall, S.L. 1981. Iron Age sequence and settlement in the Rooiberg, Thabazimbi area. Unpublished MSc Dissertation. Johannesburg: University of the Witwatersrand.

Hall, S.L. 1985. Excavations at Rooikrans and Rhenosterkloof, Late Iron Age sites in the Rooiberg area of the Transvaal. *Annals of the Cape Provincial Museums (Human Sciences)* 1(5): 131-210.

Hall, S., Miller, D., Anderson, A. & Boeyens, J. 2006. An exploratory study of copper and iron production at Marothodi, an early 19th century Tswana town, Rustenburg district, South Africa. *Journal of African Archaeology* 4 (1): 3-35.

Hall, S. & Smith, B. 2000. Empowering places: rock shelters and ritual control in farmer-forager interactions in the Northern Province. *South African Archaeology Society Goodwin Series* 8: 30-46.

Hammel, A., White, C., Pfeiffer, S. & Miller, D. 2000. Pre-colonial mining in southern Africa. *The Journal of the South African Institute of Mining and Metallurgy* 100: 49-56.

Hanisch, E.O.M. 1981. The northern Transvaal: environment and archaeology. In: E.A. Voigt (ed.) *Guide to Archaeological Sites in the Northern and Eastern Transvaal*: 1-6. Pretoria: Transvaal Museum. (for the Southern African Association of archaeologists Excursion June 6th – 11th 1981)

Higginbotham, E. 1985. Excavation techniques in historical archaeology. *Australian Historical Archaeology* 3: 8-14.

Holdaway, S. 2006. Chapter 5: Absolute Dating. In Balme, J. & Paterson, A. (eds.) *Archaeology in Practice: A student guide to archaeological analyses*, pp. 117-158. Oxford: Blackwell Publishing.

Huckleberry, G. 2006. Chapter 12: Sediments. In Balme, J. & Paterson, A. (eds.) *Archaeology in Practice: A student guide to archaeological analyses*, pp. 338-361. Oxford: Blackwell Publishing.

Huffman, T.N. 1982. Archaeology and ethnohistory of the African Iron Age. *Annual Review of Anthropology* 11: 133-50.

Huffman, T.N. 1990a. The Waterberg research of Jan Aukema. *The South African Archaeological Bulletin* 45(52): 117-119.

Huffman, T.N. 1990b. Broederstroom and the origins of cattle-keeping in southern Africa. *African Studies* 49(2): 1-12.

Huffman, T.N. 1993. Broederstroom and the Central Cattle Pattern. *South African Journal of Science* 89: 220–226.

Huffman, T.N. 2000. Mapungubwe and the Origins of the Zimbabwe Culture. *Goodwin Series* 8: 14-29.

Huffman, T.N. 2007. *Handbook to the Iron Age*. Scottsville: University of KwaZulu-Natal Press.

Jorge, M.A.B., Van de Wouw, M., Hanson, J. & Mohammed. J. 2008. Characterisation of a collection of buffel grass (*Cenchrus ciliaris*). *Tropical Grasslands* 42:27-39.

Killick, D. 1991. A tin lerale from the Soutpansberg, Northern Transvaal, South Africa. *The South African Archaeological Bulletin* 46(154): 137-141.

Killick, D. & Miller, D. in press. Late Iron Age metal working technology at Phalaborwa (northern Lowveld, South Africa). *Journal of Archaeological Science*, quoted by Miller, D. & Killick, D. 2004.

Krige, E.J. 1936. *The social systems of the Zulus*. New York: Longmans, Green and Co.

Koleini, F. 2012. Mapungubwe metals revisited: a technical and historical study of Mapungubwe material culture with an emphasis on conservation. Unpublished PhD Thesis. Pretoria: University of Pretoria.

Koursaris, A., Hall, S. & Grant, M.R. 2007. An archaeometallurgical study of iron artifacts from Mabotse. *Journal of the Minerals, Metals & Materials Society* 59(5): 22-25.

Loubser, J.H.N. 1993. Ndongondwane: the significance of features and finds from a ninth-century site on the lower Thukela River, Natal. *Natal Museum Journal of Humanities* 5: 109-151.

Lyaya, E.C. 2011. Bio-archaeometallurgy, technology, and spatial organization of ironworking at Mjimwema, Njombe Tanzania. *Papers from the Institute of Archaeology* 21:59-79.

Maggs, T. 1973. The NC3 Iron Age tradition. In Mason, R.J. (ed.), Early Iron Age settlement of southern Africa. *South Africa Journal of Science* 69: 324-326.

Maggs, T. 1980a. Msuluzi Confluence: a seventh century Early Iron Age site on the Tugela River. *Annals of the Natal Museum* 24(1): 111-145.

Maggs, T. 1980b. The Iron Age Sequence South of the Vaal and Pongola Rivers: Some Historical Implications. *The Journal of African History* 21(1): 1-15.

Maggs, T. 1980c. Mzonjani and the beginning of the Iron Age in Natal. *Annals of the Natal Museum* 24(1):71-96.

Maggs, T. 1982. Mabhija: pre-colonial industrial development in the Tugela Basin. *Annals of the Natal Museum* 25(1): 123-141.

Maggs, T. 1984. Ndongondwane: a preliminary report on an Early Iron site on the lower Tugela River. *Annals of the Natal Museum* 26: 71-94.

Maggs, T. 1991. Metalwork from Iron Age hoards as a record of metal production in the Natal Region. *The South African Archaeological Bulletin* 46(154): 131-136.

Maggs, T. 1992. 'My Father's hammer never ceased its song day and night': the Zulu ferrous metalworking industry. *Natal Museum Journal of Humanities* 4: 65-87.

Maggs, T. 1993. Three decades of Iron Age research in South Africa: Some personal reflections. *The South African Archaeological Bulletin* 48(158): 70-76.

Maggs, T. 1994. The Early Iron Age in the extreme south: some patterns and problems. *Azania: Archaeological Research in Africa* 29-30(1): 168-178.

Maggs, T.M. & Michael, M.A. 1976. Ntshekane: an Early Iron Age site in the Tugela Basin, Natal. *Annals of the Natal Museum* 23(3): 705-740.

Maggs, T. & Ward, V. 1984. Early Iron Age sites in the Muden area of Natal. *Annals of the Natal Museum* 26(1): 105-140.

Maggs, T. & Miller, D.E. 1995. Sandstone crucibles from Mhlopheni, Natal: evidence of precolonial brass-working. *Natal Museum Journal of Humanities* 7: 1-16.

Mason, R.J. 1974. Background to the Transvaal Iron Age-new discoveries at Olifantspoort and Broederstroom. *Journal of the South African Institute of Mining and Metallurgy* 74: 211-216.

Mason, R.J. 1982. Prehistoric mining in South Africa, and Iron Age copper mines in the Dwarsberg, Transvaal. *Journal of the South African Institute of Mining and Metallurgy* 82(5): 134-144.

Miller, D. 1994. Report on the analysis of slags, metals and other artefacts from the Oanob river valley, Rehoboth, Namibia. Unpublished report, University of Cape Town.

Miller, D.E. 1996. *The Tsodilo jewellery - metal work from northwestern Botswana*. Cape Town: University of Cape Town Press.

Miller, D. 2000. Report on metallographic analysis of slags from Nandoni (Bristol), submitted by Pietermaritzburg Museum. Unpublished report, University of Cape Town.

Miller, D. 2001. Metal assemblages from the Greefswald areas: K2, Mapungubwe Hill and Mapungubwe Southern Terrace. *South African Archaeological Bulletin* 56: 83-103.

Miller, D. 2002. Smelter and Smith: Iron Age metal fabrication technology in southern Africa. *Journal of Archaeological Science* 29: 1083–1131.

Miller, D. 2010. Indigenous metal melting and casting in southern Africa. *South African Archaeological Bulletin* 65(191): 45-57.

Miller, D. & Evans, G. 1992. Report on the metallurgical analysis of ferrous metal-working residues submitted by Dr J. Pistorius, University of Pretoria. Unpublished report, University of Cape Town.

Miller, D., Morris, D. & Evans, G. 1993. Metallurgical analysis of two artefacts from a burial at De Hoop, Kimberley District. *Southern African Field Archaeology* 2(1): 49-52.

Miller, D.E. & van der Merwe, N.J. 1994a. Early metal working in sub-Saharan Africa: A review of recent research. *The Journal of African History* 35(1): 1-36.

Miller, D.E. & van der Merwe, N.J. 1994b. Early Iron Age metal working at the Tsodilo Hills, Northwestern Botswana. *Journal of Archaeological Science* 21: 101-115.

Miller, D. & Whitelaw, G. 1994. Early Iron Age metal working from the site of KwaGandaganda, Natal, South Africa. *The South African Archaeological Bulletin* 49(160): 79-89.

Miller, D., Boeyens, J. & Küsel, M. 1995. Metallurgical analyses of slags, ores and metal artefacts from archaeological sites in the North-West Province and northern Transvaal. *South African Archaeological Bulletin* 50: 39-46.

Miller, D. & Sandelowsky, B. 1999. Smelting without ceramics: the Drierivier copper smelting site near Rehoboth, Namibia. *South African Archaeological Bulletin* 54, 28-37.

Miller, D. & Killick, D. 2004. Slag identification at southern African Sites. *Journal of African Archaeology* 2(1): 23-47.

Miller, D. & Hall, S. 2008. Rooiberg revisited: the analysis of tin and copper smelting debris. *Historical Metallurgy* 42(1): 23-38.

Moore, M.P.J. 1981. The Iron Age of the Makapan Valley area, central Transvaal. Unpublished MSc Dissertation. Johannesburg: University of the Witwatersrand.

O'Conner, T. & Barrett, J. 2006. Chapter 9: Animal Bones. In Balme, J. & Paterson, A. (eds.) *Archaeology in Practice: A student guide to archaeological analyses*, pp. 260-295. Oxford: Blackwell Publishing.

Pleiner, R. 2000. *Iron in Archaeology: The European Bloomery Smelters*. Praha: Archeologický Ústav Av Cr.

Pollard, M., Batt, C., Stern, B., & Young, S.M.M. 2006. *Analytical chemistry in archaeology*. Cambridge: Cambridge University Press.

Prinsloo, H.P. 1974. Early Iron Age site a Klein Afrika near Wylliespoort, Soutpansberg Mountains, South Africa. *South African Journal of Science* 70: 271-273.

Pryce, T.O. & Natapintu, S. 2009. Smelting Iron from Laterite: Technical possibility or ethnographic aberration? *Asian Perspectives* 48 (2): 249-264.

Rehren, T., Charlton, M., Chirikure, S., Humphris, J., Ige, A. & Veldhuijzen, H.A. 2007. Decisions set in slag: the human factor in African iron smelting. In: LaNiece, S., Hook, D.R., and Craddock, P.T., (eds.) *Metals and Mines: Studies in Archaeometallurgy*, pp. 211 - 218. London: Archetype/British Museum.

Robinson, K.R. 1961. Two iron-smelting furnaces from the Chibi Native Reserve, Southern Rhodesia. *The South African Archaeological Bulletin* 16(61): 20-22.

Sadr, K. & Sampson, C.G. 2006. Through thick and thin: Early pottery in southern Africa. *Journal of African Archaeology* 4(2): 235-252.

Sandelowsky, H. 1974. Prehistoric metal-working in South West Africa. *Journal of the South African institute of mining and metallurgy* 74: 363-366.

Schmidt, P.R. 1997. *Iron technology in East Africa: symbolism, science, and archaeology*. Oxford: James Currey Publishers.

Schmidt, P.R. 2009. Tropes, materiality, and ritual embodiment of African iron smelting furnaces as human figures. *Journal of Archaeological Method and Theory* 16(3):262-282.

Sheikh, M.R., Acharya, B.S. & Gartia, R.K. 2010. Characterization of iron slag of Kakching, Manipur by X-ray and optical spectroscopy. *Indian Journal of Pure & Applied Physics* 48: 632-634.

Shinnie, P. 1985. Iron working at Meroe. In: Haaland, R. & Shinnie, P. (eds.) *African Iron Working, Ancient and Traditional*: 28-35. Bergen: Norwegian University Press.

Shugar, A.N., & Mass, J.L. 2012. Introduction. In: Shugar, A.N., & Mass, J.L. (eds.) *Studies in archaeological science Vol. 3: Handheld XRF for art and archaeology*: 17-36. Leuven: Leuven University Press.

Shugar, A.N. 2013. Portable X-ray fluorescence and archaeology: limitations of the instrument and suggested methods to achieve desired results. In: Armitage, R.A. & Burton, J.H. (eds.) *Archaeological chemistry VIII*: 173-193. American Chemical Society: Washington DC.

Stockton, E.D. 1973. Shaw's Creek Shelter: Human Displacement of Artefacts and its Significance. *Mankind* 9: 112-117.

Stuiver, M. & van der Merwe, N.J. 1968. Radiocarbon chronology of the Iron Age in sub-Saharan Africa. *Current Anthropology* 9(1): 54-58.

Thondhlana, T.P. 2012. Metalworkers and smelting precincts: technological reconstructions of second millennium copper production around Phalaborwa, northern lowveld of South Africa. Unpublished PhD Thesis. London: University College London.

Unknown, Molecular weights of some oxides and factors to convert them to elements by weight. (Consulted February 2013): <http://www.geol.umd.edu/~piccoli/probe/molweight.html>.

Van der Ryst, M.M. 1998. The Waterberg Plateau in the Northern Province, Republic of South Africa, in the Later Stone Age. *Oxford: British Archaeological Reports* 715.

Van der Ryst, M.M. 2007. Seeking shelter: Later Stone Age hunters, gatherers and fishers of Olieboomspoort in the western Waterberg, south of the Limpopo. Unpublished PhD Thesis. Johannesburg: University of the Witwatersrand.

Van Doornum, B.L. 2005. Changing Places, Spaces and Identity in the Shashe-Limpopo Region of Limpopo Province, South Africa. Unpublished PhD Thesis. Johannesburg: University of the Witwatersrand.

Walter, B.S, & Schultz, J.J. 2013. Mapping simulated scenes with skeletal remains using differential GPS in open environments: An assessment of accuracy and practicality. *Forensic Sci. Int.* (Consulted October 2013): <http://dx.doi.org/10.1016/j.forsciint.2013.02.027>

Wheeler, R.E.M. 1954. *Archaeology from the earth*. Oxford: Clarendon Press.